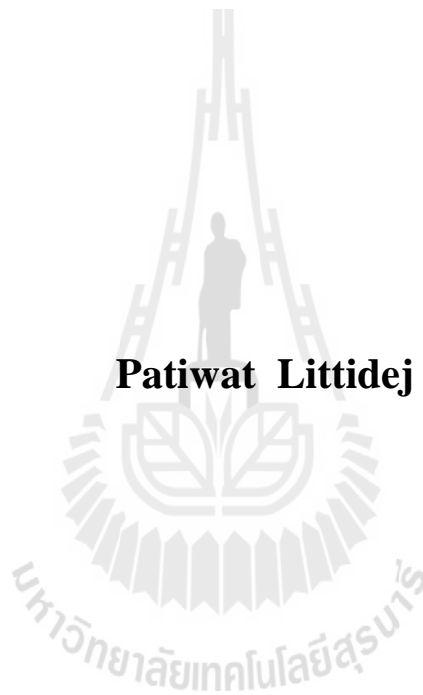


**POSITIONING AMBIENT AIR QUALITY MONITORING
STATIONS UTILIZING SPATIAL MULTI-OBJECTIVE
DECISION ANALYSES**

Patiwat Littidej



**A Thesis Submitted in Partial Fulfillment of the Requirements for the
Degree of Doctor of Philosophy in Geoinformatics**

Suranaree University of Technology

Academic Year 2013

การหาตำแหน่งสถานีตรวจวัดคุณภาพอากาศด้วยการวิเคราะห์การตัดสินใจ
แบบหลายวัตถุประสงค์



นายปฏิวัติ ฤทธิเดช

วิทยานิพนธ์นี้เป็นส่วนหนึ่งของการศึกษาตามหลักสูตรปริญญาวิทยาศาสตรดุษฎีบัณฑิต

สาขาวิชาภูมิสารสนเทศ

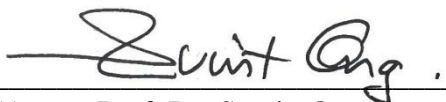
มหาวิทยาลัยเทคโนโลยีสุรนารี

ปีการศึกษา 2556


**POSITIONING AMBIENT AIR QUALITY MONITORING
STATIONS UTILIZING SPATIAL MULTI-OBJECTIVE
DECISION ANALYSES**

Suranaree University of Technology has approved this thesis submitted in partial fulfillment of the requirements for the Degree of Doctor of Philosophy.


Thesis Examining Committee


(Assoc. Prof. Dr. Suwit Ongsomwang)


Chairperson


(Asst. Prof. Dr. Sunya Sarapirome)

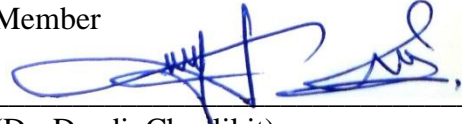
Member (Thesis Advisor)


(Asst. Prof. Dr. Nares Chuesuwan)

Member


(Asst. Prof. Dr. Songkot Dasananda)

Member


(Dr. Dusdi Chanlikit)

Member


(Prof. Dr. Sukit Limpijumnong)

Vice Rector for Academic Affairs
and Innovation


(Assoc. Prof. Dr. Prapun Manyum)

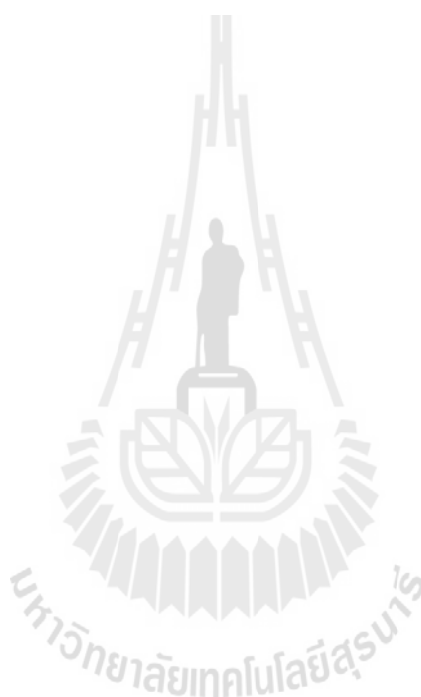
Dean of Institute of Science

ปฎิบัติ ฤทธิเดช : การหาตำแหน่งสถานีตรวจวัดคุณภาพอากาศด้วยการวิเคราะห์การ
ตัดสินใจแบบหลายวัตถุประสงค์ (POSITIONING AMBIENT AIR QUALITY
MONITORING STATIONS UTILIZING SPATIAL MULTI-OBJECTIVE DECISION
ANALYSES) อาจารย์ที่ปรึกษา : ผู้ช่วยศาสตราจารย์ ดร.สัญญา สราภิรมย์, 190 หน้า

สถานีตรวจวัดคุณภาพอากาศสำหรับตรวจวัดมลพิษที่มีแหล่งกำเนิดแบบเส้นทางการจราจรมีค่าใช้จ่ายสูง ตำแหน่งที่ตั้งของสถานีต้องตั้งอยู่ในพื้นที่ที่มีค่าดัชนีความเข้มข้นมลพิษสูง ค่าดัชนีความถี่ของความรุนแรงสูง ค่าดัชนีพื้นที่ให้บริการของสถานีที่สูง และค่าดัชนีผลกระทบต่อประชากรสูง วัตถุประสงค์ของการศึกษานี้คือเพื่อระบุตำแหน่ง และจำนวนที่เหมาะสมของสถานีตรวจวัดคุณภาพอากาศในเขตเทศบาลเมืองนครราชสีมา โดยใช้การวิเคราะห์การตัดสินใจแบบหลายวัตถุประสงค์เชิงพื้นที่ การสร้างแผนที่กระจายเชิงพื้นที่ของความรุนแรงมลพิษประเภทคาร์บอนมอนอกไซด์ ออกไซด์ของไนโตรเจน และฝุ่นอนุภาคขนาดเล็กกว่า 10 ไมครอน รวมถึงการรวมกันของแผนที่ด้วย CALINE4 และระบบสารสนเทศภูมิศาสตร์ บนพื้นฐานของการเปลี่ยนแปลงประเภทยานพาหนะ ช่วงเวลาที่ยานพาหนะเคลื่อนที่ และทิศทางลมที่พัดเข้ามาในพื้นที่ศึกษา ผลการศึกษาแสดงค่าการกระจาย ค่าความรุนแรงมลพิษสูงในพื้นที่ตามแนวถนนมิตรภาพ และถนนทางหลวงหมายเลข 224 ค่าความถี่ของความรุนแรงมลพิษได้รับจากความรุนแรงมลพิษซึ่งสามารถสังเกตค่าสูงของดัชนีได้ชัดเจนในพื้นที่รอบๆ ถนนมิตรภาพบริเวณหน้าห้างสรรพสินค้าเดอะมอลล์นครราชสีมา และเทศบาลอุตสาหกรรมมิตรภาพ ส่วนบริเวณอื่นจะแสดงค่าดัชนีปานกลางและต่ำ ตำแหน่งที่ตั้งต้องสามารถวัดค่าสูงสุดของพื้นที่ให้บริการได้ซึ่งค่าสูงสุดจะพบได้ในบริเวณรอบ ถนนมิตรภาพหน้าห้างสรรพสินค้าเดอะมอลล์นครราชสีมา และตามแนวถนนทางหลวงหมายเลข 224 ค่าดัชนีสูงสุดของการเปิดเผยผลกระทบต่อประชากรได้มาจากการวิเคราะห์ตรรกะความคลุมเครือ ซึ่งมีค่าสูงสุดอยู่ในช่วง 0.6001-0.7931 สามารถสังเกตได้ในบริเวณรอบถนนทางหลวงหมายเลข 224 ด้านหน้าโรงเรียนเมืองนครราชสีมา โรงเรียนอนุบาลนครราชสีมา วิทยาลัยอาชีวศึกษานครราชสีมา และโรงเรียนสุนารีวิทยา ลักษณะเด่นเหล่านี้จะสัมพันธ์กับความรุนแรงของมลพิษ และลักษณะเหล่านี้จะถูกนำไปกำหนดเป็นฟังก์ชันวัตถุประสงค์ของแบบจำลองการวิเคราะห์การตัดสินใจแบบหลายวัตถุประสงค์ สำหรับหาที่ตั้งที่เหมาะสมของสถานี

ผลลัพธ์แสดง 15 ที่ตั้งที่เหมาะสมซึ่งจะถูกพิจารณาอีกครั้ง ด้วยการวิเคราะห์ความอ่อนไหว ทำให้เหลือ 3 ที่ตั้งที่เหมาะสม ที่ตั้งที่มีคะแนนสูงสุดคือ 3.66 เป็นค่าของผลรวมทุกฟังก์ชันวัตถุประสงค์ ตำแหน่งดังกล่าวถูกตั้งอยู่ตรงข้ามกับห้างสรรพสินค้าเดอะมอลล์นครราชสีมาบนพิกัดแนวแกน $X_1 = 831,100$ เมตร และแกน $Y_1 = 1,658,100$ เมตร ส่วนอีกสองสถานีที่มีค่าคะแนน

รองลงมาจะตั้งอยู่บนพิกัด $X_2=833,200$ เมตร และ $Y_2=1,658,500$ เมตร และ $X_3=831,250$ เมตร และ $Y_3=1,658,200$ เมตร ซึ่งจะตั้งอยู่บริเวณหน้าโรงเรียนเมืองนครราชสีมา และใกล้กับสถานีตรวจวัดคุณภาพอากาศเดิมที่มีอยู่แล้วของกรมควบคุมมลพิษ ตำแหน่งที่มีค่าคะแนนรองลงมาจะไม่ถูกเสนอเป็นที่ตั้ง



สาขาวิชาการรับรู้จากระยะไกล
ปีการศึกษา 2556

ลายมือชื่อนักศึกษา ปฏิวัติ ฤทธิเดช
ลายมือชื่ออาจารย์ที่ปรึกษา วิวัฒน์ ฤทธิเดช

PATIWAT LITTIDEJ : POSITIONING AMBIENT AIR QUALITY
MONITORING STATIONS UTILIZING SPATIAL MULTI-OBJECTIVE
DECISION ANALYSES THESIS ADVISOR : ASST. PROF. SUNYA
SARAPIROME, Ph.D. 190 PP.

AIR QUALITY MONITORING STATION / GIS / SPATIAL MULTI-OBJECTIVE
DECISION ANALYSIS / LINEAR PROGRAMMING /AIR POLLUTION

Air quality monitoring station (AQMS) has high cost on the investment to detect pollutants from traffic line source. Its location requires maximized conditions on pollution intensity, frequency of violence, service area, and people exposure impact. The objective of the study is to determine a proper position and a number of AQMSs for Nakhon Ratchasima municipal area using the spatial multi-objective decision analysis. The spatial distributions of pollution intensity were generated in forms of carbon monoxide (CO), nitrogen oxide (NO_x) and particulate matter less than 10 micron (PM₁₀) including their combination using CALINE4 and GIS, based on varying vehicle types, time periods, and wind directions. The result shows high pollution dispersions in areas along the Mittrapap Road and Highway 224. The maximum frequency of violence index derived from pollution intensity could obviously be observed from area surrounding Mittrapap Road in front of the Mall and Tesco Lotus department stores. Apart from this, other areas showed moderate and low index. Locations provided the highest index of service area were found in the area surrounding Mittrapap Road in front of The Mall and along Highway 224. The highest index of people exposure impact determined using fuzzy logic, ranged

between 0.6001-0.7931, could be observed in the area surrounding Highway 224 in front of Mueang Nakhon Ratchasima school, Anuban Nakhon Ratchasima school, Nakhon Ratchasima vocational college, and Suranaree Wittaya school. These characteristics related to pollution intensity and its impact were then input as objective functions in spatial multi-objectives decision analysis for siting proper AQMSs. Fifteen proper sites obtained from optimization models of the analysis were reconsidered and reduced to 3 proper sites using sensitivity analysis. The site with highest score as 3.66 of combined all objective functions was located opposite to The Mall commercial center at coordinate $X_1=831,100$ m and $Y_1=1,658,100$ m. Other two second best sites at coordinates $X_2=833,200$ m and $Y_2=1,658,500$ m, and $X_3=831,250$ m and $Y_3=1,658,200$ m were located in front of Mueang Nakhon Ratchasima school and too close to the existing AQMS of the PCD, they were thus neglected.

School of Remote Sensing

Academic Year 2013

Student's Signature Patiwat Littidej

Advisor's Signature S. Sawapinome

ACKNOWLEDGEMENTS

This thesis would not have been possible without the guidance and the help of several individuals who in one way or another contributed and extended their valuable assistance in the preparation and completion of this study.

This research was granted by the Commission on Higher Education granting through Mr. Patiwat Littidej who was funded under the CHE-PHD-THA program.

First and foremost, my utmost gratitude to my advisor, Asst. Prof. Dr. Sunya Sarapirome for his invaluable advice to complete this work. He not only provided immense knowledge but his logical ways of thinking have been of great value for me.

Besides my advisor, I am deeply grateful to Assoc. Prof. Dr. Suwit Ongsomwang, Asst. Prof. Dr. Songkot Dasananda, Assit. Prof. Dr. Nares Chuesuwan for serving as committee members and appreciated suggestions. I would also like to thank Dr. Dusdi Chanlikit for his helpful guidance.

Special thanks go to student in school of Remote Sensing, Miss. Warunee Aunphoklang for guidance and preparation of network analysis and teaching me the essential techniques. My warm thanks are due to my friends from the School of Remote Sensing for their kind help and moral support that made my stay full with much joy and happy moments. I would also like to express my apology that I could not mention one by one personally.

Finally, a note of thanks goes to my beloved parents whose dedication, love and persistent confidence on me. I owe my loving thanks to them for being patient

and encouraging me to finish this work. My graduation would not be achieved without their understanding and encouragement.

Patiwat Littidej



CONTENTS

	Page
ABSTRACT IN THAI.....	I
ABSTRACT IN ENGLISH	III
ACKNOWLEDGEMENTS.....	V
CONTENTS.....	VII
LIST OF TABLES.....	XIV
LIST OF FIGURES	XVIII
LIST OF ABBREVIATIONS.....	XXVIII
CHAPTER	
I INTRODUCTION.....	1
1.1 Background problem.....	1
1.2 Study area.....	4
1.2.1 Study area selection.....	4
1.2.2 Points of interest.....	5
1.2.3 Traffic data of the study area.....	6
1.2.4 Pollutants from mobile sources	7
1.3 Research objectives	9
1.4 Scope of the study	10
1.5 Assumptions of the study	10

CONTENTS (Continued)

	Page
II LITERATURE REVIEW AND THE RESEARCH APPROACH.....	12
2.1 Meteorological conditions.....	12
2.2 Theory of Line Source Dispersion model.....	14
2.3 Fuzzy set membership.....	20
2.4 Multi-Objective Decision Analysis (MODA).....	20
2.4.1 Linear programming (LP).....	21
2.5 Previous researches.....	23
2.5.1 Application of line source air dispersion modeling.....	23
2.5.2 Application of GIS to analyse urban traffic air pollution.....	26
2.5.3 Multi-objective modeling to locate Air Quality Monitoring Stations.....	28
2.6 Synthesis of the research approach.....	31
III RESEARCH METHODOLOGY.....	32
3.1 Overview of the research methodology.....	32
3.2 Data collection, refinement, and manipulation.....	33
3.2.1 Traffic and emission coefficient data.....	33
3.3 Potential impact points.....	36
3.4 Pollution and network mapping.....	37
3.4.1 CALINE4 model.....	38

CONTENTS (Continued)

	Page
3.4.2 Spatial pollution interpolation	41
3.4.3 Combined pollution map	42
3.4.4 frequency of violence.....	45
3.4.5 Pollution network map.....	45
3.4.6 Service area determination.....	46
3.5 People exposure impact determination.....	46
3.6 Optimization process using multi-objective decision analysis.....	47
3.6.1 Design of objective functions	47
3.6.1.1 Maximization of pollution intensity (Z_1)	47
3.6.1.2 Maximization of the frequency of pollution violence (Z_2)	47
3.6.1.3 Maximization of service area (Z_3).....	48
3.6.1.4 Maximization of people exposure impact (Z_4).....	48
3.6.2 Design of constraint functions.....	49
3.6.2.1 A number of alternatives	49
3.6.2.2 Service area and spatial autocorrelation	49
3.6.2.3 Effective service area	51
3.6.3 The multi-objective model.....	52
3.7 Sensitivity analysis using value function of MODA	53

CONTENTS (Continued)

	Page
IV RESULTS AND DISCUSSION	54
4.1 Data Collection.....	54
4.1.1 Meteorological Data	54
4.1.2 Ambient concentration determination of CO, NO _x and PM ₁₀	57
4.2 Pollution intensity	60
4.2.1 Estimation of pollutants concentration from CALINE4	60
4.2.2 Diagnostic evaluation of emission rates.....	61
4.2.3 Evaluation of the results from CALINE4 model	62
4.2.4 Surface maps obtained from IDW Interpolation	64
4.2.5 Pollution intensity varied with types of vehicle, pollutants and time periods	65
4.2.6 Combined pollution map.....	67
4.2.7 Classification of pollution intensity	71
4.3 Frequency of violence	72
4.4 Constraint and objective function used on service area and Moran's I.....	76
4.4.1 Pollution network map	76
4.4.2 Proper search tolerance of service area	77
4.4.3 Service area constraint based on Moran's I	77
4.4.4 Discussion of service area.....	79

CONTENTS (Continued)

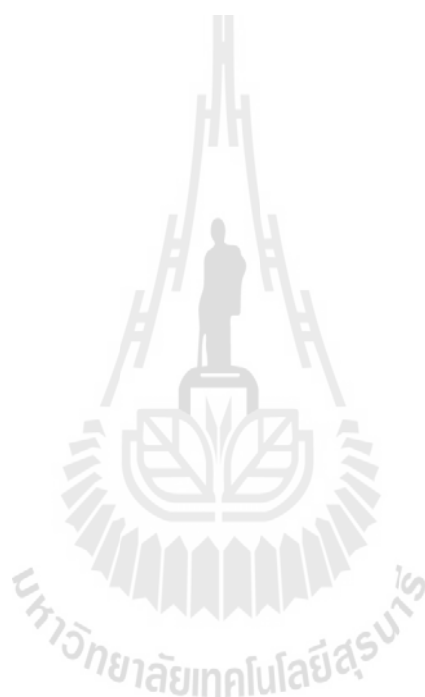
	Page
4.5 People exposure impact.....	81
4.5.1 Fuzzy number determination.....	81
4.6 Combination of all distribution of variables in objective function	82
4.7 Sensitivity analysis of spatial multi-objective model.....	86
4.8 Screening a suitable position.....	93
V CONCLUSIONS AND RECOMMENDATIONS	96
5.1 Conclusions	96
5.1.1 Pollution distribution and people exposure impact	96
5.1.2 Spatial multi-objective and constraint functions	98
5.2 Recommendations for future improvements.....	99
REFERENCES	100
APPENDICES	107
APPENDIX A TRAFFIC VOLUME (VEHICLE/HOUR) OF 21 ROAD SECTIONS	108
APPENDIX B A NUMBER OF POPULATION AT POINTS OF INTEREST AND DESCRIPTIVE STATISTICS.....	116
APPENDIX C FIELD OBSERVATION OF AMBIENT (CO) AND COUNTING POPULATION.....	119
APPENDIX D THE PROCESS OF CALINE4 RUNNING	121

CONTENTS (Continued)

	Page
APPENDIX E NO _x EMISSION (G/HR./LINK) ON LINK (BIG-C 3- JUNCTION TO MUEANG NAKHON RATCHASIMA SCHOOL)	125
APPENDIX F WIND ROSE DIAGRAM OF ALL TIME PERIODS (07:00- 19:00).....	130
APPENDIX G CO CONCENTRATION (PPM) DISPERSION MAPS VARIED WITH VEHICLE TYPES AND WIND DIRECTION IN (0-315 DEGREE) AT TIME PERIODS: (07:00-19:00).....	134
APPENDIX H NOX CONCENTRATION (PPB) DISPERSION MAPS VARIED WITH VEHICLE TYPES AND WIND DIRECTION IN (0-315 DEGREE) AT TIME PERIODS: (07:00-19:00).....	155
APPENDIX I PM10 CONCENTRATION ($\mu\text{G}/\text{M}^3$) DISPERSION MAPS VARIED WITH VEHICLE TYPES AND WIND DIRECTION IN (0-315 DEGREE) AT TIME PERIODS: (07:00-19:00).....	166
APPENDIX J FREQUENCY OF VIOLENCE MAPS VARIED WITH VEHICLE TYPES AT TIME PERIODS: (07:000-19:00) ...	177
APPENDIX K FUZZY NUMBER (A, B, C, AND D) OF CLASS LOW AND HIGH.....	186

CONTENTS (Continued)

	Page
CURRICULUM VITAE	190



LIST OF TABLES

Table	Page
1.1 Concentration of PM10 ($\mu\text{g}/\text{m}^3$) on different road network of Nakhon Ratchasima municipality in August 2004	8
2.1 Beaufort scale of wind velocities	15
2.2 Pasquill stability categories.....	16
2.3 The coefficient of Pasquill-Gifford (σ_y) and (σ_z) of urban area	18
3.1 Required data and their sources	35
3.2 Emission coefficients of CO (g/km/v) with respect to different types of vehicles and speed.....	35
3.3 Emission coefficients of NO _x (g/km/v) with respect to different types of vehicles and speed.....	36
3.4 Emission coefficients of PM10 (g/km/v) with respect to different types of vehicles and speed.....	36
3.5 The correlation analysis between (MC+PLDGV) and (LDDT+HDDT+BUS) with NO _x	43
3.6 Result of t-Test (Two-Sample Assuming Unequal Variances).....	44
4.1 Weighted extraction of wind direction in each time periods using wind rose diagram	56
4.2 Observations of CO ambient concentrations at 21 links during time observed at 07:00-19:00, 19 th January -12 nd February 2012	58

LIST OF TABLES (Continued)

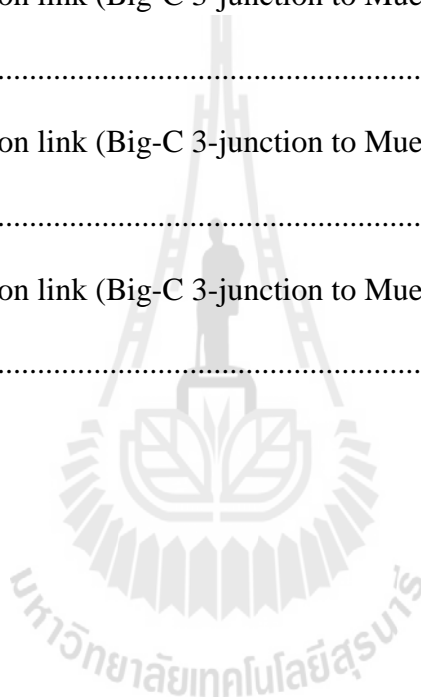
Table	Page
4.3 Estimation of PM10 ambient concentrations at 21 links	59
4.4 Estimation of NOx ambient concentrations at 21 links	59
4.5 Relationship between service area and Moran's I of each frequency of violence points	79
4.6 Influence of changing score weight pattern to related with co-ordinate, maximum spatial autocorrelation and total score of all objectives function ..	94
A.1 Traffic volume (V/H) of Mittrapap Rd. (Samyakpak to Jet-gas station).....	109
A.2 Traffic volume (V/H) of Mittrapap Rd. (Jet-gas station to Tesco lotus)	109
A.3 Traffic volume (V/H) of Mittrapap Rd. (Tesco lotus to The Mall).	109
A.4 Traffic volume (V/H) of Mittrapap Rd. (The Mall to 3-junction Big-C).	110
A.5 Traffic volume (V/H) of Mittrapap Rd. (3-junction Big-C to Pigasus).....	110
A.6 Traffic volume (V/H) of Highway 224. (3-junction Big-C to Sunararee wittaya school)	110
A.7 Traffic volume (V/H) of Suranarai Rd. (3-junction)	111
A.8 Traffic volume (V/H) of Suranarai Rd. (3-junction to Rajaphat Korat)	111
A.9 Traffic volume (V/H) of Highway 224 (Suranararee wittaya school to Huatalay junction).....	111
A.10 Traffic volume (V/H) of Mukkamontri Rd. (Sawairiang)	112
A.11 Traffic volume (V/H) of Soiking sawairiang	112

LIST OF TABLES (Continued)

Table	Page
A.12 Traffic volume (V/H) of Mukkamontri Rd. (St. Maries school)	112
A.13 Traffic volume (V/H) of Suebsiri Rd.....	113
A.14 Traffic volume (V/H) of Detudom Rd.....	113
A.15 Traffic volume (V/H) of Phoklang Rd.....	113
A.16 Traffic volume (V/H) of Chan Rd	114
A.17 Traffic volume (V/H) of Changpuek Rd.....	114
A.18 Traffic volume (V/H) of Chainarong Rd	114
A.19 Traffic volume (V/H) of Prachak Rd	115
A.20 Traffic volume (V/H) of Ratchadamnoen Rd	115
A.21 Traffic volume (V/H) of Chumphon Rd.....	115
B.1 A number of population at each points of interest.....	117
B.2 Descriptive statistic of number of population at each points of interest.....	118
E.1 NOx emission on link (Big-C 3-junction to Mueang school) of date 06/02/2012	126
E.2 NOx emission on link (Big-C 3-junction to Mueang school) of date 07/02/2012	126
E.3 NOx emission on link (Big-C 3-junction to Mueang school) of date 08/02/2012	127

LIST OF TABLES (Continued)

Table		Page
E.4	NOx emission on link (Big-C 3-junction to Mueang school) of date 09/02/2012	127
E.5	NOx emission on link (Big-C 3-junction to Mueang school) of date 10/02/2012	128
E.6	NOx emission on link (Big-C 3-junction to Mueang school) of date 11/02/2012	128
E.7	NOx emission on link (Big-C 3-junction to Mueang school) of date 12/02/2012	129



LIST OF FIGURES

Figure	Page
1.1 The study area within Nakhon Ratchasima municipality	5
1.2 Points of interest in the study area	6
1.3 Traffic volumes on road network in the study area at 07:00-08:00 am and 17:00-18:00 pm collected between 1-20 February 2007.....	8
1.4 Comparison locations of actual AQMS with other temporarily monitoring sites.....	9
2.1 (a) and (b) The effect of wind speed on air pollution dispersion and dilution.....	13
2.2 Coefficient distribution of pollution along the horizontal σ_y and vertical σ_z	18
2.3 Element series represented by series of equivalent finite line sources (FLS).....	19
2.4 Converting linguistic to fuzzy numbers	20
3.1 Steps of the research conceptual framework	34
3.2 Points of interest of people exposure impact in the study area.....	37
3.3 Process of pollutants concentration mapping	40
3.4 Pairs of CO, NO _x , and PM ₁₀ with type of vehicles, time periods and wind .	42
3.5 The analytical framework of pollution network and a cut-off service area....	50

LIST OF FIGURES (Continued)

Figure	Page
4.1	An example of wind rose diagram to average mean speed and direction of the 45 degree according to the clockwise from north of Nakhon Ratchasima municipality during 1 th January 2010 to 31 th May 2011 at 18:00-19:00 pm 55
4.2	Ambient concentrations observing points at 21 road junctions in the study area 58
4.3	Pollution concentrations were estimated at receptor points with varying wind directions in a range of 0-315 degree 61
4.4	Observed versus Predicted CO concentration (within 10 m buffer only)..... 63
4.5	Validation points of observed versus predicted CO concentration (within 10 m buffer only) 63
4.6	CO dispersion based on PLDGV vehicle type along 45 degree of receptor points at 18:00-19:00 pm 65
4.7	NO _x dispersion based on LDDT vehicle type along 45 degree of receptor points at 18:00-19:00 pm 66
4.8	PM ₁₀ dispersion based on HDDT vehicle type along 45 degree of receptor points at 18:00-19:00 pm 66
4.9	Average CO concentration map of results estimated from all vehicle types, time periods, and wind directions 69

LIST OF FIGURES (Continued)

Figure	Page
4.10 Average NO _x concentration map of results estimated from all vehicle types, time periods, and wind directions	69
4.11 Average PM ₁₀ concentration map of results estimated from all vehicle types, time periods, and wind directions	70
4.12 Pollution intensity map of the integrated normalized CO, NO _x , and PM ₁₀ concentrations (Z_1).....	70
4.13 Frequency of violence of emitted CO from all time periods and vehicle types.....	73
4.14 Frequency of violence of emitted NO _x from all time periods and vehicle types.....	73
4.15 Frequency of violence of emitted PM ₁₀ from all time periods and vehicle types.....	74
4.16 Combined frequency of violence of emitted CO, NO _x , and PM ₁₀ from all time periods and vehicle types (Z_2)	74
4.17 Pollution network map based on attribute of L_n	76
4.18 Comparison of service area based on varying search tolerances.....	78
4.19 Relationship between service area and Moran's I	78
4.20 Map showing service area (Z_3) of each cell of alternatives.....	80
4.21 People exposure impact map (Z_4).....	82

LIST OF FIGURES (Continued)

Figure	Page
4.22 Map of combined all objective function (Z_1 to Z_4).....	83
4.23 Result of optimal location of AQMS using multi-objective without constraint U_z	84
4.24 Result of optimal locations of AQMS using multi-objective function subject to all constraints	85
4.25 Location of AQMSs with varying weighted of objective functions as ($0.4Z_1, 0.2Z_2, 0.2Z_3$, and $0.2Z_4$).....	87
4.26 Location of AQMSs with varying weighted of objective functions as ($0.5Z_1, 0.167Z_2, 0.167Z_3$, and $0.167Z_4$).....	88
4.27 Location of AQMSs with varying weighted of objective functions as ($0.6Z_1, 0.133Z_2, 0.133Z_3$, and $0.133Z_4$).....	88
4.28 Location of AQMSs with varying weighted of objective functions as ($0.2Z_1, 0.4Z_2, 0.2Z_3$, and $0.2Z_4$).....	89
4.29 Location of AQMSs with varying weighted of objective functions as ($0.167Z_1, 0.5Z_2, 0.167Z_3$, and $0.167Z_4$).....	89
4.30 Location of AQMSs with varying weighted of objective functions as ($0.133Z_1, 0.6Z_2, 0.133Z_3$, and $0.133Z_4$).....	90
4.31 Location of AQMSs with varying weighted of objective functions as ($0.2Z_1, 0.2Z_2, 0.4Z_3$, and $0.2Z_4$).....	90

LIST OF FIGURES (Continued)

Figure	Page
4.32	Location of AQMSs with varying weighted of objective functions as $(0.167Z_1, 0.167Z_2, 0.5Z_3, \text{ and } 0.167Z_4)$ 91
4.33	Location of AQMSs with varying weighted of objective functions as $(0.133Z_1, 0.133Z_2, 0.6Z_3, \text{ and } 0.133Z_4)$ 91
4.34	Location of AQMSs with varying weighted of objective functions as $(0.2Z_1, 0.2Z_2, 0.2Z_3, \text{ and } 0.4Z_4)$ 92
4.35	Location of AQMSs with varying weighted of objective functions as $(0.167Z_1, 0.167Z_2, 0.167Z_3, \text{ and } 0.5Z_4)$ 92
4.36	Location of AQMSs with varying weighted of objective functions as $(0.133Z_1, 0.133Z_2, 0.133Z_3, \text{ and } 0.6Z_4)$ 95
4.37	Positioning of proposed AQMSs compared with existing AQMS 93
C.1	Measurement of ambient CO at Mittrapap Road (17:00-18:00)..... 120
C.2	Counting population at local market using (Counter instrument) 120
D.1	(Step 1) Job parameters..... 122
D.2	(Step 2) Run conditions 122
D.3	(Step 3) Link geometry 123
D.4	(Step 4) Link activity 123
D.5	(Step 5) Receptor positions..... 124
D.6	(Step 6) Result of CALINE4..... 124

LIST OF FIGURES (Continued)

Figure	Page
F.1 Wind rose diagram at 07:00-08:00..	131
F.2 Wind rose diagram at 09:00-10:00	131
F.3 Wind rose diagram at 12:00-13:00..	132
F.4 Wind rose diagram at 15:00-16:00..	132
F.5 Wind rose diagram at 18:00-13:00..	133
G.1 CO concentration (ppm) dispersion maps of PLDGV vehicle type during 07:00-08:00 am..	135
G.2 CO concentration (ppm) dispersion maps of PLDGV vehicle type during 09:00-10:00 am..	136
G.3 CO concentration (ppm) dispersion maps of PLDGV vehicle type during 12:00-13:00 pm..	137
G.4 CO concentration (ppm) dispersion maps of PLDGV vehicle type during 15:00-16:00 pm..	138
G.5 CO concentration (ppm) dispersion maps of PLDGV vehicle type during 18:00-19:00 pm..	139
G.6 CO concentration (ppm) dispersion maps of MC vehicle type during 07:00-08:00 am..	140
G.7 CO concentration (ppm) dispersion maps of MC vehicle type during 09:00-10:00 am..	141

LIST OF FIGURES (Continued)

Figure	Page
G.8 CO concentration (ppm) dispersion maps of MC vehicle type during 12:00-13:00 pm.....	142
G.9 CO concentration (ppm) dispersion maps of MC vehicle type during 15:00-16:00 pm.....	143
G.10 CO concentration (ppm) dispersion maps of MC vehicle type during 18:00-19:00 pm.....	144
G.11 CO concentration (ppm) dispersion maps of HDDT vehicle type during 07:00-08:00 am.....	145
G.12 CO concentration (ppm) dispersion maps of HDDT vehicle type during 12:00-13:00 pm.....	146
G.13 CO concentration (ppm) dispersion maps of HDDT vehicle type during 12:00-13:00 pm.....	147
G.14 CO concentration (ppm) dispersion maps of HDDT vehicle type during 15:00-16:00 pm.....	148
G.15 CO concentration (ppm) dispersion maps of HDDT vehicle type during 18:00-19:00 pm.....	149
G.16 CO concentration (ppm) dispersion maps of LDDT vehicle type during 07:00-08:00 am.....	150
G.17 CO concentration (ppm) dispersion maps of LDDT vehicle type during 09:00-10:00 am.....	151

LIST OF FIGURES (Continued)

Figure	Page
G.18 CO concentration (ppm) dispersion maps of LDDT vehicle type during 12:00-13:00 pm.....	152
G.19 CO concentration (ppm) dispersion maps of LDDT vehicle type during 15:00-16:00 pm.....	153
G.20 CO concentration (ppm) dispersion maps of LDDT vehicle type during 18:00-19:00 pm.....	154
H.1 NO _x concentration (ppb) dispersion maps of LDDT vehicle type during 07:00-08:00 am.....	156
H.2 NO _x concentration (ppb) dispersion maps of LDDT vehicle type during 09:00-10:00 am.....	157
H.3 NO _x concentration (ppb) dispersion maps of LDDT vehicle type during 12:00-13:00 pm.....	158
H.4 NO _x concentration (ppb) dispersion maps of LDDT vehicle type during 15:00-16:00 pm.....	159
H.5 NO _x concentration (ppb) dispersion maps of LDDT vehicle type during 18:00-19:00 pm.....	160
H.6 NO _x concentration (ppb) dispersion maps of HDDT vehicle type during 07:00-08:00 am.....	161
H.7 NO _x concentration (ppb) dispersion maps of HDDT vehicle type during 09:00-10:00 am.....	162

LIST OF FIGURES (Continued)

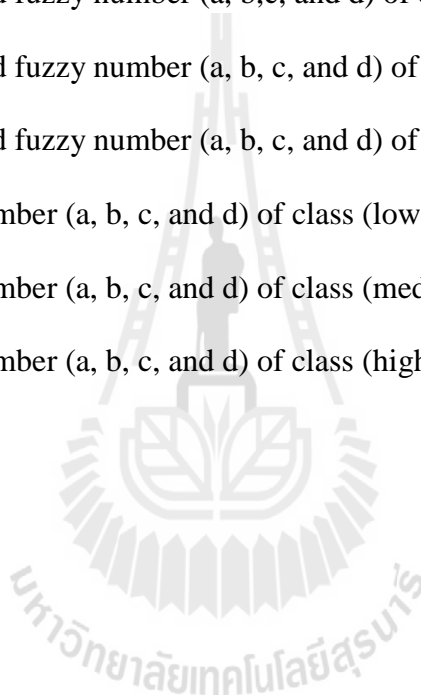
Figure	Page
H.8	NO _x concentration (ppb) dispersion maps of HDDT vehicle type during 12:00-13:00 pm..... 163
H.9	NO _x concentration (ppb) dispersion maps of HDDT vehicle type during 15:00-16:00 pm..... 164
H.10	NO _x concentration (ppb) dispersion maps of HDDT vehicle type during 18:00-19:00 pm..... 165
I.1	PM ₁₀ concentration ($\mu\text{g}/\text{m}^3$) dispersion maps of HDDT vehicle type during 07:00-08:00 am..... 167
I.2	PM ₁₀ concentration ($\mu\text{g}/\text{m}^3$) dispersion maps of HDDT vehicle type during 09:00-10:00 am..... 168
I.3	PM ₁₀ concentration ($\mu\text{g}/\text{m}^3$) dispersion maps of HDDT vehicle type during 12:00-13:00 pm..... 169
I.4	PM ₁₀ concentration ($\mu\text{g}/\text{m}^3$) dispersion maps of HDDT vehicle type during 15:00-16:00 pm..... 170
I.5	PM ₁₀ concentration ($\mu\text{g}/\text{m}^3$) dispersion maps of HDDT vehicle type during 18:00-19:00 pm..... 171
I.6	PM ₁₀ concentration ($\mu\text{g}/\text{m}^3$) dispersion maps of LDDT vehicle type during 07:00-08:00 am..... 172
I.7	PM ₁₀ concentration ($\mu\text{g}/\text{m}^3$) dispersion maps of LDDT vehicle type during 09:00-10:00 am..... 173

LIST OF FIGURES (Continued)

Figure	Page
I.8	PM10 concentration ($\mu\text{g}/\text{m}^3$) dispersion maps of LDDT vehicle type during 12:00-13:00 pm..... 174
I.9	PM10 concentration ($\mu\text{g}/\text{m}^3$) dispersion maps of LDDT vehicle type during 15:00-16:00 pm.....175
I.10	PM10 concentration ($\mu\text{g}/\text{m}^3$) dispersion maps of LDDT vehicle type during 18:00-19:00 am..... 176
J.1	CO frequency of violence map of HDDT vehicle type at 07:00-08:00, 09:00-10:00, 12:00-13:00, 15:00-16:00, and 18:00-19:00.....178
J.2	CO frequency of violence map of LDDT vehicle type at 07:00-08:00, 09:00-10:00, 12:00-13:00, 15:00-16:00, and 18:00-19:00.....179
J.3	CO frequency of violence map of MC vehicle type at 07:00-08:00, 09:00-10:00, 12:00-13:00, 15:00-16:00, and 18:00-19:00.....180
J.4	CO frequency of violence map of PLDGV vehicle type at 07:00-08:00, 09:00-10:00, 12:00-13:00, 15:00-16:00, and 18:00-19:00.....181
J.5	NO _x frequency of violence map of HDDT vehicle type at 07:00-08:00, 09:00-10:00, 12:00-13:00, 15:00-16:00, and 18:00-19:00.....182
J.6	NO _x frequency of violence map of LDDT vehicle type at 07:00-08:00, 09:00-10:00, 12:00-13:00, 15:00-16:00, and 18:00-19:00.....183
J.7	PM10 frequency of violence map of HDDT vehicle type at 07:00-08:00, 09:00-10:00, 12:00-13:00, 15:00-16:00, and 18:00-19:00.....184

LIST OF FIGURES (Continued)

Figure		Page
J.8	PM10 frequency of violence map of LDDT vehicle type at 07:00-08:00, 09:00-10:00, 12:00-13:00, 15:00-16:00, and 18:00-19:00.....	185
K.1	The normalized fuzzy number (a, b,c, and d) of calss (low).....	187
K.2	The normalized fuzzy number (a, b, c, and d) of class (medium).	187
K.3	The normalized fuzzy number (a, b, c, and d) of class (high)	188
K.4	Total fuzzy number (a, b, c, and d) of class (low)	188
K.5	Total fuzzy number (a, b, c, and d) of class (medium)	189
K.6	Total fuzzy number (a, b, c, and d) of class (high)	189



LIST OF ABBREVIATIONS

AQMS	=	Air Quality Monitoring Station
BUS	=	Bus
C	=	n th receptor concentration
CALINE4	=	California line source dispersion model version 4
Caltrans	=	California Department of Transportation
FLS	=	Finite line source
g/m ³	=	Gram per cubic meter
g/mi/s	=	Gram per mile per section
GIS	=	Geographic Information System
H	=	Source height
HDDT	=	Heavy duty diesel truck
IDW	=	Inverse distance weighted
km	=	kilometer
LDDT	=	Light duty diesel truck
LP	=	Linear programming
km	=	Kilometer
m	=	Meter
m/s	=	Meter per second

LIST OF ABBREVIATIONS (Continued)

MADA	=	Multi-Attribute Decision Analysis
MC2	=	2-stroke motorcycle
MC4	=	4-stroke motorcycle
MCDA	=	Multi-Criteria Decision Analysis
MODA	=	Multi-Objective Decision Analysis
NA	=	Network analysis
PCD	=	Pollution Control Department
PLDGV	=	Private light duty gasoline vehicle
PPB	=	Parts per billion
PPM	=	Parts per million
SA	=	Service area
SOI	=	Sphere of influence
sq. km	=	Square Kilometer
TMD	=	Thai Meteorological Department
US EPA	=	United States Environmental Protection Agency
V/H	=	Vehicle per hour
$\mu\text{g}/\text{m}^3$	=	Microgram per cubic meter

CHAPTER I

INTRODUCTION

1.1 Background problem

Protection of human health and the environment from pollutants effects is the primary goal of all air pollution control programs. In order to evaluate the direct and indirect effects caused by emissions from air pollution sources, the Air Quality Monitoring Station (AQMS) is an essential tool to monitor and control the atmospheric pollution. The scale of AQMS should be in the neighbourhood scale. As reported by the United States Environmental Protection Agency - USEPA (2006) neighbourhood scale defines concentrations within some extended area of the city that has relatively uniform land use with dimensions in the 0.5 to 4.0 kilometres range. Determination of how many monitoring stations to have and on which site to build them is the most important factor to be taken into account when designing the AQMS network. The AQMS design objective is usually to provide maximum information about the air quality in a given area with minimum number of monitoring stations. It is required to determine the minimum number of monitoring stations due to budget constraints. Providing the minimum number of stations minimizes the installation, maintenance, and management costs.

The only one existing AQMS in the center of municipality of Nakhon Ratchasima province was installed by the Pollution Control Department (PCD). The

data from the PCD station were not enough to represent the air quality of the municipality as a whole. More stations should be additionally installed in an area with high concentration of air pollutants and near major sources. Conversely, the background station should be installed in area with low pollution and no major source. Therefore, the current AQMSs or air quality monitoring network (AQMN) of the area is necessary to be reviewed and restructured.

In most cases, AQMS is designed to measure the concerned pollutants such as particulate matter (PM), carbon monoxide (CO), sulfur dioxide (SO₂), ozone (O₃), nitrogen oxides (NO_x), and total hydrocarbons (Chang and Tseng, 1999). Most of the reported AQMS design methods were applied to a specific situation in which one or two specific objectives are considered. However, design of AQMS considering the multiple-criteria including multiple pollutants is complicated because air pollution phenomena are complex and dynamic in nature, depends on the meteorological and topographical conditions and involves not only irregularity of atmospheric movement but also uncertainty of human activities. As reported by Modak and Lohani (1985), when AQMSs are really set up at the proper locations, their data and information provided can be effectively served for several purposes, i.e. (1) planning and implementing air quality protection and air pollution control strategies; (2) ensuring that the air quality standard is achieved; (3) preventing or responding quickly to air quality deterioration; (4) evaluating the people exposure and other potential receptors; and (5) controlling emissions from significantly important sources. It is difficult to find an AQMS location that can cover all objectives stated above. Frequently, the methods used to position AQMS have achieved merely one or two of those objectives.

Recent studies, using the utility function in a multi-objective model has become one of the main focuses. Arbeloa (1993) developed a technique for designing an optimal air quality monitoring networks. The concept of potential of violation and the spatial correlation analysis technique were used to compare the information given by the potential sites. McElroy, Behar, Meyers, and Liu, (1986) applied air quality simulation models and population exposure information to produce representative combined patterns and then employed the concept of sphere of influence (SOI). However, different decision makers may have different objectives and scope of interest constrained by limited budget.

In this study, the objective of the study is to generate new objective and constraint functions approach for locating urban AQMS considering multi-criteria including multiple air pollutants in the system. The optimization is approached based on the linear programming (LP) gained from the spatial multi-objective decision analysis associated with a candidate station, which is estimated over the representative site of the potential station. The four objectives of determining a proper number of AQMSs and locating them on proper positions are of interest in the study. They include the capability to locate AQMSs on the positions of: (1) maximum pollution potential, (2) highest frequency of pollution violence, (3) mostly dense population subject to exposure impact, and (4) maximum service area. Almost all of the previous studies normally contained only the first two objectives. The last two objectives are specifically included in this study so that the better and more complete results can be achieved as expected.

The model deals with spatial multi-objectives with a budget and other constraints via geographic information system (GIS). GIS has been better known as a

tool to greatly assist this kind of analyses, for examples, service area of AQMS and spatial autocorrelation. A sensitivity analysis on optimum locations using value function of the spatial multi-objective decision analysis (SMODA) through weight variation is also performed.

1.2 Study area

1.2.1 Study area selection

The study area is the municipality of Nakhon Ratchasima province, Thailand, commonly referred to as Korat with area of 37.2 km² and population density of 7,496 persons/km² (กรมการปกครอง, 2552). A map of study area is displayed in Figure 1.1 and points of interest showed in Figure 1.2.

Nakhon Ratchasima has been long known as the large province and big gateway to the northeastern part of Thailand. Increasing of traffic activities in Nakhon Ratchasima municipality has led to an increase in the consumption of fossil fuels and subsequent air pollution. This causes air quality and human health deterioration in this municipality. Air pollutants can cause a variety of health problems such as breathing difficulty, lung damage, bronchitis, cancer, and nervous system damage. Air quality is necessary to be monitored from the AQMS installed in the proper position in order to monitor pollution to levels which minimize harmful effects on human health and the environment.

1.2.2 Points of interest

Points of interest for air pollution impact of the study area include hotel, hospital, government office, education, local markets and commercial centers. They can be evaluated in terms of people exposure opportunity. The municipality area with points of interests or people exposure targets and its road network is illustrated in Figure 1.2.

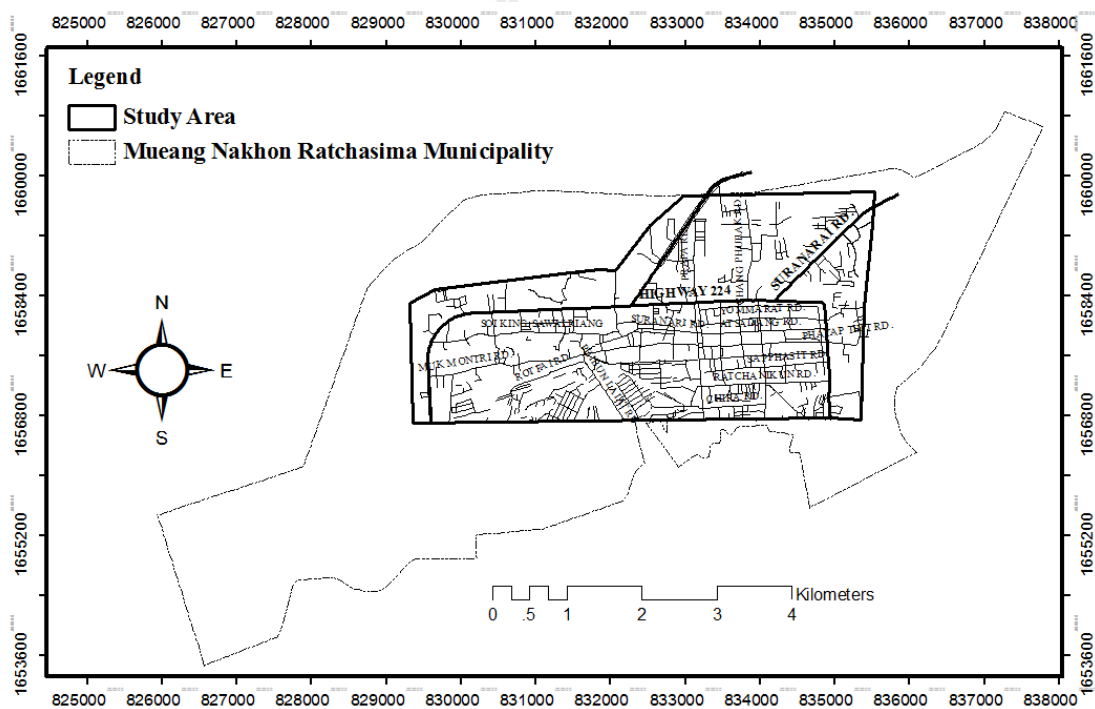
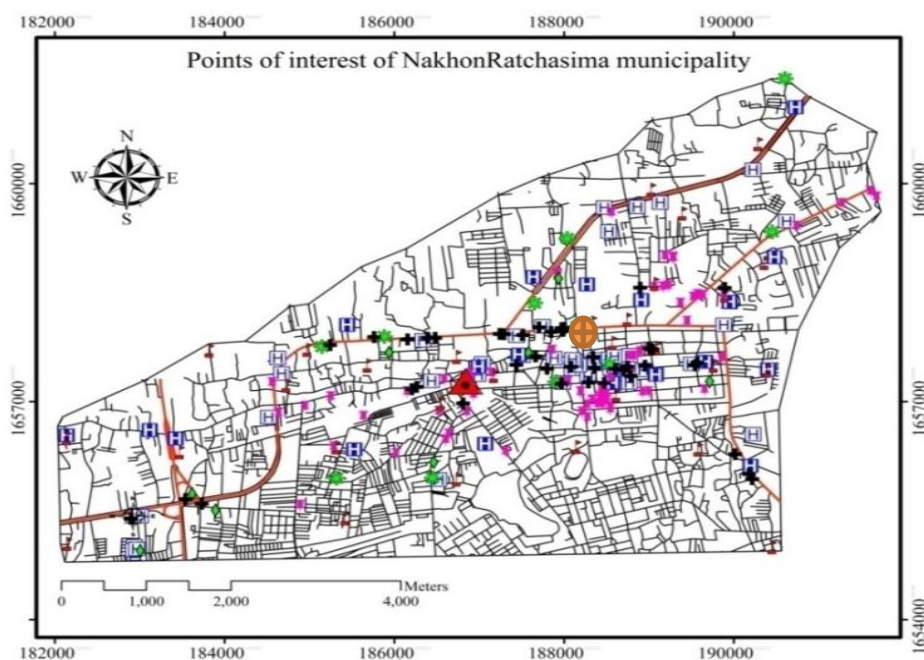


Figure 1.1 The study area within Nakhon Ratchasima municipality.



Legend

- ▲ Old existing AQMS (2002-2008) ● new station (2010-present)
- ✚ Bank
- ✱ Commercial_Center
- 🏫 Education
- ◆ Local market
- 🏛️ Government office
- 🏥 Hospital
- 🏨 Hotel

Figure 1.2 Points of interest in the study area.

1.2.3 Traffic data of the study area

The traffic volume data (Vehicle per Hour, V/H) of major and minor roads were derived from records of traffic data at 34 main intersections, collected by the Office of Transport and Traffic Policy and Planning (สำนักงานนโยบายและแผนการขนส่งและจราจร, 2550). Nine categories of the vehicles are private light duty gasoline

vehicles (PLDGV), business light duty gasoline vehicles (BLDGV), light duty gasoline trucks (LDGT), light duty diesel trucks (LDDT), heavy duty diesel trucks (HDDT), heavy duty gasoline vehicles (HDGV), bus (BUS), 2-stroke motorcycles (MC2), and 4-stroke motorcycles (MC4). The pollutants being investigated were CO, NO_x and PM₁₀. All road segments were processed as line sources and the vehicle fleet of the local city roads was classified in accordance with Figure 1.2. Table 1.1 and Figure 1.3 show locations and variation of PM₁₀ concentration between actual AQMS with other temporarily monitoring sites. However, since the traffic volume data of Highway No. 2 and 224 did not contain so many categories of vehicles, its vehicle fleet was classified as only PLDGV, LDDT, HDDT and MC.

1.2.4 Pollutants from mobile sources

The increase of vehicles in Nakhon Ratchasima is not proportionate to the increase of roads and has caused traffic congestion and delay in transportation. Traffic speed surveyed in 2007 (สำนักงานนโยบายและแผนการขนส่งและจราจร, 2550) showed that during the rush hour, average speed was 20 km/hour in the inner area, whereas it was 30 km/hour in the outer area. These large numbers of vehicles and traffic congestion have put severe impact on air quality of Nakhon Ratchasima. The motor vehicle engine emits many types of pollutants including (NO_x), volatile organic compounds (VOCs), carbon monoxide (CO), carbon dioxide (CO₂), particulates, sulphur dioxide (SO₂) and lead. From the annual report of (สำนักงานนโยบายและแผนการขนส่งและจราจร, 2550) shows emissions from different mobile sources which

are the major emitters of NO_x (80%), CO (75%), and PM₁₀ (54%) in Nakhon Ratchasima municipality.

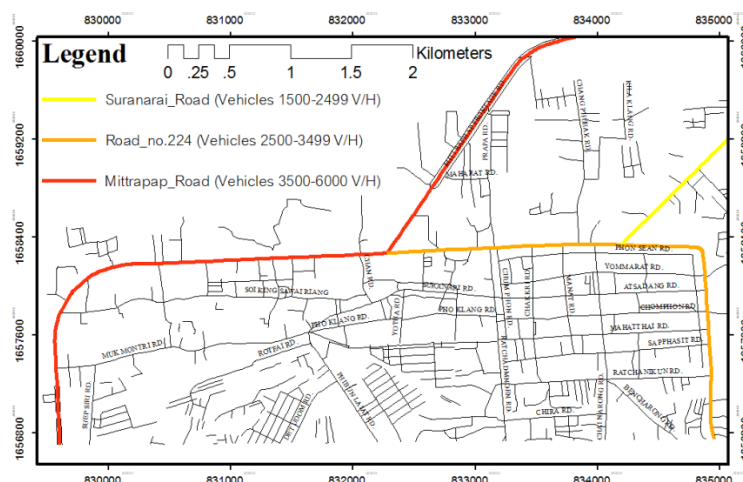


Figure 1.3 Traffic volumes on road network in the study area at 07:00-08:00 am and 17:00-18:00 pm collected between 1-20 February 2007. (สำนักงานนโยบายและแผนการขนส่งและจราจร (สนข), 2550).

Table 1.1 Concentration of PM₁₀ ($\mu\text{g}/\text{m}^3$) on exposure study different road network of Nakhon Ratchasima municipality in August 2004 (กุลธิดา ตระสินธุ์, 2547).

Station	Dates	PM10	PM10	PM10	PM10	PM10
		($\mu\text{g}/\text{m}^3$)	($\mu\text{g}/\text{m}^3$)	($\mu\text{g}/\text{m}^3$)	($\mu\text{g}/\text{m}^3$)	($\mu\text{g}/\text{m}^3$)
	28-29-30	4-5-6	13-14-15	18-19-20	25-26-27	
	Jul 2004	Aug 2004	Aug 2004	Aug 2004	Aug 2004	
Existing AQMS	43-47-35	19-27-33	36-28-44	36-34-32	31-38-33	
Anuban	23-35-37	-	-	-	-	
Samyak Mitrapap	-	58-63-117	-	-	-	
Pratu Chainaronk	-	-	28-34-44	-	-	
Hayak Huarotfai	-	-	-	90-49-42	-	
Yamo	-	-	-	-	57-72-45	

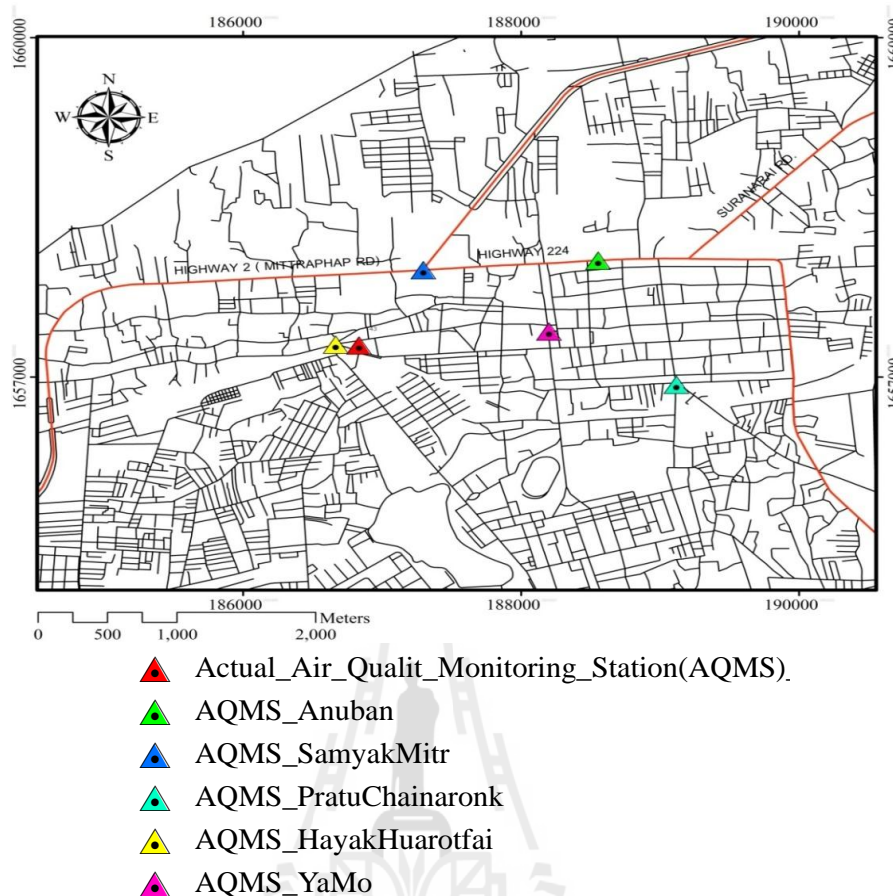


Figure 1.4 Comparison locations of actual AQMS with other temporarily monitoring sites (กุลธิดา ตระสินธุ์, 2547).

1.3 Research objectives

The ultimate goal of the research is to raise the quality of life with respect to efficient protection and control of air pollution which is ever-increasing in all fast-growing and densely-populated towns. The proper AQMSs in terms of number and position can provide effective data and information advantage for protection and control planning. To fulfill this goal, the research objectives are set up as follows:

- (1) to generate the representative spatial distributions of air pollution (CO, NO_x, and PM₁₀) in the study area using CALINE4 Gaussian model, and

(2) to determine proper positions of AQMSs using the spatial multi-objective decision analyses.

1.4 Scope of the study

The scope of the study covers:

(1) traffic and ambient pollution data observed on March 2007 and 2010 were used for analysis. Additional field observation of ambient pollution could be partly operated,

(2) meteorological data during dry seasons of 2010 were used for analysis,

(3) traffic data, meteorological data, and ambient pollution concentrations were analyzed mainly during daytime of 5 periods i.e. 07:00-08:00, 09:00-10:00, 12:00-13:00, 15:00-16:00, and 18:00-19:00,

(4) the CALINE4 Gaussian model performed under the Worst Case Wind Angle run type,

(5) the proper grid size is 50mx50m and the numbers of decision variables are not over 8000 due to the capacity of hardware and software, and

(6) extents of constraints were determined by the cut-off value.

1.5 Assumptions of the study

(1) The wind direction coincides with the positive direction of the axis X based on different and most of wind speeds and wind directions on all seasons. The direction the wind is blowing from, measured clockwise in degrees from the north (0 - north, 90 = east, 180 = south, 270 = west). In the study, Worst case wind angle is selected, CALINE4 does not use this input.

(2) Due to the limitation of data availability, traffic and ambient pollution data of the year 2010 and 2012 can be used together and are considered to express the same behavior during dry seasons.

(3) Pollution estimation was operated during daytime due to its peak. Therefore, the point of interests which are highly populated and obviously active during daytime rather than general residential area were brought to count on people exposure impact. These are schools, markets, hospitals, commercial centers, government and private offices, etc.

(4) The dispersion model based on the Gaussian diffusion equation employs a homogeneous mixing zone wind flow and steady state meteorological conditions.

(5) The speed of vehicles are assumed that all vehicles moved at the speed up to 20 km/h.

(6) Network analysis was relied on the field length impedance of air concentration network data set.

(7) Sphere of influence (SOI) was used to determine the service area under the GIS function.

(8) Linear programming (LP) performed through the simplex algorithm was used for multi-objective analysis.

CHAPTER II

LITERATURE REVIEW AND THE RESEARCH APPROACH

The main objective of this chapter is to explain the data composition, theory of fuzzy set membership, air dispersion modeling and optimization modeling literature as well as to review relevant literatures to find where this study fits into debates around the subject. This chapter contains four sections. The first section described the study of meteorological conditions of air dispersion model. The second section elaborated the theory of CALINE4 model, fuzzy set membership and optimization modeling. The third section discussed about the literatures showing the linkages between air dispersion modeling, spatial distribution with GIS and spatial multi-objective modeling. The final section deal about literatures showing different factors affecting spatial multi-objective modeling.

2.1 Meteorological conditions

Air pollution concentrations are influenced by prevailing weather conditions and vary considerably with time. These variations are largely determined by meteorological factors. The extent to which pollutants are dispersed and diluted is dependent on wind speed, turbulence, mixing depth, topography, etc. Air pollution can be dispersed, diffused and diluted by a number of factors. It is these factors that

must be considered in CALINE4 dispersion modeling study. The principal factors of concern include:

- Meteorological conditions

(a) Wind speed and direction

Wind speed is determined by atmospheric pressure gradients. Low wind speeds tend to result in the accumulation of pollutants. Pollution concentrations are inevitably inversely proportional to the wind speed (Figure 2.1a). Table 2.1 lists typical terms given to describe wind speed (Parker, 1978).

Wind speed also varies with height over the lowest few hundred meters of the earth's atmosphere due to the frictional effect of the earth's surface (Figure 2.1b). The variation is greatest over rough surfaces (e.g. cities), effecting the reduction of wind speed up to 40%. Over smooth surfaces (e.g. sea) the effect is less and the reduction may only be 20% (Parker, 1978).

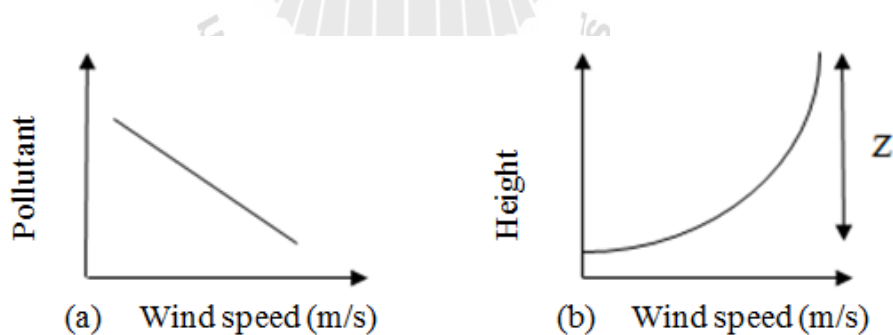


Figure 2.1 (a) and (b) The effect of wind speed on air pollution dispersion and dilution (Parker, 1978).

The frictional drag retards motion close to the ground and therefore gives rise to a sharp decrease of mean horizontal wind speed as the surface is approached (Oke, 1978).

(b) Atmospheric stability

Turbulence in the atmosphere is created by two principal factors, the minor of which is surface roughness. This occurs when blowing over a surface creates mechanical mixing in the atmosphere. Greater surface roughness, due to buildings and topography, generally acts to increase turbulence, and therefore encourages dispersion.

Atmospheric stability used in air quality dispersion is often divided into 7 categories from A (very unstable), through D (neutral) to G (very stable). In addition, hybrid categories A/B, B/C, and C/D which are intermediate between A and B, B and C, and C and D, are also defined. The atmospheric stability classes are generally referred to as the Pasquill -Gifford categories. Category A is often associated with a more rapid dispersion of pollution and category G with temperature inversions and possible accumulation of pollution. The stability categories are estimated from the total cloud cover, wind speed and time of day. During daytime an estimate is made of the incident solar radiation and this is combined with wind speed to estimate the stability category (Parker, 1978). At nighttime, stability is a simple function of cloud cover and wind speed as shown in Table 2.2.

2.2 Theory of Line Source Dispersion model

CALINE4 is the last in a series of line source air quality models developed by the California Department of Transportation (Caltrans). It is based on the Gaussian

diffusion equation and employs a mixing zone concept to characterize pollutant dispersion over the roadway.

The purpose of the model is to assess air quality impacts near transportation facilities. Given source strength, meteorology and site geometry, CALINE4 can predict pollutant concentrations for receptors located within 500 meters of the roadway. In addition to predicting concentrations of relatively inert pollutants such as CO, the model can predict NO_x and PM₁₀ (Caltrans, 1989).

Table 2.1 Beaufort scale of wind velocities (Parker, 1978).

Force	Beaufort scale description	Velocity (mph)	Velocity (km/h)
0	Calm	0	0
1	Light	1-3	1.6-5
2	Light	4-7	6-11
3	Light	8-12	13-19
4	Moderate	13-18	21-29
5	Fresh	19-24	30-38
6	Strong	25-31	40-50
7	Strong	32-38	51-61
8	Fresh gale	39-46	62-74
9	Strong gale	47-54	75-86
10	Whole gale	55-63	88-101
11	Storm gale	64-72	102-115
12	Hurricane	73-82	117-147

CALINE4 is a computer-based line source Gaussian dispersion model that uses solutions to the Gaussian dispersion in Equation (2.1). It was developed to calculate CO concentrations, but it can be used to predict the concentrations of various other pollutants (NO_x, inert gases and particulates) in a variety of road networks (Marmur and Mamane, 2003). The input parameters required for the model involve roadway geometry, meteorological parameters and measured traffic flow. The emission factors used for computation are considered in grams per mile for each vehicle (Gramotnev, Brown, Ristovski, Hitchins, and Morawska, 2003).

Table 2.2 Pasquill stability categories (Pasquill and Smith, 1982).

Wind speed (m/s)	Daytime incoming solar radiation				Within 1 hr of sunrise or sunset	Night-time cloud amount (oktas)		
	Strong >59	Moderate 30-59	Slight <29	Overcast		0-3	4-7	8
<2	A	A-B	B	C	D	F	F	D
2-3	A-B	B	C	C	D	F	E	D
3-5	B	B-C	D	D	D	D	D	D
5-6	C	C-D	D	D	D	D	D	D
>6	C	D	D	D	D	D	D	D

Central to the CALINE4 model is the concept of a “mixing zone” that exists above the roadway where the intense mechanical turbulence, results in enhanced mixing of pollutants (Held, Chang, and, Niemeier, 2003). The primary role of the

mixing zone is to establish initial Gaussian dispersion parameters at a reference distance near the edge of the roadway.

The dispersion concentration at the downwind receptors can be expressed by Gaussian formulation. Each element is modeled as an “equivalent” finite line source (FLS) positioned normal to the wind direction and centered at the element mid-point. The receptor concentration attributable to an infinitesimal FLS segment, dy , can be calculated as (Caltrans, 1989):

$$dC = \frac{qdy}{2\pi u \sigma_y \sigma_z} \left[\exp\left(\frac{-y^2}{2\sigma_y^2}\right) \right] \times \left\{ \exp\left[\frac{-(z-H)^2}{2\sigma_z^2}\right] + \exp\left[\frac{-(z+H)^2}{2\sigma_z^2}\right] \right\} \quad (2.1)$$

where C is n th receptor concentration (g/m^3), q is the linear source strength ($\text{g}/\text{kg}/\text{link}$), u is wind speed (m/s), H is source height (m), and σ_y, σ_z is horizontal and vertical dispersion parameters.

The integral of the whole FLS becomes (Caltrans, 1989):

$$C = \frac{q}{\sqrt{2\pi u \sigma_z}} \left\{ \exp\left[\frac{-(z-H)^2}{2\sigma_z^2}\right] + \exp\left[\frac{-(z+H)^2}{2\sigma_z^2}\right] \right\} \quad (2.2)$$

From Equation (2.1), to calculate the concentration of pollutants must know the C, q, u, H, σ_y and σ_z where the σ_y and σ_z are the dependent position in the spread of pollution and atmospheric stability condition derived from the experiment. There were many experiments but one that has been accepted and used most is an experiment of Turner (Turner, 1970).

The results can show in form to present the relationship of $\log \sigma_y$, and σ_z to the log distance. The graph can be used directly to calculate the σ_y and σ_z values when the distance is known. In addition, Turner (1970) has created a relationship of σ_z to x

which is the distance, α and β is constant, and m is stability level. It can be calculated as:

$$\sigma_z(m) = \alpha x^\beta \quad (2.3)$$

where x is distance along leeward axis (km), the stability levels shown in Table 2.3.

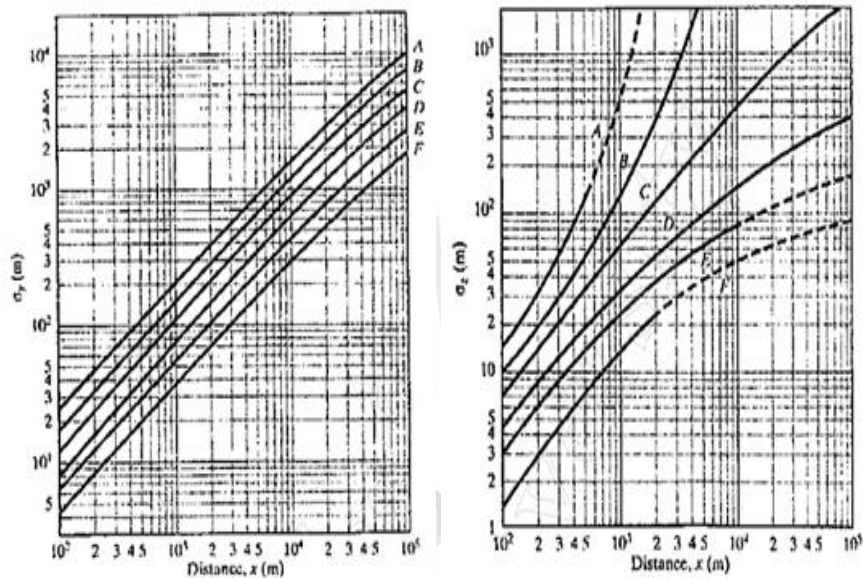


Figure 2.2 Coefficient distribution of pollution along the horizontal σ_y and vertical σ_z (Turner, 1970).

Table 2.3 The coefficient of Pasquill-Gifford (σ_y) and (σ_z) of urban area (Turner, 1970).

Stability	σ_y (m)	σ_z (m)
A-B	$0.32x(1+0.0004x)^{-1/2}$	$0.24x(1+0.0001x)^{-1/2}$
C	$0.22x(1+0.0004x)^{-1/2}$	$0.20x$
D	$0.16x(1+0.0004x)^{-1/2}$	$0.14x(1+0.0003x)^{-1/2}$
E-F	$0.11x(1+0.0004x)^{-1/2}$	$0.08x(1+0.0015x)^{-1/2}$

CALINE4 computes receptor concentration as a series of incremental contributions from each element FLS. The source strength for each segment needs to be modified by a weighting factor, then the emission contribution from a given road segment to the receptor can be calculated.

CALINE4 divides individual road segments into a series of elements from which incremental concentrations are computed and then summed to form a total concentration estimate for a particular receptor. Each element is modeled as an equivalent FLS positioned normal to the wind direction and centered at the element midpoint, and the dispersion concentration at the downwind receptors can be expressed by Gaussian formulation (Caltrans, 1989) as shown in Figure 2.3.

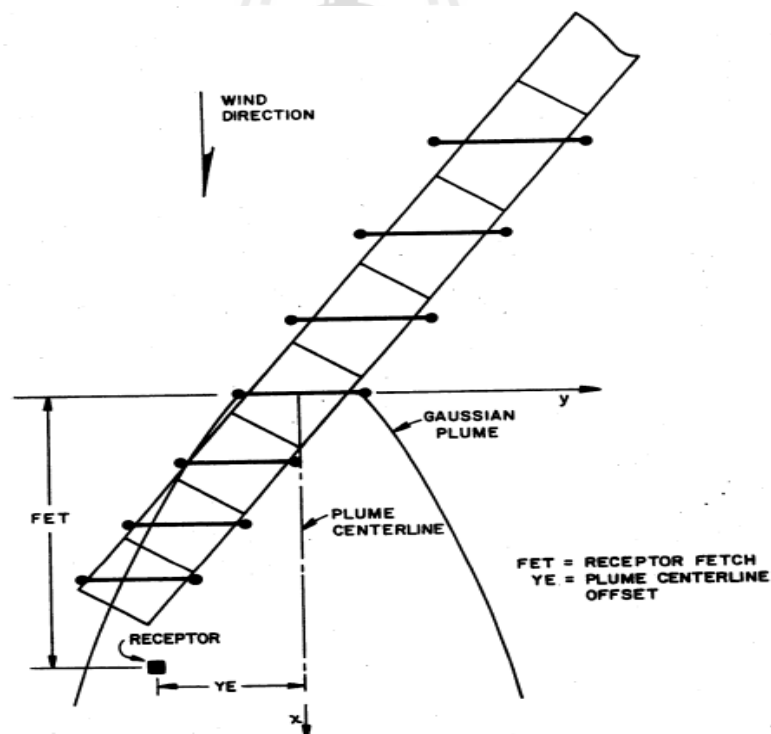


Figure 2.3 Element series represented by series of equivalent finite line sources (FLS) (Caltrans, 1989).

2.3 Fuzzy set membership

The concept of a fuzzy number provides us with the basis for defining linguistic of fuzzy variables (Klir and Yuan, 1995). Specifically, the fuzzy numbers are states of linguistic variable. The states are represented by linguistic concepts such as “very short,” “short,” “medium,” “long,” “very long,” “very steep,” “steep,” “low,” “medium,” “high” and so on. These concepts are defined in terms of a basic variable, the values of which are real numbers within a specific range. A base variable is a variable in the conventional sense. The fuzzy numbers mostly used often include triangular type (Figure 2.4) as well as fuzzy numbers (Chen and Hwang, 1992).

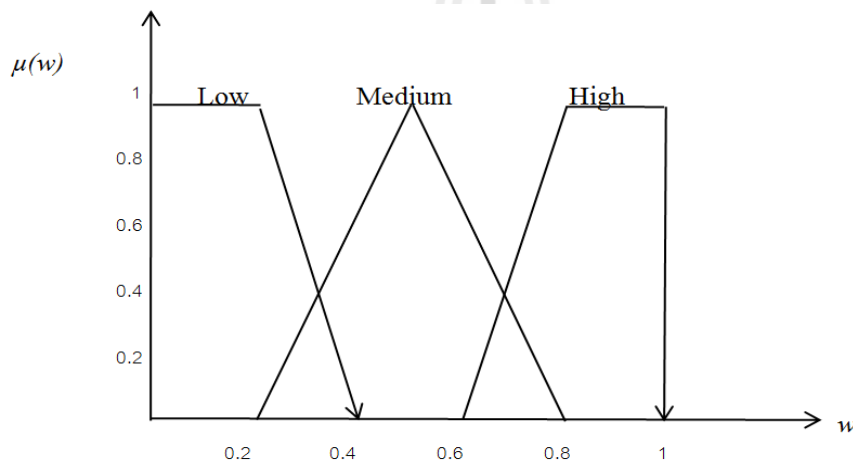


Figure 2.4 Converting linguistic to fuzzy numbers (Chen and Hwang, 1992).

2.4 Multi-Objective Decision Analysis (MODA)

Multi-criteria Decision Analysis (MCDA) is organized into two sections dealing with multi-attribute and multi-objective spatial decision problems. The aim of Multi-attribute Decision Analysis (MADA) is to choose the best or the most preferred alternative, and to rank the alternatives in descending order of preference. In MADA methods the attributes serve as both decision variables and decision criteria, whereas

in the Multi-objective Decision Analysis (MODA) approaches, a distinction is made between decision criteria (objective functions) and decision variables. MODA decision rules define the set of alternatives in terms of a decision model consisting of a set of objective functions and a set of constraints imposed on the decision variables (Malczewski, 1999). The processing of MODA in this research can be formulated into maximization linear programming (LP).

2.4.1 Linear programming (LP)

Bazaraa (1990) explained the general concept of the LP. It is concerned with the optimization (minimization or maximization) of a linear function while satisfying a set and/or inequality of constraints or restrictions. The concept explanation begins by formulating a particular type of linear programming problem. The following example case presents maximization as the optimization function. As previously described (Bazaraa, Jarvis, and Sherali, 1990) any general linear programming problem can be manipulated in canonical form.

Maximize

$$c_1x_1 + c_2x_2 + \dots + c_nx_n \quad (a)$$

Subject to

$$\left. \begin{aligned} a_{11}x_1 + a_{12}x_2 + \dots + a_{1n}x_n &\leq b_1 \\ a_{21}x_1 + a_{22}x_2 + \dots + a_{2n}x_n &\leq b_2 \\ &\vdots \\ a_{m1}x_1 + a_{m2}x_2 + \dots + a_{mn}x_n &\leq b_m \end{aligned} \right\} \quad (b)$$

$$\text{And} \quad x_1, x_2, \dots, x_n \geq 0 \quad (c)$$

In this linear programming, objective function and the others are listed as follows.

(a) Objective function: here $c_1x_1 + c_2x_2 + \dots + c_nx_n$ is the objective function (or criterion function) to be maximized and will be denoted by z . The coefficients c_1, c_2, \dots, c_n are the (known) cost coefficients and x_1, x_2, \dots, x_n are the decision variables (unknown) to be determined.

(b) Constraint set: the inequality $\sum_{j=1}^n a_{ij}x_j \leq b_i$ denotes the i th constraints. The coefficients a_{ij} for $i = 1, 2, \dots, m, j = 1, 2, \dots, n$ are called the technological coefficients. The technological coefficients form the constraint matrix A .

$$A = \begin{bmatrix} a_{11} & a_{12} & \dots & a_{1n} \\ a_{21} & a_{22} & \dots & a_{2n} \\ \cdot & \cdot & \dots & \cdot \\ \cdot & \cdot & \dots & \cdot \\ \cdot & \cdot & \dots & \cdot \\ a_{m1} & a_{m2} & \dots & a_{mn} \end{bmatrix}$$

The column vector whose i th component is b_i , which is referred to as the right-hand-side vector, represents the maximal requirement to be satisfied.

(c) Non-negativity constraints: the constraints $x_1, x_2, \dots, x_n \geq 0$ are the non-negativity constraints. A set of variables x_1, x_2, \dots, x_n satisfying all the constraints is called feasible points or a feasible vector.

(d) Linear programming can be a decision rule for multi-objective function. This research proposed the linear programming as the decision rule for four purposes which are to maximize pollution potential, people exposure impact, pollution violence and service area.

2.5 Previous researches

2.5.1 Application of line source air dispersion modeling

Saghoun Kamolwat studied the comparison of air pollutants concentrations, which are CO, NO, SO₂, and PM, at Thon Buri-Pak Tho and Suksawas highways, using mathematical model, HIWAY. The period of the study is 20 days with sample collection 3 hours a day. The result of this research was that only CO and PM could be observed. CO concentration at Thon Buri-Pak Tho highway was similar to the observed data but the model under estimated about 80 per cent at Suksawas highway (สงวน กมลวัฒน์, 2537).

Chumpol Sriprapakorn applied the air quality model, CALINE4, to predict PM10 concentration at Lat Phrao and Din Daeng road. The CO concentration calculated by CALINE4 was compared with the observed concentration from the PCD and the RMSE was 0.9733 ppm as for the PM10, the model result was calculated by applying the proportion of CO and PM10 molecular weight. The RMSE from this model was between 0.33 and 1.30 ppm while the best RMSE was about 0.94 ppm. This explains that the CALINE4 can predict CO and PM10 concentration and can evaluate the dispersion of PM10 from source to the closer areas at lee wind side (ชุมพล ศรีประภากร, 2544).

Sivapan Choo-in developed the model to predict CO and NO₂ concentration in tunnel road by using Microsoft Visual Basic. The study area was under BTS station at Phaya Thai and Sala Daeng. The wind speed in tunnel, traffic volume and types of vehicles (private car, motorcycle, light truck, and heavy truck), pollutants concentration in and out tunnel, and structure of tunnel were collected. This

information was used to develop the model based on the principle of box model. The results demonstrated that the developed model can estimate the concentration of CO and NO₂ at Sala Daeng station with R² is 0.98 and 0.846, respectively. The pollutant concentrations inside was higher than outside the tunnel road. However, these concentrations were lower than the air quality standard (ศิวพันธุ์ ชูอินทร์, 2544).

Dusadee Mougya and Sawitree Kudeesuk studied CO concentration at the road beside Suan Sunandha Rajabhat University compared with the result from CALINE4 and HIWAY2 model by using the Paired t-test. The results showed that CALINE4 was the most effective model in prediction of CO concentration from non-rush hour traffics (คุษฎี ม่วงชา และสาวิตรี กุฎีสุข, 2545)

Dabberdt, Hoydysh, Schorling, Yang, and Holynskyj (1995) studied about ambient concentrations at urban intersections using Gaussian dispersion models (HIWAY and CALINE4). These Gaussian modeling experiments served to quantify some of the complex aspects of the variability of locally-generated pollutant concentrations at and near urban intersections where there was a significant influence of buildings on dispersion. The application of the two mathematical models illustrated the challenges of estimating concentrations in complex urban environments such as intersections where concentrations are observed to be high and highly variable.

Gramotnev, Brown, Ristovski, Hitchins, and Morawska (2003) applied CALINE4 to measure concentration of CO near a busy road for the analysis of aerosols of fine and ultra-fine particles, generated by vehicles on the road. This method was based on measurements of the average particle number concentration at just one point near the road. The results showed that the dependencies of the

experimental and the predicted concentrations on distance from the road clearly confirms the applicability of the Caline4 package for the analysis of propagation of fine particle aerosols from a busy road.

Levitin, HarKonen, Kukkonen, and Nikmo (2005) studied on evaluation of the CALINE4 and CAR-FMI models against measurements near a major road. The concentrations of NO_x, NO₂, and O₃ were measured simultaneously at three locations and at three heights (3.5, 6, and 10 m) on both sides of the road. Traffic densities and relevant meteorological parameters were also measured on-site. The results showed that the performance of both models was better at a distance of 34 m, compared with that at a distance of 17 m.

Holmes and Morawska (2006) provided the review of dispersion modeling packages with reference to the dispersion of particles in the atmosphere. The models reviewed included: Box models, Gaussian models, Lagrangian/Eulerian models, and CFD models. The models fit to particle dispersion modeling depend heavily on the nature of the concentration desired.

Kenty et al. (2007) applied Caline4 to measure concentration of NO_x and NO₂ near Gandy Boulevard in Tampa, FL (USA) during May 2002. A comparison of measured and calculated NO₂ concentrations indicated that for ambient O₃ concentrations less than 40 ppb the model under-predicts the chemical transformation of NO.

Ganguly, Broderick, and O'Donoghue (2009) studied on assessment of GFLSM and CALINE4 for vehicular pollution prediction in Ireland. The concentrations predicted by these models were compared with background-corrected ambient concentrations measured at three different distances from a motorway and the

performance of model assessed in the context of integrated transport-environment modeling for regulatory purposes. The result showed that the performance of GFLSM was similar to that of CALINE4 at a receptor distance of 120 m. This indicated the agreement between the measured and modeled long-term average concentrations over the three different receptor distances of 25, 120, and 240 m.

2.5.2 Application of GIS to analyse urban traffic air pollution

Atit Tippichai applied GIS to simulating air pollution from urban road traffic. This paper described the application development of such tools for analyzing air pollution from road traffic in urban areas both from abroad and in Thailand. It was concluded that the application of GIS and mathematical air pollution models can help traffic and transport planners to evaluate the proposed projects/plans efficiency (อาทิตย์ ทิพย์พิชัย, 2548).

Moragues and Alcaide (1996) used GIS to assess the effect of traffic pollution. In the study, GIS provided a suitable instrument for assessing and locating traffic effects before and after the new infrastructure enters service. The pollution map was cross-referenced with the standard maps in order to locate and quantify the population affected by the different pollution levels including to identify the wildlife and historic and/or archaeological features at risk. The utilization of GIS methodology allowed the environmental changes to be automatically located with the use of a personal computer.

Gualtieri and Tartaglia (1998) predicted urban traffic air pollution with a GIS framework. This research presented a comprehensive model for the evaluation of air pollution caused by road traffic in urban areas, depending on site geometric and

morphological conditions. The model was integrated in a GIS that allows the use of spatial co-ordinates to describe the structure of urban areas, road networks, and distribution of pollutants in the atmosphere. Conclusively, GIS has provided a suitable tool for assessing urban traffic air pollution.

Fouda (2001) used GIS to environmental assessment of air pollution impacts on urban clusters and natural landscape. A model for pollutants plumes was designed through a GIS to calculate the dispersal of TSP loads over the landscape and to estimate its spatial distribution and to analyze its relationship with other geographic land use attributes. The major objective of the modeling process was generating concentration maps. The results showed that, two-dimensional contour maps were essential information layers for the completion of the geographic base of the GIS. The plume plots for the three wind directions were subjected to adaptation for scale, rotation, and shifting so that they would match the master plan of the region's land cover and urban land use.

Li, Tao, Dawson, Cao, and Lam (2002) used a GIS based model to predict noise from the road traffic. This model was based on local environmental standards, vehicle types and traffic conditions. The model was accurate to 0.8 dB at locations near the road carriage way and 2.1 dB within the housing estate. An integrated noise-GIS system was developed to provide general functions for noise modeling and an additional tool for noise design.

Lin and Lin (2002) had applied GIS to air quality analysis in Taichung City, Taiwan. The research utilized a GIS which integrates a vehicle emission model, Gaussian pollutant dispersion model, backward trajectory model and related databases to estimate the emissions and spatial distribution of traffic pollutants. The results

showed that there were higher CO emissions around downtown areas, and the areas along highway sustained higher NO_x, SO_x, and TSP pollutions. Predictions of several hypothetical scenarios indicated that the major effect of upgrading motorcycles was the reduction of TSP emission by more than 10%, while increasing average traffic speed of city roads may reduce more than 14% of CO emissions.

Kang, Chun, Jie, and Qi (2009) studied about urban air pollution based on GIS. The framework of urban air pollution was used a GIS-based spatial distribution of air pollution. It included three sections in sequence of data acquisition, model running and result applications. The research utilized spatial data management and analysis provided by GIS to organize the data and implement urban air pollution. The results showed that the spatial distribution trends were much better represented and learned. The interrelationships between the involved methods were strengthened.

Jerrett, Gale, and Kontgis (2010) reviewed on spatial modeling in environmental and public health research. This paper has two aims: (1) to summarize various geographic information science methods; and (2) to provide a review of studies that have employed such methods. It can be concluded that GIS and allied methods were now essential components in the larger fields of epidemiology and public health. This influence was evidence with growing used for informing public health prevention policies and practices.

2.5.3 Multi-objective modeling to locate Air Quality Monitoring Stations

Chang and Tseng (1999) had designed a multi-pollutant air quality monitoring network in a metropolitan. This paper presented optimal searches for siting pattern of AQMNs using both simulation and optimization models as a combined tool. While conservative, quasi-stable, and reactive pollutants were

considered in the design principles, cost, coverage effectiveness, and spatial correlation characteristics were included in the multi-criteria decision making process. The results of the objective on detecting the highest concentrations of a set of pollutants can be very different from the objective on detecting the highest frequency of violations in AQMN design.

Kao and Hsieh (2006) utilized multi-objective analysis to determine an air quality monitoring network in an industrial district. A dispersion model was employed to simulate hourly distribution of pollutant concentrations in the study area. Models optimizing pollution detection, coverage, and population protection were established. Alternative AQMNs with varied station numbers and spatial distributions were obtained using the models. AQMNs were ranked for effectiveness in monitoring the spatial variation of pollutants. This multi-objective analysis was expected to facilitate a decision-making process for determining an appropriate AQMN.

Chen, Liu, and Chen (2006) developed a multiple objective planning theory and system for sustainable air quality monitoring networks. The environmental, social, and economic objectives and sub-objectives, and their weights were identified using multiple objective optimizations. The objective value was identified as the sum of each sub-objective value multiplied by the weight. The results showed that this study generated better alternatives than the actual monitoring network. An installation schedule for the alternative was proposed. The procedure and computer system developed in this study can be used to assist the competent and different alternatives for air quality monitoring networks planning.

Elkamel, Fatehifar, Taheri, Al-Rashidi, and Lohi (2007) used a heuristic optimization approach for air quality monitoring network design with the

simultaneous consideration of multiple pollutants. A mathematical model based on the multiple cell approach (MCA) was used to create monthly spatial distributions for the concentrations of the pollutants emitted from different emission sources. The objective of the optimization was to provide maximum multi-pollutants of CO, NO_x, and SO₂ emitted from each source within a given area. The effect of the spatial correlation coefficient (R_c) was analyzed. The number of monitoring stations required for total coverage was increased. A high R_c based network may not necessarily cover the entire region, but the covered region will be well represented.

Lozano et al. (2009) designed air quality monitoring networks for nitrogen dioxide and ozone. The proposed method consists of four steps for choosing the best locations for the monitoring stations: (1) preliminary evaluation; (2) sampling campaigns with passive diffusion samplers; (3) spatial interpolation; and (4) selection of best locations for the monitoring stations. The results were affirmative for nitrogen dioxide and the stations could be kept as traffic-orientated, urban and suburban background stations. For ozone assessment, it was detected that the control station should move slightly.

Mofarrah and Husain (2010) used a holistic approach for optimal design of air quality monitoring network expansion in an urban area. An objective methodology for determining the optimum number of ambient air quality stations in a monitoring network. The methodology integrated the multiple-criteria method with the spatial correlation technique. The pollutant concentration and population exposure data were used in this methodology in different ways. In the first stage, the Fuzzy Analytic Hierarchy Process (FAHP) with triangular fuzzy numbers (TFNs) was used to identify the most desirable monitoring locations. The alternatives configuration

were then determined on the basis of the concept of sphere of influences (SOIs). The SOIs were dictated by a predetermined cut-off value (R_c) in the spatial correlation coefficients (r) between the pollutant concentrations at the monitoring stations identified from first step and the corresponding concentrations at neighboring locations in the region. Finally, the optimal station locations could be ranked using combined utility scores gained from the first and second steps.

2.6 Synthesis of the research approach

In general, different decision-makers may have different objectives, criteria, and pollutants of interest so that the considerations of a number of alternatives and effectiveness can be satisfied at the same time when siting AQMS in the urban region. Most AQMS utilize three types of monitoring sites: (1) background sites to detect regional transport; (2) population-oriented sites to detect population exposure (persons/km²); and (3) impacted sites of different types of sources, e.g. vehicular or industrial purposes. The selection of objectives for optimal location of AQMS may have to cover several design principles. In this study, the optimization analysis considers objective and constraint functions (details in research procedure) in relation to monitoring a set of reactive regulatory pollutants. Moreover, the work describes a new method to design sphere of influences (SOIs) via the air concentration network using GIS network analysis. The SOIs will be dictated by a predetermined cut-off value Moran's I, as the spatial autocorrelation coefficient.

CHAPTER III

RESEARCH METHODOLOGY

Having considered the different theories to this study in the literature review and the research questions in the previous chapter, this chapter describes the methodology to analyze the data in connection with investigating the relationship between vehicles emission and ambient concentration. This chapter contains five sections. The first section discuss about data collection; the second section elaborate air dispersion modeling; the third section explain the procedure of spatial distribution; the fourth section mention about the optimization process; and the last section mention on sensitivity analysis. The conceptual framework in this study is illustrated in Figure 3.1. It includes data acquisition, model of dispersion and fuzzy set membership, GIS processes of time-series pollution dispersion and service area determination, and optimization analysis using LP.

3.1 Overview of the research methodology

The final achievement of this research aims at locating proper AQMSs through maximizing objective functions so that they can detect the maximum pollution potential, maximum pollution violence, and maximum people exposure impact, and each can serve the largest area. The purpose of the study is to determine the AQMSs in terms of proper positions that can provide effective data and information advantage

for protection and control planning. The potential location selection in form of grid cells comprises 3 steps of model running. First, concentration maps was created by interpolation of pollutions resulted from the emission and dispersion model of each type of vehicles with varying wind directions and time periods. Second, the objective and constraint functions prepared to achieve such planning goal include 4 maximizing objective functions and constraints. Constraints for the analysis will cover spatial autocorrelation, effective service area, alternative constraints, and minimum concentration difference. The major constraints are criteria on effective service area or often called sphere of influence (SOI) determined through network analysis (NA) and alternatives which cover a maximum number of stations. The effective area is determined. A number of alternatives is set up as a constraint. The sensitivity analysis is performed using the value function of the MODA.

3.2 Data collection, refinement, and manipulation

Input data required for the research as listed in Table 3.1 were collected. These data were firstly refined and manipulated, for example, road segmentation, receptor position generation, etc. in order that they can be used properly and effectively to serve the research objectives.

3.2.1 Traffic and emission coefficient data

The emission of the entire vehicle fleet was calculated on the basis of emission coefficients (g/km/vehicle), traffic volume (vehicles/hour) of all road section showed in Appendix A, and road segment length (kilometer). The traffic volume can be estimated by counting. The average speed from field observation and traffic volume of each link were then input to estimate CO, NO_x, and PM10 of each link.

The set of the emission coefficients with respect to different types of pollutants, vehicles, and speeds was developed and updated by the Pollution Control Department (PCD) of Thailand in 2005 as shown in Tables 3.2-3.4.

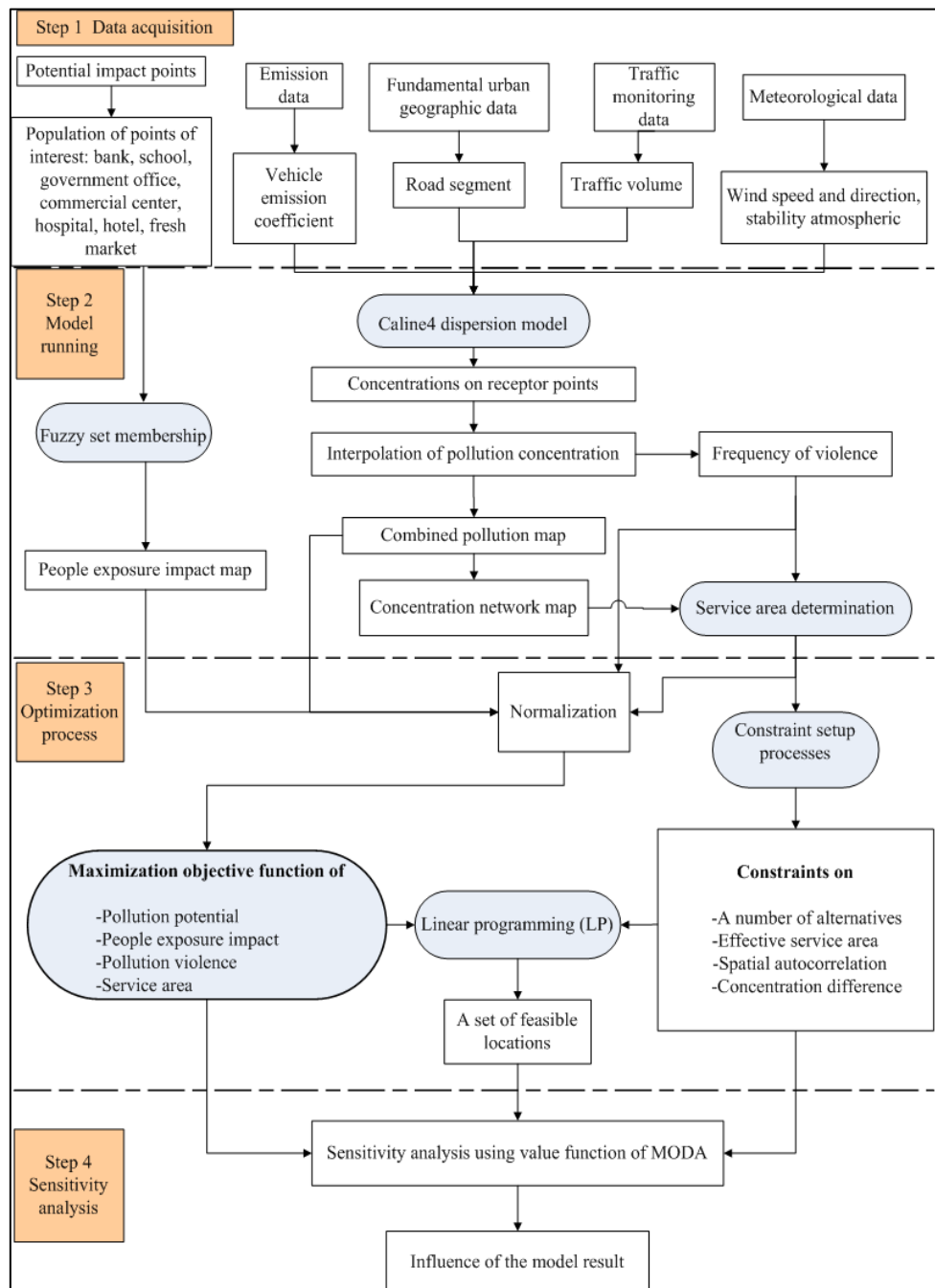


Figure 3.1 Steps of the research conceptual framework.

Table 3.1 Required data and their sources.

Type of data	Source	Year
1) Traffic data	Field counting	2010, 2012
2) Meteorology	Thai Meteorological Department (TMD)	2010-2011
3) Emission factor	Pollution Control Department (PCD)	2005
4) Road network	Thai Transport Portal	2010
5) Points of interest (Potential impact points)	Observed	2012
6) Ambient pollution concentrations	Observed	2012

Table 3.2 Emission coefficients of CO (g/km/v) with respect to different types of vehicles and speed (กรมควบคุมมลพิษ, 2550).

Speed (km/hr.)	PLDGV	LDDT	HDDT	MC
5	121.58	3.84	23.46	101.72
7.5	83.75	3.38	20.68	72.58
10	64.60	3.00	18.31	54.66
15	43.38	2.39	14.54	35.27
20	35.78	1.92	11.75	25.78
30	26.31	1.33	8.12	17.12
40	20.72	0.98	5.99	12.78

Table 3.3 Emission coefficients of NO_x (g/km/v) with respect to different types of vehicles and speed (กรมควบคุมมลพิษ, 2550).

Speed (km/hr.)	PLDGV	LDDT	HDDT	MC
5	1.44	2.03	15.46	0.51
7.5	1.28	1.90	14.47	0.48
10	1.21	1.79	13.59	0.46
15	1.13	1.59	12.11	0.43
20	1.09	1.44	10.94	0.43
30	1.05	1.22	9.32	0.46
40	1.08	1.10	8.38	0.53

Table 3.4 Emission coefficients of PM₁₀ (g/km/v) with respect to different types of vehicles and speed (กรมควบคุมมลพิษ, 2550).

Speed (km/hr.)	LDDT	HDDT
5	0.20	0.35
7.5	0.18	0.30
10	0.18	0.30
15	0.18	0.30
20	0.15	0.30
30	0.15	0.25
40	0.15	0.20

3.3 Potential impact points

These data include impact points related to intensity of people exposure to pollutions. They can be separated into six categories: hospital, education, local

market, hotel, transport terminal and commercial center which were considered in terms of linguistic fuzzy and fuzzy numbers. Figure 3.2 shows positions of points of interest and a number of population of points of interest showed in Appendix B and field observation showed in Appendix C.

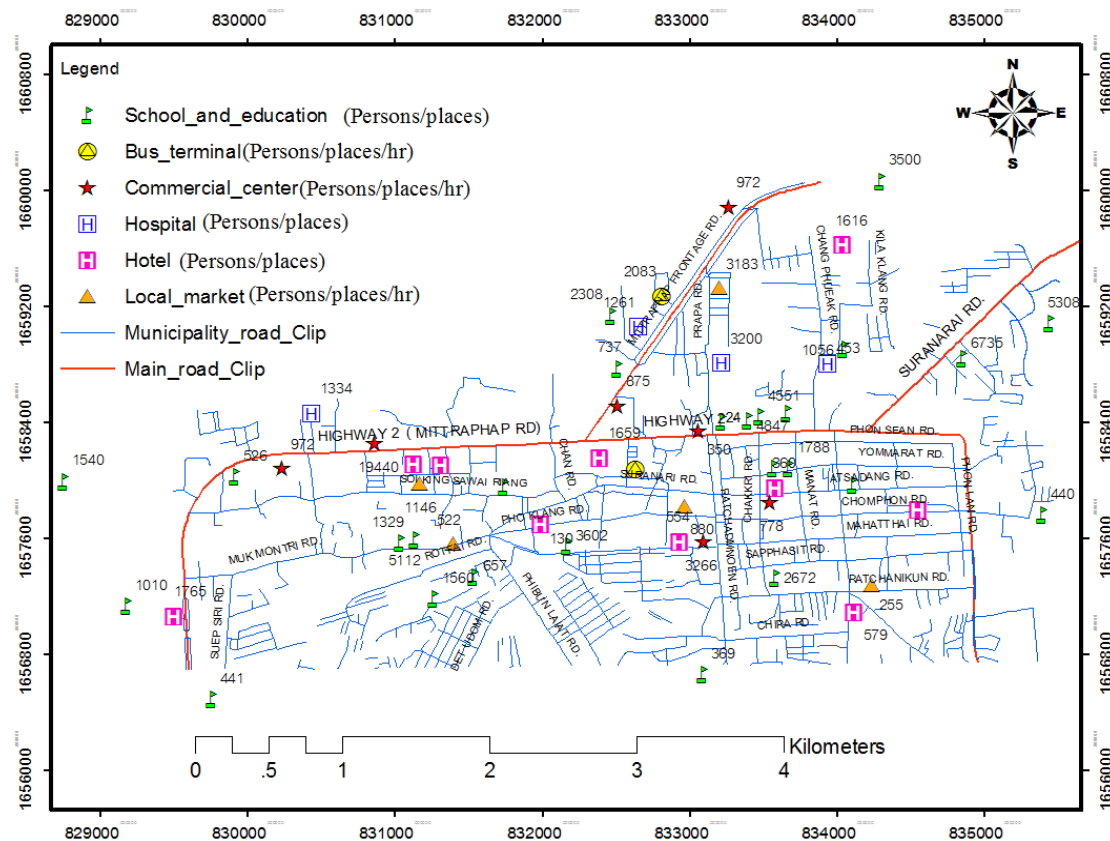


Figure 3.2 Points of interest of people exposure impact in the study area.

3.4 Pollution and network mapping

The pollution mapping process was performed using the vehicle emission and pollutant dispersion model. Each type of traffic volume varying upon multi-time periods and a set of receptor positions with varying wind directions of each road segment were input into the CALINE4, a tool with Gaussian dispersion model. The

pollution concentrations in receptor positions were then interpolated to be in form of the grid. The results of interpolation were employed for combined pollution mapping. The concentration network map was then generated from the combined pollution map for further service area analysis.

3.4.1 CALINE4 model

To obtain the emission of each link, the processes include dividing roads into segments/links according to the change of traffic and emission rates varied by traffic volume of a day. The figures of CALINE4 running showed in Appendix D.

The pollution dispersion process using CALINE4 model includes configuring parameters and the model run types.

(1) Parameter configuration

- Job parameters contain general information that identifies the job, defines general modeling parameters, run type, aerodynamic roughness coefficient, model information, and sets the units (meters) that are used as input data for the link geometry and receptor positions.

- Link geometry is filled in the matrix to define the roadway network to be modeled. Each row in the matrix defines a single link and up to 21 links are entered. Links are defined as straight-line segments.

- Link activity defines the level of traffic and auto emission rate observed at each link. Traffic volume is the hourly traffic volume anticipated to travel on each link, in units of vehicles per hour. If a multi-run scenario is selected, traffic volume must be defined for 5 hours. Emission factor is the weighted average emission rate of the local vehicle fleet, expressed in terms of grams per kilometer per vehicle. The above mentioned emission obtained is used in the model.

(2) Run type selection

The run type in the study will be worst case wind angle. The emission factors must be defined in the time period of 5 hours. The parameters required by the run type are:

- wind speed, wind direction, atmospheric stability, mixing height and ambient pollutant concentration, and

- receptor positions designed based on wind speed and direction of the links. Cartesian coordinate system and units of measurement pertaining to receptors should be the same as the link geometry. Each receptor contains attributes of the X-Y coordinates and the height (Z). The maximum number of receptors is limited at 20. Each contains the data from the links.

(3) The model operation

The model running results in concentrations attached to each receptor points along links of the road network. The distributions of pollution concentrations for the whole study area are further generated by means of the spatial interpolation of data from those receptors. The overall process is shown in Figure 3.3.

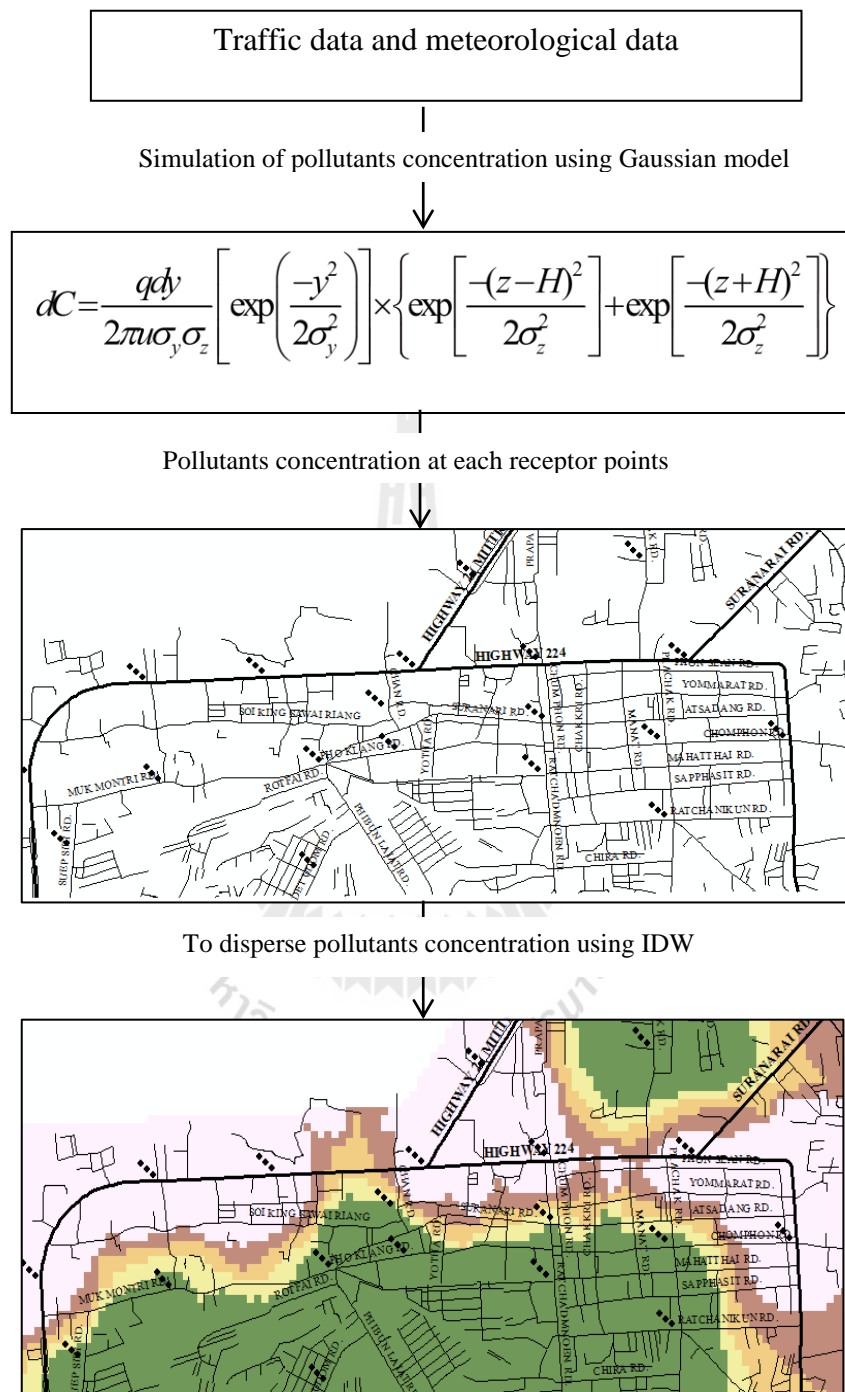


Figure 3.3 Process of pollutants concentration mapping.

3.4.2 Spatial pollution interpolation

The predicted CO, NO_x, and PM10 concentrations varying with wind directions and time periods from CALINE4 in the receptors along the road network are interpolated to predict the raster-based concentrations over the study area. Inverse Distance Weighting (IDW) method is chosen to express more local influence. IDW is a method of interpolation that estimates cell values by averaging the values of sample data points in the neighborhood of each processing cell and can be expressed as Equations (3.1) and (3.2) (ESRI, 2010). A general form of finding an interpolated value u data given point x based on samples $u_i = u(x_i)$ for $i = 0, 1, 2, \dots, N$ using IDW as an interpolating function:

$$u(x) = \frac{\sum_{i=0}^N w_i(x) u_i}{\sum_{j=0}^N w_j(x)}, \quad (3.1)$$

where

$$w_i(x) = \frac{1}{d(x, x_i)^p}, \text{ and} \quad (3.2)$$

is a simple IDW weighting function, x denotes an interpolated point, x_i is an interpolating (known) point, d is a given distance from the known point x_i to the unknown point x , N is the total number of known points used in interpolation and p is a positive real number, called the power parameter.

3.4.3 Combined pollution map

All types of pollution concentrations are weighted by percentage of all wind directions and varied with time periods, types of vehicle, and types of pollutant and combined to be the map of pollution intensity as shown in Figure 3.4. This intensity was normalized, and then input for generating pollution network map and for one of the maximized objective functions.

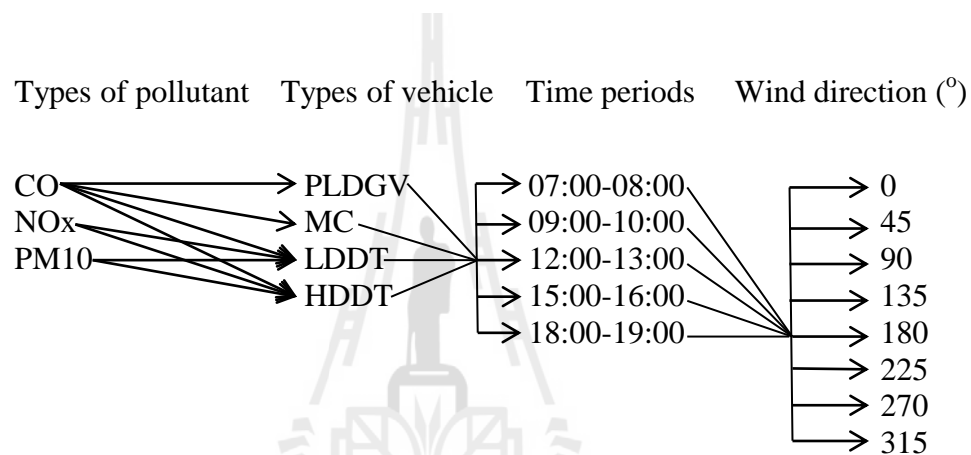


Figure 3.4 Pairs of CO, NO_x, and PM₁₀ with type of vehicles, time periods and wind direction.

The PM₁₀ emitted from MC and PLDGV was excluded in this study because in the annual reports of the PCD the PM₁₀ from these two types of vehicles was considered very low and never include in the annual test of emission coefficient. In the study area, it could be concluded that NO_x from MC and PLDGV has been very low compared to the one from LDDT, and HDDT and will not be included in this study. According to the correlation test based on all time periods in 7 days data on the link containing the highest traffic density to check the relationship between emitted NO_x and types of vehicles, it could be observed that the NO_x and the group of LDDT and HDDT showed significantly higher relationship as shown in Table 3.5.

Table 3.5 The correlation analysis between (MC+PLDGV) and (LDDT+HDDT) with NO_x.

	NO _x	MC+PLDGV	LDDT+HDDT
NO _x	1		
MC+PLDGV	0.4127	1	
LDDT+HDDT	0.7656	0.7439	1

From the Table 3.5, NO_x shows high correlation (0.77) to the group of LDDT and HDDT while the correlation to the group of MC and PLDGV is only 0.41. This explains that, in term of NO_x, the emission from the group of LDDT and HDDT was related to NO_x emission more than MC and PLDGV adequately.

The t-Test was also deployed to test the significant difference of NO_x from the group of MC and PLDGV and group of LDDT and HDDT. The result showed that the emitted NO_x from LDDT and HDDT was significantly higher than from MC and PLDGV. The emission of NO_x from the link could be obtained from emission model in Equation (3.3) (สำนักงานนโยบายและแผนการขนส่งและจราจร, 2550).

$$\text{Emission of Link} = \sum_k \sum_i D_k \times T_{ki} \times Ef_{ki}, \quad (3.3)$$

where, k is link number. i is vehicle type (Car, Light Duty Truck, Motorcycle, and Truck). D_k is link length (km). $T_{k,i}$ is traffic volume in link k of vehicle type i (Vehicle/hr.). $Ef_{k,i}$ is the amount of NO_x Emission on link k of vehicle type i

(g/km/vehicle). The NO_x emission of all time periods of the link showed in Appendix E.

The hypotheses of t-Test could be separated to be H_0 and H_1 . H_0 is accepted if the mean emissions of the link of all types of vehicles are not significant difference, otherwise H_1 , the opposite hypothesis is accepted. The test results are displayed in Table 3.6.

Therefore, to reduce the number of CALINE4 operations based on the tests of correlation and t-Test, NO_x from MC and PLDGV was reasonably excluded from the study.

Table 3.6 Result of t-Test (Two-Sample Assuming Unequal Variances).

t-Test: Two-Sample Assuming Unequal Variances		
	LDDT+HDDT+BUS	MC+PLDGV
Mean	4382.378734	1116.013165
Variance	1597913.327	62218.34344
Observations	79	79
df	84	
t Stat	22.53238003	
P(T<=t) two-tail	2.30216E-37	
t Critical two-tail	1.988609667	

From the Table 3.6, P-value [P(T<=t) two-tail] is 2.30216E-37 which is less than 0.05(∞) and t Stat (22.5323) is higher than t Critical two-tail (1.9886). Therefore, the H_0 is rejected. It can be explained that the mean of NO_x emission from the group LDDT and HDDT is significantly difference from the group of MC and PLDGV.

3.4.4 Frequency of violence

The results of pollution raster-based maps varied with wind directions and time periods are then used for determining the violence defined by the frequency of pollution concentration which is more than the mean and standard deviation of its own pollutant of every time period in each alternative (cell).

The frequency of violence is counted. The frequency of violence at any grid cell is the sum of pollution of each type of pollutants, vehicles, and time periods as expressed in Equation (3.4):

$$V_j = [C_{jivtd}] > [C_{jivtd} (mean+S.D.)], \quad (3.4)$$

where, V_j is the frequency of violence index detected at grid j . C_{jivtd} is the concentration at cell j of pollutant i of traffic volume of vehicle type v according to time having concentration above their mean and positive standard deviation. This determination results in the sum of their frequencies of each time instant. It implies that the higher the frequency of violation, the larger impact would appear for an area. The resulting frequency of violence was further used as one of the maximized objective functions and for further proper service area and Moran's I determination

3.4.5 Pollution network map

The network map is composed of a set of nodes and links in form of grid. The proper size of a network cell is 50 m x 50 m. The concentration of each node was adopted from the input combined pollution map at a corresponding position. The concentration impedance of each link was obtained from the following Equation (3.5):

$$L_n = L_j e^{|C_i - C_j|_d}, \quad (3.5)$$

where

L_n = the concentration impedance of network link,

L_{ij} = the length of the network link from node i to node j ,

C_i = the concentration of pollutants at node i , $i \neq j$,

C_j = the concentration of pollutants at node j , $j \neq I$, and

d = directions of links connecting to node i .

3.4.6 Service area determination

Alternatives obtained from the frequency of violence and nodes and links from pollution network map were used for service area determination. Its determination is as same as determining sphere of influence (SOI) using NA with varying thresholds of concentration impedance. The service area of a monitoring location also called sphere of influence (SOI) by (Modak and Lohani, 1985) is defined as the zone over which the air quality data for a given monitoring location can be considered representative. The Moran's I of each determined service area is calculated and plotted against its service area extent. The peak of the plot indicates the proper Moran's I for a constraint and the upper limit of the service area of candidate alternatives as input of one of the maximized objective functions.

3.5 People exposure impact determination

People exposure impact is determined based on types of impact points which are hospital, education, local market, hotel, transport terminal and commercial center. Due to lack of actual people density data, descriptive statistic of population density of each category during day time is determined and then normalized to be linguistic fuzzy and fuzzy number. Final result is the interpolation of raster-based fuzzy number obtained from kernel density estimation.

3.6 Optimization process using multi-objective decision analysis

To locate a proper set of AQMSs in the study area, the optimization process of multi-objective decision analysis is applied. The process includes a set of maximized objective functions and constraints which are conditions that the results are necessary to consent. The final output of the process, a set of ranked alternatives, is achieved under the constraint on the limited number.

3.6.1 Design of objective functions

The objective functions designed in the study are to maximize pollution potential, people exposure impact, pollution violence, and service area as follows. The higher the result of these functions in any alternatives indicates that those alternatives are more suitable to be the efficient AQMS.

3.6.1.1 Maximization of pollution intensity (Z_1)

The pollution intensity at any alternative is the sum of pollution of each type of pollutants, vehicles, and time periods as expressed in Equation (3.6):

$$Z_1 = \left(\sum_{t=1}^T \sum_{v=1}^V \sum_{i=1}^I C_{jivt} \right) / T_o \times Y_j, \quad (3.6)$$

where C_{jivt} is the concentration at cell j of pollutant i of traffic volume of vehicle type v according to time instant t . T_o is the total number of time periods. Y_j is the binary integer variable; it is equal to 1 if a cell j is selected as monitoring station, 0 otherwise.

3.6.1.2 Maximization of the frequency of pollution violence (Z_2)

This consideration is relevant to the impact on pollution concentrations in terms of the frequency of having concentration above the sum of their mean and positive standard deviation. This determination results in the sum of

their frequencies of each time instant. It implies that the higher the frequency of violation, the larger impact would appear for an area. Its maximization function can be performed as Equation (3.7).

$$Z_2 = V_j Y_j, \quad (3.7)$$

where V_j is the frequency of violation being detected at grid j . Y_j is the binary integer variable; it is equal to 1 if a cell j is selected as monitoring station, 0 otherwise.

3.6.1.3 Maximization of service area (Z_3)

The services areas determined for all cells having the frequency of violence and the cut-off by Moran's I are input of this function. A cell with the bigger service area is the better to serve objective of this function.

$$Z_3 = A_j Y_j, \quad (3.8)$$

where A_j is the service area of a monitoring station, when monitoring station is located at grid j . Y_j is the binary integer variable; it is equal to 1 if a cell j is selected as monitoring station, 0 otherwise.

3.6.1.4 Maximization of people exposure impact (Z_4)

Maximum population should be able to protect when an AQMS is sited. This is an important purpose. The people exposure impact of each cell can be expressed in Equation (3.9).

$$Z_4 = E_j Y_j, \quad (3.9)$$

where E_j is the fuzzy number indicating the degree of population density of each cell. Y_j is the binary integer variable; it is equal to 1 if a cell j is selected as monitoring station, 0 otherwise.

3.6.2 Design of constraint functions

The constraint set defined in this analysis covers two conditions including a number of alternatives and effective service area.

3.6.2.1 A number of alternatives

This constraint deals with the limit of a number of alternatives or the potential sites of monitoring stations designed.

$$\sum_{j=1}^N Y_j \leq U \quad ; \forall_j \quad (3.10)$$

$$\sum_{j=1}^N Y_j \leq U_z \quad ; \forall_j \quad (3.11)$$

where U is the upper bound of the maximum number of alternatives designed and U_z is the upper bound of the maximum number of alternatives designed from class of the pollutants intensity. Y_j is the binary integer variable; it is equal to 1 if a cell j is selected as monitoring station, 0 otherwise. N is the total number of designed alternatives.

3.6.2.2 Service area and spatial autocorrelation

This constraint is the cut-off A_c in term of Moran's I obtained from of the plot between service areas and Moran's I mentioned above. Actually the higher the Moran's I means that the measurement of concentration by an AQMS in its service area will be better representative. However, if the Moran's I is higher than the one associated with the peak of the plot, it will not be consistent with the constraint on service area. The constraint is performed as steps shown in Figure 3.5.

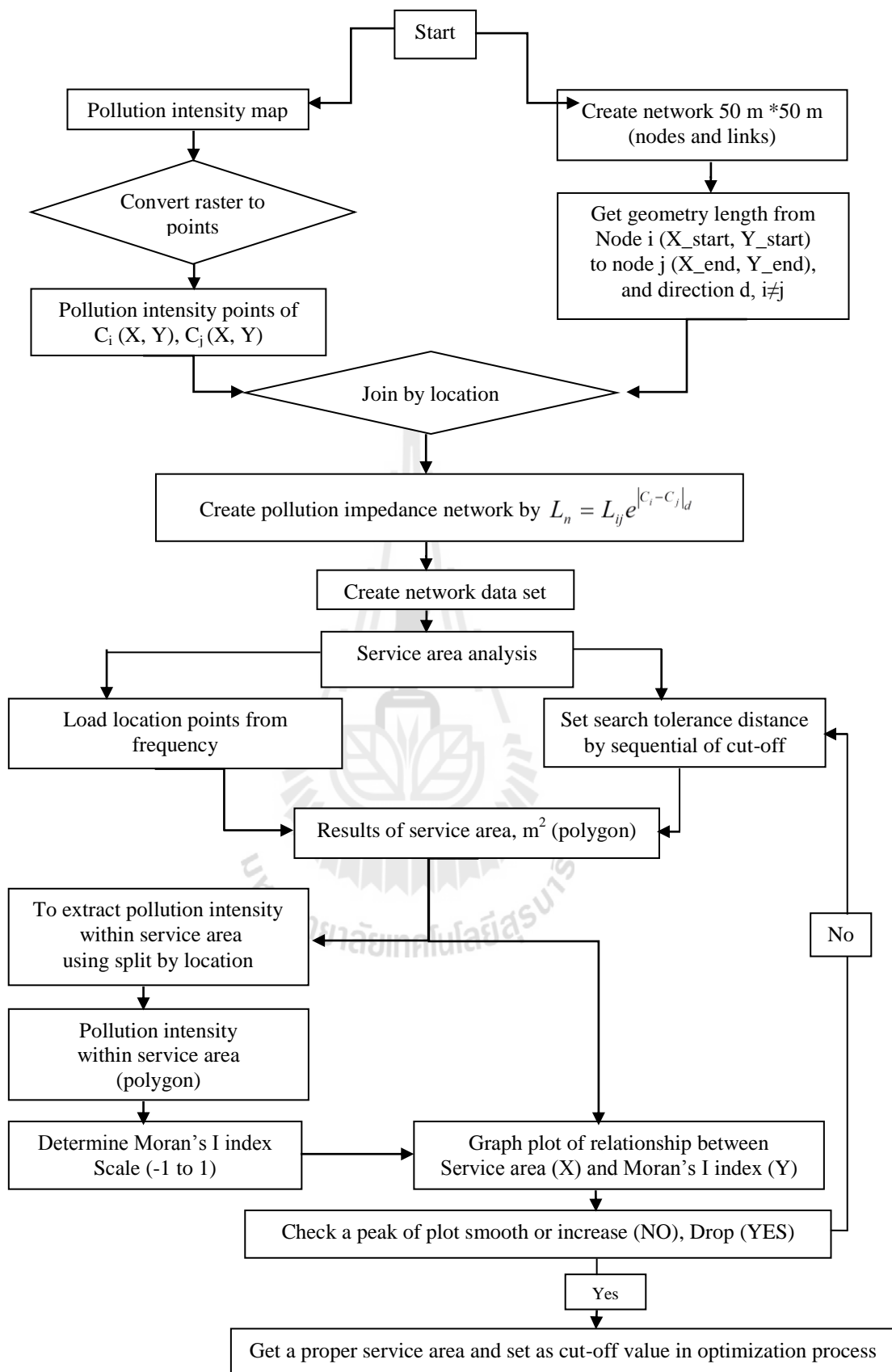


Figure 3.5 The analytical framework of pollution network and a cut-off service area.

3.6.2.3 Effective service area

The extent of the effective service area will be under the upper limit of the size of the area obtained from the peak of the plot between service areas and Moran's I mentioned above. Therefore, the alternatives chosen from the process will have service areas not larger than the upper limit.

$$A_j Y_j \leq A_c \quad ; \forall_j \quad (3.12)$$

where A_j is the service area of a monitoring station installed at grid j . A_c is the cut-off value of service area that is determined prior to the optimization analysis. Y_j is the binary integer variable; it is equal to 1 if a cell j is selected as monitoring station, 0 otherwise.

The spatial autocorrelation coefficient in term of Moran's I or M_i can be defined as (Moran, 1950):

$$M_i = \frac{\sum_{i=1}^n \sum_{j=1}^m w_{ij} (x_i - x_m)(x_j - x_m) / \sum_{i=1}^n \sum_{j=1}^m w_{ij}}{\sum_{i=1}^n (x_i - x_m)^2 / n}, \quad (3.13)$$

where x_i is the value of cell i , x_j is the value of cell j neighbor i , x_m is the mean cell value of the grid, w_{ij} is a coefficient, and n is the total number of cells in the grid. The coefficient w_{ij} has a value of 1 if j is one of the four cells directly adjacent to i and a value of 0 for other cells or cells with no data. Moran's I is positive when nearby areas have similar attribute values, negative when they have dissimilar values, and close to zero when attribute values are arranged randomly. The values of Moran's I tend to range between -1 and 1.

3.6.3 The multi-objective model

To achieve proper sites for AQMSs, all objective functions designed above are applied. The purpose of designing these objectives function is more likely to let them become the universal process to siting proper positions of AQMSs from all alternatives. However, in some given areas, some of these functions might not be performed due to their specific conditions do not meet.

A general multi-objective model for all objectives is expressed as follows:

Objective functions

$$\text{Maximization } Z \quad C_j Y_j + V_j Y_j + A_j Y_j + E_j Y_j \quad (3.14)$$

Subject to constraints:

$$\sum_{j=1}^N Y_j \leq U \quad ; \forall_j \quad (3.15)$$

$$\sum_{j=1}^N Y_j \leq U_z \quad ; \forall_j \quad (3.16)$$

$$A_j Y_j \leq A_c \quad ; \forall_j \quad (3.17)$$

$$Y_j \geq 0 \quad ; \forall_j \quad \text{and} \quad (3.18)$$

$$Y_j = 0, 1 \quad (3.19)$$

All restrictions have been described by Equations (3.15) to (3.17). In addition, from Equation (3.18) binary constraints and Equation (3.19) non-negativity constraints are: $Y_1, Y_2, \dots, Y_n \geq 0$.

3.7 Sensitivity analysis using value function of MODA

The purpose of the sensitivity analysis in this study is to examine which objective function(s) can influence to the model result the most, specifically for this area. The method selected to apply is the value function of the MODA as expressed in Equation (3.20) (Malczewski, 1999). It is performed by assigning the weights for all objective functions. Performing one function at a time, its weight will be increased, while others are still equal, until the Y_j change the position. An objective function with the least increment indicates the highest influence or the most sensitive to the model result.

$$F(x) = \max \left\{ w_k v(f_k(x)) \right\}, \quad (3.20)$$

where w_k is the weight of importance assigned to the k^{th} objective.



CHAPTER IV

RESULTS AND DISCUSSION

The results and discussion of the study are presented in this chapter. It includes results of data collection and data analysis, combined pollution map, frequency of violence map, service area determination, people exposure impact and optimization analysis using LP.

4.1 Data Collection

4.1.1 Meteorological Data

As elements of parameters input for the Gaussian distribution model, wind speed and wind direction are meteorological factors that vary significantly and cause variation of pollutant distribution in the atmosphere. Figure 4.1 shows the wind rose diagram of all seasons when traffic data were collected during January 2010 to May 2011. Wind speed and directions changed remarkably in every month, which imposed uncertainty on the pollution distribution. This study employed hourly data of all dates from the 1st January 2010 to 31st May 2011 recorded by the Nakhon Ratchasima Meteorological Department

All wind rose diagrams of all time periods were displayed in Appendix F. Figure 4.1 is an example depicting the weight of wind direction extracted. All types of pollution concentrations were weighted by the percentage of all wind directions (Table 4.1) and combined to be the map of pollution intensity. For example, the

frequency of winds over a five-time period is plotted by wind direction, with color bands showing wind ranges. The directions of the diagrams with the longest spoke show the wind direction with the greatest frequency. The wind rose shows the frequency of winds blowing from particular directions over a thirteen-month period with regardless rainy season. The length of each “spoke” around the circle is related to the frequency that the wind blows from a particular direction per unit time. Each concentric circle represents a different frequency, emanating from zero at the center to increasing frequencies at the outer circles.

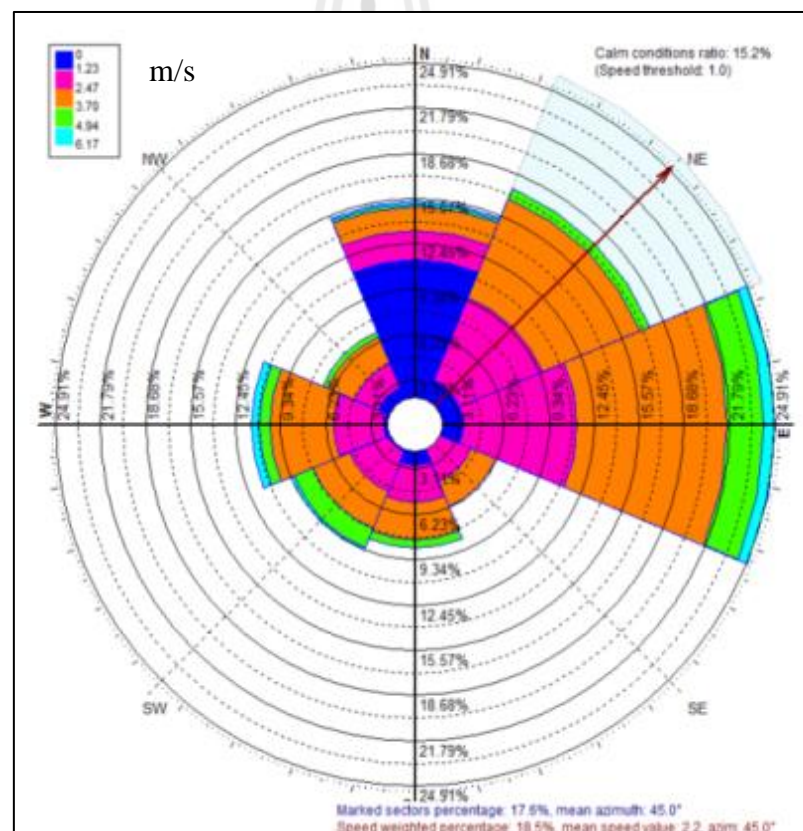


Figure 4.1 An example of wind rose diagram showing average mean speed and direction (45 degree, NE) of Nakhon Ratchasima municipality during 1st January 2010 to 31st May 2011 at 18:00-19:00 pm.

Table 4.1 Weighted extraction of wind direction in each time period using wind rose diagram.

Time periods	Wind direction (degrees)	Weights of wind direction on scale (0-1)
07:00-08:00	0	0.61
	45	0.093
	90	0.139
	135	0.02
	180	0.016
	225	0.051
	270	0.042
	315	0.029
09:00-10:00	0	0.22
	45	0.103
	90	0.218
	135	0.053
	180	0.066
	225	0.108
	270	0.156
	315	0.076
12:00-13:00	0	0.139
	45	0.119
	90	0.209
	135	0.064
	180	0.081
	225	0.123
	270	0.168
	315	0.097
15:00-16:00	0	0.139
	45	0.108
	90	0.233
	135	0.071
	180	0.103
	225	0.117
	270	0.15
	315	0.079
18:00-19:00	0	0.154
	45	0.176
	90	0.249
	135	0.06
	180	0.084
	225	0.093
	270	0.114
	315	0.07

4.1.2 Ambient concentrations determination of CO, NO_x and PM₁₀

Measurement of CO content in proximity to the road was obtained using a QRAES 2000, a carbon monoxide measurement tool. The instrument was operated over a scaled range of 0-500 ppm with 1 ppm resolution and provided 1-min averaged records. Locations of the emitters and receivers were at the middle of 21 segments of the road or links and were represented by points at the middle of links as shown in Figure 4.2.

Due to a lack of an instrument for NO_x and PM₁₀ measurement, they were obtained using backward stepwise regression in determining a relationship between traffic volume of each vehicle type on Highway 224 and hourly records of an existing air quality monitoring station near the highway. This technique allows linear regression to calculate NO_x and PM₁₀ contents hourly traffic volume with a minimum parameters in the final equation as follows:

$$\text{NO}_x = -0.43 + 0.19(\text{LDDT}) + 0.18(\text{BUS}) + 0.532(\text{HDDT}), R^2 = 0.60,$$

$$\text{PM}_{10} = -5.6 + 0.12(\text{LDDT}) + 0.1(\text{BUS}) + 1.01(\text{HDDT}), R^2 = 0.66.$$

A multiple linear regression models relating vehicle types which are LDDT, BUS, and HDDT to NO_x and PM₁₀ concentration were developed. These models were utilized to estimate ambient concentrations of CO, NO_x and PM₁₀ as results displayed in Tables 4.2-4.4.

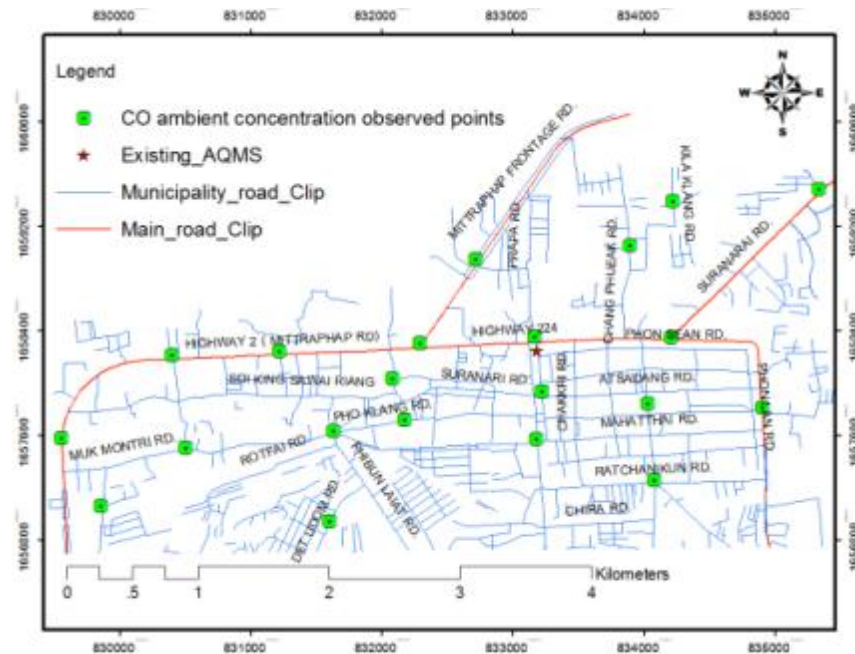


Figure 4.2 Ambient concentrations observing points at 21 road junctions in the study area.

Table 4.2 Observations of CO ambient concentrations at 21 links during time observed at 07:00-19:00, 19th January -12th February 2012.

Links	CO (ppm)	CO (ppm)	CO (ppm)	CO (ppm)	CO (ppm)
	07:00-08:00	09:00-10:00	12:00-13:00	15:00-16:00	18:00-19:00
Chang Phuaek RD.	1.28	1.08	0.80	1.10	1.90
Highway 224 Mueang school	2.85	2.40	1.90	2.65	2.10
Suebsiri RD.	1.48	1.72	1.34	1.20	2.10
Rodfai RD.	1.58	1.78	1.53	1.33	2.50
Phibun Laiat RD.	1.63	1.78	3.18	1.58	1.88
Phoklang RD.	0.88	0.53	0.28	0.33	0.95
Chakri mid RD.	1.48	1.73	2.58	1.88	2.08
Assadang RD.	0.76	0.56	0.46	0.71	0.86
Ratchanikun RD.	1.08	0.78	1.58	1.68	1.88
Suranari RD.	0.88	0.53	0.28	0.33	0.95
Kilaklang RD.	0.88	0.53	0.28	0.33	0.95
Mukmontri RD.	1.38	1.58	1.33	1.13	1.90
Chakri RD.	1.35	1.58	1.45	1.35	2.30
Highway 224 Jaosua	2.85	2.40	1.90	2.65	2.10
Phonlan RD.	2.40	2.25	2.15	3.80	3.60
Suranarai RD.	1.60	1.75	2.85	1.95	1.85
Highway 2 The mall	2.95	2.50	2.00	2.75	2.20
Highway 2 Kokprom	2.35	2.10	1.70	2.45	2.50
Highway 2 PTT	2.95	2.60	2.45	3.65	3.90
Highway 2 Big-C three junction	2.95	2.60	2.45	3.65	3.90
Highway 2 Bus terminal 2	1.20	1.07	0.80	2.13	0.95

Table 4.3 Estimation of PM10 ambient concentrations at 21 links.

Links	PM10	PM10	PM10	PM10	PM10
	($\mu\text{g}/\text{m}^3$)	($\mu\text{g}/\text{m}^3$)	($\mu\text{g}/\text{m}^3$)	($\mu\text{g}/\text{m}^3$)	($\mu\text{g}/\text{m}^3$)
	07:00-08:00	09:00-10:00	12:00-13:00	15:00-16:00	18:00-19:00
Chang Phuaek RD.	9.35	9.40	9.20	9.40	9.45
Highway 224 Mueang school	106.42	66.60	57.10	81.10	108.30
Suebsiri RD.	18.20	18.35	18.30	18.25	18.48
Rodfai RD.	19.00	19.35	18.80	18.75	19.48
Phibun Laiat RD.	6.80	7.40	7.80	6.90	7.50
Phoklang RD.	9.28	9.15	9.00	9.10	9.20
Chakri mid RD.	28.10	28.20	28.45	28.40	28.47
Assadang RD.	10.56	10.30	10.20	10.50	10.60
Ratchanikun RD.	19.12	19.00	19.15	19.70	19.18
Suranari RD.	9.28	9.15	9.00	9.10	9.20
Kilaklang RD.	9.28	9.15	9.00	9.10	9.20
Mukmontri RD.	18.50	19.10	18.60	18.55	19.20
Chakri RD.	19.00	19.35	18.80	18.75	19.48
Highway 224 Jaosua	106.42	66.60	57.10	81.10	108.30
Phonlan RD.	95.20	64.60	53.50	78.10	102.40
Suranarai RD.	88.60	56.60	48.20	74.50	86.40
Highway 2 The mall	109.42	76.50	67.20	92.10	115.20
Highway 2 Kokprom	106.42	86.50	98.40	92.50	121.10
Highway 2 PTT	125.60	106.60	97.10	101.30	118.50
Highway 2 Big-C three junction	125.60	106.60	97.10	101.30	118.50
Highway 2 Bus terminal 2	106.42	86.50	98.40	92.50	121.10

Table 4.4 Estimation of NOx ambient concentrations at 21 links.

Links	NOx (ppb)	NOx (ppb)	NOx (ppb)	NOx (ppb)	NOx (ppb)
	07:00-08:00	09:00-10:00	12:00-13:00	15:00-16:00	18:00-19:00
Chang Phuaek RD.	12.10	11.80	11.70	12.25	12.35
Highway 224 Mueang school	89.50	57.60	43.50	69.60	103.60
Suebsiri RD.	20.80	21.50	21.20	20.60	21.60
Rodfai RD.	26.80	27.50	25.20	24.60	28.80
Phibun Laiat RD.	10.00	10.20	11.20	9.60	10.10
Phoklang RD.	12.50	12.30	11.80	12.10	12.90
Chakri mid RD.	42.10	42.20	42.55	42.45	42.50
Assadang RD.	14.00	14.00	13.80	14.10	14.20
Ratchanikun RD.	7.20	6.80	7.45	7.50	7.58
Suranari RD.	12.50	12.30	11.80	12.10	12.90
Kilaklang RD.	12.50	12.30	11.80	12.10	12.90
Mukmontri RD.	26.60	27.30	25.10	24.30	28.60
Chakri RD.	26.80	27.50	25.20	24.60	28.80
Highway 224 Jaosua	89.50	57.60	43.50	69.60	103.60
Phonlan RD.	78.50	60.60	55.50	71.60	98.60
Suranarai RD.	79.50	47.30	42.80	59.20	93.80
Highway 2 The mall	98.50	68.80	54.50	78.60	108.40
Highway 2 Kokprom	104.80	64.80	74.50	78.20	111.40
Highway 2 PTT	104.50	97.60	103.50	99.60	113.40
Highway 2 Big-C three junction	104.50	97.60	103.50	99.60	113.40
Highway 2 Bus terminal 2	104.80	64.80	74.50	78.20	111.40

4.2 Pollution intensity

4.2.1 Estimation of pollutants concentration from CALINE4

The purpose of the model is to assess air quality impacts near transportation facilities. Given source strength, meteorology and site geometry, CALINE4 can predict pollutant concentrations for receptors located within 500 meters of the roadway.

The model running resulted in concentrations attached to each receptor point along links of the road network and varying wind directions as depicted in Figure 4.3. The distributions of pollution concentrations for the whole study area were further generated by means of the spatial interpolation (IDW) of data from those receptors. The pollution concentration in form of raster-based maps varying with wind directions, vehicle types and time periods were then used for determining the frequency of violence from the combined pollution. This resulted in the total 160, 80, and 80 maps of CO, NO_x, and PM₁₀, respectively.

The road network was divided into 21 links represented by points at the middle. At each represented point, 3 receptor points in the distance of 10 m, 50 m, and 150 m were created along each wind direction. Thus, at each represented point, there were total 24 receptor points where pollutant concentrations were estimated by the CALINE4. In total, 504 receptor points were created systematically distributed in the study area. To evenly represent each receptor point, 3 receptors were marked along the sideways of all the eight wind direction. Twenty-four receptor points are added across the sideways of the study area to uniformly represent the study area. Therefore, the CALINE4 model was run for five periods with different input in each time of

Concerning the types of vehicle, the numbers of vehicles of each type and their speeds were about the same in each sampling hour. The emission rates of CO, NO_x, and PM₁₀ were a range of 25.78-35.78, 0.43-1.09, and 0.15-0.30 g/km/vehicle, respectively (กรมควบคุมมลพิษ, 2550).

4.2.3 Evaluation of the results from CALINE4 model

Due to the lack of instrument for NO_x and PM₁₀ measurement, regression method was carried out to evaluate the model performance by comparing the predicted and observed only CO concentration within area of 10 meters buffered from the 8 study sites. The assessment could not be carried out for the other areas due to unavailability of data. The data for observed CO concentration within 10 meters buffered area from the study area was collected as secondary data. The data was primarily collected using a QRAES 2000 sampler on the 19 January to 12 February 2012 from 7:00 to 8:00 am (peak hour) during stable and clear climatic condition. The decimal value of the predicted CO concentration was not taken into account.

The observed versus predicted CO concentrations were plotted as a graph in Figure 4.4 and validation points showed in Figure 4.5. The value of R-square is 0.7634 which suggests that the CALINE4 model is able to explain 76% of the variation in the model within the 10 meters buffered area from the main road network. The result indicates that CALINE4 has satisfactorily predicted CO concentration in the study area. Additionally, the coefficient value of confidence also supports that CALINE4 model could be performed to predict the CO concentration with acceptable level.

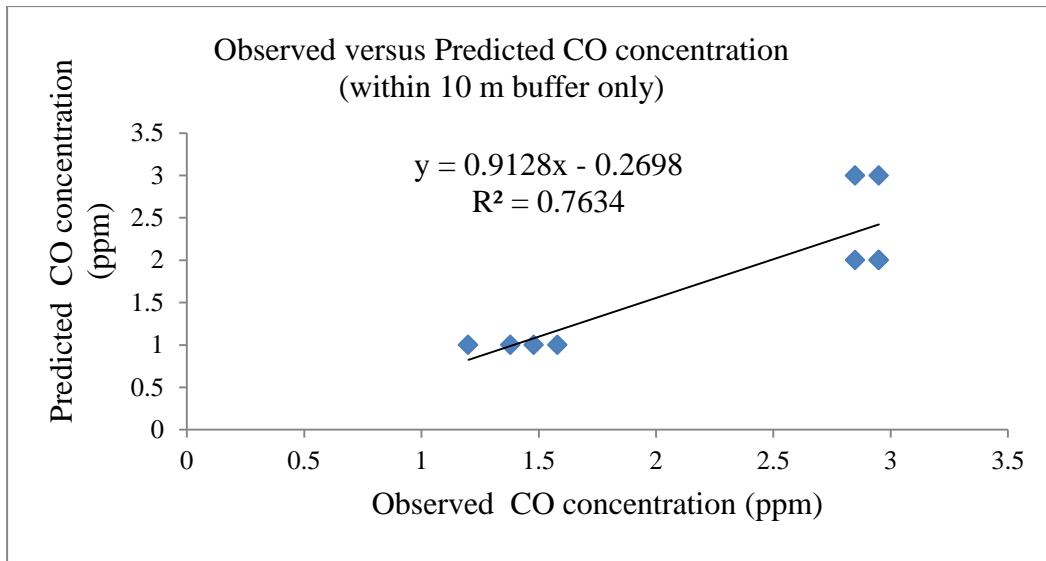


Figure 4.4 Observed versus Predicted CO hourly concentration (within 10 m buffer only).

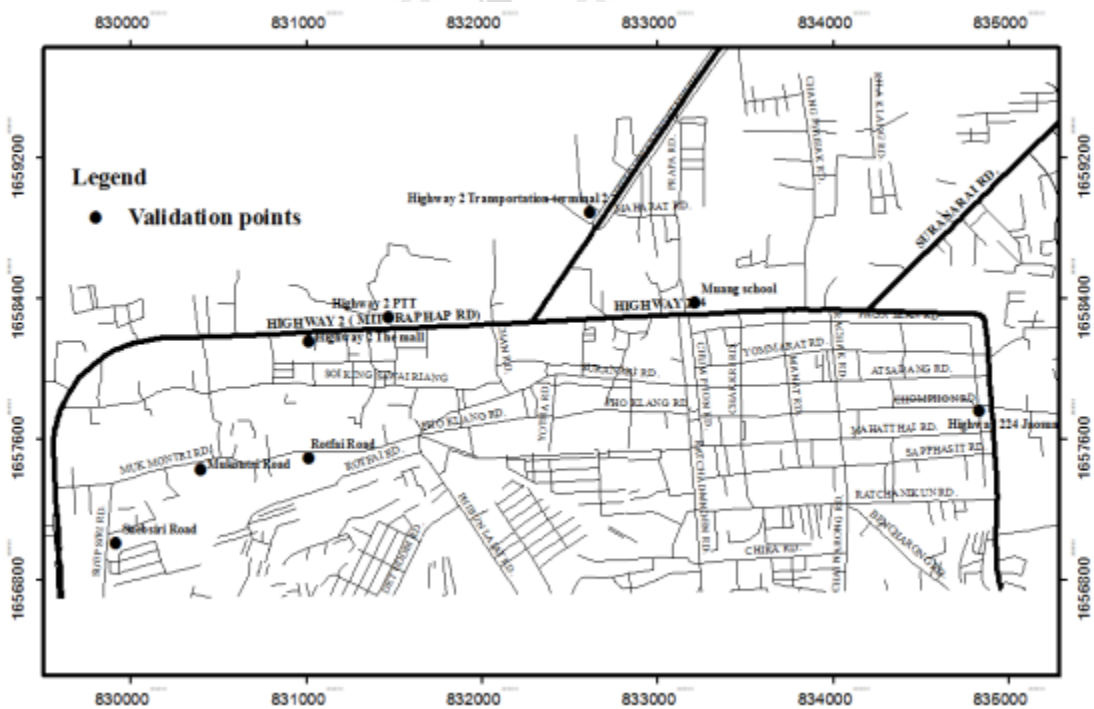


Figure 4.5 Validation points of observed versus predicted CO concentration (within 10 m buffer only).

Some roads in the study area are not a perfect street canyon, and not completely closed. There are also several accessible open spaces exist in sub-main road and non-uniformity of the building height. These characteristics of Highway 224 caused CO concentrations leaking off.

The PCD air quality monitoring station is located at the front of Mueang school which is about 10 meters from the nearby building. This open area enhanced the dilution of CO concentration in the Highway 224. For this reason, the predicted CO concentration was lower than the measured CO concentration.

Most of the time wind speeds at the TMD's station were less than 1.5 m/s. Therefore, wind circulation in street canyon tends to disappear and the mechanical turbulence is induced only by wind from vehicles and local wind. Low wind speed may be due to the obstacle from the buildings or from the advertisement signboard. Whenever the wind speeds at roof level were lower than 1.5 m/s, according to TMD's wind speed data at the height of 10 meters, the local wind speeds were not often higher than 1.5 m/s. As the wind speeds at roof level, which was less than the local wind speed, was used as an input for the model. This caused the observed CO concentrations to be higher than the predicted CO concentrations.

4.2.4 Surface maps obtained from IDW interpolation

The inverse distance weighted (IDW) interpolation explicitly implements the assumption that things that are close to one another are more alike than those that are farther apart. The IDW distributed the CO, NO_x, and PM₁₀ concentrations to the surrounding area based on the neighboring control points. In case of pollution mapping, the prediction based on the neighboring points may not be effective.

The output of IDW interpolation showed the trends of the predicted CO, NO_x and PM₁₀ concentrations over the study area. It can be clearly noted that the trends of CO, NO_x and PM₁₀ concentrations increased from the south to the north direction showed in Figures 4.6-4.8.

4.2.5 Pollution intensity varied with types of vehicle, pollutants and time periods

Figures 4.6-4.8 demonstrate examples of the raster-based simulation results of the peak of CO, NO_x, and PM₁₀ from different kinds of vehicles. All of these results were displayed in Appendices G, H, and I. Figure 4.6 illustrates that the downtown area experienced the lowest CO emission during 18:00-19:00 pm. Dispersion of CO during 15:00-19:00 pm was higher in areas along the Highway 2 and 224. PLDGV and MC of the main roads were the most significant CO emission sources while LDDT and HDDT of both municipality roads and Highway 224 were the major sources of NO_x, and PM₁₀ emissions.

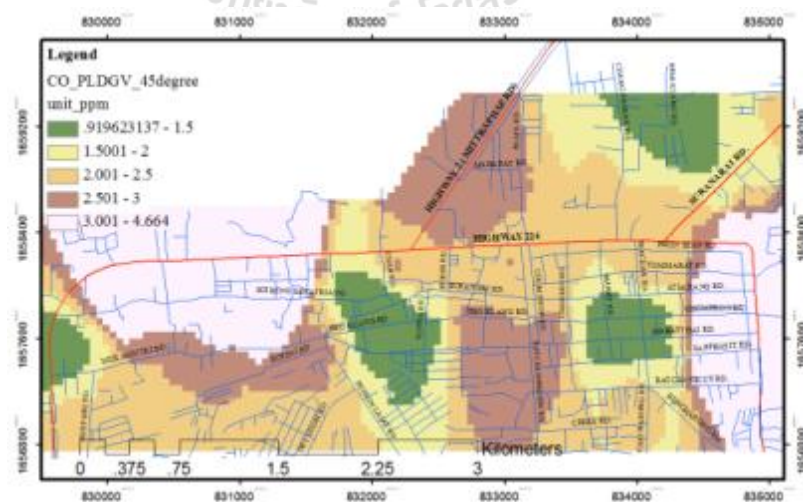


Figure 4.6 CO dispersion based on PLDGV vehicle type along 45 degree of receptor points at 18:00-19:00 pm.

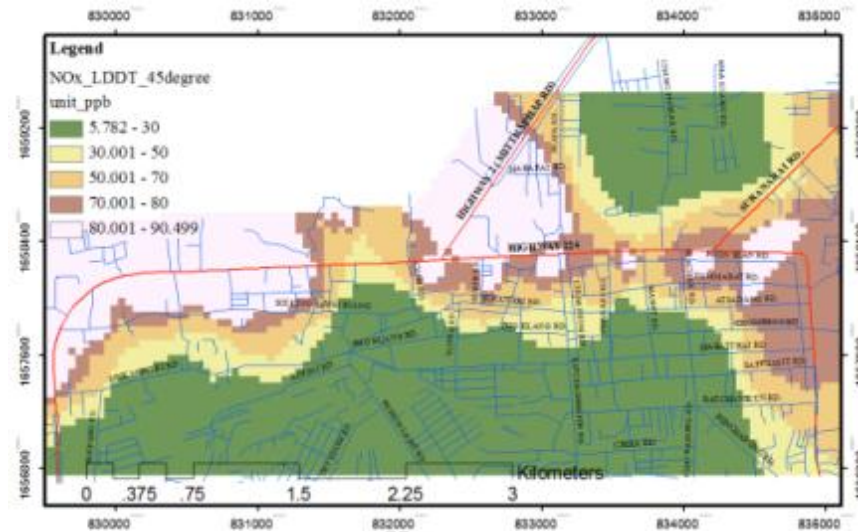


Figure 4.7 NO_x dispersion based on LDDT vehicle type along 45 degree of receptor points at 18:00-19:00 pm.

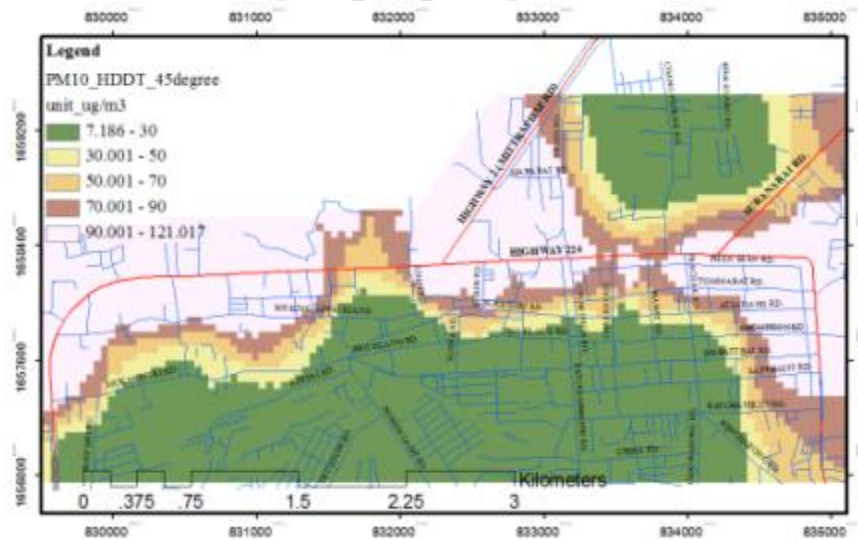


Figure 4.8 PM₁₀ dispersion based on HDDT vehicle type along 45 degree of receptor points at 18:00-19:00 pm.

The result of the simulation showed that there was a trend of increasing of all pollutants in area where road network contain high traffic volume. The resulting

distribution maps of CO, NO_x, and, PM₁₀ were as integrating spatial variations of traffic volume, types of vehicle, wind directions and speeds at different time periods. The maximum distribution areas of these pollutants at five time periods were overlapped. This corresponds to the high traffic volume always available in the main roads falling into this area at those time periods.

4.2.6 Combined pollution map

Figures 4.9-4.11 demonstrate the results of CO, NO_x, and PM₁₀ of all vehicle types, time periods, and wind directions. The results described that the downtown area had the lowest NO_x and PM₁₀ emission in municipality road. However, there were higher dispersions of NO_x and PM₁₀ in areas along the Highway 2 and 224. LDDT and HDDT of the main roads were the most significant NO_x emission sources while PLDGV and MC of municipality roads were the minor sources of NO_x and PM₁₀ emission. The downtown area had the lowest NO_x and PM₁₀ emission in during 07:00-10:00 am, but higher during 12:00-19:00 pm.

To consider the overview of the distribution of these pollutants at the peak time periods, normalized attributes of maps on the scale of 0-1 were integrated with equal weight and result in the pollution intensity map as displayed in Figure 4.12. The integrated normalized attributes were expressed as the indexes related to the concentration of the total pollution (CO, NO_x, and PM₁₀) distributed in the area. Concentration levels were highest during daylight and early night time. The results showed that the main roads contributed over 90% of all pollutants emission, although its segment length within municipality area was only 2.3 km of Highway 2 and Highway 224. PLDGV and MC of the main roads caused the most significant CO

emission while LDDT, HDDT, and BUS caused the most significant PM10 and NOx emission, respectively.

Each of these index levels imposed over a map of the municipality with classified potential pollution zone. It represented the geographical extents and the intensity and frequency of violence levels of all pollutants and wind directions. It was noticed that high index of the landscape surrounding main road, beside the municipality road itself were subjected to the impact of lower concentrations of the major pollutant.

Intensity grid illustrating the influence of different concentration levels extend through the commercial complex, queuing of van near local famous schools and the truck carrying sugarcane including several road intersections were situated in the patch. This spot and the surroundings have become well known as the worst traffic to the municipality. Estimating results of potential pollution concentration indicated that frequencies probably have the most contribution to pollution potential concentrations in Nakhon Ratchasima municipality, as the exposure concentration distribution caused by vehicle polluting types were in strong agreement. Further, the indexes of pollution intensity were used as input of one of the maximized objective functions (Z_1).

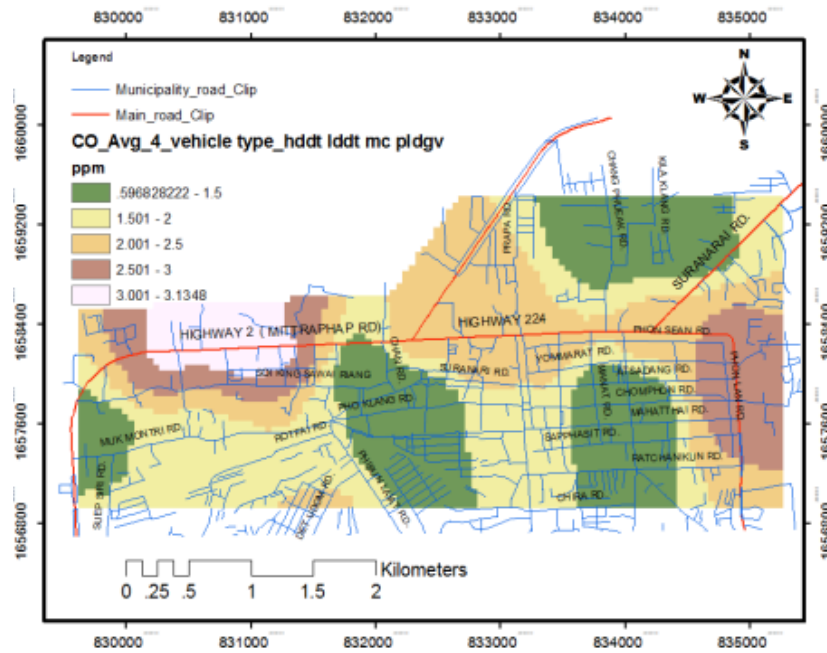


Figure 4.9 Average CO concentration map of results estimated from all vehicle types, time periods, and wind directions.

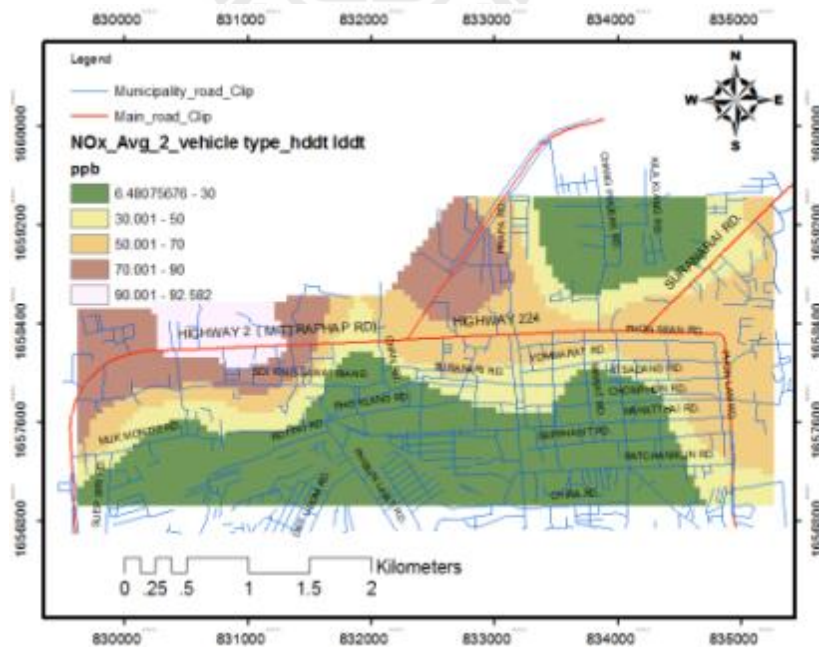


Figure 4.10 Average NO_x concentration map of results estimated from all vehicle types, time periods, and wind directions.

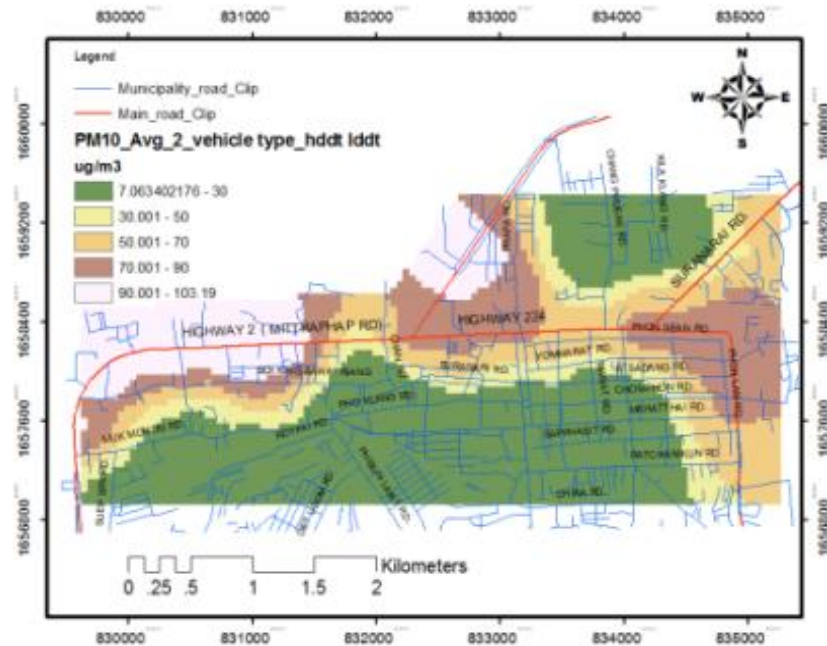


Figure 4.11 Average PM10 concentration map of results estimated from all vehicle types, time periods, and wind directions.

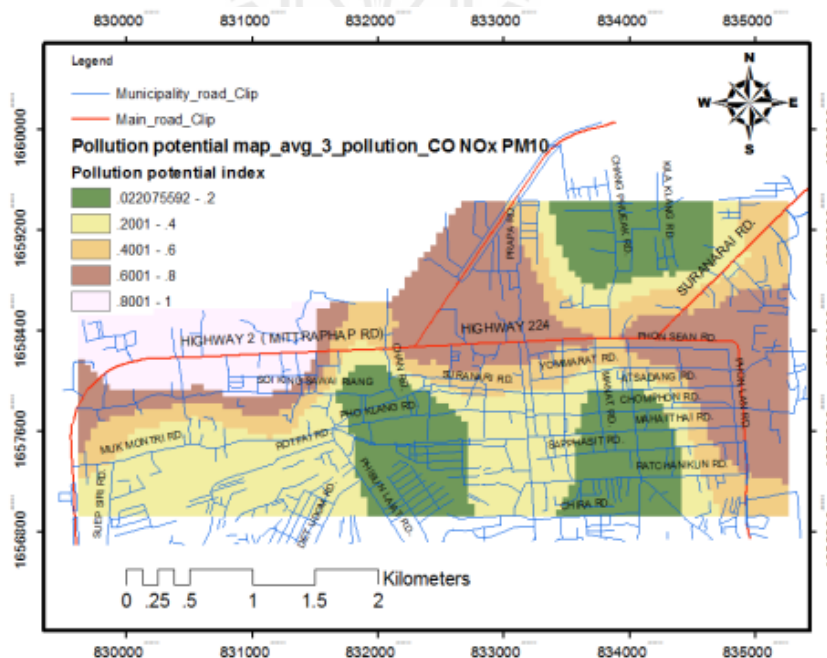


Figure 4.12 Pollution intensity map of the integrated normalized CO, NO_x, and PM10 concentrations (Z_1).

4.2.7 Classification of pollution intensity

According to the US Ambient Air Quality criteria set by the US-EPA (2006), CO, NO_x, and PM₁₀ concentrations less than 3 ppm, 90 ppb, and 120 µg/m³, respectively, in hemoglobin are not harmful for human health. The high CO, NO_x, and PM₁₀ concentrations can cause death. These criteria were used to reclassify the predicted surface from IDW to create the normalized pollution intensity over the study area. The normalized pollution intensity was classified to be 5 classes based on equal interval, namely, >0-0.2, >0.2-0.4, >0.4-0.6, >0.6-0.8, and >0.8-1. The area of class with intensity higher than 0.8 should be carefully monitored.

It is noted that the CALINE4 was able to predict pollutants concentration around 150 meters from the road. The predicted surface is therefore acceptably accurate within the 150 meters buffered area. Most of the area has moderate level of normalized pollution intensity, within a range from 0.02 to 0.60. The areas with pollution intensity predicted to be higher than 0.6 are around the Mall commercial center and school along Highway 224. This result was quite sensible as in 2011, approximately 2,832 and 3,893 vehicles a day were using the Highway 2 and 224 respectively, and higher than vehicles running in any other links. This section is the area where most of the facilities such as office premises, shopping malls, restaurants, hospital are located. It is not surprising to see high concentrations of CO, NO_x and PM₁₀ around that area. Similarly, the junction nearby Big-C shopping mall is the major road intersection of the Nakhon Ratchasima city where vehicles mainly head to KhonKaen and BuriRam province. Therefore, the vehicles in Nakhon Ratchasima are at unprecedented level, and it is sensible to predict pollution intensity of this link to be at unhealthy high level.

4.3 Frequency of violence

The violence levels were simulated to evaluate the air quality of the municipality of Nakhon Ratchasima. The result of the analysis showed that there was a trend of frequency of violence increasing for all pollutants in high traffic volume road network. The resulting frequency of violence was normalized and further used as one of the maximized objective functions. Their positions in form of cells were further input for service area determination using a Moran's I approach.

The resulting frequency maps of CO, NO_x, and PM₁₀ from all time periods and vehicle types were shown in Figures 4.13.-4.15, respectively and all frequency maps showed in Appendix J. Their integration was shown in Figure 4.16. This consideration was to estimate how frequent the pollution concentrations were above their mean plus standard deviation. The classes of combined frequency of violence were divided to be 0-10, >10-20, >20-30, >30-35 and >35-40 based on equal interval method. The distribution of higher frequency indicated the area of higher pollution intensity. It implies that an area with higher frequency could cause more severe impact for the area.

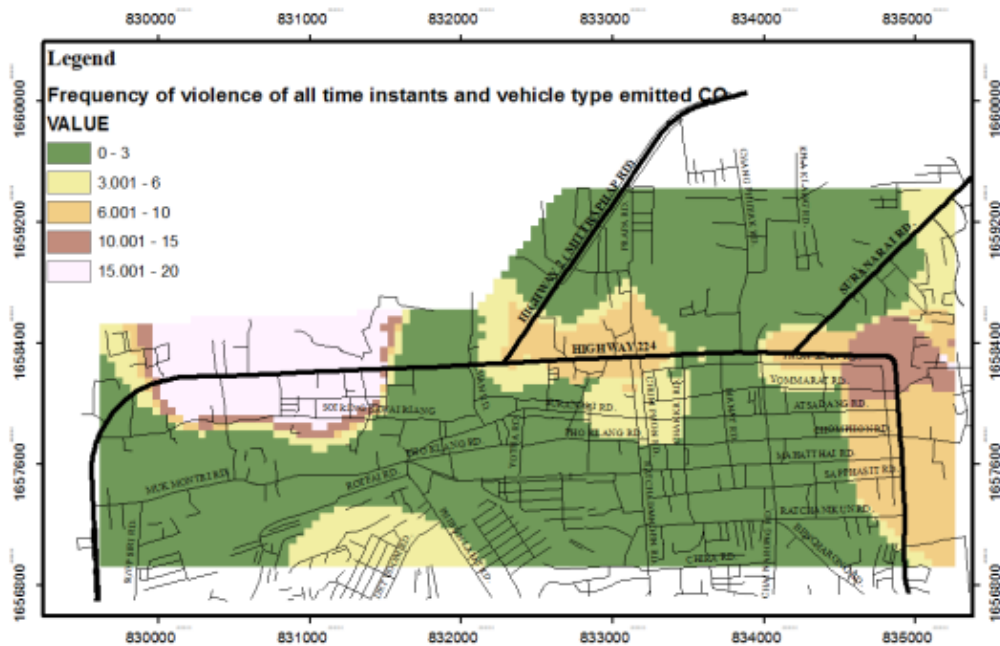


Figure 4.13 Frequency of violence of emitted CO from all time periods and vehicle types.

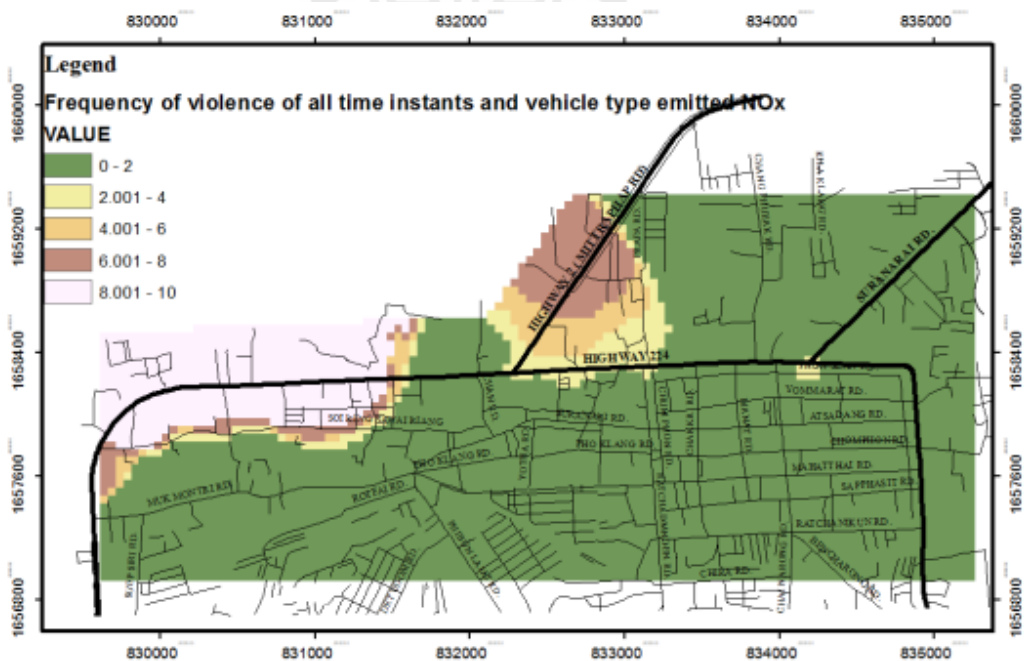


Figure 4.14 Frequency of violence of emitted NOx from all time periods and vehicle types.

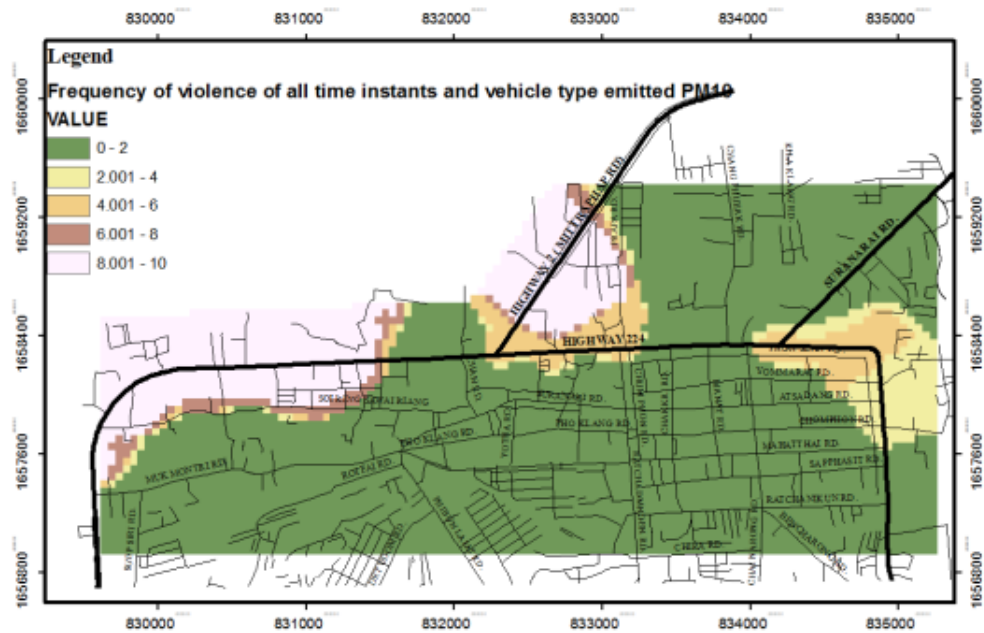


Figure 4.15 Frequency of violence of emitted PM10 from all time periods and vehicle types.

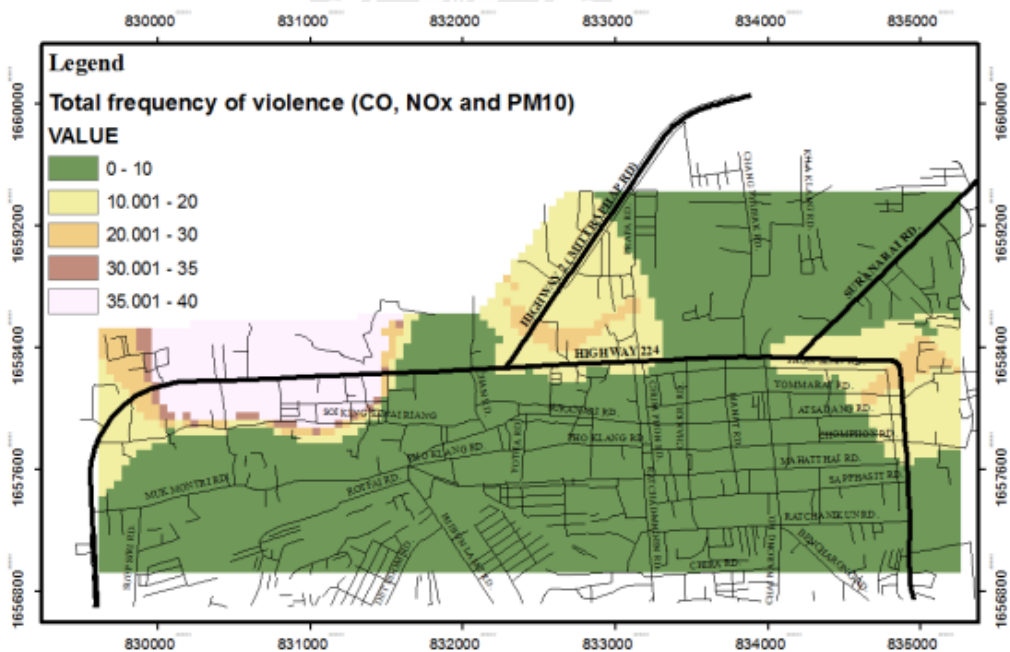


Figure 4.16 Combined frequency of violence of emitted CO, NOx, and PM10 from all time periods and vehicle types (Z_2).

The integrated normalized attributes were expressed as the indexes related to the concentration of all pollutants at all time periods distributed in the area. The violence areas with maximum frequencies of these pollutants at all time periods were quite associated spatially. This corresponded to the main roads with high traffic volume. The higher index comparatively indicates the higher pollutions and higher frequency of violence. The highest combined frequency that severely threatened to the area at morning time was caused by the traffic congestion at several intersections along roads. In major roads, traffic volume was extremely large during periods of rush hours. Exceptionally, traffic upstream of obstructions, such as cycle time of junction, bus stop, and construction, might also be constrained and resulted in traffic jams. Such dynamics of traffic congestion was known as traffic flow. The maximum frequency of violence patches could be obviously observed on the area surrounding Mittrapap Road in front of the Mall and Tesco Lotus department stores. Apart from this, other areas show did not very high frequency of the combined pollution.

The frequency of violence map showed characteristics corresponding to the distribution of pollution intensity. The locations of the impact points depended mainly upon the ambient concentration and wind direction transporting the effluent from vehicle types. Further, the normalized index of frequency of violence was used as input of one of the maximized objective functions (Z_2).

4.4 Constraint and objective function based on service area and Moran's I

4.4.1 Pollution network map

The use of pollution network map for determining a proper service area of each AQMS alternative was obviously the first contribution in this study. Normally, when a buffered operation invoked area of influence (or so-called “polygon feature”), the buffer will create a circular region around the polygon and the region is functioned as a service area. By using pollution network map, centers of cells in the study area were connected to each other by the links. Attribute of each center of cell contained combined pollution concentration. Therefore, impedance or attribute of each link was the exponential of difference of the combined pollutions between its two end nodes. This structure of nodes, links, and the difference of combined pollution became the pollution network map, shown as examples in Figure 4.17.

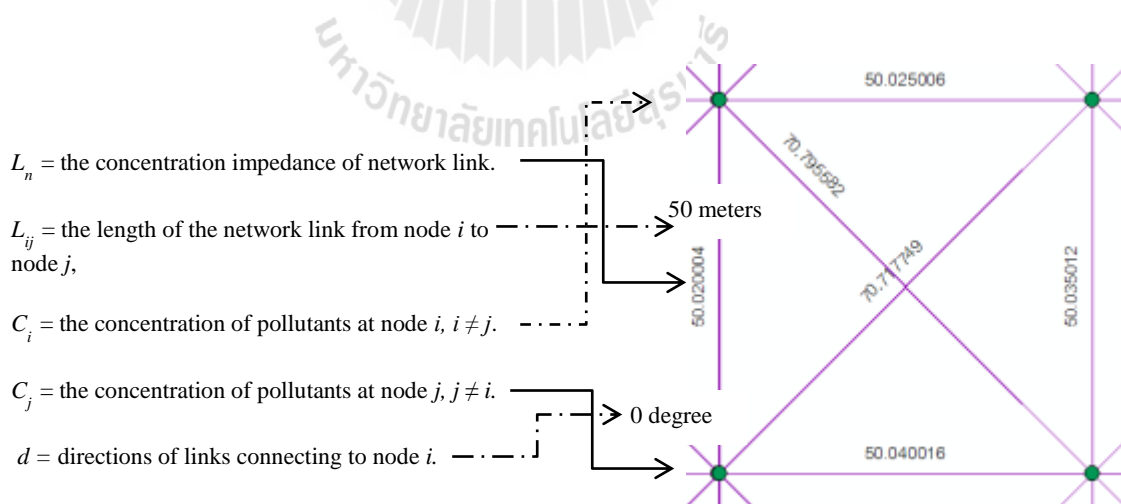


Figure 4.17 Pollution network map based on attribute of L_n .

4.4.2 Proper search tolerance of service area

The impedance of link in concentration network had effect on extents of service area. The different service area extents led to different score of alternative sites. The service area determination was based on search tolerance in term of cut-off value. The search tolerance of service area was important factor to be considered when the link impedance was applied. A unit of length of links indexed in term of L_n . The maximum distance of search tolerance was not exceeded 200 because urban areas surrounding the road in the range 200 to 500 meters were classified as agricultural lands which were not applied in the analysis procedure.

4.4.3 Service area constraint based on Moran's I

To estimate the maximum extent of service area used as the constraint in the objective function for proper AQMS siting, the process and results can be described in the following. A number of the centers of cells fall into the highest zone of the frequency of violence, 19 cells, were used as candidates or alternatives for proper AQMS sites. Service area determination of each center was operated by varying search tolerance (L_n) of 150, 175, and 200, shown as examples in Figure 4.18. The process resulted in a polygon of each service area. Combined pollution concentrations of cells falling into each service area were extracted to perform spatial autocorrelation using the Moran's I approach. Area extent of candidate service areas and their Moran's I are listed in Table 4.5. The peak of the plots between area extent of services areas and their Moran's I (as shown in Figures 4.19) were extracted. At the peak the area extent is 102,755.89 m² and Moran's I is 0.76. Herein, the area extent of the extracted service area (A_c), 102,755.89 m², was identified to be one of the constraints for the proper AQMS siting.

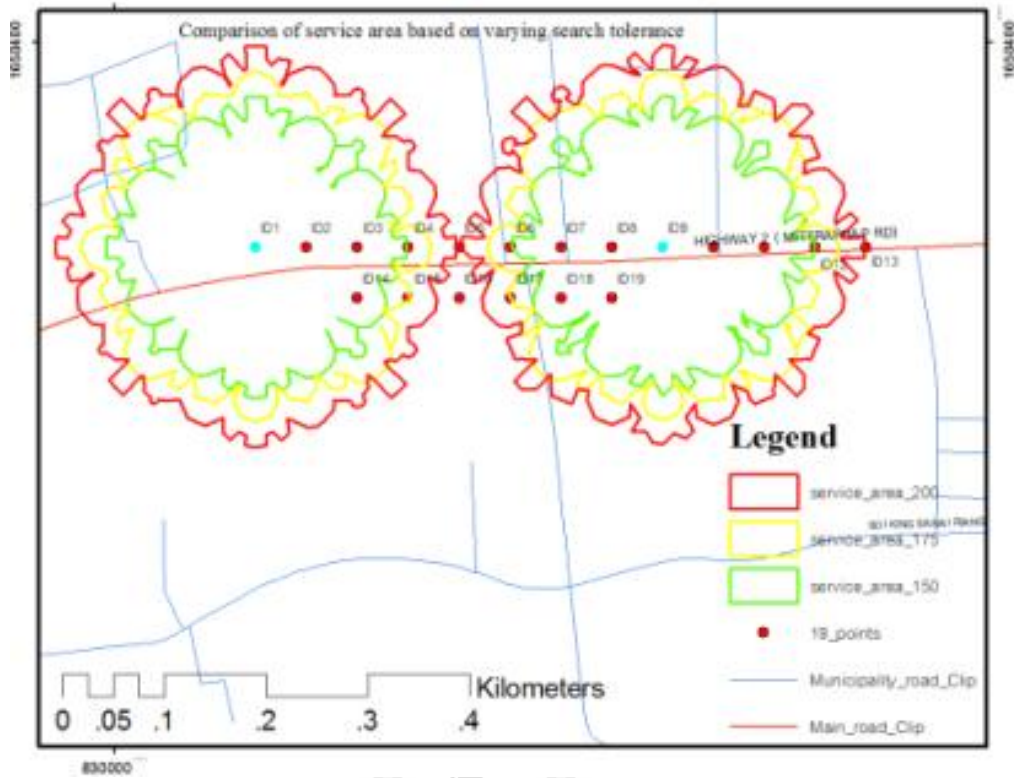


Figure 4.18 Comparison of service area based on varying search tolerances.

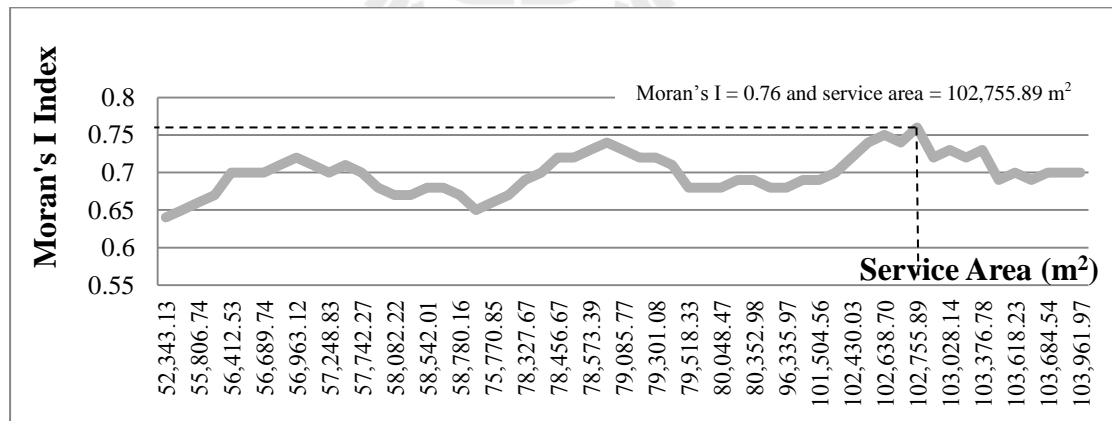


Figure 4.19 Relationship between service area and Moran's I.

Table 4.5 Relationship between service area and Moran's I of each frequency of violence points.

Frequency of violence points	Service area of search tolerance with $Ln = 150$ (m ²)	Moran's I of $Ln = 150$	Service area of search tolerance with $Ln = 175$ (m ²)	Moran's I of $Ln = 175$	Service area of search tolerance with $Ln = 200$ (m ²)	Moran's I of $Ln = 200$
ID1	52,343.13	0.64	72,757.98	0.65	96,335.97	0.68
ID2	54,663.62	0.65	75,770.85	0.66	99,786.25	0.69
ID3	55,806.74	0.66	77,646.38	0.67	101,504.56	0.69
ID4	56,321.29	0.67	78,327.67	0.69	102,199.10	0.7
ID5	56,412.53	0.7	78,381.45	0.7	102,430.03	0.72
ID6	56,518.39	0.7	78,456.67	0.72	102,568.48	0.74
ID7	56,689.74	0.7	78,506.60	0.72	102,638.70	0.75
ID8	56,792.38	0.71	78,573.39	0.73	102,694.76	0.74
ID9	56,963.12	0.72	79,057.90	0.74	102,755.89	0.76
ID10	57,195.73	0.71	79,085.77	0.73	102,828.23	0.72
ID11	57,248.83	0.7	79,125.44	0.72	103,028.14	0.73
ID12	57,532.20	0.71	79,301.08	0.72	103,195.98	0.72
ID13	57,742.27	0.7	79,416.23	0.71	103,376.78	0.73
ID14	57,937.94	0.68	79,518.33	0.68	103,487.94	0.69
ID15	58,082.22	0.67	79,772.38	0.68	103,618.23	0.7
ID16	58,317.80	0.67	80,048.47	0.68	103,623.29	0.69
ID17	58,542.01	0.68	80,196.38	0.69	103,684.54	0.7
ID18	58,596.33	0.68	80,352.98	0.69	103,902.80	0.7
ID19	58,780.16	0.67	80,449.86	0.68	103,961.97	0.7

4.4.4 Discussion of service area

The smaller size of cell used to determine the service area could provide the more accurate result. The proper grid-cell size used for the study was 50 m x 50 m which was proportionated to extent of service area. The smaller cell size could provide smaller or larger service area. The ideal service area should be bigger area extent. Service area extent was used as one of the objective function in the spatial optimization models which maximized all objective functions.

The area that provided the highest spatial autocorrelation, closer to 1, was considered to be proper for being service area and the bigger area was the better so that a minimum number of AQMS required could be kept.

The alternatives ID3 to ID15 from Table 4.5 provided highly spatial index ranged between 0.7-0.76. For other study areas, cut-off value of search tolerance

could be changed depending on pollution network characteristic of the area. The index of service area was identified to be one of the maximized objective functions (Z_3). Figure 4.20 showed the normalized service area at each cell of alternatives.

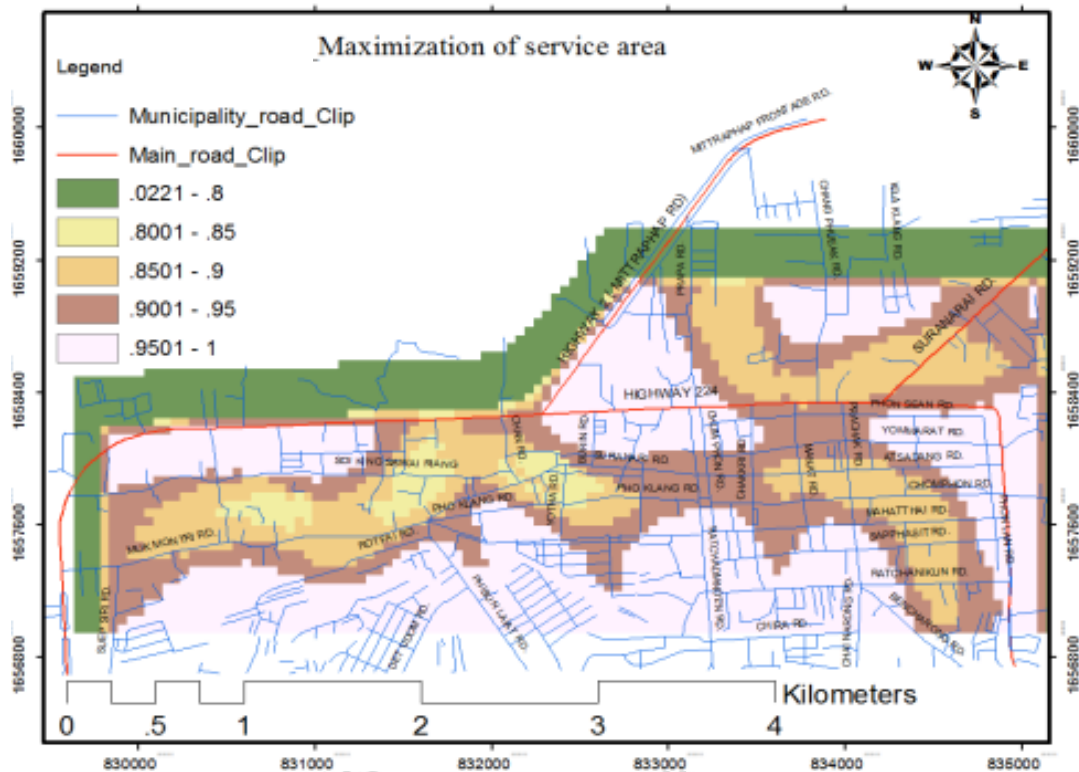


Figure 4.20 Map showing service area (Z_3) of each cell of alternatives.

4.5 People exposure impact

4.5.1 Fuzzy number determination

Due to a lack of data on population density in each cell (50m x 50m), therefore they were estimated in term of fuzzy indexes from points tending to have high people exposure instead. These points included hospital, education, local market, hotel, transport terminal and commercial center. The index of each point was derived based on theory of fuzzy set membership. The data on population present at each

impact point were collected only day time period for most active days. Descriptive statistic was used to classify impact category to be 3 classes of linguistic fuzzy, namely low (0-673), medium (674-5061), and high (more than 5061). Finally, the linguistic fuzzy classes were changed to fuzzy numbers obtained from graph (Chen and Hwang, 1992) as (0, 0, 0.2, 0.4), (0.2, 0.5, 0.5, 0.8), and (0.6, 0.8, 0.8, 1), respectively. Each point contained 4 fuzzy values from the triangle class of fuzzy graph as attributes which could be displayed as 4 raster-based data layers. These layers were then interpolated by kernel density function (with 1,000 bandwidth) to obtain distribution of impact for each fuzzy number (Figures K.4-K.6 in Appendix K). The total distribution of impact indexes, as shown in Figure 4.21, were the sum and normalization of all distribution data layers as local operation. The high impact cells became high potential for being AQMS and were further used as one of the maximized objective function (Z_4).

The result revealed that the total impact distribution was corresponded the most with the distribution of the medium class. This was because the people exposure appeared more at points with frequency and quantity corresponding to the medium class than other classes. Points with obviously high impact were education institutes which were Mueang school, Nakhon Ratchasima Vocation College, and Suranaree Wittaya school, and local markets. These points have been always located very close to arterial and minor roads where people are active during day time.

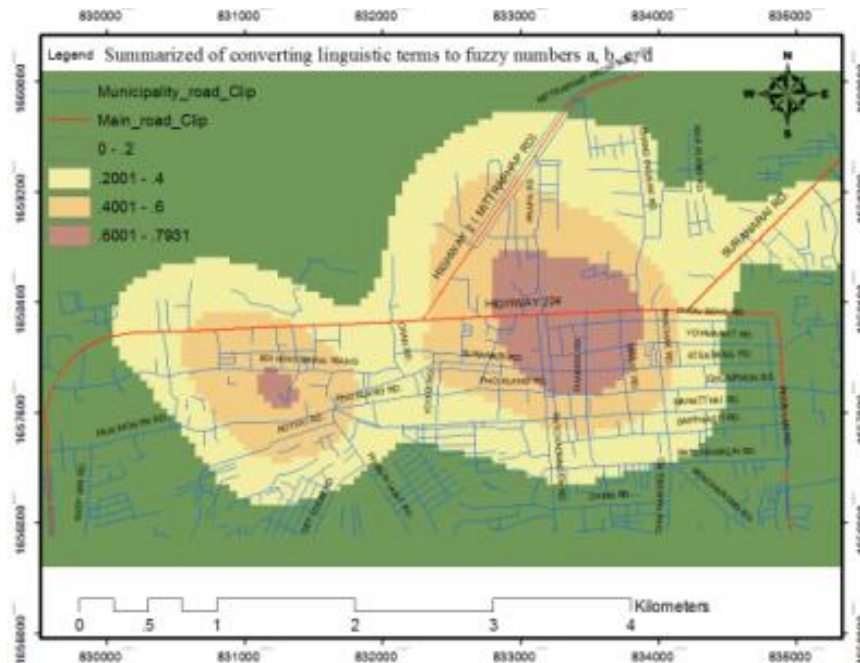


Figure 4.21 People exposure impact map (Z_4).

4.6 Combination of all distribution of variables in objective functions

The objective functions in the study were the combination of maximization of pollution intensity, frequency of violence, service area, and people exposure impact. The distribution map of the combination without any constraints considered is shown in Figure 4.22. The map was classified into five classes using equal interval method. It is obvious that potential alternatives of AQMS would mainly fall into the area corresponding to high pollution intensity and frequency of violence. The people exposure impact and service area seemed to be subordinate.

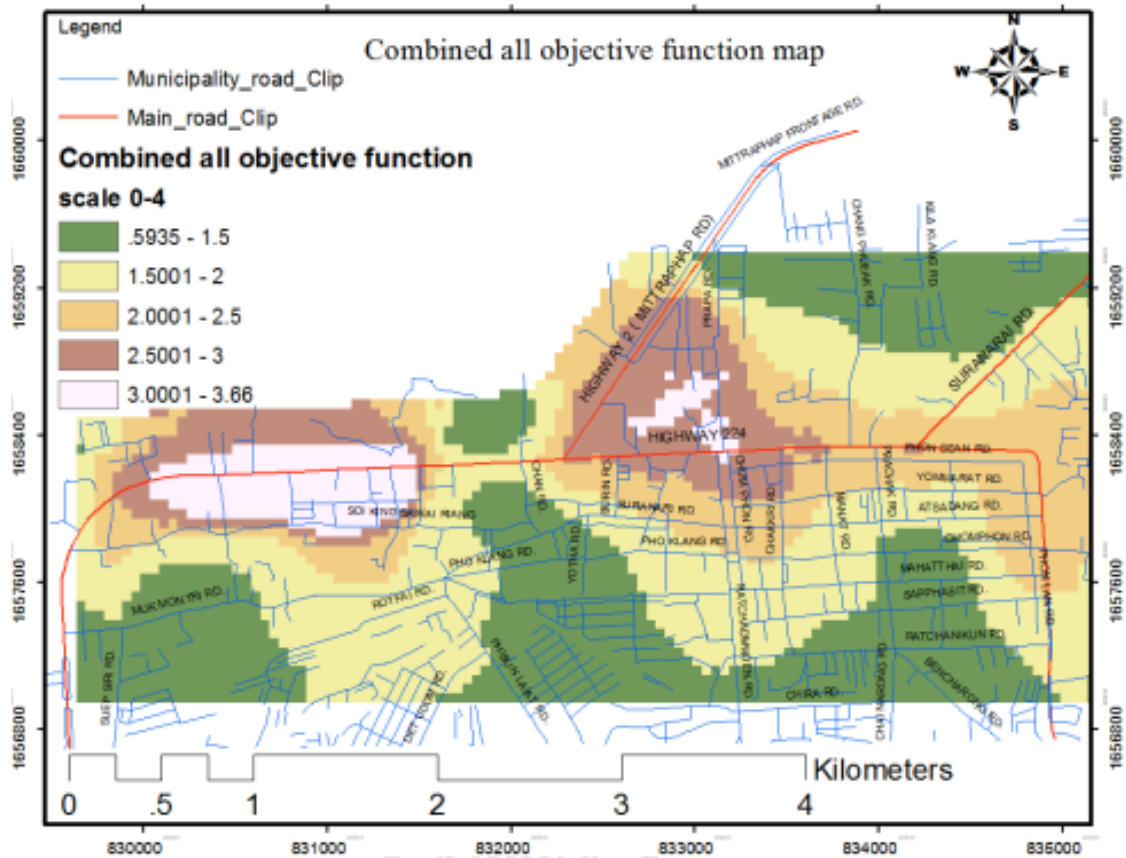


Figure 4.22 Map of combined all objective function (Z_1 to Z_4).

The highest indexes appear in the area surrounding the Mittrapap road, particularly in the vicinity of the Mall. However, the solution approach of siting has to consider many constraints in objective functions. Therefore, the optimization models through the LP should be used to determine the optimal solution of an AQMS siting.

The total number of AQMS candidates (U) was initially set up to be 15. Fortunately, this number could provide observable change of AQMS positions that met the requirement when sensitivity analysis was operated. The selected alternatives from the LP (Y_j) would be fallen only in the class of highest index alone. As a result in Figure 4.23, all AQMS candidates were only fallen into the high index class area. In

practice, the resulting selected alternatives were not suitable to station installation management.

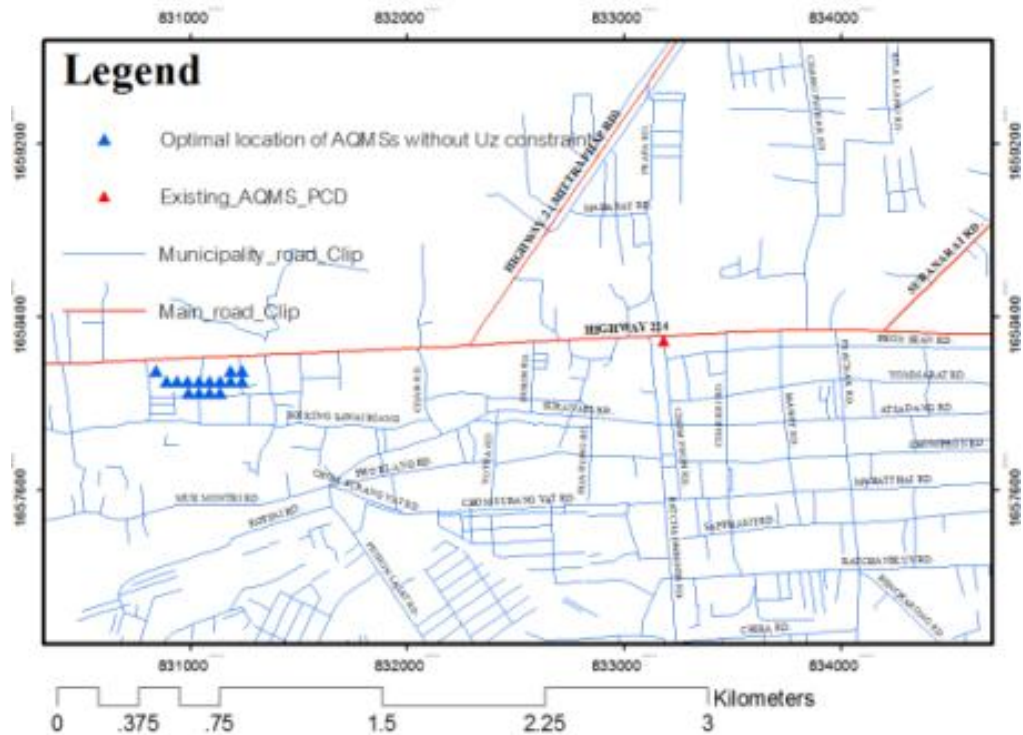


Figure 4.23 Result of optimal location of AQMS using multi-objective without constraint U_z .

To cope with this undesirable solution, the addition constraint was added. The fix numbers of AQMS in certain classes (U_z) were identified to allow distribution of AQMS candidates in selected class areas. All classes excluding the lowest index one were input into the LP for AQMS siting analysis with the constraint number of AQMS as 6, 4, 3, and 2 for higher to low index class areas, respectively. Corresponding to the result without constraint consideration, as a result in Figure 4.24, six sites of AQMS candidates were located in the class area covering the

Mittrapap road in front of the Mall department store. The coordinates of the highest score point of optimization model was located at X= 831,100 m and Y= 1,658,100m. This point was proposed to be the best position of AQMS. These sites indicated the highest index area of combined objective functions. The rests seemed to rely more on people exposure impact as they were fallen into the high index area of people exposure impact. Few of the rests were located not far from the existing AQMS of the PCD.

The weights were then applied to objective functions so that the variation of suitable AQMS sites could be observed. According to different policies, the weights on different variables in objective functions can be varied and the preferred result could be selected. This trial was operated as the following sensitivity analysis.

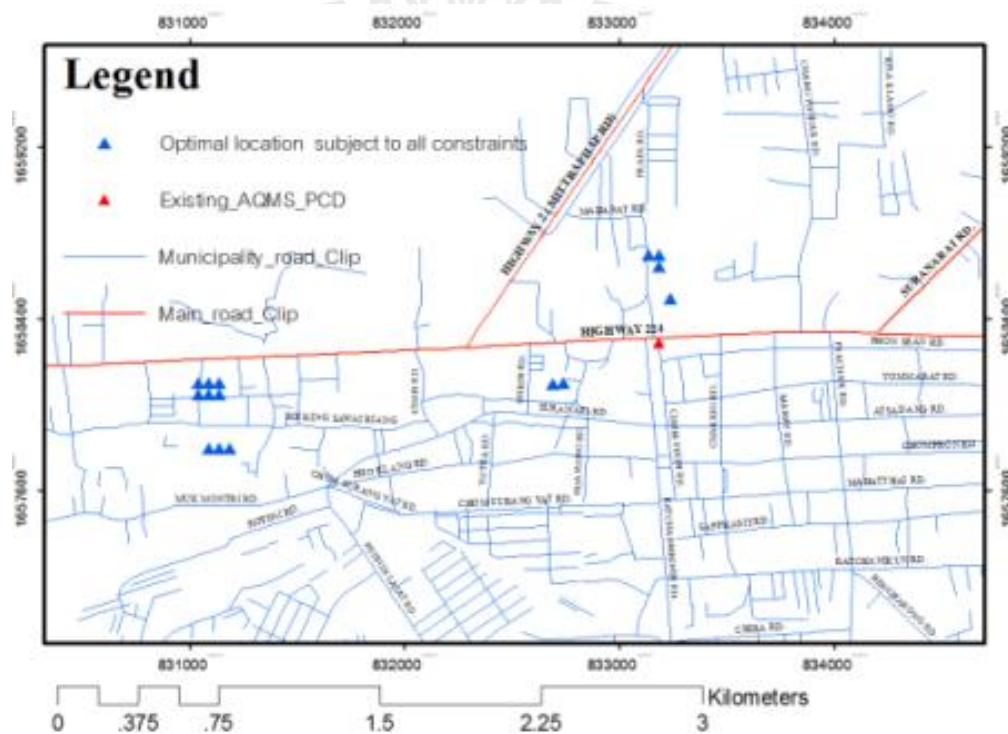


Figure 4.24 Result of optimal locations of AQMS using multi-objective function subject to all constraints.

4.7 Sensitivity analysis of spatial multi-objective model

The purpose of the sensitivity analysis was to examine which objective function(s) could influence the model result. The analysis was performed by varying weights of all objective functions. The weight of each objective function was increased, one at a time, while others were still kept the same.

The groups of weight assigned to objective functions, 12 variations, were: $(0.4Z_1, 0.2Z_2, 0.2Z_3, 0.2Z_4)$, $(0.5Z_1, 0.167Z_2, 0.167Z_3, 0.167Z_4)$, $(0.6Z_1, 0.133Z_2, 0.133Z_3, 0.133Z_4)$, $(0.2Z_1, 0.4Z_2, 0.2Z_3, 0.2Z_4)$, $(0.167Z_1, 0.5Z_2, 0.167Z_3, 0.167Z_4)$, $(0.133Z_1, 0.6Z_2, 0.133Z_3, 0.133Z_4)$, $(0.2Z_1, 0.2Z_2, 0.4Z_3, 0.2Z_4)$, $(0.167Z_1, 0.167Z_2, 0.5Z_3, 0.167Z_4)$, $(0.133Z_1, 0.133Z_2, 0.6Z_3, 0.133Z_4)$, $(0.2Z_1, 0.2Z_2, 0.2Z_3, 0.4Z_4)$, $(0.167Z_1, 0.167Z_2, 0.167Z_3, 0.5Z_4)$, and $(0.133Z_1, 0.133Z_2, 0.133Z_3, 0.6Z_4)$, where Z_1 , Z_2 , Z_3 , and Z_4 are pollution intensity, frequency of violence, service area and, people exposure impact, respectively.

Locations of 15 alternative sites resulted from weighting objective functions in range of 0.4 to 0.6 were displayed in Figures 4.25-4.36. Figures 4.25-4.27 show a location of 15 alternative sites resulted from higher weighting to pollution intensity (0.4-0.6). They were located at the same positions. It indicated that the pollution intensity played important role in location. Likewise, Figures 4.28-4.35, resulted from higher weighting to frequency of violence and service area, show similar tendency of proposed AQMS locations. This was because frequency of violence and service area were determined based on pollution intensity. However, the distribution of alternative locations was obviously different when weight of 0.6 was applied to people exposure impact (Figure 4.36). The alternative sites determined were located nearby Mueang school and existing AQMS of the PCD. From results of sensitivity analysis, the

positions of AQMSs could be located in two different zones depending on application approaches between monitoring the highest pollution and population impact. However, the results were not specified a number of sites. This required screening the number of AQMSs.

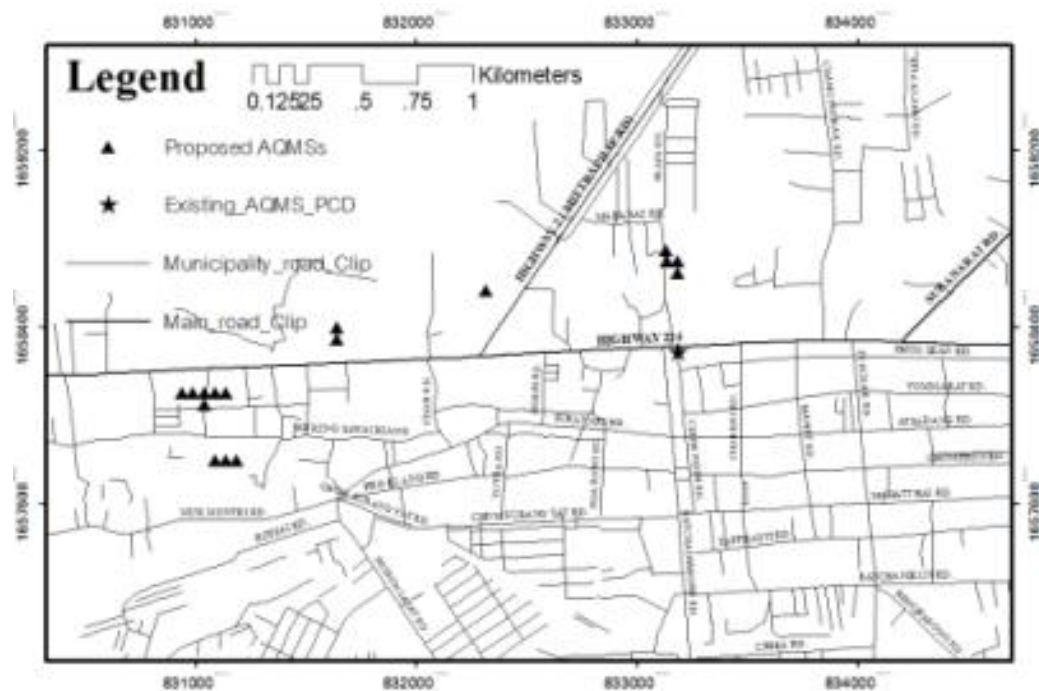


Figure 4.25 Location of AQMSs with varying weighted of objective functions as $(0.4Z_1, 0.2Z_2, 0.2Z_3, \text{ and } 0.2Z_4)$.

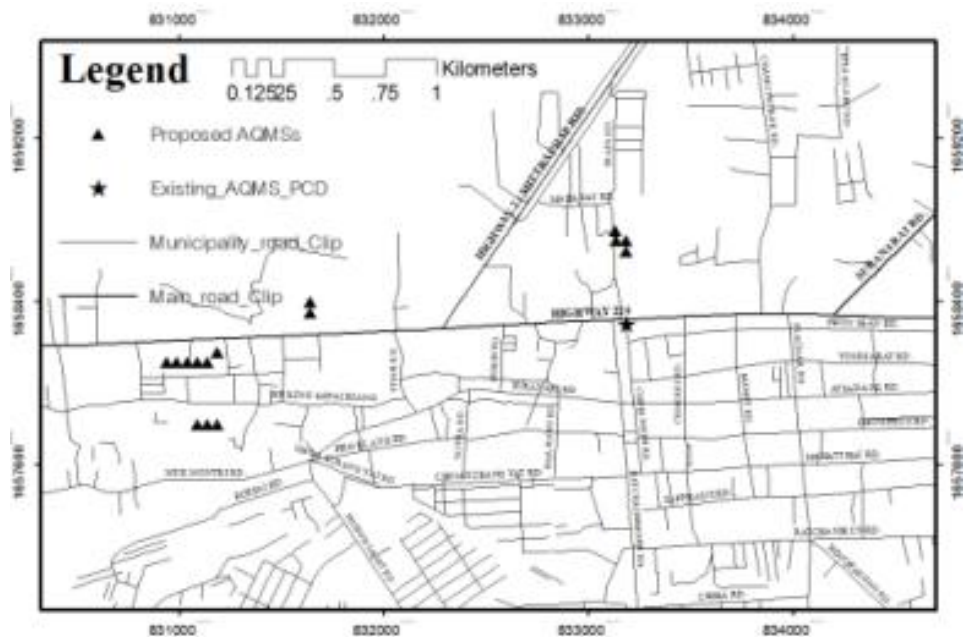


Figure 4.26 Location of AQMSs with varying weighted of objective functions as $(0.5Z_1, 0.167Z_2, 0.167Z_3, \text{ and } 0.167Z_4)$.

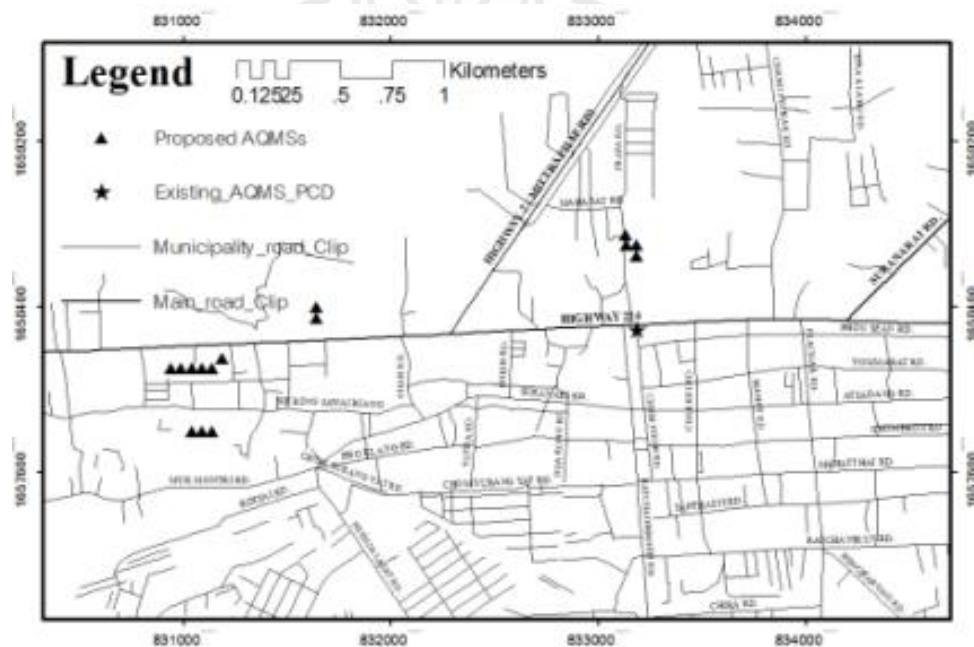


Figure 4.27 Location of AQMSs with varying weighted of objective functions as $(0.6Z_1, 0.133Z_2, 0.133Z_3, \text{ and } 0.133Z_4)$.

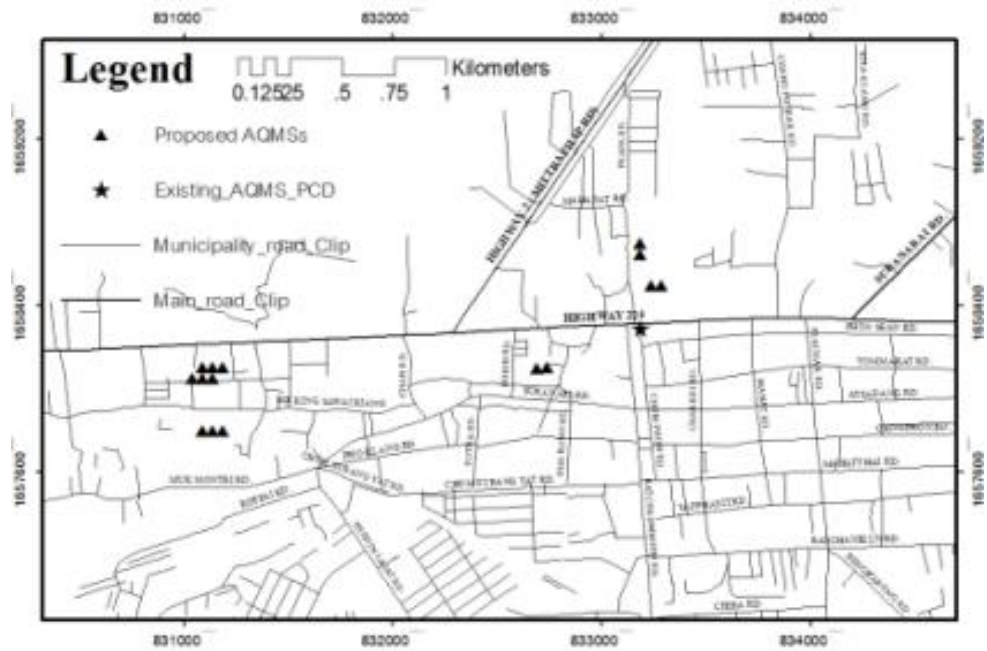


Figure 4.28 Location of AQMSs with varying weighted of objective functions as $(0.2Z_1, 0.4Z_2, 0.2Z_3, \text{ and } 0.2Z_4)$.

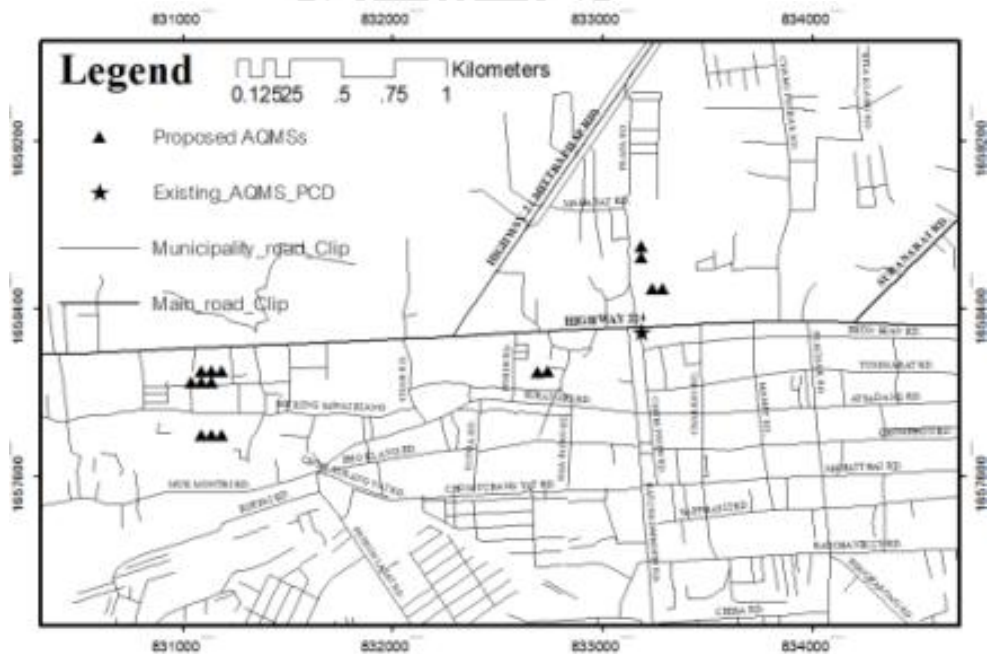


Figure 4.29 Location of AQMSs with varying weighted of objective functions as $(0.167Z_1, 0.5Z_2, 0.167Z_3, \text{ and } 0.167Z_4)$.

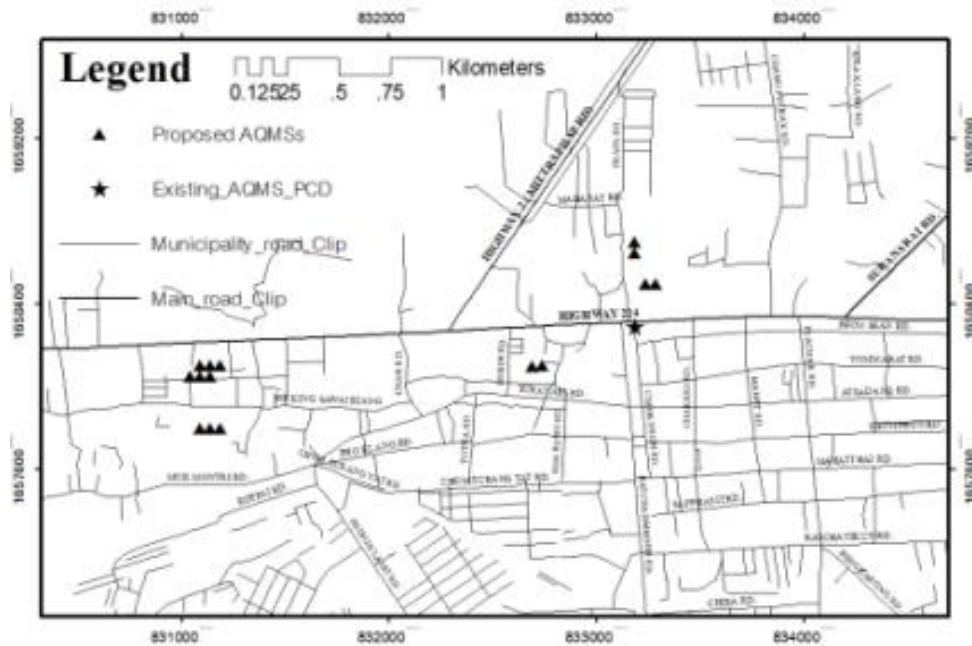


Figure 4.30 Location of AQMSs with varying weighted of objective functions as $(0.133Z_1, 0.6Z_2, 0.133Z_3, \text{ and } 0.133Z_4)$.

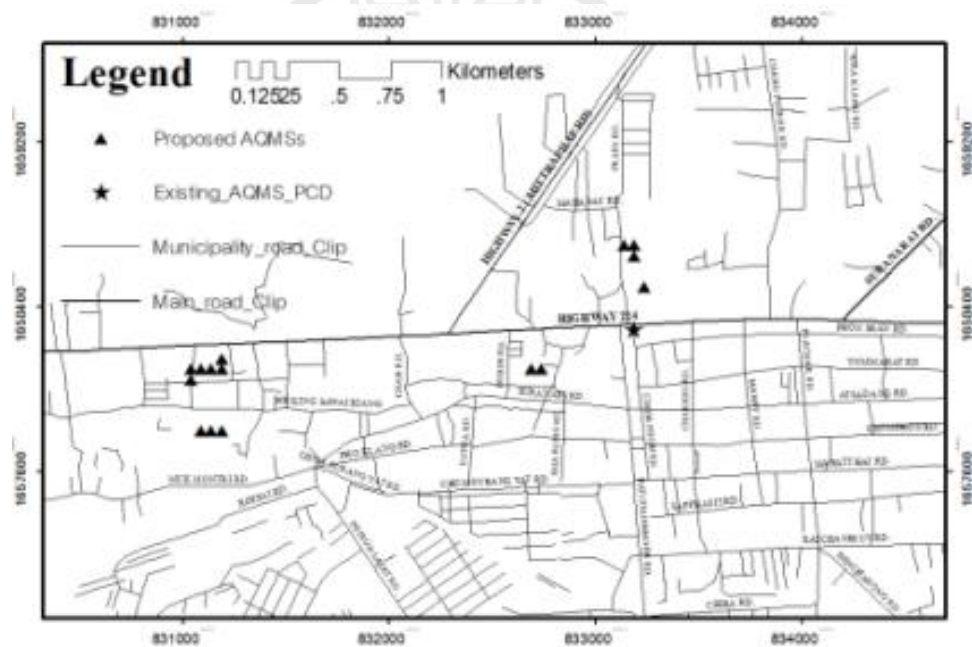


Figure 4.31 Location of AQMSs with varying weighted of objective functions as $(0.2Z_1, 0.2Z_2, 0.4Z_3, \text{ and } 0.2Z_4)$.

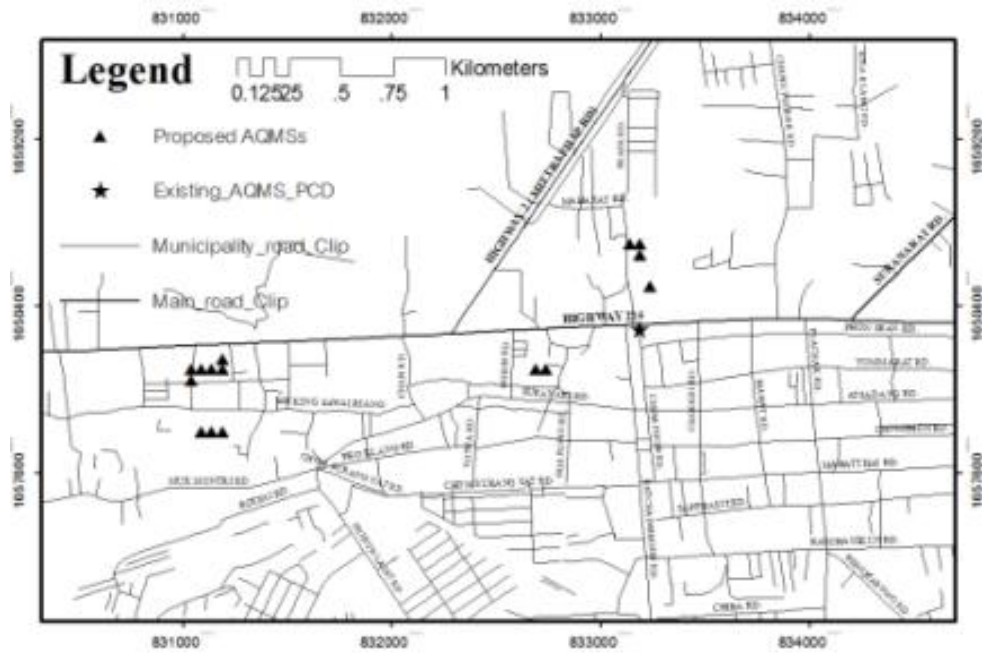


Figure 4.32 Location of AQMSs with varying weighted of objective functions as $(0.167Z_1, 0.167Z_2, 0.5Z_3, \text{ and } 0.167Z_4)$.

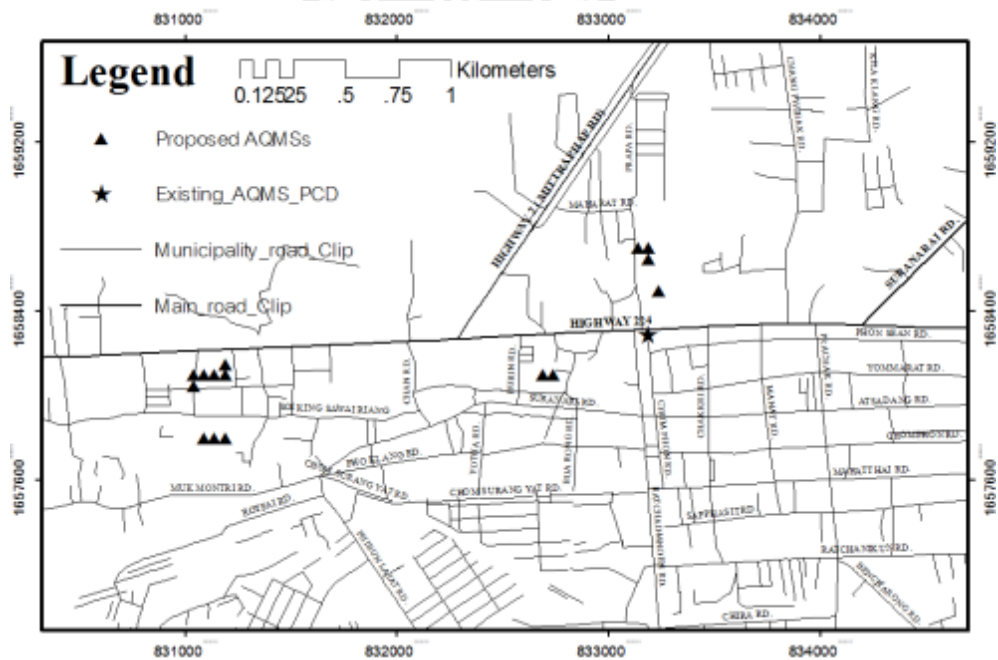


Figure 4.33 Location of AQMSs with varying weighted of objective functions as $(0.133Z_1, 0.133Z_2, 0.6Z_3, \text{ and } 0.133Z_4)$.

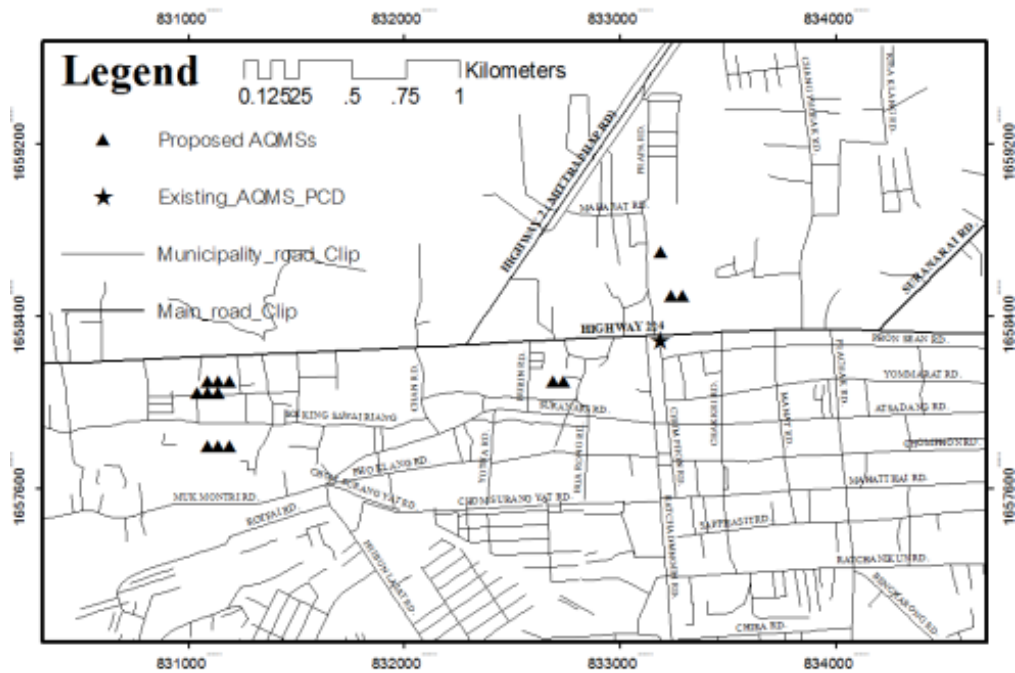


Figure 4.34 Location of AQMSs with varying weighted of objective functions as $(0.2Z_1, 0.2Z_2, 0.2Z_3, \text{ and } 0.4Z_4)$.

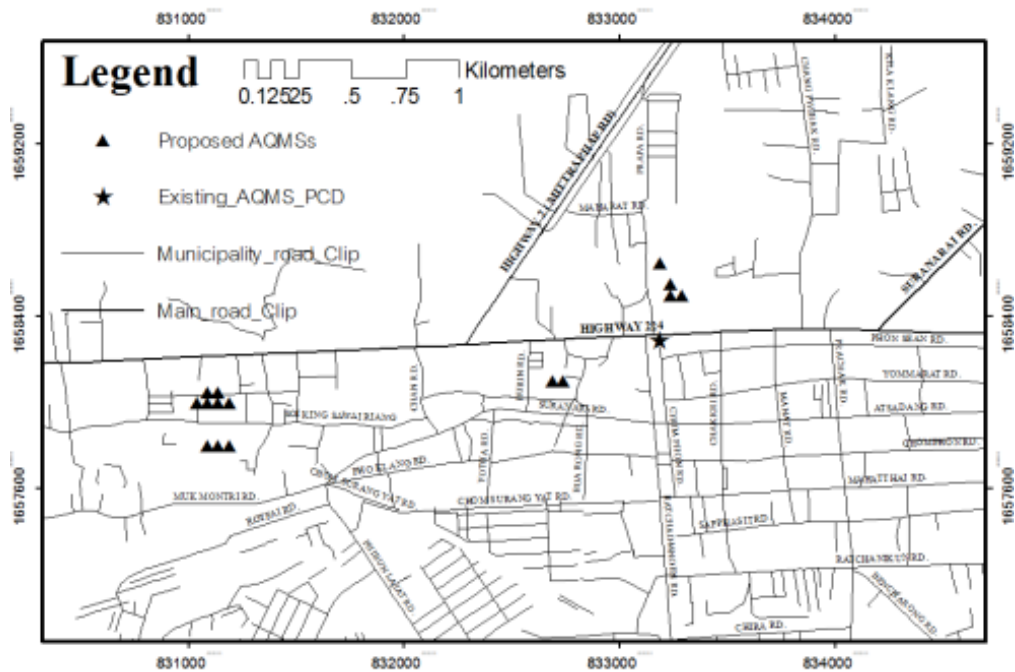


Figure 4.35 Location of AQMSs with varying weighted of objective functions as $(0.167Z_1, 0.167Z_2, 0.167Z_3, \text{ and } 0.5Z_4)$.

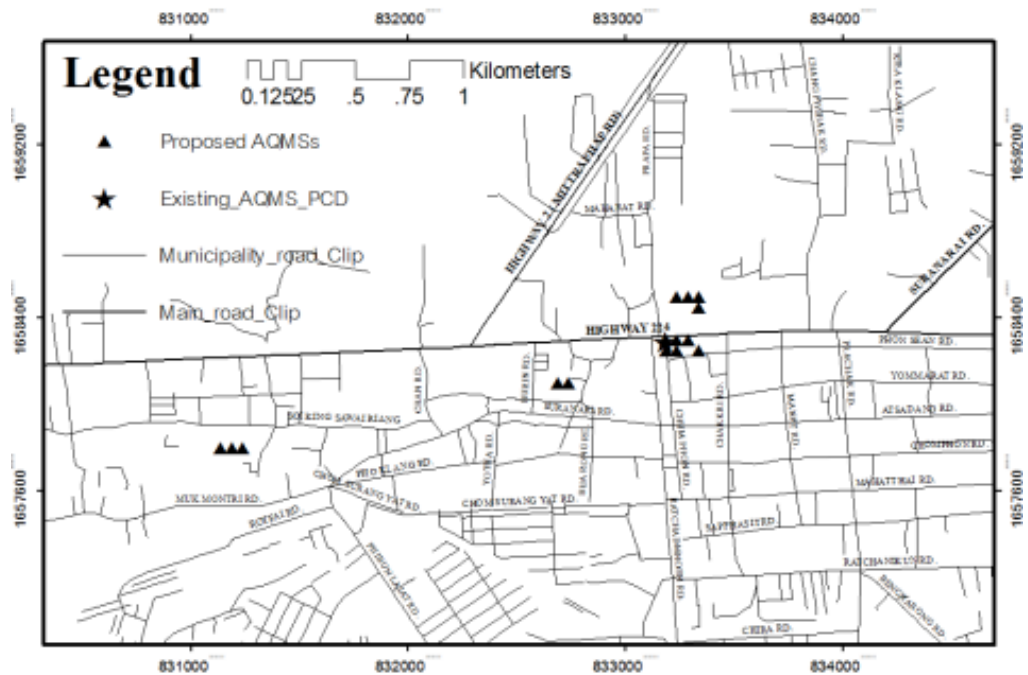


Figure 4.36 Location of AQMSs with varying weighted of objective functions as $(0.133Z_1, 0.133Z_2, 0.133Z_3, \text{ and } 0.6Z_4)$.

4.8 Screening a suitable position

From the total 12 variations of sensitivity analysis, the position providing the highest score of total objective functions of each variation were put in order according to its Moran's I and its score as shown in Table 4.6. Their Moran's I were determined from the service area with $200(L_n)$ searching tolerance and each cell contained total score from all objective functions. Weighting from 0.4 to 0.6 of each objective function provided the highest spatial autocorrelation ranged 0.70-0.76 and highest score of all objective functions in range of 3.15 to 3.66.

From the Table 4.6, three best positions could be extracted. Their coordinates were $X_1 = 831,100$ m and $Y_1 = 1,658,100$ m, $X_2 = 833,200$ m and $Y_2 = 1,658,500$ m, and $X_3 = 833,200$ m and $Y_3 = 1,658,300$ m. The first best position reflected the

influence from pollution intensity (Z_1), frequency of violence (Z_2), and service area (Z_3) while the last two positions reflected the influenced from people exposure impact (Z_4). Therefore, the only three potential points of new stations were suggested from the study (Figure 4.37). However, the last two positions were located very close to the existing PCD station. Therefore, the first best position with coordinate $X_1 = 831,100$ m and $Y_1 = 1,658,100$ m was strongly recommended to be the new station required.

Table 4.6 Influence of changing score weight pattern to related with co-ordinate, maximum spatial autocorrelation and total score of all objectives function.

Weighting with objectives function scale ranged (0.4-0.6)	Optimal location on coordinate (X, Y) (meter)	Highest spatial autocorrelation based search tolerance $L_n = 200$	Highest combined objectives function (Z_1 to Z_4)
$0.4Z_1, 0.2Z_2, 0.2Z_3, 0.2Z_4$	(831100, 1658100)	0.76	3.66
$0.5Z_1, 0.167Z_2, 0.167Z_3, 0.167Z_4$	(831100, 1658100)	0.76	3.66
$0.6Z_1, 0.133Z_2, 0.133Z_3, 0.133Z_4$	(831100, 1658100)	0.76	3.66
$0.2Z_1, 0.4Z_2, 0.2Z_3, 0.2Z_4$	(831100, 1658100)	0.76	3.66
$0.167Z_1, 0.5Z_2, 0.167Z_3, 0.167Z_4$	(831100, 1658100)	0.76	3.66
$0.133Z_1, 0.6Z_2, 0.133Z_3, 0.133Z_4$	(831100, 1658100)	0.76	3.66
$0.2Z_1, 0.2Z_2, 0.4Z_3, 0.2Z_4$	(831100, 1658100)	0.76	3.66
$0.167Z_1, 0.167Z_2, 0.5Z_3, 0.167Z_4$	(831100, 1658100)	0.76	3.66
$0.133Z_1, 0.133Z_2, 0.6Z_3, 0.133Z_4$	(831100, 1658100)	0.76	3.66
$0.2Z_1, 0.2Z_2, 0.2Z_3, 0.4Z_4$	(833200, 1658500)	0.72	3.45
$0.167Z_1, 0.167Z_2, 0.167Z_3, 0.5Z_4$	(833200, 1658500)	0.72	3.45
$0.133Z_1, 0.133Z_2, 0.133Z_3, 0.6Z_4$	(833200, 1658300)	0.70	3.15

The new proposed AQMS location resulted from the study could monitor the area expressing highest pollution intensity, frequency of violence, and service area. Even though this position reflected less people exposure impact when compared to the other two proposed positions, in fact, it was located opposite to the mall commercial center where big amount of people have been present. The position expressed high pollution intensity due to being nearby road section with heavy traffic. Also, it was close to the section of the Mittrapap road where traffic always drained from all nearby road connection. Finally, it is fair to say that the developed model in this study does not merely provide new location of station that meet regulatory requirements, but also provide the second best station locations which were located very near to the existing PCD station.

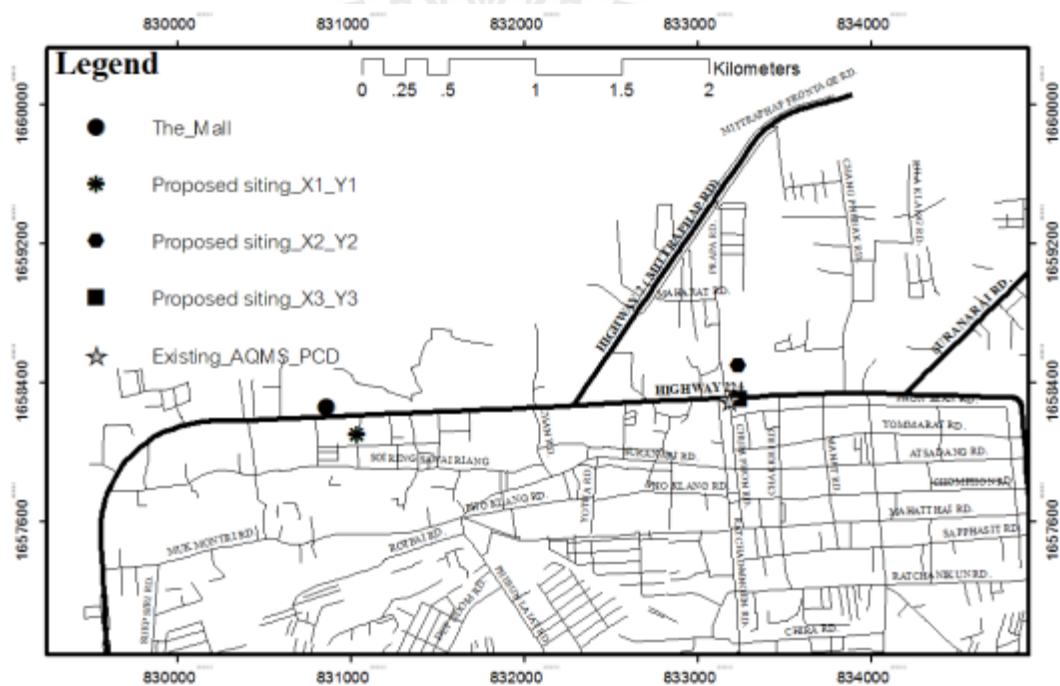


Figure 4.37 Positioning of proposed AQMSs compared with existing AQMS.

CHAPTER V

CONCLUSIONS AND RECOMMENDATION

5.1 Conclusions

The objectives of the study include: (1) to generate the representative spatial distributions of air pollution (CO, NO_x, and PM10) in the Nakhon Ratchasima municipality area using CALINE4 Gaussian model and people exposure impact using fuzzy membership, and (2) to determine proper positions of AQMSs using the spatial multi-objective decision analyses. Results and findings can be herein summarized as follows.

5.1.1 Pollution distribution and people exposure impact

The simulation of pollutant concentrations was obtained from a Gaussian diffusion equation/model (CALINE4). In order to evaluate the accuracy of the model, the R-square method was carried out by comparing predicted and observed CO concentration within 10 meters buffer from the eight study sites. The results of R-square value as 0.76 suggested that the CALINE4 model could predict satisfactory CO concentration. However, a lack of NO_x and PM10 measurement instrument were caused some inaccurate results of pollutant mapping. Therefore, for more effective future study, information of ground measurement of both pollutants should be available for modeling and validation. This requires tools for both pollutants measurement.

In recent years, the application of GIS has increased in order to identify and assess various polluted areas. Spatial distribution maps of all pollutants were generated using the GIS interpolation approach. It can combine automated cartographic features with database management capabilities. For this study, the strengths of GIS in data management, spatial analysis, and raster modeling were incorporated into three critical steps of pollution distribution modeling: wind speed and directions, ambient concentration of gases, and concentration of particulate matter. The results were presented as pollution maps.

The finding on highest pollution intensity area covered where most of the facilities such as commercial center and education have been located. They are the area surrounding Mittrapap Road in front of the Mall and Mueang Nakhon Ratchasima school. Likewise, almost of alternatives falling into this area rather provided the highest service area.

Slightly different, the maximum frequency of violence patches could be obviously observed on the area surrounding Mittrapap Road in front of the Mall and Tesco Lotus department stores. The frequency of violence of all pollutants tended to increase in high-traffic-volume road network. Temporally, the highest pollution intensity and frequency of violence severely threatened to the area at two peak hours which was caused by the traffic congestion at several intersections along roads.

Map of people exposure impact displayed that the high impact was subject to the area of education institutes which were Mueang Nakhon Ratchasima school, Nakhon Ratchasima Vocation College, and Suranaree Wittaya school, and local markets. Nonetheless, these maps could not identify a number and location of

AQMSs. Therefore, the determination of proper location of AQMSs was achieved using spatial multi-objective method.

Conclusively, the study showed that GIS and the Gaussian model through CALINE4 which is proper for line-source pollution distribution could be used to simulate pollution distribution and derivative map successfully.

5.1.2 Positions of AQMSs using the spatial multi-objective decision analyses

The study described problems and solutions of optimization models for determining the optimal locations of Air Quality Monitoring Stations (AQMSs) in urban area of Nakhon Ratchasima municipality using various objective functions. These functions included maximization pollution intensity, frequency of violence, service area, and people exposure impact. Constraints set up as input for the linear programming of MODA covered a number of alternatives, specified numbers of alternatives in certain zones classified based on the map resulting from combining all objective function products, and cut-off proper service area.

The results of finding a proper position of AQMSs were shown as points/sites located in the highest-score area of combined objective functions. These candidate sites were reassessed using sensitivity analysis. The results found that the best position with coordinate $X_1 = 831,100$ m and $Y_1 = 1,658,100$ m was strongly recommended to be the new station required. The new proposed AQMS location was located at area expressing highest pollution intensity, frequency of violence, and service area. This is implied that the spatial multi-objective models could identify a proper position of AQMS attributing all specifications.

5.2 Recommendations for future improvements:

To consider various objective functions under conflict constraint functions. The results of a proper position may not located on optimal location. Several forms of non-linear programming could find optimal solution. For example, the min-max optimization model is designed objective function. The proposed objective function should be simultaneously designed for both of minimal a number of station and maximal objective function based on same constraint functions .

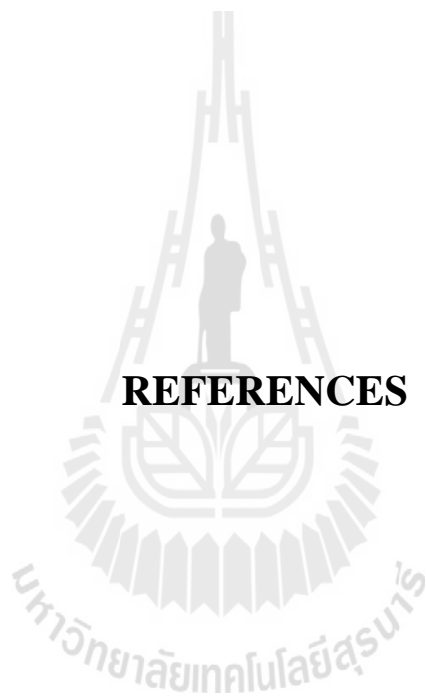
For further study in this field of research, some points could be recommended as follows.

(1) Pollution intensity of other kinds of pollutants such as ozone and hydrocarbons could be included in the optimization procedures in case field data are available.

(2) This study considered only line source of pollution as determined by CALINE 4, No pollution from hot spots is combined to the one from the line source. The whole regime of pollution intensity in the area could be clearer figured out if this is included.

(3) Finally, it is highly recommended to reevaluate the appropriate locations of stations after 5 years of operation, as the tendency of traffic volume on minor roads are expected to increase by an average of 5 per cent every year (สำนักงานนโยบายและแผนการขนส่งและจราจร, 2550). By doing so, modeling of air pollution and optimization models will be extremely useful tool for future assessment of proper zone of the AQMSs.

REFERENCES



REFERENCES

- กรมการปกครอง. (2552). การบริการข้อมูลด้านสถิติ ข้อมูลจำนวนประชากรประจำปี [ออนไลน์] : http://203.113.86.149/stat/y_stat50.html.
- กรมควบคุมมลพิษ. (2550). รายงานประจำปีห้องปฏิบัติการตรวจวัดมลพิษจากยานพาหนะ [ออนไลน์]: <http://www.pcd.go.th/download/air.cfm>.
- กุลธิดา ตระสินธุ์. (2547). มลพิษอากาศที่บุคคลได้รับจากการเดินทางและการจราจรในเขตเทศบาลนครนครราชสีมา. วิทยานิพนธ์ปริญญาโทบริหารธุรกิจ. สาขาวิชาวิศวกรรมสิ่งแวดล้อม. มหาวิทยาลัยเทคโนโลยีสุรนารี.
- ชุมพล ศรีประภากร. (2544). การประยุกต์แบบจำลองคุณภาพอากาศริมถนน CALINE4 เพื่อการพยากรณ์ระดับปริมาณฝุ่นละอองริมถนนกรุงเทพมหานคร. วิทยานิพนธ์ปริญญาโทบริหารธุรกิจ. สาขาวิชาวิทยาศาสตร์สภาวะแวดล้อม. จุฬาลงกรณ์มหาวิทยาลัย.
- คุณหญิง ม่วงยา และสาวิตรี กุฎิสุข. (2545). โครงการศึกษาปริมาณก๊าซคาร์บอนมอนนอกไซด์จากการจราจรและเปรียบเทียบแบบจำลองทางคณิตศาสตร์ สำหรับการแพร่กระจายมลพิษทางอากาศบนถนนรอบสถาบันราชภัฏสวนสุนันทา. กรุงเทพฯ.
- ศิวพันธุ์ ชูอินทร์. (2544). แบบจำลองทางคณิตศาสตร์เพื่อประมาณความเข้มข้นก๊าซคาร์บอนมอนอกไซด์และก๊าซออกไซด์ของไนโตรเจนในถนนที่มีลักษณะคล้ายอุโมงค์. วิทยานิพนธ์ปริญญาโทบริหารธุรกิจ. สาขาวิชาวิทยาศาสตร์สิ่งแวดล้อม. มหาวิทยาลัยธรรมศาสตร์.
- สงวน กมลวัฒน์. (2537). การศึกษาปริมาณการปลดปล่อยก๊าซมลพิษจากการจราจรบริเวณ ใกล้ทางด่วนและเปรียบเทียบกับแบบจำลองคณิตศาสตร์. วิทยานิพนธ์ปริญญาโทบริหารธุรกิจ. สาขาเทคโนโลยีสิ่งแวดล้อม. มหาวิทยาลัยเทคโนโลยีพระจอมเกล้าธนบุรี.
- สำนักงานนโยบายและแผนการขนส่งและจราจร. (2550). โครงการศึกษาวางแผนแม่บทด้านการจราจรและขนส่งเมืองในภูมิภาค: จังหวัดนครราชสีมา.
- อาทิตย์ ทิพย์ชัย. (2548). การประยุกต์ใช้ระบบสารสนเทศภูมิศาสตร์สำหรับวิเคราะห์มลพิษทางอากาศจากการจราจรในเขตเมือง. วารสารวิจัย มหาวิทยาลัยขอนแก่น. 10(4).

- Arbeloa F.J.S., Caseiras C.P., and Andres P.M.L. (1993). Air quality monitoring: optimization of a network around a hypothetical potash plant in open countryside. **Atmospheric Environment**. 27A(5): 729–38.
- Bazaraa, M.S., Jarvis, J.J., and Sherali, H.D. (1990). **Linear programming and network flows**. New York: John Wiley & Sons.
- Caltrans (1989). **CALINE4—A dispersion model for predicting air pollutant concentrations near roadways, Final Report prepared by the Caltrans Division of New Technology and Research**. FHWA/CA/TL: 84/15.
- Chang, N.B. and Tseng, C.C. (1999). Optimal design of a multi-pollutant air quality monitoring network in a metropolitan region using Khohsiung, Taiwan as an example. **Environmental Monitoring and Assessment**. 57: 121–148.
- Chen, C.H., Liu, W.L., and Chen, C.H. (2006). Development of a multiple objective planning theory and system for sustainable air quality monitoring networks. **Science of the Total Environment**. 354: 1–19.
- Chen, S.J. and Hwang, C.L. (1992). Fuzzy multiple attribute decision making. **Berlin: Springer-Verlag**.
- Dabberdt, W., Hoydyshb, W., Schorling, M., Yangb, F., and Holynskyjb, O. (1995). Dispersion modeling at urban intersections. **The Science of the Total Environment**. 169: 93–102.
- Elkamel, A., Fatehifar, E., Taheri, M., Al-Rashidi M.S., and Lohi, A. (2007). A heuristic optimization approach for Air Quality Monitoring Network design with the simultaneous consideration of multiple pollutants. **Journal of Environmental Management**. 88: 507–516.
- ESRI. (2010). ArcMap 9.3 [Computer software]. New York: ESRI.

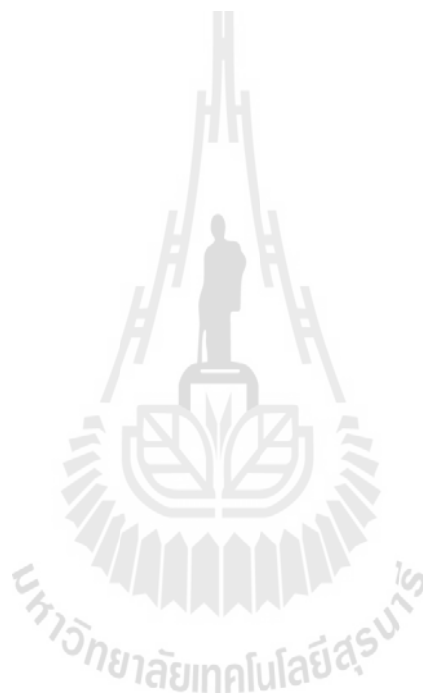
- Fouda, Y.E. (2001). A GIS for environmental assessment of air pollution impacts on urban clusters and natural landscape at Rosetta City and region, Egypt. **Urban Ecosystems**. 5: 5–25.
- Ganguly, R., Broderick, B.M., and Donoghue, R.O. (2009). Assessment of a General Finite Line Source Model and CALINE4 for Vehicular Pollution Prediction in Ireland. **Environ Model Assess**. 14: 113–125.
- Gramotnev, G., Brown, R., Ristovski, Z., Hitchins, J., & Morawska, L. (2003). Determination of average emission factors for vehicles on a busy road. **Atmospheric Environment**. 37(4): 465–474.
- Gualtieri, G. and Tartaglia, M. (1998). Predicting urban traffic air Pollution: A GIS framework. **Transportation Research**. 3: 329–336.
- Gualtieri, G. and Tartaglia, M. (1998). Predicting urban traffic air pollution: A GIS framework. *Transportation Research Part D: Transport and Environment*. 3(5): 329–336.
- Held, T., Chang, D.P.Y., and Niemeier, D.A. (2003). UCD 2001: An improved model to simulate pollutant dispersion from road ways. **Atmospheric Environment**. 37(38): 5325–5336.
- Holmes, N.S. and Morawska L. (2006). A review of dispersion modeling and its application to the dispersion of particles: An overview of different dispersion models available. **Atmospheric Environment**. 40: 5902–5928.
- Jerrett, M., Gale, S., and Kontgis, C. (2010). Spatial modeling in environmental and public health research. **International Journal of Environmental Research and Public Health**. ISSN 1660–4601.

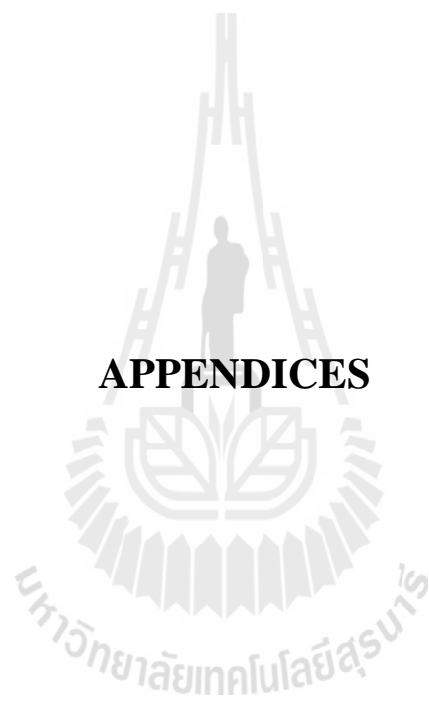
- Kang, Y., Chun, L.M., Jie, C.Z., and Qi, L. (2009). Urban air pollution study based on GIS. **Urban Remote Sensing Joint Event**.
- Kao, J.J. and Hsieh, M.R. (2006). Utilizing multi-objective analysis to determine an air quality monitoring network in an industrial district. **Atmospheric Environment**. 40: 1092–1103.
- Kenty, K.L., Poor, N.D., Kronmiller, K.G., McClenny W., Kinge C., Atkesonf T., and Campbell S.W. (2007). Application of CALINE4 to roadside NO/NO₂ transformations. **Atmospheric Environment**. 41: 4270–4280.
- Klir, G.J. and Yuan B. (1995). **Fuzzy sets and fuzzy logic: theory and applications**. Upper Saddle River, Nj: Prentice Hall.
- Levitin, O., Harkonenb, J., Kukkonenb, J., and Nikmob, J. (2005). Evaluation of the CALINE4 and CAR–FMI models against measurements near a major road. **Atmospheric Environment**. 39: 4439–4452.
- Li, B., Tao, S., Dawsona, R.W., Caoa, J., and Lamb, K. (2002). A GIS based road traffic noise prediction model. **Applied Acoustics**. 63: 679–691.
- Lin, M.D. and Lin, Y.C. (2002). The application of GIS to air quality analysis in Taichung City, Taiwan, ROC. **Environmental Modeling & Software**. 17: 11–19.
- Lozano, A., Usero, J., Vanderlinden, E., Raez, J., Contreras, J., and Navarrete, B. (2009). Air quality monitoring network design to control nitrogen dioxide and ozone, applied in Malaga, Spain. **Microchemical Journal**. 93: 164–172.
- Malczewski, J. (1999). **GIS and Multi Criteria Decision Analysis**. New York: John Wiley& Sons.

- Marmur, A. and Mamane, Y. (2003). Comparison and evaluation of several mobile-source and line-source models in Israel. *Transportation Research Part D: Transport and Environment*. 8(4): 249–265.
- McElroy, J.L., Behar, J.V., Meyers, T.C., and Liu, M.K., (1986). Methodology for designing air quality monitoring networks: II. Application to Las Vegas, Nevada, for carbon monoxide. *Environmental Monitoring and Assessment*. 6: 13.
- Modak, P.M. and Lohani, B.N. (1985). Optimization of ambient air quality monitoring networks: part I. *Environmental Monitoring and Assessment*. 5: 1–19.
- Mofarrah, A. and Husain, T. (2010). A holistic approach for optimal design of air quality monitoring network expansion in an urban area. *Atmospheric Environment*. 44: 432–440.
- Moragues, A. and Alcaide, T. (1996). The use of a geographical information system to assess the effect of traffic pollution. *The Science of the Total Environment*. 189/190: 267–273.
- Moran, P. A. P. (1950). Notes on Continuous Stochastic Phenomenon. *Biometrika* 37 (1): 17–23.
- Oke, T.R. (1978). *Boundary Layer Climates*. Methun & Co Ltd, London, p.372.
- Parker, A. (1978). *Industrial Air Pollution Handbook*. McGraw-Hill Book Company (UK) Limited, London, p.658.
- Pasquill, F. and Smith, F.B. (1982). *Atmospheric diffusion (3rd ed)*. Ellis Horwood. Chichester.

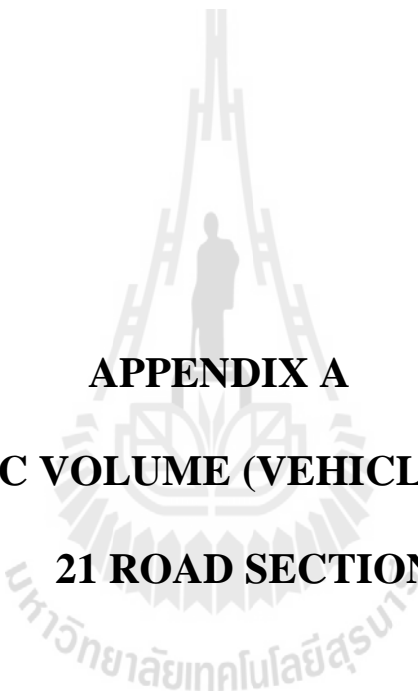
Turner, D.B. (1970). **Workbook of Atmospheric Dispersion Estimates**. Lewis Publishers. Boca Raton.

USEPA. (2006). Planning and standards. [On-line]. Available: <http://www.epa.gov/ttn/amtic/pamsgram.html>.





APPENDICES



APPENDIX A
TRAFFIC VOLUME (VEHICLE/HOUR) OF
21 ROAD SECTIONS

Table A.1 Traffic volume (V/H) of Mittrapap Rd. (Samyakpak to Jet-gas station).

Time periods (24/03/2010)	PLDGV	LDDT	HDDT	BUS	MC2	MC4
(07:00-08:00)	1518	341	125	234	1498	20
(08:00-09:00)	1651	154	120	148	1090	12
(09:00-10:00)	1012	542	370	349	1067	17
(12:00-13:00)	1437	193	65	136	1058	20
(14:00-15:00)	1327	146	78	110	971	28
(15:00-16:00)	1525	88	130	220	1053	7
(16:00-17:00)	1527	137	62	92	1119	20
(18:00-19:00)	1505	70	115	219	1128	27

Table A.2 Traffic volume (V/H) of Mittrapap Rd. (Jet-gas station to Tesco lotus).

Time periods (25/03/2010)	PLDGV	LDDT	HDDT	BUS	MC2	MC4
(07:00-08:00)	1851	309	155	285	1145	21
(08:00-09:00)	1958	143	135	176	1013	33
(09:00-10:00)	1213	498	442	418	980	41
(12:00-13:00)	1655	184	76	157	1012	24
(14:00-15:00)	1501	142	87	124	948	30
(15:00-16:00)	1781	83	147	257	995	7
(16:00-17:00)	1767	130	71	106	1066	19
(18:00-19:00)	1762	66	133	256	1062	25

Table A.3 Traffic volume (V/H) of Mittrapap Rd. (Tesco lotus to The Mall).

Time periods (25/03/2010)	PLDGV	LDDT	HDDT	BUS	MC2	MC4
(07:00-08:00)	1851	309	155	285	1145	21
(08:00-09:00)	1958	143	135	176	1013	33
(09:00-10:00)	1213	498	442	418	980	41
(12:00-13:00)	1655	184	76	157	1012	24
(14:00-15:00)	1501	142	87	124	948	30
(15:00-16:00)	1781	83	147	257	995	7
(16:00-17:00)	1767	130	71	106	1066	19
(18:00-19:00)	1762	66	133	256	1062	25

Table A.4 Traffic volume (V/H) of Mittrapap Rd. (The Mall to 3-junction Big-C).

Time periods (25/03/2010)	PLDGV	LDDT	HDDT	BUS	MC2	MC4
(07:00-08:00)	1851	309	155	285	1145	21
(08:00-09:00)	1958	143	135	176	1013	33
(09:00-10:00)	1213	498	442	418	980	41
(12:00-13:00)	1655	184	76	157	1012	24
(14:00-15:00)	1501	142	87	124	948	30
(15:00-16:00)	1781	83	147	257	995	7
(16:00-17:00)	1767	130	71	106	1066	19
(18:00-19:00)	1762	66	133	256	1062	25

Table A.5 Traffic volume (V/H) of Mittrapap Rd. (3-junction Big-C to Pigasus).

Time periods (26/03/2010)	PLDGV	LDDT	HDDT	BUS	MC2	MC4
(07:00-08:00)	1228	205	103	190	760	16
(08:00-09:00)	1384	102	96	125	716	23
(09:00-10:00)	836	343	304	288	675	28
(12:00-13:00)	1245	139	58	118	761	18
(14:00-15:00)	1176	111	69	98	743	23
(15:00-16:00)	1305	61	109	189	729	7
(16:00-17:00)	1318	97	54	79	795	14
(18:00-19:00)	1281	48	96	186	773	18

Table A.6 Traffic volume (V/H) of Highway 224. (3-junction Big-C to Sunararee withthaya school).

Time periods (27/03/2010)	PLDGV	LDDT	HDDT	BUS	MC2	MC4
(07:00-08:00)	1775	302	149	274	1198	22
(08:00-09:00)	1888	131	130	170	1277	31
(09:00-10:00)	1168	465	426	403	1243	33
(12:00-13:00)	1606	135	73	152	1382	21
(14:00-15:00)	1461	143	84	120	1023	21
(15:00-16:00)	1722	101	141	248	1156	12
(16:00-17:00)	1712	129	70	103	1236	14
(18:00-19:00)	1703	255	128	248	1214	28

Table A.7 Traffic volume (V/H) of Suranarai Rd. (3-junction).

Time periods (28/03/2010)	PLDGV	LDDT	HDDT	BUS	MC2	MC4
(07:00-08:00)	753	291	63	116	1298	23
(08:00-09:00)	948	124	64	85	1117	34
(09:00-10:00)	547	468	117	188	1243	39
(12:00-13:00)	931	148	42	88	1085	32
(14:00-15:00)	926	154	53	76	1256	26
(15:00-16:00)	941	189	77	135	1243	19
(16:00-17:00)	975	133	39	57	1034	21
(18:00-19:00)	915	167	69	133	1112	26

Table A.8 Traffic volume (V/H) of Suranarai Rd. (3-junction to Rajaphat Korat).

Time periods (28/03/2010)	PLDGV	LDDT	HDDT	BUS	MC2	MC4
(07:00-08:00)	753	291	63	116	1298	23
(08:00-09:00)	948	124	64	85	1117	34
(09:00-10:00)	547	468	117	188	1243	39
(12:00-13:00)	931	148	42	88	1085	32
(14:00-15:00)	926	154	53	76	1256	26
(15:00-16:00)	941	189	77	135	1243	19
(16:00-17:00)	975	133	39	57	1034	21
(18:00-19:00)	915	167	69	133	1112	26

Table A.9 Traffic volume (V/H) of Highway 224 (Suranaree wittaya school to Huatalay junction).

Time periods (29/03/2010)	PLDGV	LDDT	HDDT	BUS	MC2	MC4
(07:00-08:00)	2451	296	6	19	1098	23
(08:00-09:00)	2211	138	13	16	977	29
(09:00-10:00)	1590	479	17	15	943	7
(12:00-13:00)	2453	179	17	37	982	23
(14:00-15:00)	2303	139	28	41	923	29
(15:00-16:00)	2386	80	25	45	963	8
(16:00-17:00)	2575	126	14	23	1033	11
(18:00-19:00)	2474	64	21	40	1027	21

Table A.10 Traffic volume (V/H) of Mukkamontri Rd. (Sawairiang).

Time periods (01/03/2010)	PLDGV	LDDT	HDDT	BUS	MC2	MC4
(07:00-08:00)	945	296	1	4	598	21
(08:00-09:00)	1021	138	3	2	677	32
(09:00-10:00)	1211	479	2	8	743	39
(12:00-13:00)	1034	179	9	2	782	23
(14:00-15:00)	1045	139	11	0	723	29
(15:00-16:00)	932	80	9	4	663	15
(16:00-17:00)	832	126	11	0	833	18
(18:00-19:00)	929	64	11	0	827	24

Table A.11 Traffic volume (V/H) of Soiking sawairiang.

Time periods (02/03/2010)	PLDGV	LDDT	HDDT	BUS	MC2	MC4
(07:00-08:00)	614	156	3	3	498	22
(08:00-09:00)	599	138	9	1	677	32
(09:00-10:00)	459	179	10	8	743	36
(12:00-13:00)	628	139	6	1	652	23
(14:00-15:00)	611	129	7	0	783	23
(15:00-16:00)	635	101	6	3	753	12
(16:00-17:00)	634	122	7	0	873	15
(18:00-19:00)	626	125	8	0	895	21

Table A.12 Traffic volume (V/H) of Mukkamontri Rd. (St. Maries school).

Time periods (03/03/2010)	PLDGV	LDDT	HDDT	BUS	MC2	MC4
(07:00-08:00)	1018	256	16	3	1498	20
(08:00-09:00)	1051	148	20	4	1090	12
(09:00-10:00)	1112	139	12	4	1067	17
(12:00-13:00)	1237	129	9	8	1058	20
(14:00-15:00)	1027	135	15	2	971	28
(15:00-16:00)	1025	111	16	3	1053	7
(16:00-17:00)	1127	129	20	8	1119	20
(18:00-19:00)	1135	138	19	9	1128	27

Table A.13 Traffic volume (V/H) of Suebsiri Rd.

Time periods (04/03/2010)	PLDGV	LDDT	HDDT	BUS	MC2	MC4
(07:00-08:00)	1111	186	6	1	498	21
(08:00-09:00)	1102	128	9	1	377	32
(09:00-10:00)	1006	179	14	5	443	39
(12:00-13:00)	1121	176	11	1	582	23
(14:00-15:00)	1110	187	18	0	533	29
(15:00-16:00)	1126	149	12	1	543	7
(16:00-17:00)	1126	129	6	0	653	18
(18:00-19:00)	1121	221	5	0	677	24

Table A.14 Traffic volume (V/H) of Detudom Rd.

Time periods (05/03/2010)	PLDGV	LDDT	HDDT	BUS	MC2	MC4
(07:00-08:00)	568	136	2	1	367	21
(08:00-09:00)	690	145	5	1	58	32
(09:00-10:00)	702	114	8	4	561	39
(12:00-13:00)	856	125	14	2	753	23
(14:00-15:00)	783	168	12	0	619	39
(15:00-16:00)	667	146	11	1	628	23
(16:00-17:00)	852	129	4	4	763	25
(18:00-19:00)	802	226	2	5	833	7

Table A.15 Traffic volume (V/H) of Phoklang Rd.

Time periods (06/03/2010)	PLDGV	LDDT	HDDT	BUS	MC2	MC4
(07:00-08:00)	694	114	2	1	569	26
(08:00-09:00)	706	125	5	1	768	18
(09:00-10:00)	114	168	8	4	561	15
(12:00-13:00)	782	149	14	2	853	22
(14:00-15:00)	662	110	12	0	919	24
(15:00-16:00)	692	112	11	1	553	12
(16:00-17:00)	714	126	4	4	419	24
(18:00-19:00)	843	162	2	5	628	29

Table A.16 Traffic volume (V/H) of Chan Rd.

Time periods (07/03/2010)	PLDGV	LDDT	HDDT	BUS	MC2	MC4
(07:00-08:00)	518	341	5	1	971	23
(08:00-09:00)	651	154	12	1	683	15
(09:00-10:00)	712	242	3	0	569	18
(12:00-13:00)	537	193	6	0	768	25
(14:00-15:00)	1327	146	8	0	561	28
(15:00-16:00)	525	188	11	1	853	14
(16:00-17:00)	527	137	4	0	919	22
(18:00-19:00)	505	170	6	1	928	22

Table A.17 Traffic volume (V/H) of Changpuek Rd.

Time periods (08/03/2010)	PLDGV	LDDT	HDDT	BUS	MC2	MC4
(07:00-08:00)	1016	166	4	3	1198	26
(08:00-09:00)	1105	188	3	4	1077	36
(09:00-10:00)	1009	156	6	4	1232	32
(12:00-13:00)	1124	189	8	6	1089	23
(14:00-15:00)	1115	186	5	2	1021	26
(15:00-16:00)	1129	159	8	6	1110	19
(16:00-17:00)	1426	163	6	7	1023	18
(18:00-19:00)	1321	198	4	8	1159	26

Table A.18 Traffic volume (V/H) of Chainarong Rd.

Time periods (09/03/2010)	PLDGV	LDDT	HDDT	BUS	MC2	MC4
(07:00-08:00)	618	321	6	0	881	21
(08:00-09:00)	655	345	10	3	653	17
(09:00-10:00)	724	248	6	1	679	14
(12:00-13:00)	547	245	9	1	728	22
(14:00-15:00)	568	345	8	2	741	24
(15:00-16:00)	529	277	9	1	743	18
(16:00-17:00)	526	268	4	4	932	24
(18:00-19:00)	598	321	5	1	914	26

Table A.19 Traffic volume (V/H) of Prachak Rd.

Time periods (10/03/2010)	PLDGV	LDDT	HDDT	BUS	MC2	MC4
(07:00-08:00)	616	328	5	0	875	20
(08:00-09:00)	652	348	9	3	652	19
(09:00-10:00)	725	243	6	1	674	14
(12:00-13:00)	537	237	9	1	728	22
(14:00-15:00)	561	348	8	2	746	24
(15:00-16:00)	522	272	9	1	749	11
(16:00-17:00)	526	264	4	4	931	28
(18:00-19:00)	594	328	5	1	919	26

Table A.20 Traffic volume (V/H) of Ratchadamnoen Rd.

Time periods (11/03/2010)	PLDGV	LDDT	HDDT	BUS	MC2	MC4
(07:00-08:00)	1116	366	5	5	1218	25
(08:00-09:00)	1135	388	6	6	1117	32
(09:00-10:00)	1219	356	8	10	1032	39
(12:00-13:00)	1224	389	7	12	1219	22
(14:00-15:00)	1315	486	6	14	1461	27
(15:00-16:00)	1359	459	7	16	1230	15
(16:00-17:00)	1316	363	8	17	1143	16
(18:00-19:00)	1421	498	4	12	1319	21

Table A.21 Traffic volume (V/H) of Chumphon Rd.

Time periods (12/03/2010)	PLDGV	LDDT	HDDT	BUS	MC2	MC4
(07:00-08:00)	1106	369	5	5	1118	21
(08:00-09:00)	1125	389	6	6	1217	34
(09:00-10:00)	1269	347	8	10	1132	34
(12:00-13:00)	1235	376	7	12	1145	28
(14:00-15:00)	1315	494	6	14	1312	24
(15:00-16:00)	1346	458	7	16	1236	19
(16:00-17:00)	1321	375	8	17	1144	14
(18:00-19:00)	1465	486	4	12	1312	28



APPENDIX B

**A NUMBER OF POPULATION AT POINTS OF
INTEREST AND DESCRIPTIVE STATISTICS**

Table B.1 A number of population at each points of interest.

Institutions/educations	A number of population (persons/places)
Rajamangala University of Technology Isan	5308
Nakhon Ratchasima Rajabhat University	6735
Suranaree Wittaya school	4515
Korat Pittayakhom school	1540
Assumption college Nakhon Ratchasima school	2308
Ruammitr Wittaya school	2739
Somboon Wittayanukoon school	1010
Ubonratch school	441
st. Mary's Wittaya school	5112
st. Mary's Business Administration College	1560
Nakhon Ratchasima Engineering Commercial Tech	3500
Nakhon Ratchasima Technical College	4860
Nakhon Ratchasima Vocational College	4847
Tessabarn 1 school	1771
Tessabarn 2 school	1329
Tessabarn 3 school	1788
Tessabarn 4 school	737
Samakhee huarodfai school	657
Muang Nakhon Ratchasima school	3015
Anubarn school	4551
Sukhanaree school	3602
Watsakaew school	2672
Suamon school	1056
Wattoongsawang school	440
Yotinnukoon school	369
Watkhoprom school	526
Bus terminals	A number of population (persons/hour)
Terminal old	1250
Terminal new	2083
Commercial centers	A number of population (persons/hour)
Klang plaza (old)	778
Klang plaza (new)	3266
The mall Korat	19440
Lotus	972
Big-C	875
IT plaza	350
Makro	972

Table B.1 A number of population at each points of interest (continued)

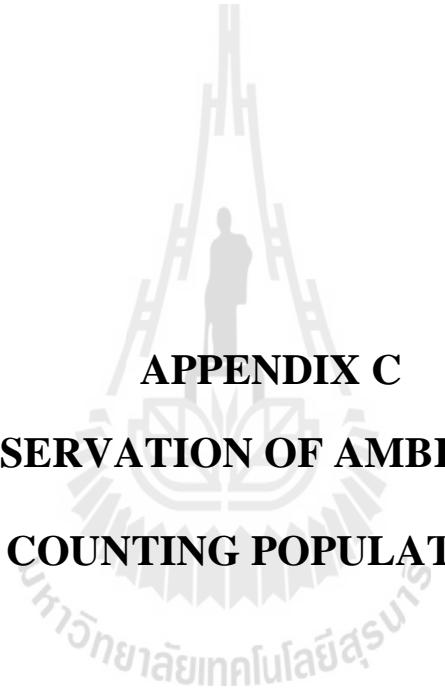
Hospitals	A number of population (persons/hour)
Bangkok Ratchasima hospital	1334
Maharaj Nakhon Ratchasima hospital	3200
Jittavech Nakhon Ratchasima hospital	453
Saint Mary hospital	1261

Hotels	A number of population (persons/places)
Sima thani hotel Korat	1765
V-one hotel Korat	1616
Ratchaphruk grand hotel Korat	1659
The Iyara hotel Korat	1652
Punjadara hoyel Korat	579
Chao phayainn hotel Korat	554
KR hotel	360
KS hotel	569
Siri hotel	130
City park hotel	379

Local markets	A number of population (persons/hour)
Talad_Huarodfai	522
Talad_Yamo	1146
Talad_Maekimheng	880
Talad_Suranakorn	3183
Talad_Prutuphee	255

Table B.2 Descriptive statistic of number of population at each points of interest

Descriptive statistics	
Mean	2193.907407
Standard Error	390.202561
Median	1331.5
Mode	972
Standard Deviation	2867.391512
Sample Variance	8221934.086
Kurtosis	24.76699958
Skewness	4.359402645
Range	19310
Minimum	130
Maximum	19440
Sum	118471
Count	54



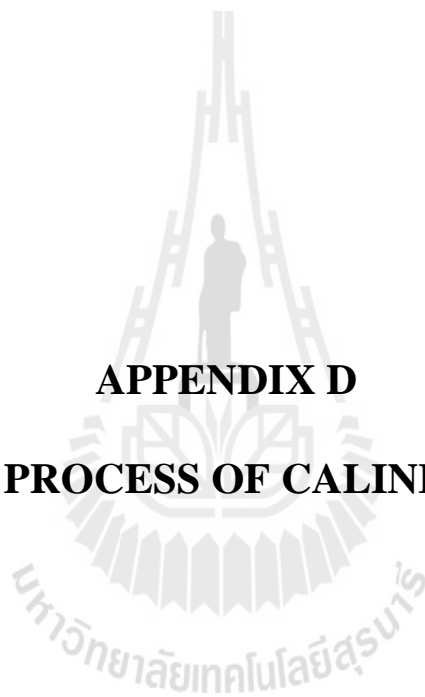
APPENDIX C
FIELD OBSERVATION OF AMBIENT (CO) AND
COUNTING POPULATION



Figure C.1 Measurement of ambient CO at Mittrapap Road (17:00-18:00).



Figure C.2 Counting population at local market using (Counter instrument).



APPENDIX D

THE PROCESS OF CALINE4 RUNNING

CL4 v2.1

Job Parameters | Run Conditions | Link Geometry | Link Activity | Receptor Positions | Results | Help | About

Job Filename: E:\Software_Air pollution\CL4 v2.1\Input-Output\Pollutants simulation.dat

Job Title: Korat

Pollutants

Pollutant Type: Carbon Monoxide Nitrogen Dioxide Particulates

Molecular Weight: 28 Settling Velocity: n/a cm/s Deposition Velocity: 0 cm/s

Aerodynamic Roughness Coefficient: Rural Suburban Central Business District Other: _____ centimeters

Run Type

Standard Worst-Case Wind Direction Multi-Run Multi-Run / Worst-Case Hybrid

Model Information

Link/Receptor Geometry Units: Meters Feet Altitude Above Sea Level: 200 meters

Number of Links: 0 Number of Receptors: 0 Averaging Interval: 1 hour

Figure D.1 (Step 1) Job parameters.

CL4 v2.1

Job Parameters | Run Conditions | Link Geometry | Link Activity | Receptor Positions | Results | Help | About

	Run: Hour 1
Wind Speed (≥0.5 m/sec)	1.2
▶ Wind Direction (0-360°)	90
Wind Direction Std. Dev. (5-60°)	22.5
Atmospheric Stability Class (1-7)	7
Mixing Height (≥5 m)	1000
Ambient Temperature (°C)	31
Ambient CO Concentration (ppm)	2.3

Atmospheric Stability Class	Valid Wind Speed (m/s)
1	< 4.0
2	< 5.5
3	< 1000
4	< 1000
5	< 5.5
6	< 4.5
7	< 3.5

Figure D.2 (Step 2) Run conditions.



APPENDIX E

**NO_x EMISSION (G/HR./LINE) ON LINE
(BIG-C 3-JUNCTION TO MUEANG NAKHON
RATCHASIMA SCHOOL)**

Table E.1 NO_x emission on linE (Big-C 3-junction to Mueang school) of date 06/02/2012.

Date/Time 06/02/2012	NOX (ppb)	Emission by MC (g/hr/line)	Emission by PLDGV (g/hr/line)	Emission by LDDT (g/hr/line)	Emission by HDDT+BUS (g/hr/line)	Emission by MC+PLDGV (g/hr/line)	Emission by LDDT+HDDT+BUS (g/hr/line)
07:00-8:00	74.4	455.8	1057.3	1913.76	4660.44	1513.1	6574.2
8:00-9:00	61.3	172	839.3	1789.92	2822.52	1011.3	4612.44
9:00-10:00	51.5	184.9	626.75	1648.8	2002.02	811.65	3650.82
10:00-11:00	59.2	125.99	926.5	1664.64	2319.28	1052.49	3983.92
11:00-12:00	50.3	187.05	615.85	1463.04	1947.32	802.9	3410.36
12:00-13:00	47.3	123.41	931.95	1409.76	1575.36	1055.36	2985.12
13:00-14:00	42.3	161.25	752.1	1362.24	1586.3	913.35	2948.54
14:00-15:00	33.7	87.72	773.9	1329.12	1378.44	861.62	2707.56
15:00-16:00	86.4	176.3	806.6	1668.96	2866.28	982.9	4535.24
16:00-17:00	138.1	379.26	1079.1	2052	3971.22	1458.36	6023.22
17:00-18:00	95.3	311.75	1068.2	1887.84	3610.2	1379.95	5498.04
18:00-19:00	99.5	167.27	1106.35	1968.48	3883.7	1273.62	5852.18

Table E.2 NO_x emission on linE (Big-C 3-junction to Mueang school) of date 07/02/2012.

Date/Time 07/02/2012	NOX (ppb)	Emission by MC (g/hr/line)	Emission by PLDGV (g/hr/line)	Emission by LDDT (g/hr/line)	Emission by HDDT+BUS (g/hr/line)	Emission by MC+PLDGV (g/hr/line)	Emission by LDDT+HDDT+BUS (g/hr/line)
07:00-8:00	94.2	465.26	1079.1	1820.16	4452.58	1544.36	6272.74
8:00-9:00	70.4	175.44	856.74	1702.08	2702.18	1032.18	4404.26
9:00-10:00	51.2	188.77	639.83	1566.72	1816.04	828.6	3382.76
10:00-11:00	71.2	128.57	945.03	1553.76	2220.82	1073.6	3774.58
11:00-12:00	37.1	190.92	628.93	1290.24	1706.64	819.85	2996.88
12:00-13:00	37.4	125.99	951.57	1340.64	1630.06	1077.56	2970.7
13:00-14:00	41.2	164.69	767.36	1369.44	1881.68	932.05	3251.12
14:00-15:00	35.3	94.17	790.25	1262.88	1323.74	884.42	2586.62
15:00-16:00	44.9	180.17	822.95	1350.72	2341.16	1003.12	3691.88
16:00-17:00	86.6	323.79	1100.9	1827.36	3555.5	1424.69	5382.86
17:00-18:00	177.5	315.62	1097.63	1938.24	3785.24	1413.25	5723.48
18:00-19:00	136.3	170.71	1129.24	1872	3686.78	1299.95	5558.78

Table E.3 NO_x emission on linE (Big-C 3-junction to Mueang school) of date 08/02/2012.

Date/Time 08/02/2012	NOX (ppb)	Emission by MC (g/hr/line)	Emission by PLDGV (g/hr/line)	Emission by LDDT (g/hr/line)	Emission by HDDT+BUS (g/hr/line)	Emission by MC+PLDGV (g/hr/line)	Emission by LDDT+HDDT+BUS (g/hr/line)
07:00-8:00	92.4	488.05	1153.22	1782.72	4540.1	1641.27	6322.82
8:00-9:00	87.6	163.4	906.88	1738.08	2756.88	1070.28	4494.96
9:00-10:00	83.3	188.77	676.89	1601.28	2242.7	865.66	3843.98
10:00-11:00	55.5	163.83	954.84	1473.12	2012.96	1118.67	3486.08
11:00-12:00	54.8	193.07	634.38	1376.64	1892.62	827.45	3269.26
12:00-13:00	42.6	127.28	960.29	1304.64	1531.6	1087.57	2836.24
13:00-14:00	58.5	177.59	827.31	1425.6	1783.22	1004.9	3208.82
14:00-15:00	53.8	96.75	851.29	1326.24	1542.54	948.04	2868.78
15:00-16:00	87.3	190.49	872	1620	2570.9	1062.49	4190.9
16:00-17:00	168.6	375.82	1166.3	1910.88	3818.06	1542.12	5728.94
17:00-18:00	137.9	276.92	1100.9	1889.28	3577.38	1377.82	5466.66
18:00-19:00	92.4	488.05	1153.22	1782.72	4540.1	1641.27	6322.82

Table E.4 NO_x emission on linE (Big-C 3-junction to Mueang school) of date 09/02/2012.

Date/Time 09/02/2012	NOX (ppb)	Emission by MC (g/hr/line)	Emission by PLDGV (g/hr/line)	Emission by LDDT (g/hr/line)	Emission by HDDT+BUS (g/hr/line)	Emission by MC+PLDGV (g/hr/line)	Emission by LDDT+HDDT+BUS (g/hr/line)
07:00-8:00	101.6	497.94	1177.2	1794.24	4912.06	1675.14	6706.3
8:00-9:00	93.9	166.84	925.41	1592.64	2986.62	1092.25	4579.26
9:00-10:00	23.4	192.64	691.06	1306.08	2045.78	883.7	3351.86
10:00-11:00	28.8	167.27	974.46	1317.6	2089.54	1141.73	3407.14
11:00-12:00	42.2	196.94	648.55	1496.16	2209.88	845.49	3706.04
12:00-13:00	39.9	129.86	981	1523.52	1870.74	1110.86	3394.26
13:00-14:00	37.2	181.46	844.75	1465.92	1739.46	1026.21	3205.38
14:00-15:00	29.4	103.63	869.82	1401.12	1717.58	973.45	3118.7
15:00-16:00	44.4	194.79	889.44	1667.52	2811.58	1084.23	4479.1
16:00-17:00	62.9	422.26	1189.19	1997.28	3807.12	1611.45	5804.4
17:00-18:00	82.1	175.87	1197.91	2155.68	3905.58	1373.78	6061.26
18:00-19:00	101.6	497.94	1177.2	1794.24	4912.06	1675.14	6706.3

Table E.5 NO_x emission on linE (Big-C 3-junction to Mueang school) of date 10/02/2012.

Date/Time 10/02/2012	NOX (ppb)	Emission by MC (g/hr/line)	Emission by PLDGV (g/hr/line)	Emission by LDDT (g/hr/line)	Emission by HDDT+BUS (g/hr/line)	Emission by MC+PLDGV (g/hr/line)	Emission by LDDT+HDDT+BUS (g/hr/line)
07:00-8:00	75.7	542.66	1258.95	2059.2	3260.12	1801.61	5319.32
8:00-9:00	68.2	204.68	999.53	1896.48	2395.86	1204.21	4292.34
9:00-10:00	69.9	220.16	746.65	1916.64	2494.32	966.81	4410.96
10:00-11:00	48	150.07	1103.08	1684.8	2188	1253.15	3872.8
11:00-12:00	36.7	222.74	733.57	1622.88	1870.74	956.31	3493.62
12:00-13:00	48.7	147.06	1109.62	1956.96	1881.68	1256.68	3838.64
13:00-14:00	39.9	177.59	827.31	1729.44	2023.9	1004.9	3753.34
14:00-15:00	76.9	96.75	851.29	1887.84	2964.74	948.04	4852.58
15:00-16:00	79.7	193.93	887.26	2361.6	4288.48	1081.19	6650.08
16:00-17:00	109.7	424.84	1175.02	2172.96	4419.76	1599.86	6592.72
17:00-18:00	93.6	184.04	1217.53	2265.12	4386.94	1401.57	6652.06
18:00-19:00	75.7	542.66	1258.95	2059.2	3260.12	1801.61	5319.32

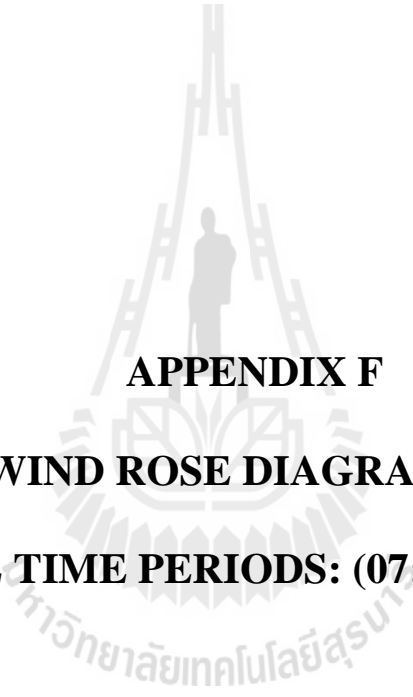
Table E.6 NO_x emission on linE (Big-C 3-junction to Mueang school) of date 11/02/2012.

Date/Time 12/02/2012	NOX (ppb)	Emission by MC (g/hr/line)	Emission by PLDGV (g/hr/line)	Emission by LDDT (g/hr/line)	Emission by HDDT+BUS (g/hr/line)	Emission by MC+PLDGV (g/hr/line)	Emission by LDDT+HDDT+BUS (g/hr/line)
07:00-8:00	95	439.46	1038.77	1876.32	5141.8	1478.23	7018.12
8:00-9:00	79.5	147.06	816.41	1756.8	3128.84	963.47	4885.64
9:00-10:00	68.4	170.28	609.31	1617.12	2450.56	779.59	4067.68
10:00-11:00	62.4	213.28	984.27	1632.96	2133.3	1197.55	3766.26
11:00-12:00	48.1	199.09	654	1435.68	1881.68	853.09	3317.36
12:00-13:00	38.2	131.15	989.72	1382.4	1750.4	1120.87	3132.8
13:00-14:00	30.5	195.65	910.15	1336.32	1476.9	1105.8	2813.22
14:00-15:00	42.1	106.64	937.4	1474.56	1914.5	1044.04	3389.06
15:00-16:00	93.5	273.91	1049.67	2011.68	4244.72	1323.58	6256.4
16:00-17:00	87.9	335.4	990.81	1918.08	4200.96	1326.21	6119.04
17:00-18:00	80.4	155.23	1056.21	1863.36	4190.02	1211.44	6053.38
18:00-19:00	95	439.46	1038.77	1876.32	5141.8	1478.23	7018.12

Table E.7 NO_x emission on linE (Big-C 3-junction to Mueang school) of date 12/02/2012.

Date/Time 11/02/2012	NOX (ppb)	Emission by MC (g/hr/line)	Emission by PLDGV (g/hr/line)	Emission by LDDT (g/hr/line)	Emission by HDDT+BUS (g/hr/line)	Emission by MC+PLDGV (g/hr/line)	Emission by LDDT+HDDT+BUS (g/hr/line)
07:00-8:00	93	341.85	793.52	1723.68	4222.84	1135.37	5946.52
8:00-9:00	72.1	129	630.02	1612.8	2549.02	759.02	4161.82
9:00-10:00	55.5	138.89	470.88	1484.64	1848.86	609.77	3333.5
10:00-11:00	58.3	94.6	695.42	1499.04	1728.52	790.02	3227.56
11:00-12:00	35	193.07	634.38	1319.04	1794.16	827.45	3113.2
12:00-13:00	31.9	127.28	960.29	1270.08	1531.6	1087.57	2801.68
13:00-14:00	47.1	177.59	827.31	1226.88	1673.82	1004.9	2900.7
14:00-15:00	51.2	190.49	872	1503.36	2406.8	1062.49	3910.16
15:00-16:00	N/A	N/A	N/A	N/A -	N/A	N/A	N/A
16:00-17:00	76.3	248.11	863.28	1848.96	3500.8	1111.39	5349.76
17:00-18:00	85.5	210.27	854.56	1761.12	3457.04	1064.83	5218.16
18:00-19:00	95.6	134.16	885.08	1712.16	3675.84	1019.24	5388





APPENDIX F
WIND ROSE DIAGRAM OF
ALL TIME PERIODS: (07:00-19:00)

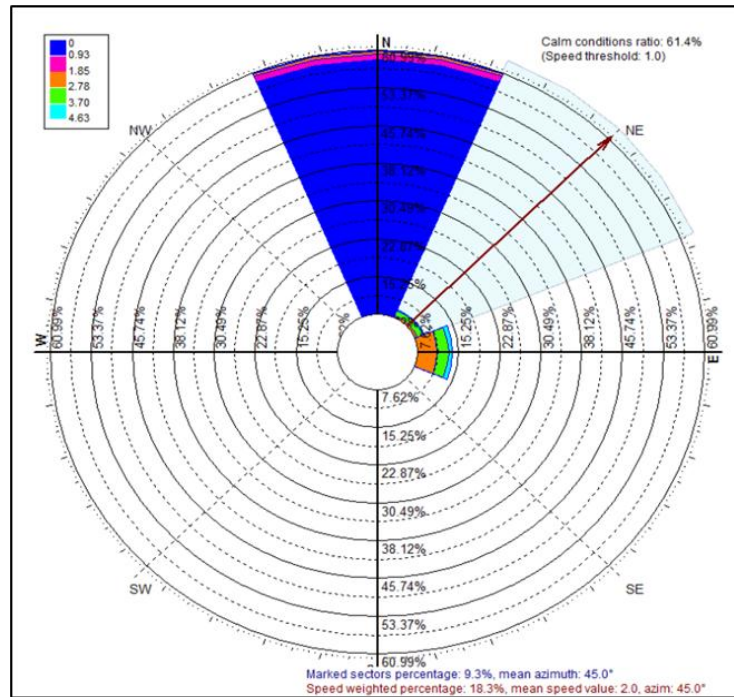


Figure F.1 Wind rose diagram at 07:00-08:00.

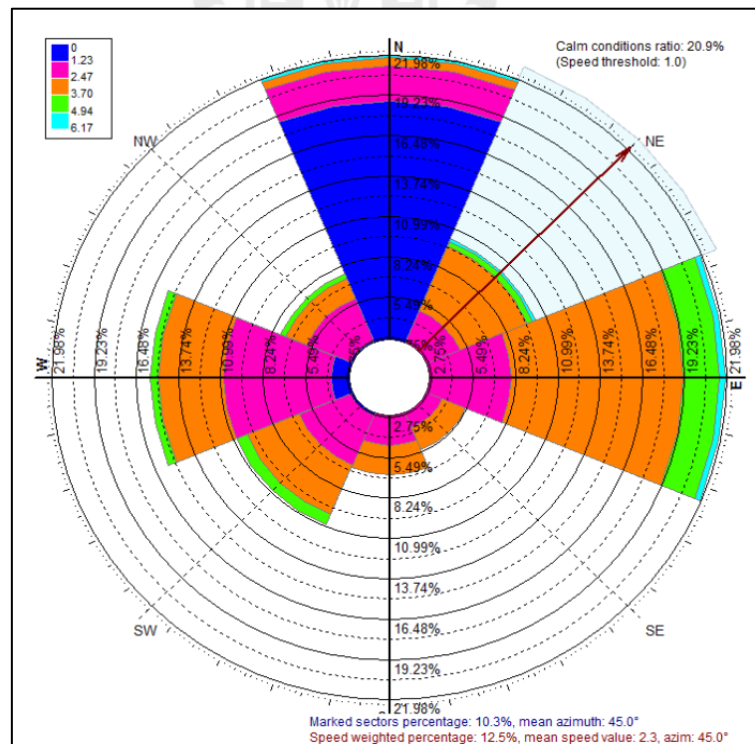


Figure F.2 Wind rose diagram at 09:00-10:00.

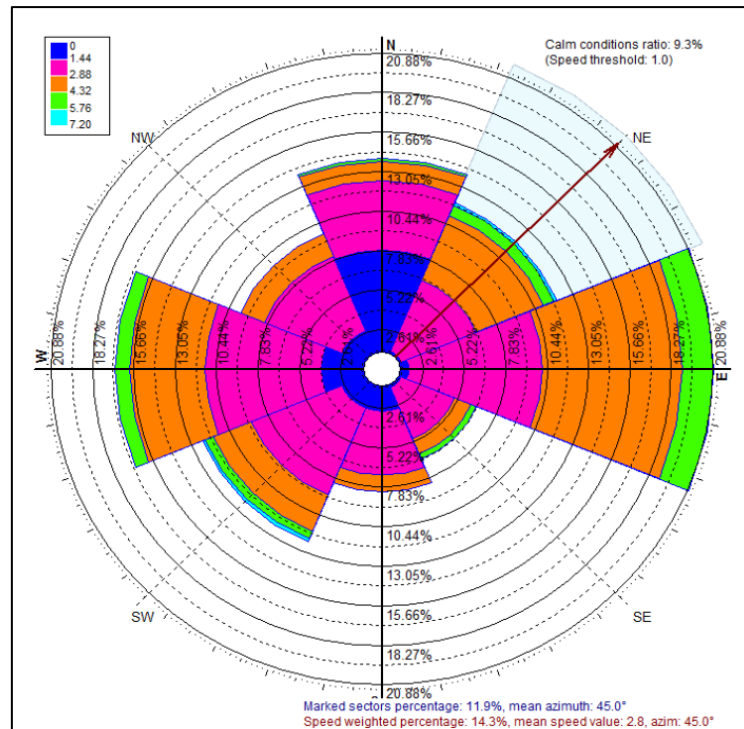


Figure F.3 Wind rose diagram at 12:00-13:00.

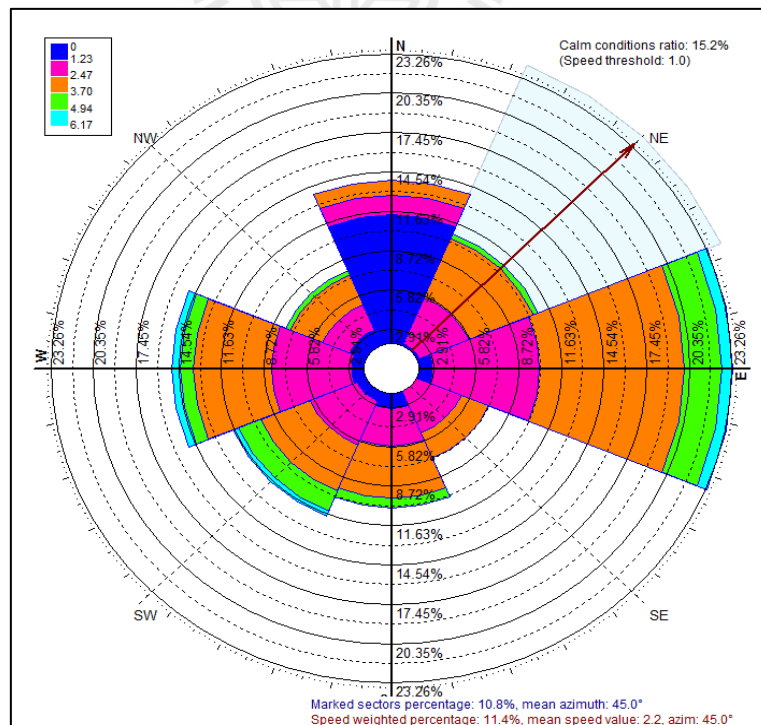


Figure F.4 Wind rose diagram at 15:00-16:00.

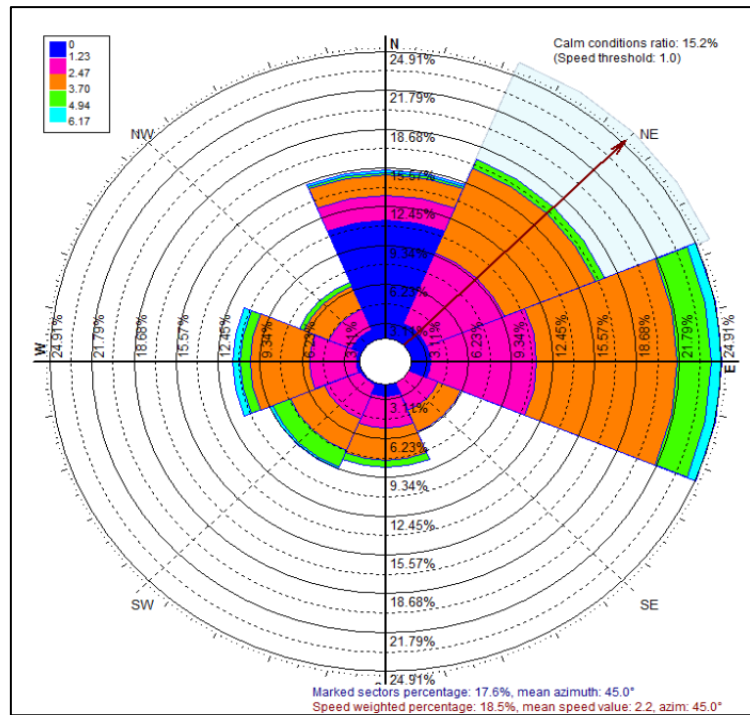


Figure F.5 Wind rose diagram at 18:00-19:00.





APPENDIX G

CO CONCENTRATION (PPM) DISPERSION MAPS

VARIED WITH VEHICLE TYPES AND WIND

DIRECTION IN (0-315 DEGREE)

AT TIME PERIODS: (07:00 -19:00)

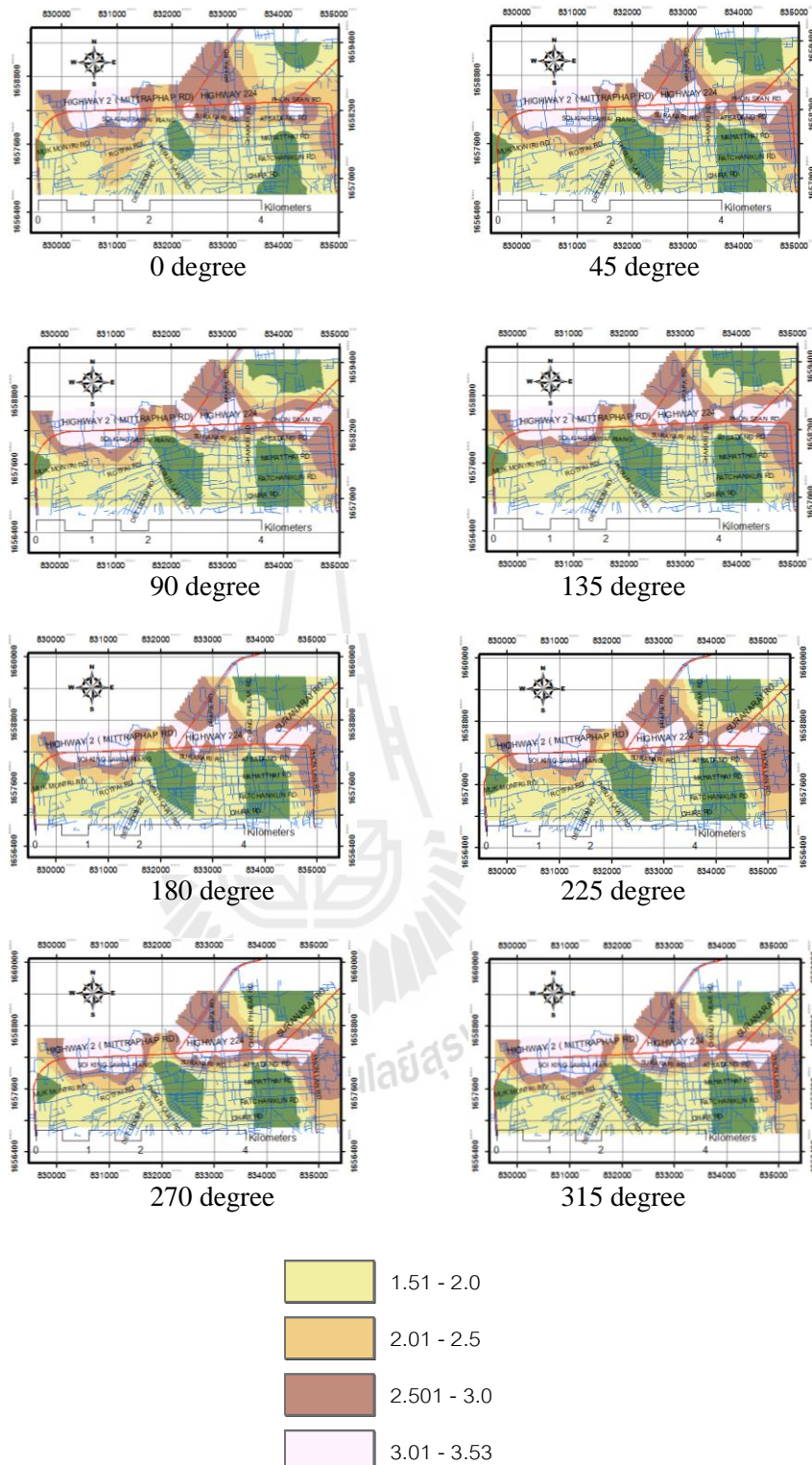


Figure G.1 CO concentration (ppm) dispersion maps of PLDGV vehicle type during 07:00-08:00.

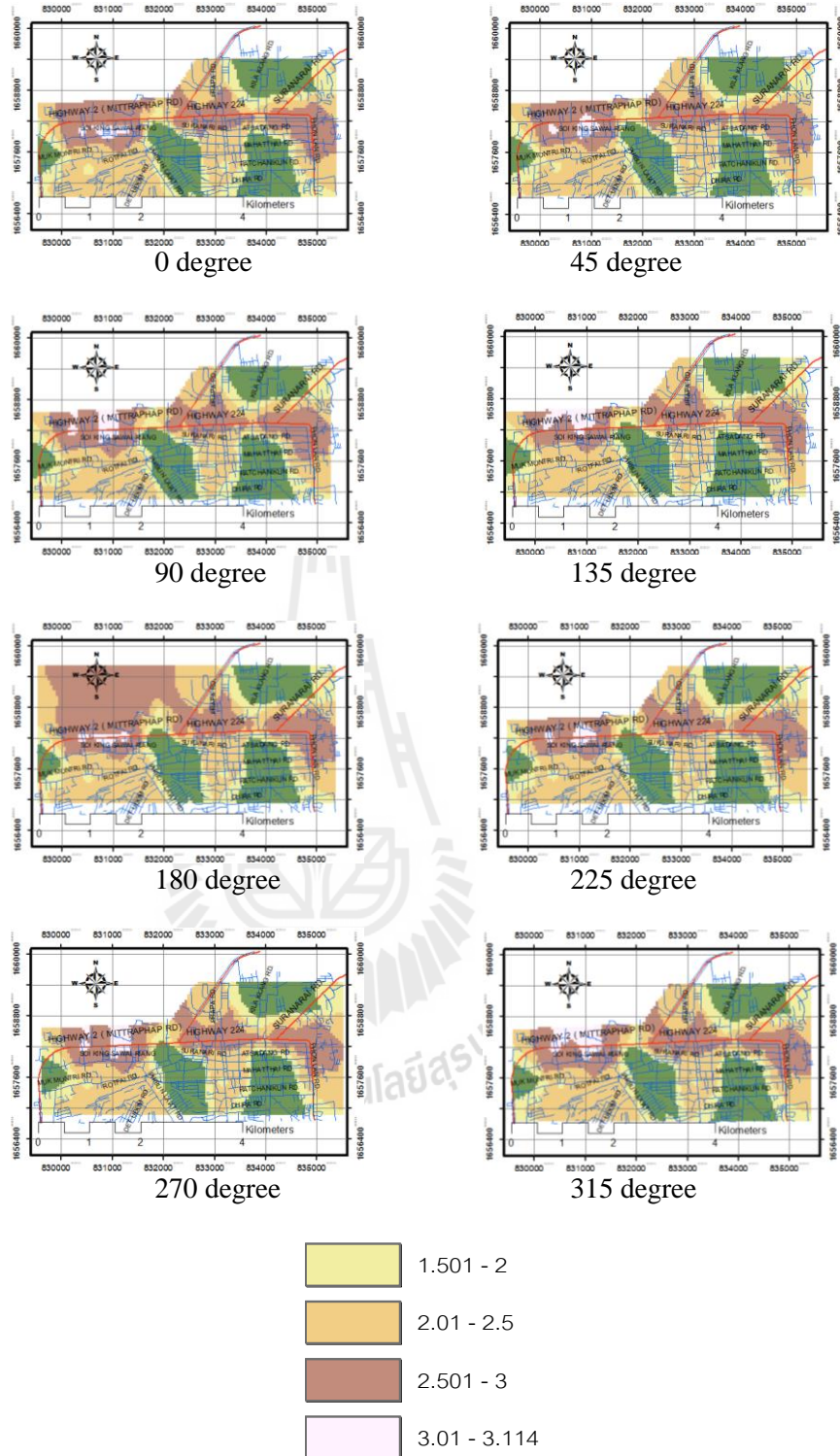


Figure G.2 CO concentration (ppm) dispersion maps of PLDGV vehicle type during 09:00-10:00.

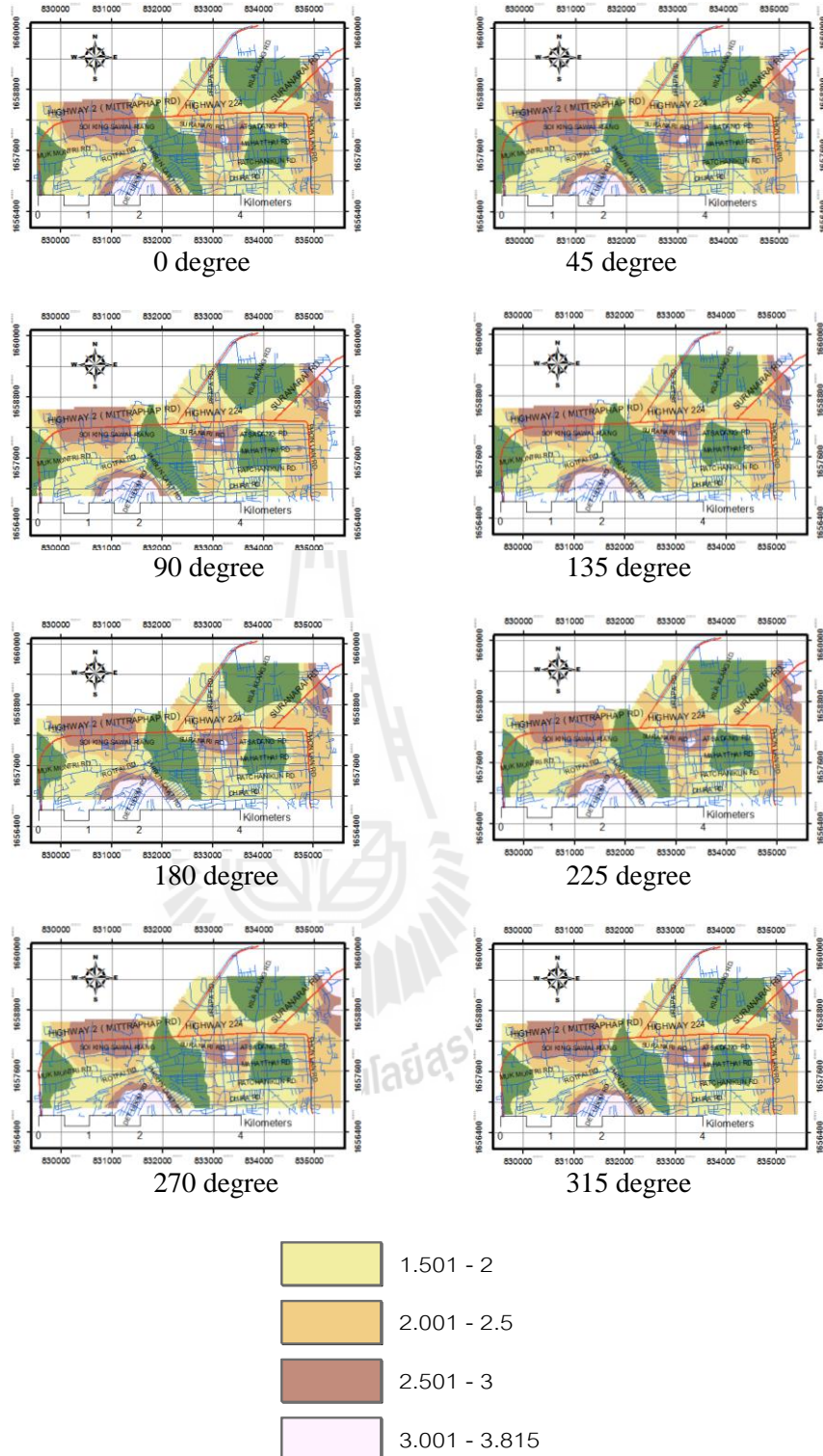


Figure G.3 CO concentration (ppm) dispersion maps of PLDGV vehicle type during 12:00-13:00.

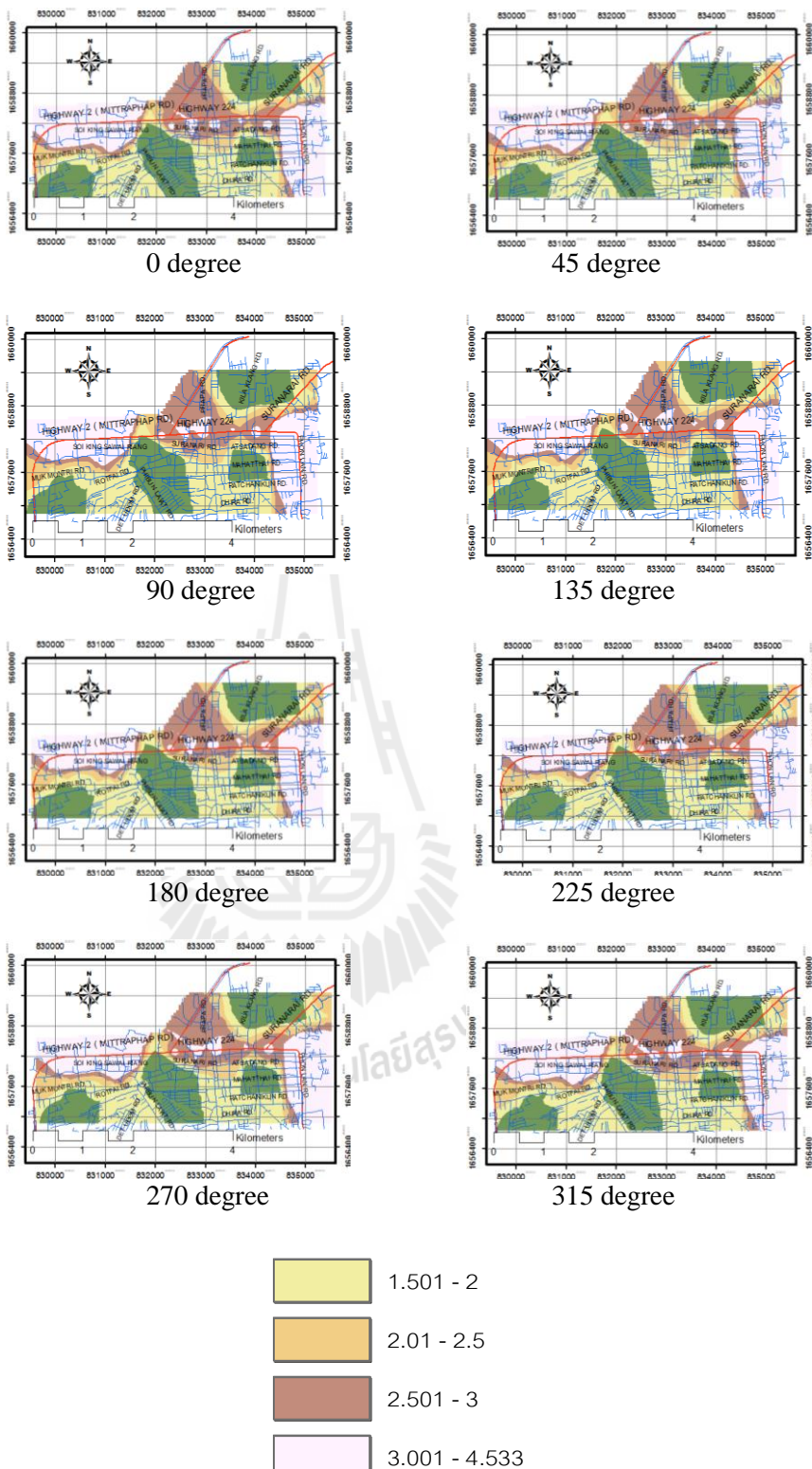


Figure G.4 CO concentration (ppm) dispersion maps of PLDGV vehicle type during 15:00-16:00.

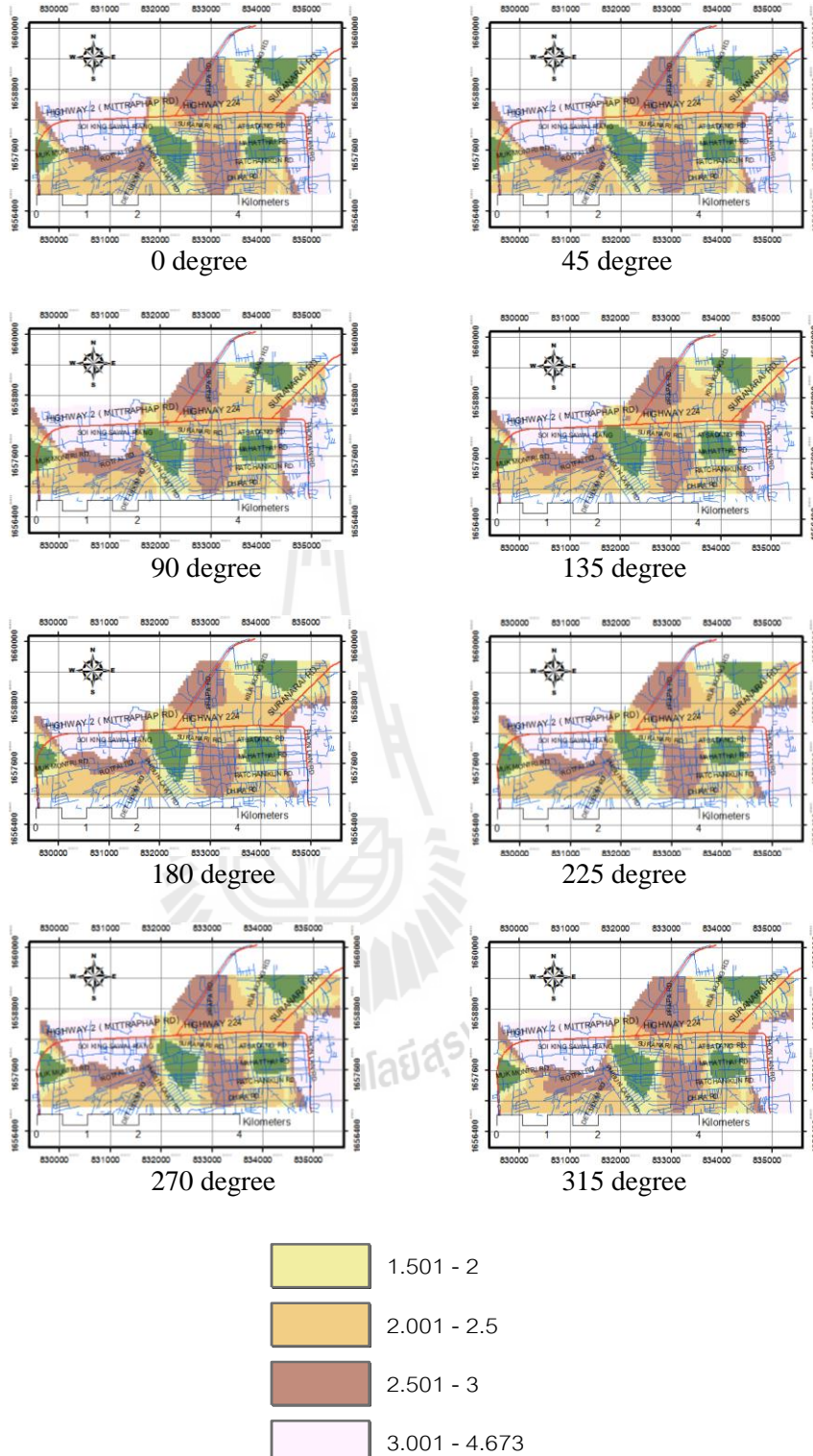


Figure G.5 CO concentration (ppm) dispersion maps of PLDGV vehicle type during 18:00-19:00.

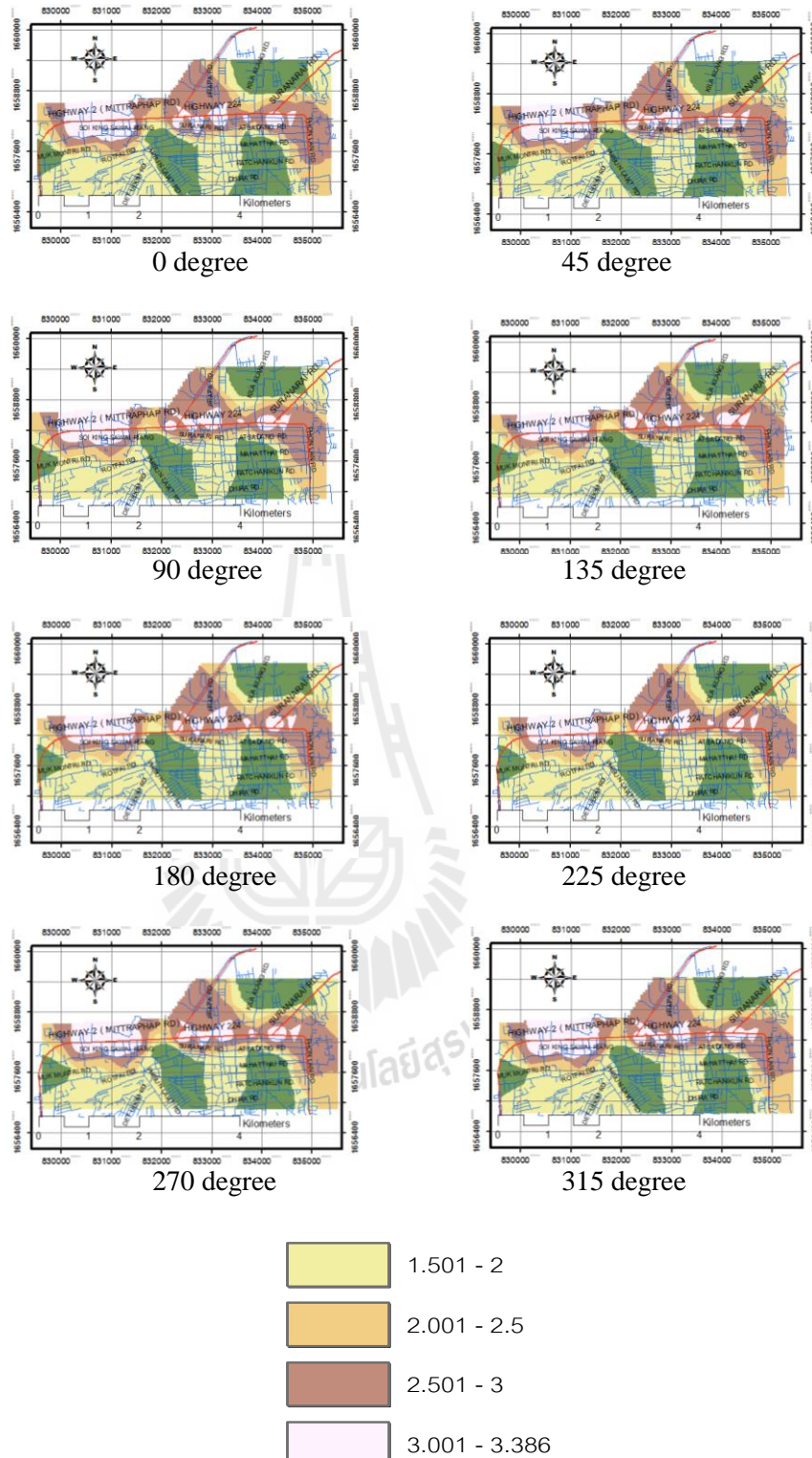


Figure G.6 CO concentration (ppm) dispersion maps of MC vehicle type during 07:00-08:00.

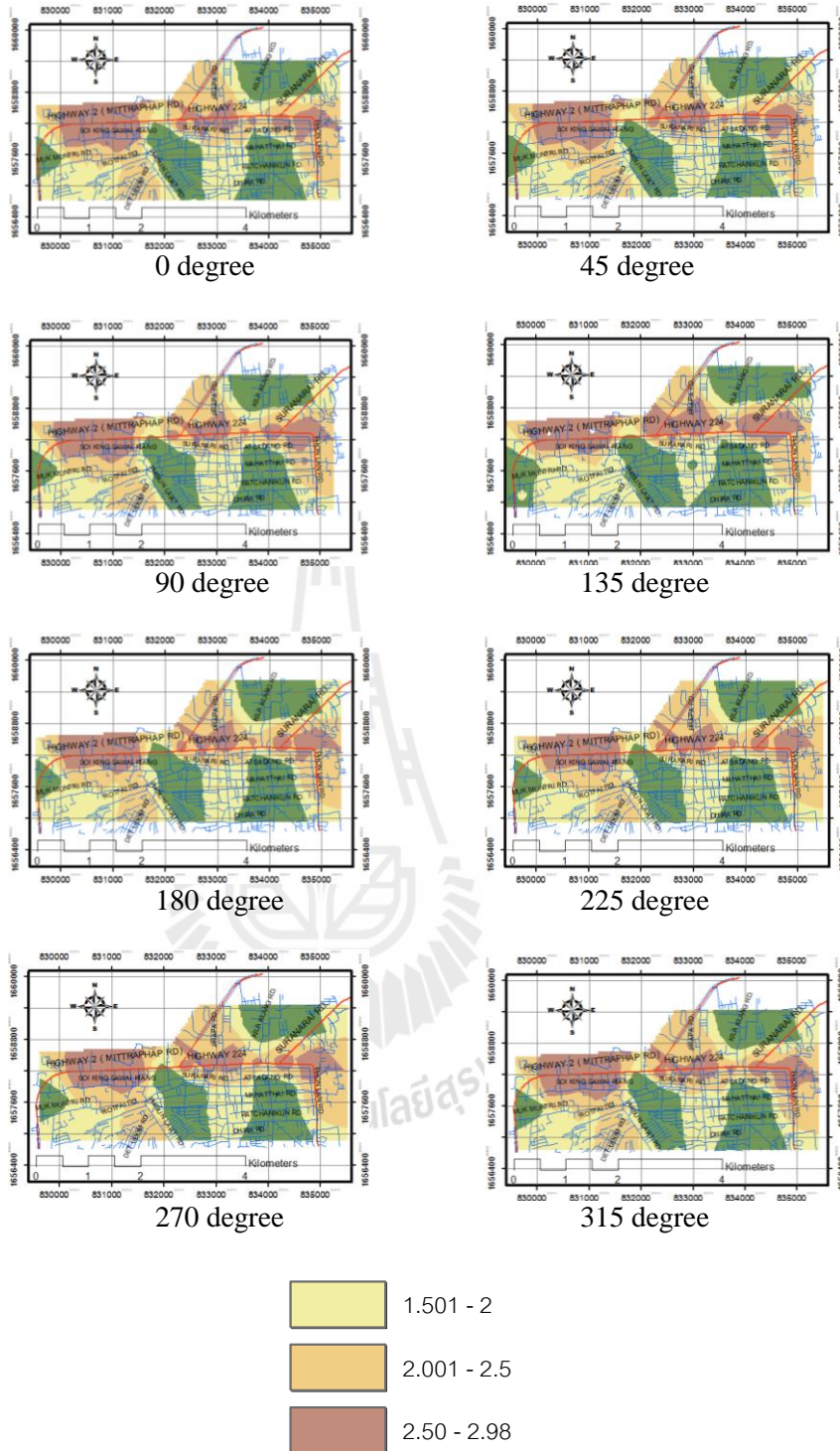


Figure G.7 CO concentration (ppm) dispersion maps of MC vehicle type during 09:00-10:00.

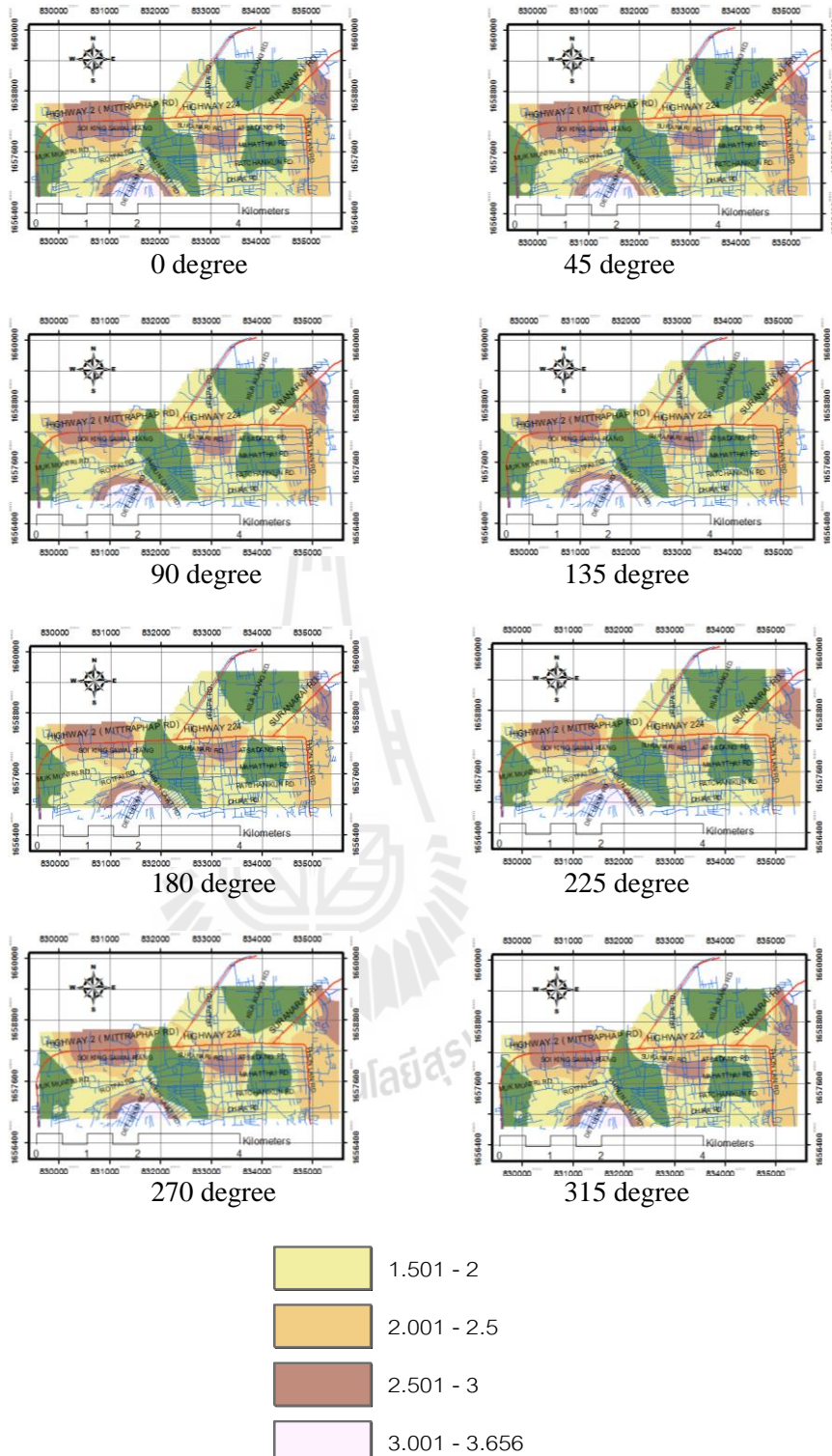


Figure G.8 CO concentration (ppm) dispersion maps of MC vehicle type during 12:00-13:00.

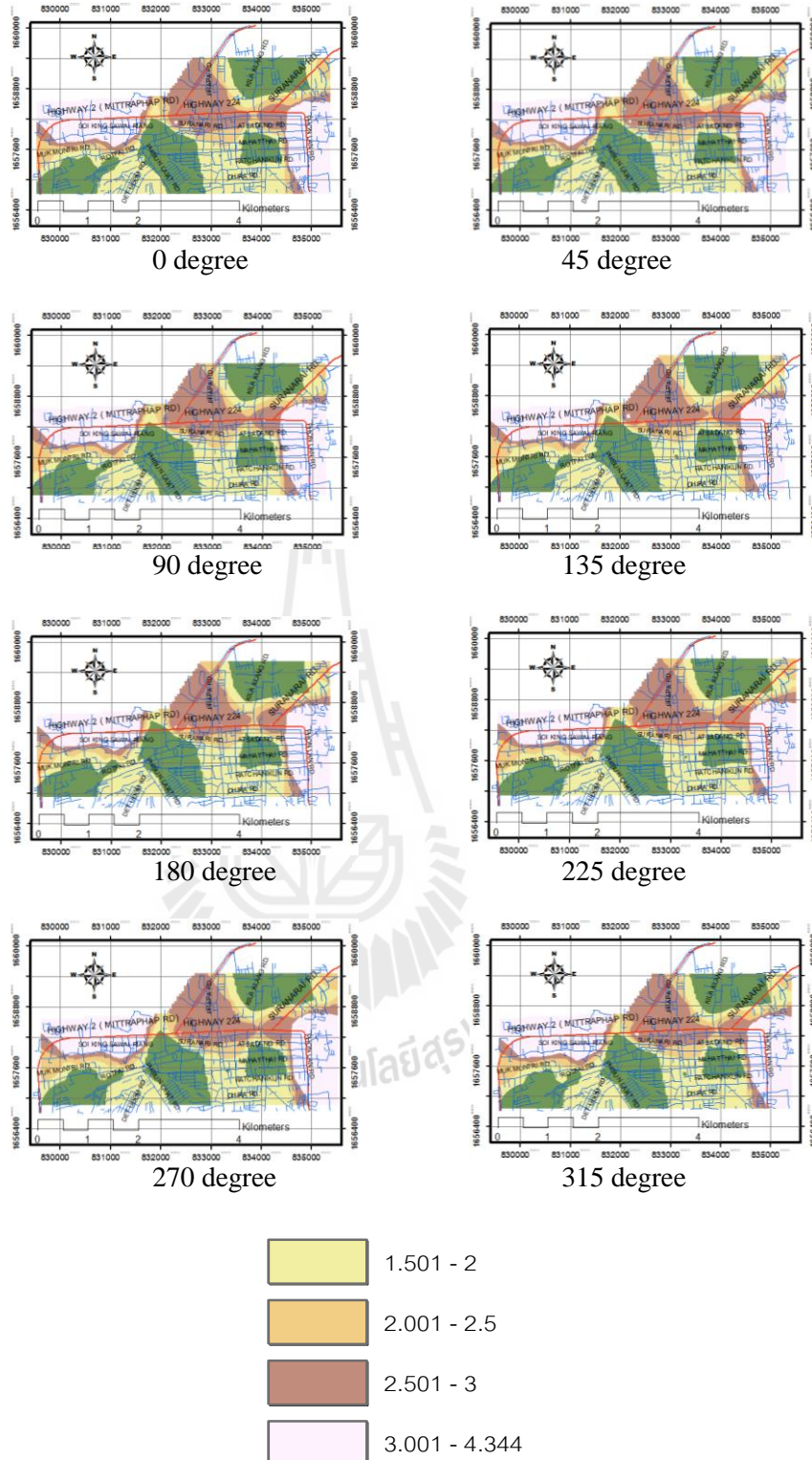


Figure G.9 CO concentration (ppm) dispersion maps of MC vehicle type during 15:00-16:00.

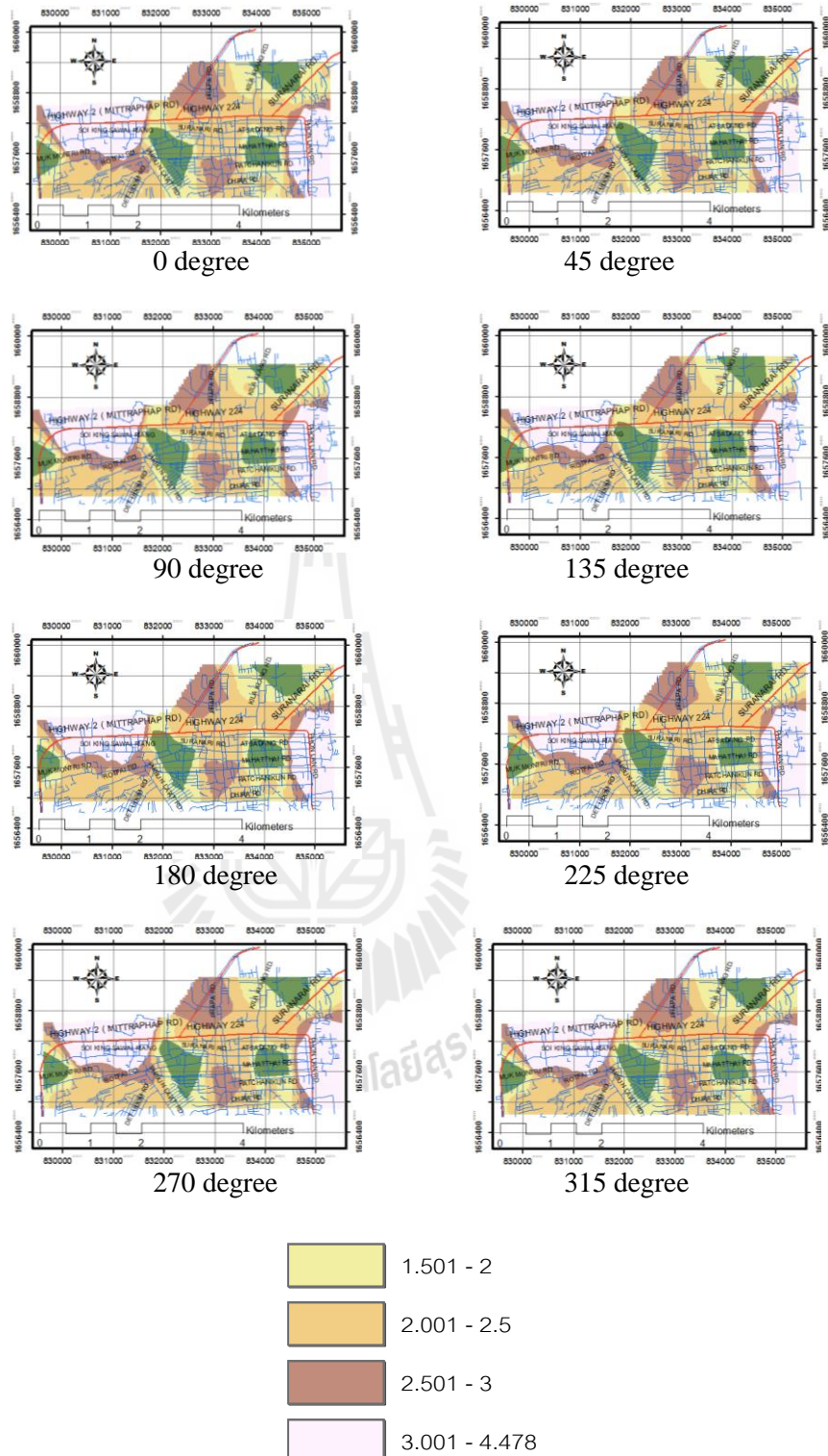


Figure G.10 CO concentration (ppm) dispersion maps of MC vehicle type during 18:00-19:00.

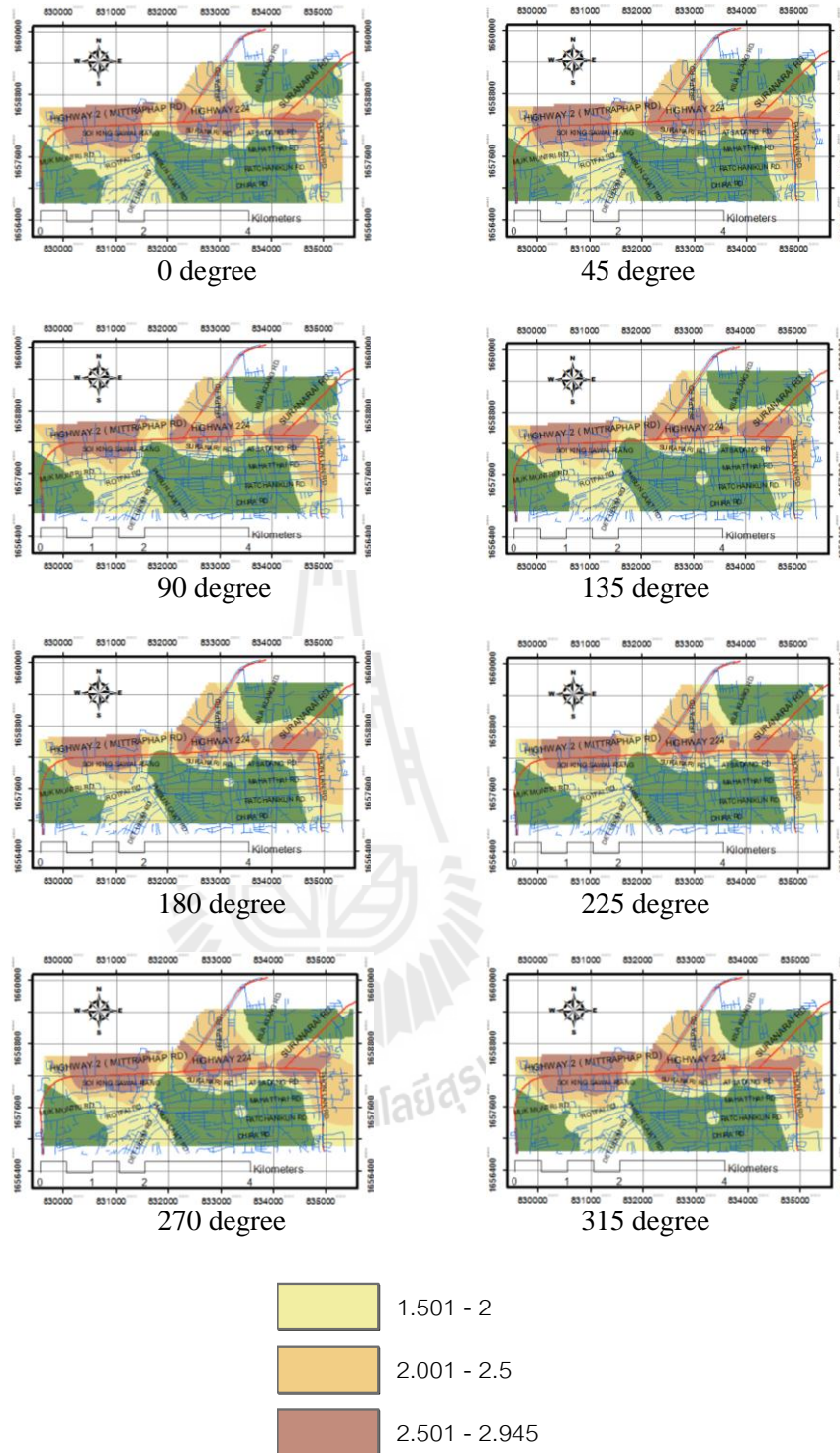


Figure G.11 CO concentration (ppm) dispersion maps of HDDT vehicle type during 07:00-08:00.

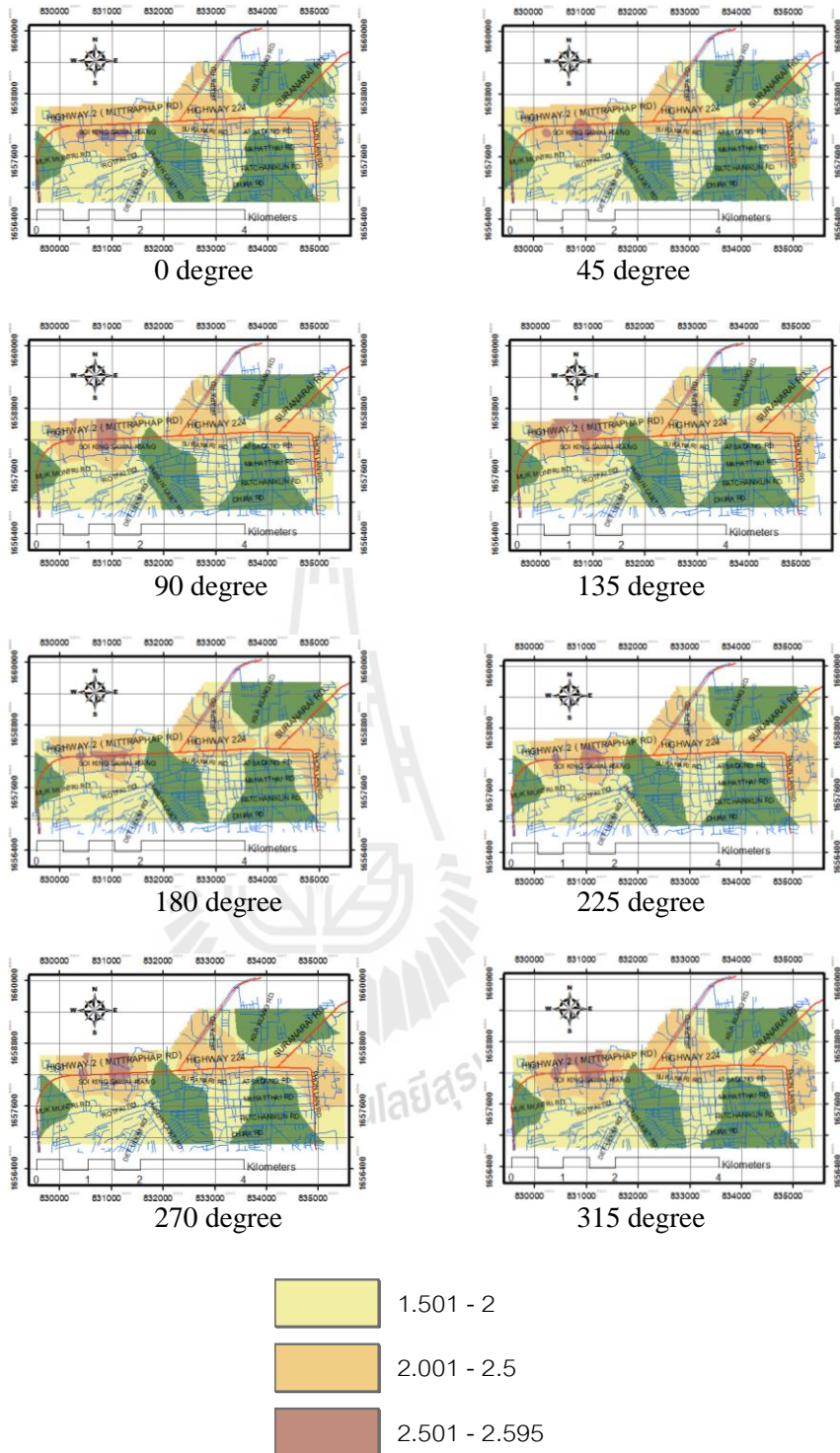


Figure G.12 CO concentration (ppm) dispersion maps of HDDT vehicle type during 12:00-13:00.

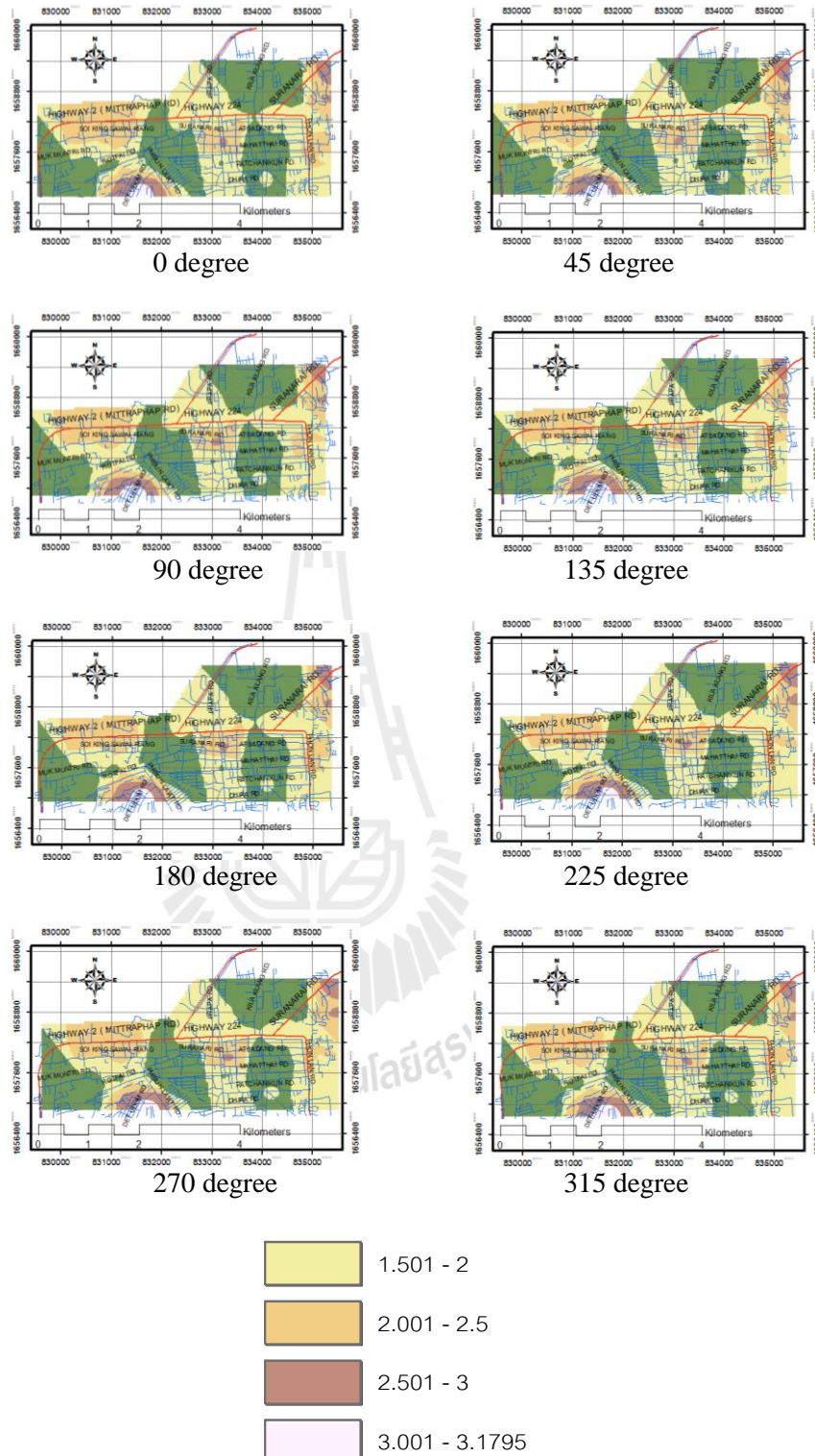


Figure G.13 CO concentration (ppm) dispersion maps of HDDT vehicle type during 12:00-13:00.

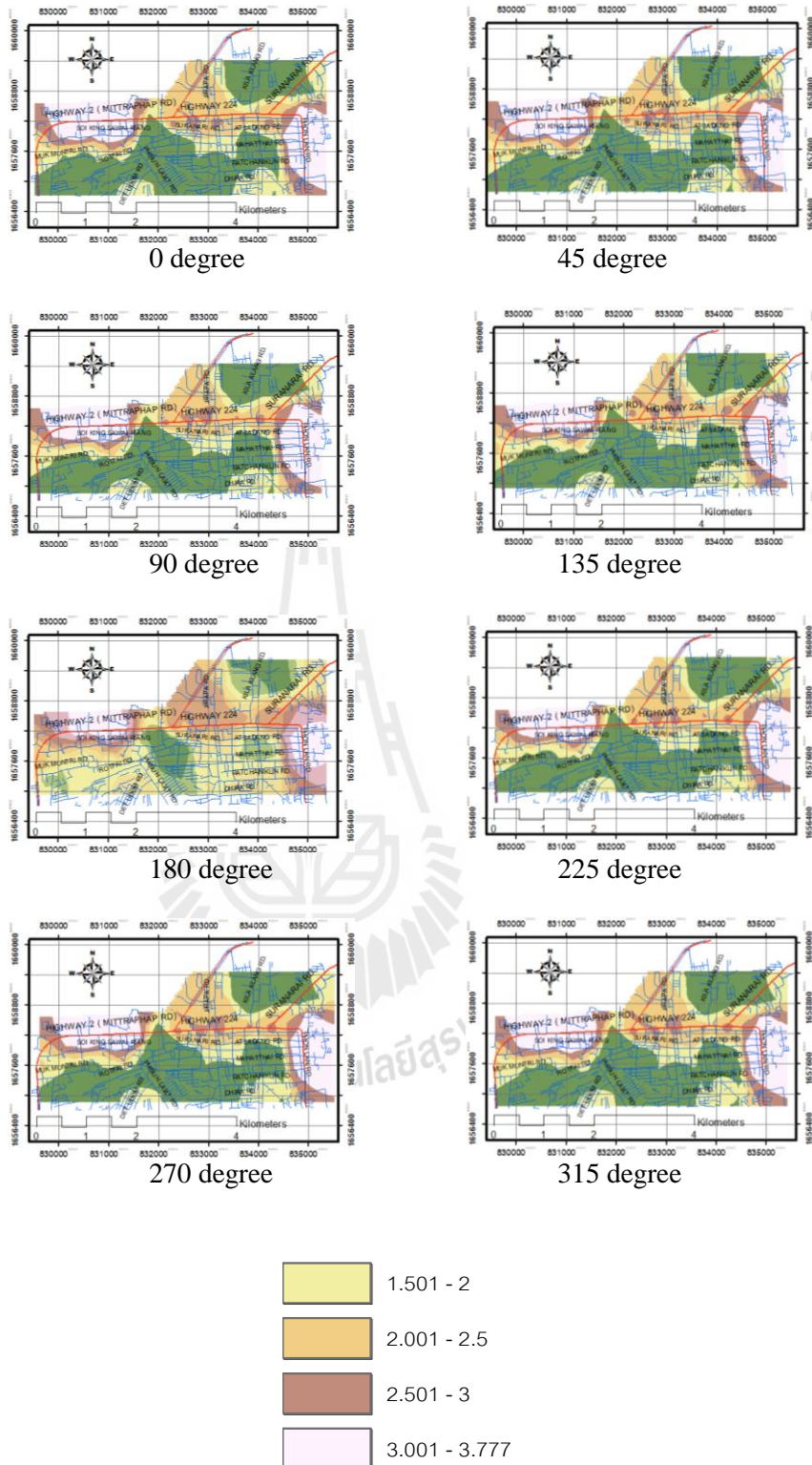


Figure G.14 CO concentration (ppm) dispersion maps of HDDT vehicle type during 15:00-16:00.

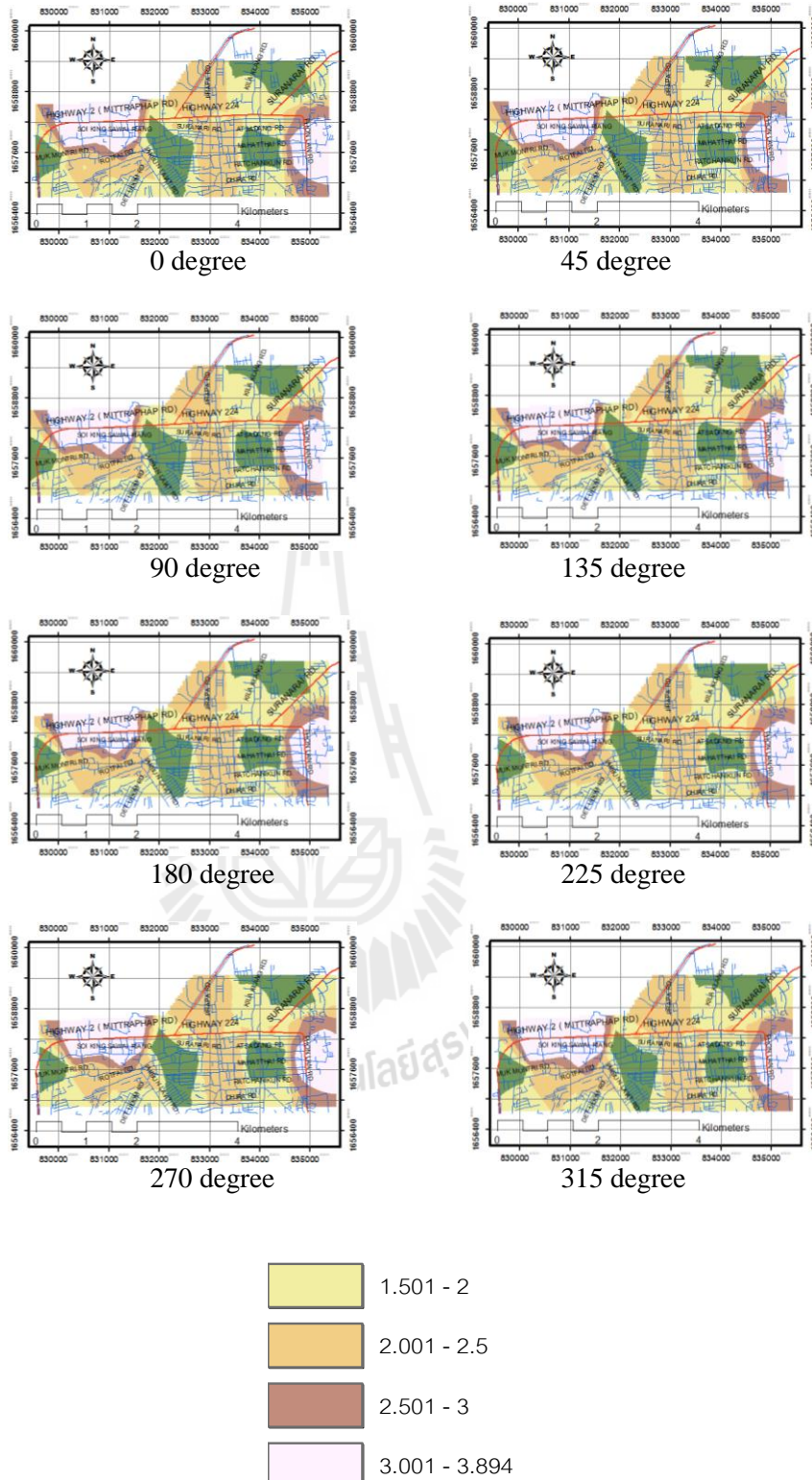


Figure G.15 CO concentration (ppm) dispersion maps of HDDT vehicle type during 18:00-19:00.

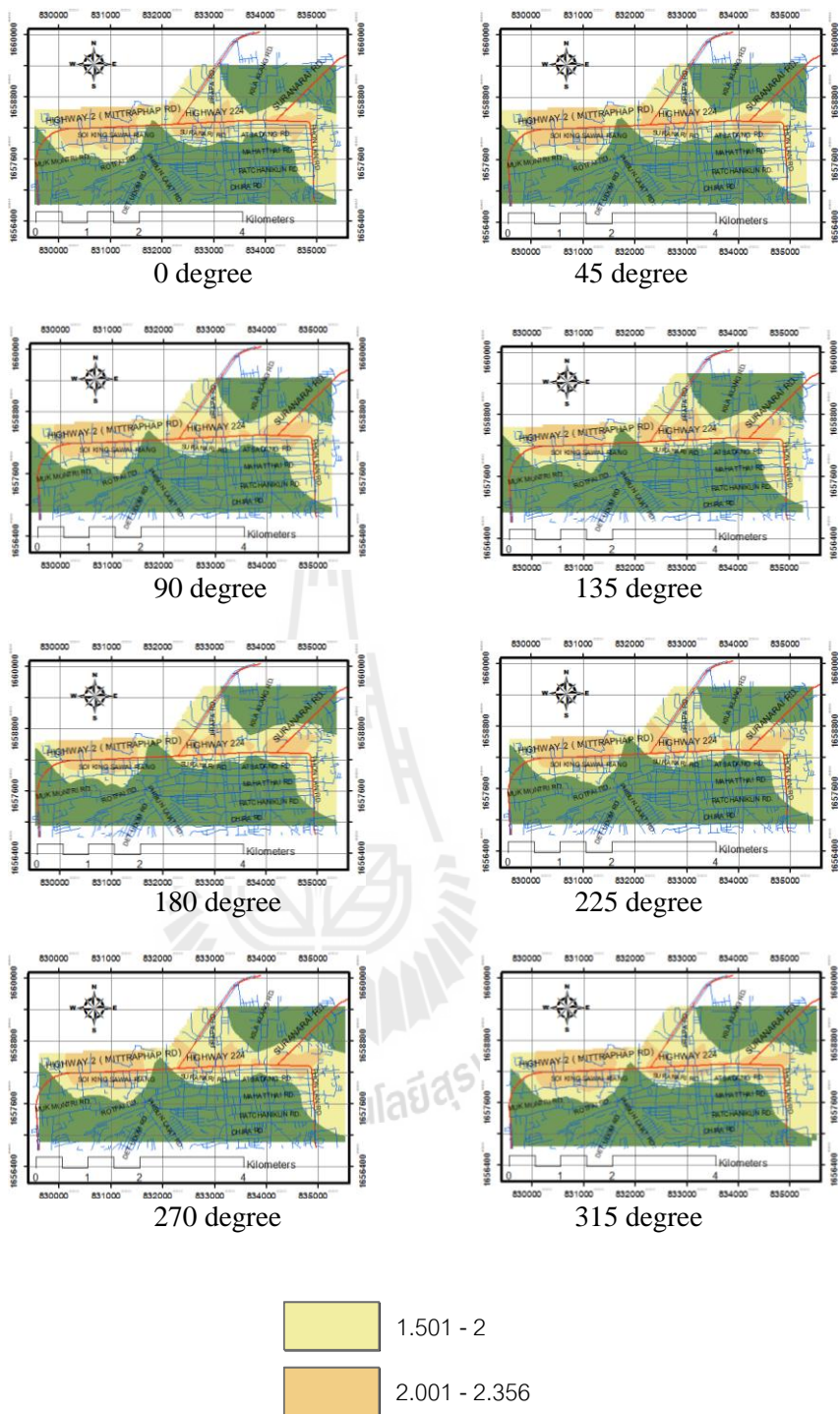


Figure G.16 CO concentration (ppm) dispersion maps of LDDT vehicle type during 07:00-08:00.

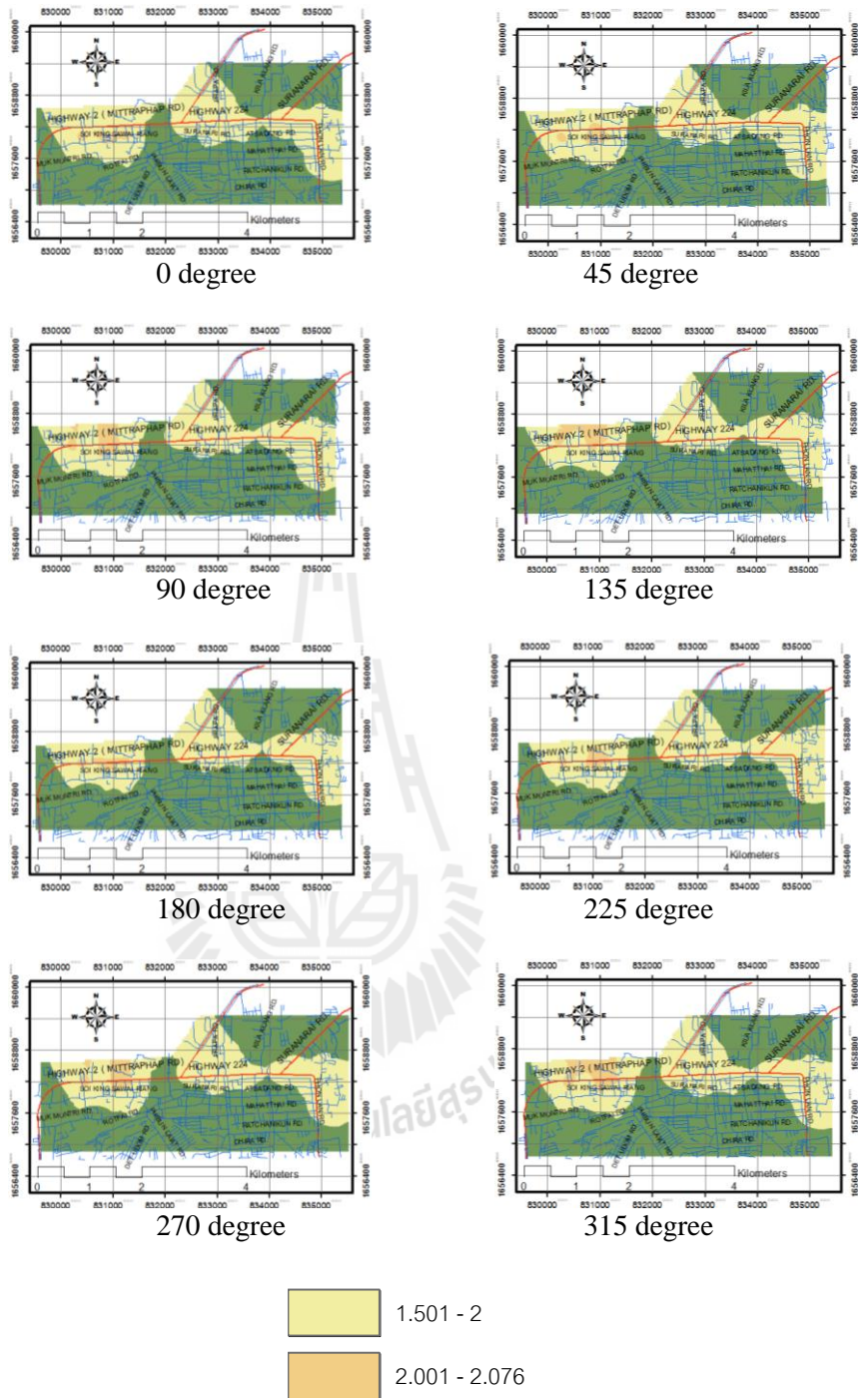


Figure G.17 CO concentration (ppm) dispersion maps of LDdT vehicle type during 09:00-10:00.

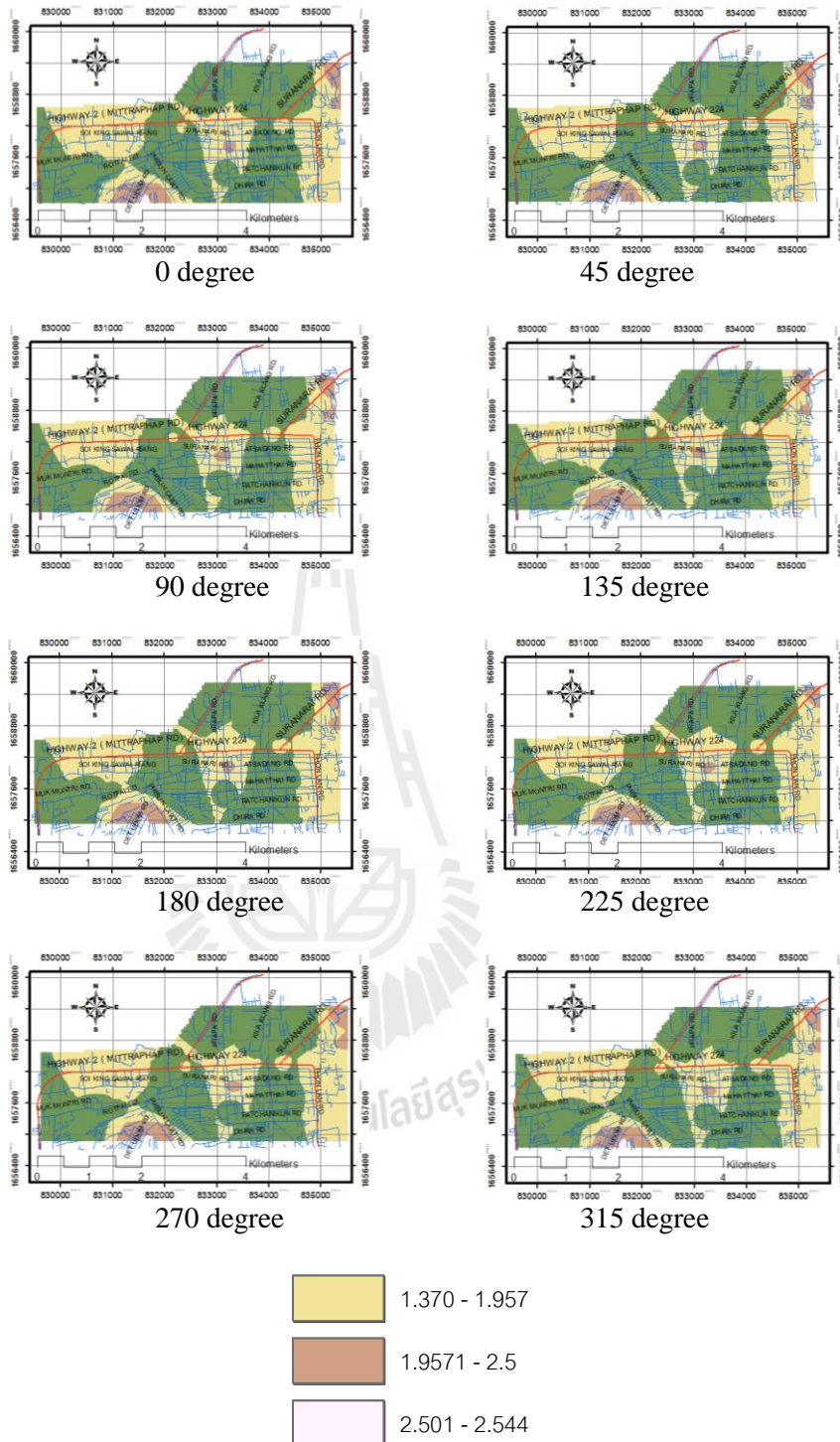


Figure G.18 CO concentration (ppm) dispersion maps of LDDT vehicle type during 12:00-13:00.

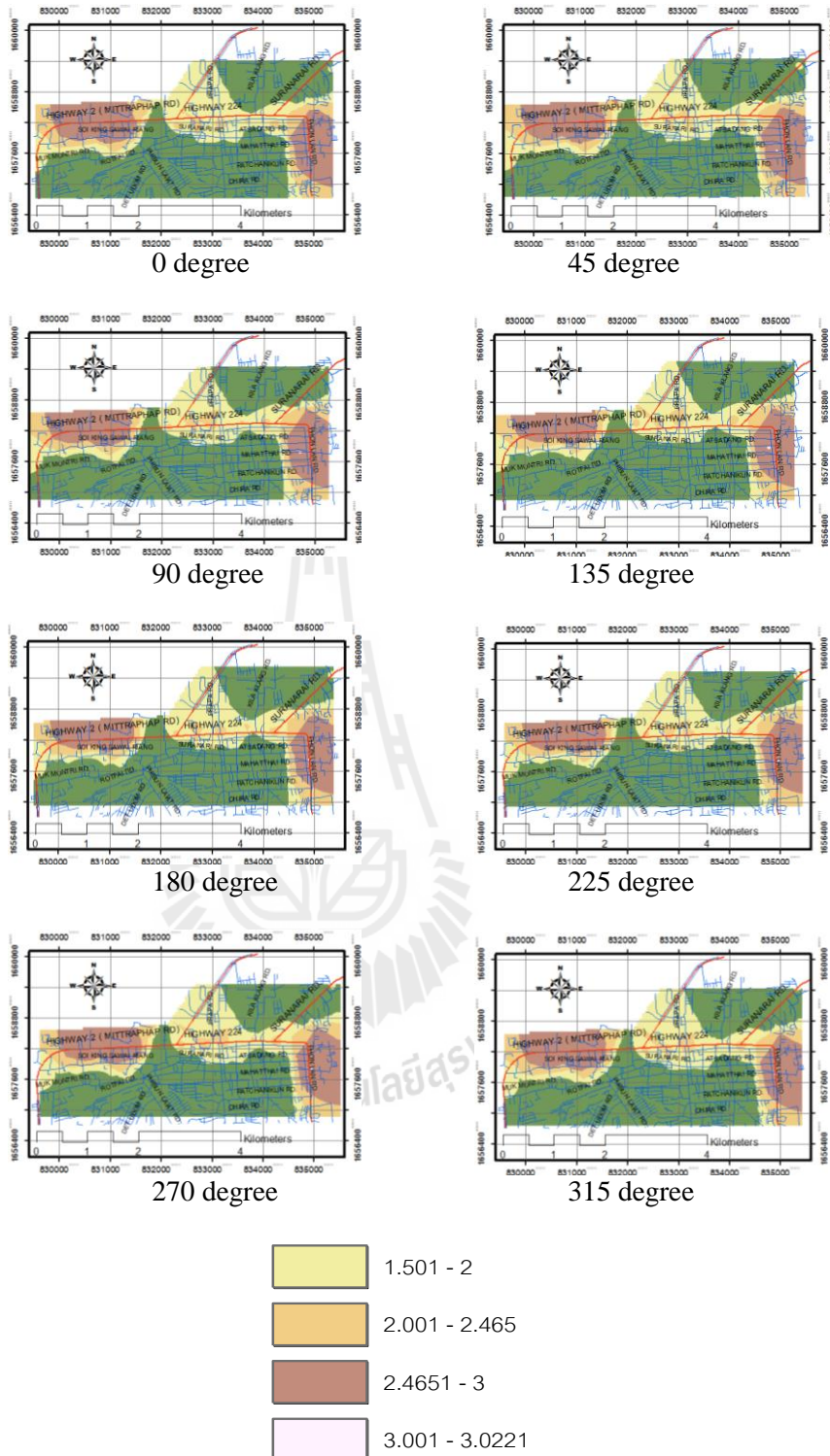


Figure G.19 CO concentration (ppm) dispersion maps of LDdT vehicle type during 15:00-16:00.

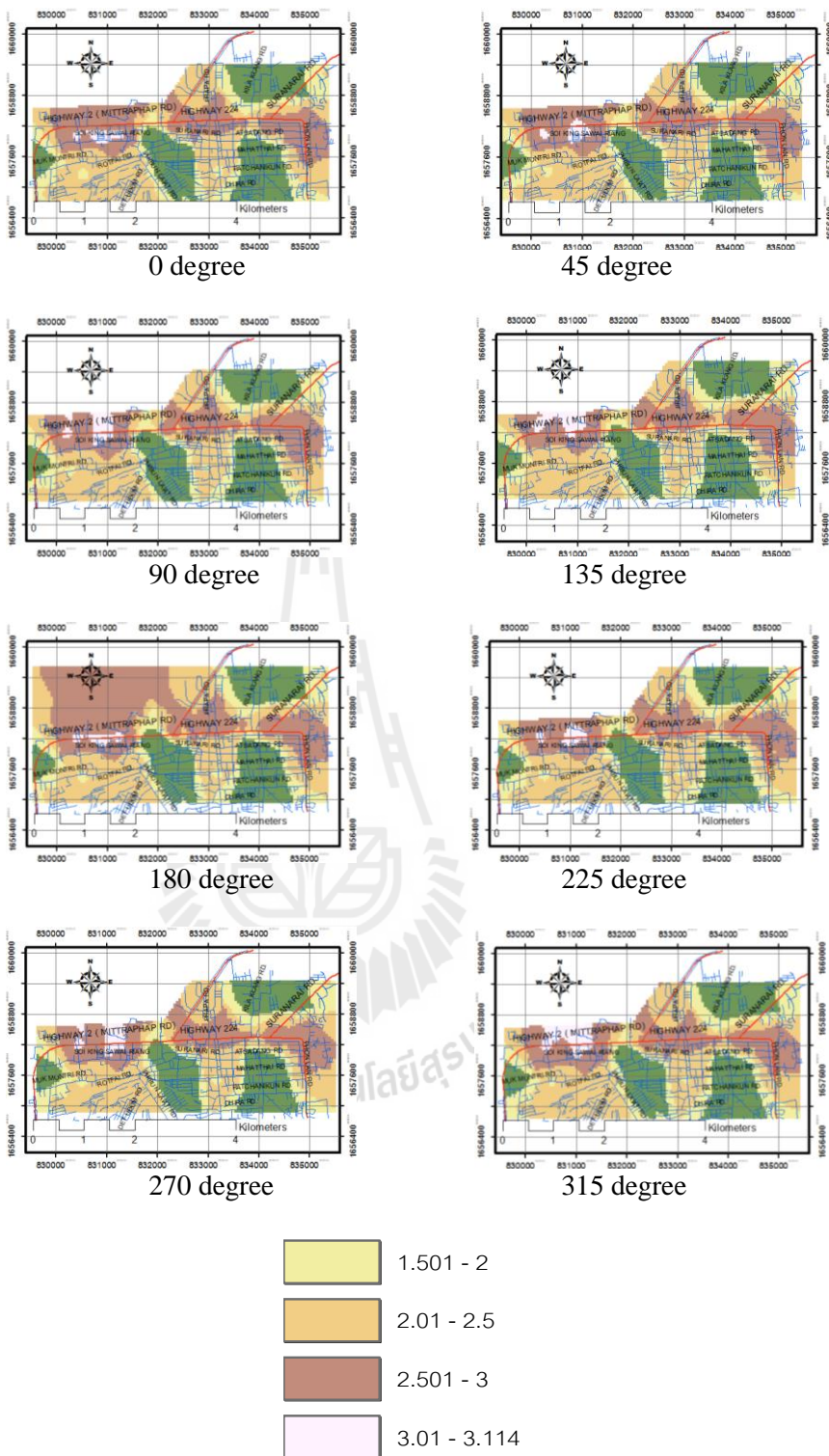


Figure G.20 CO concentration (ppm) dispersion maps of LDDT vehicle type during 18:00-19:00.



APPENDIX H

NOX CONCENTRATION (PPB) DISPERSION MAPS

VARIED WITH VEHICLE TYPES AND WIND

DIRECTION IN (0-315 DEGREE)

AT TIME PERIODS: (07:00-19:00)

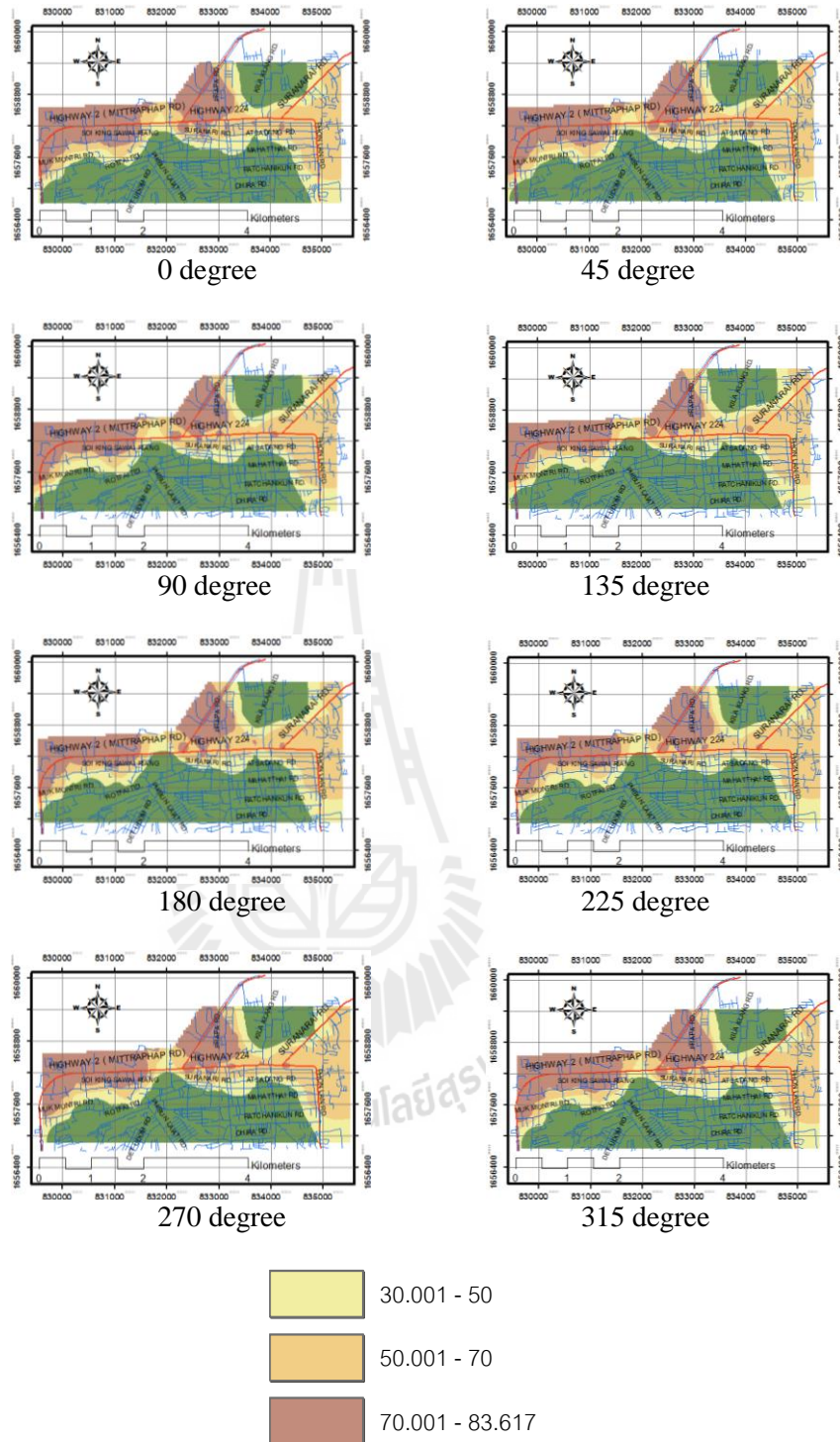


Figure H.1 NO_x concentration (ppb) dispersion maps of LDDT vehicle type during 07:00-08:00.

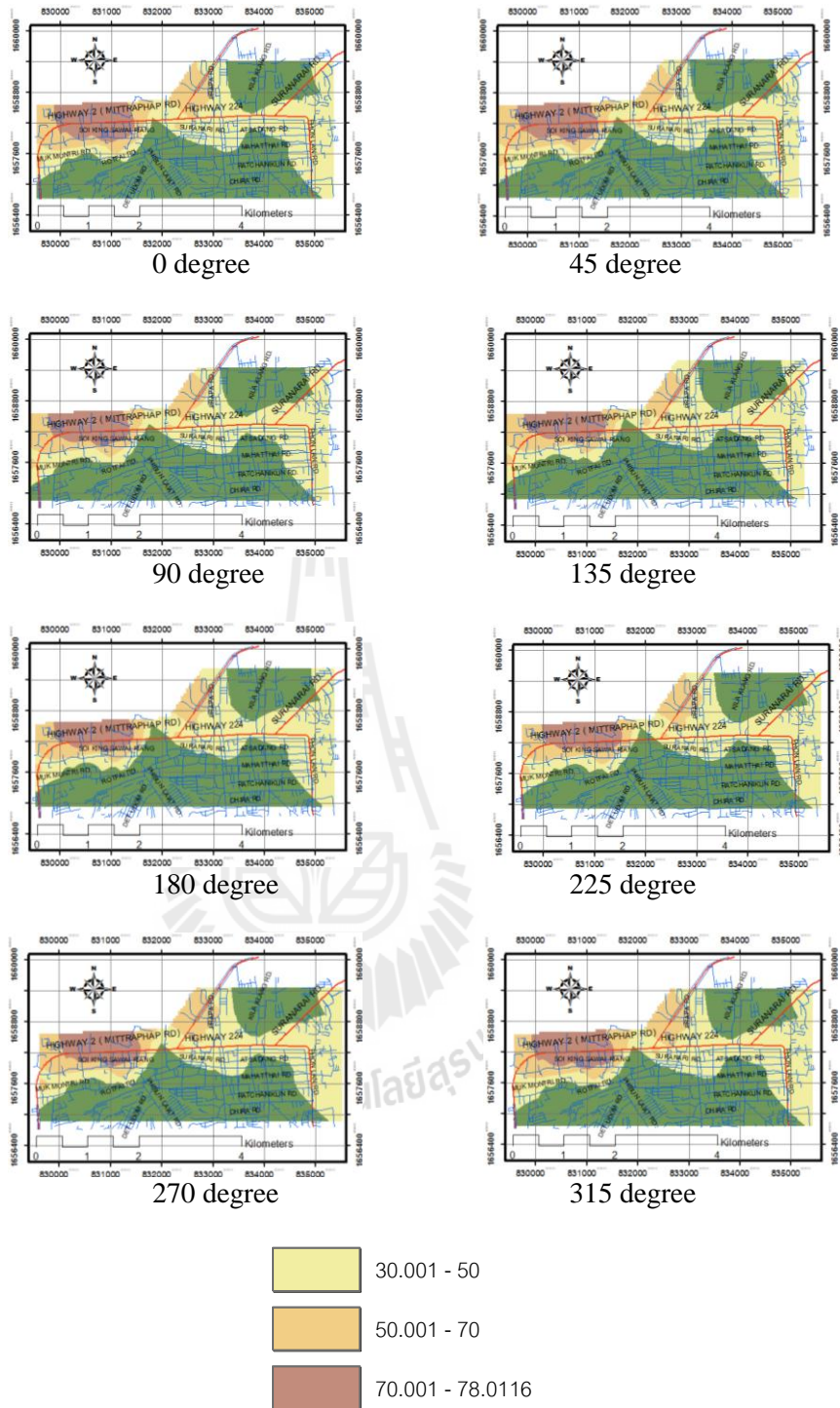


Figure H.2 NOx concentration (ppb) dispersion maps of LDDT vehicle type during 09:00-10:00.

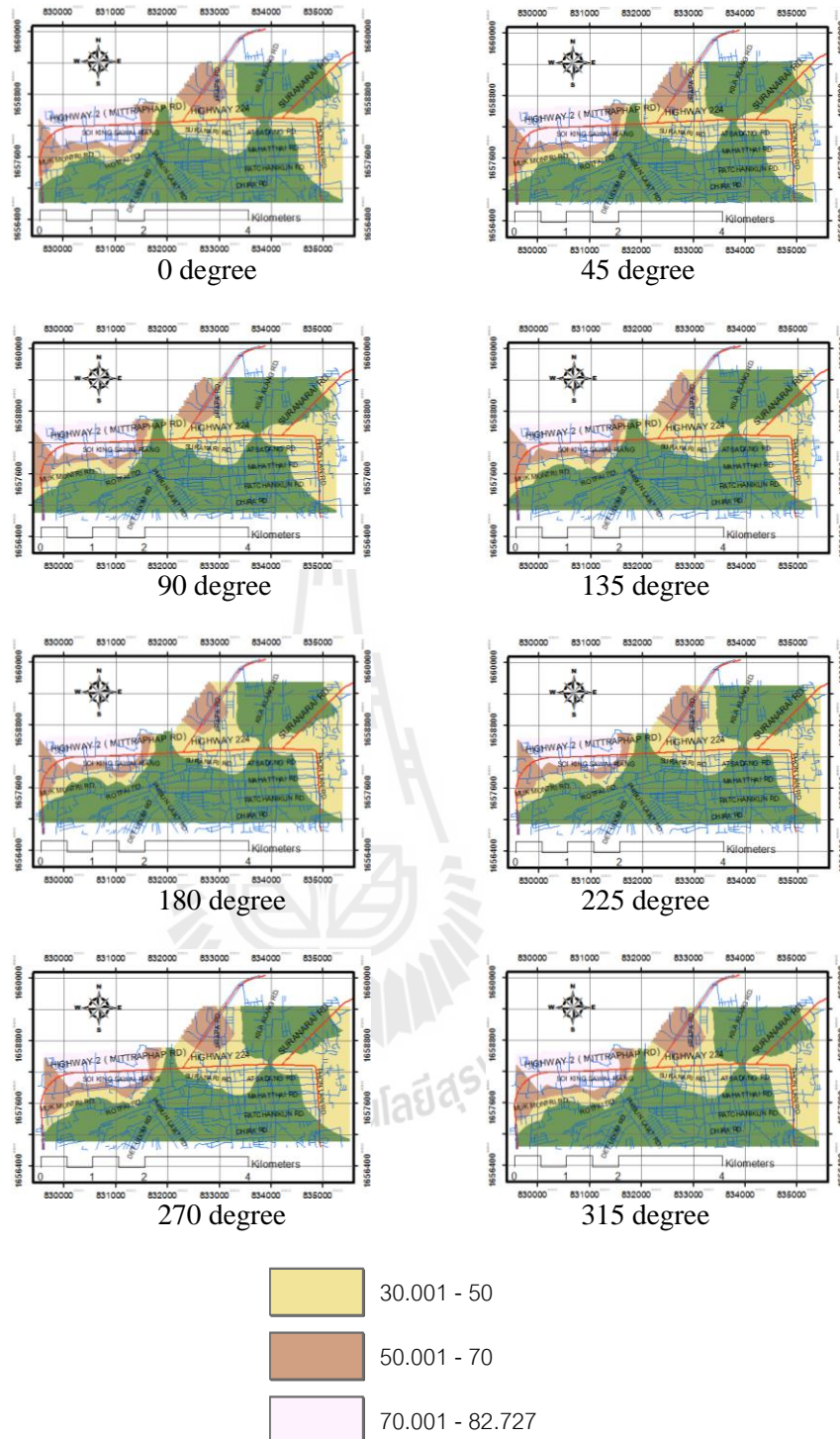


Figure H.3 NO_x concentration (ppb) dispersion maps of LDDT vehicle type during 12:00-13:00.

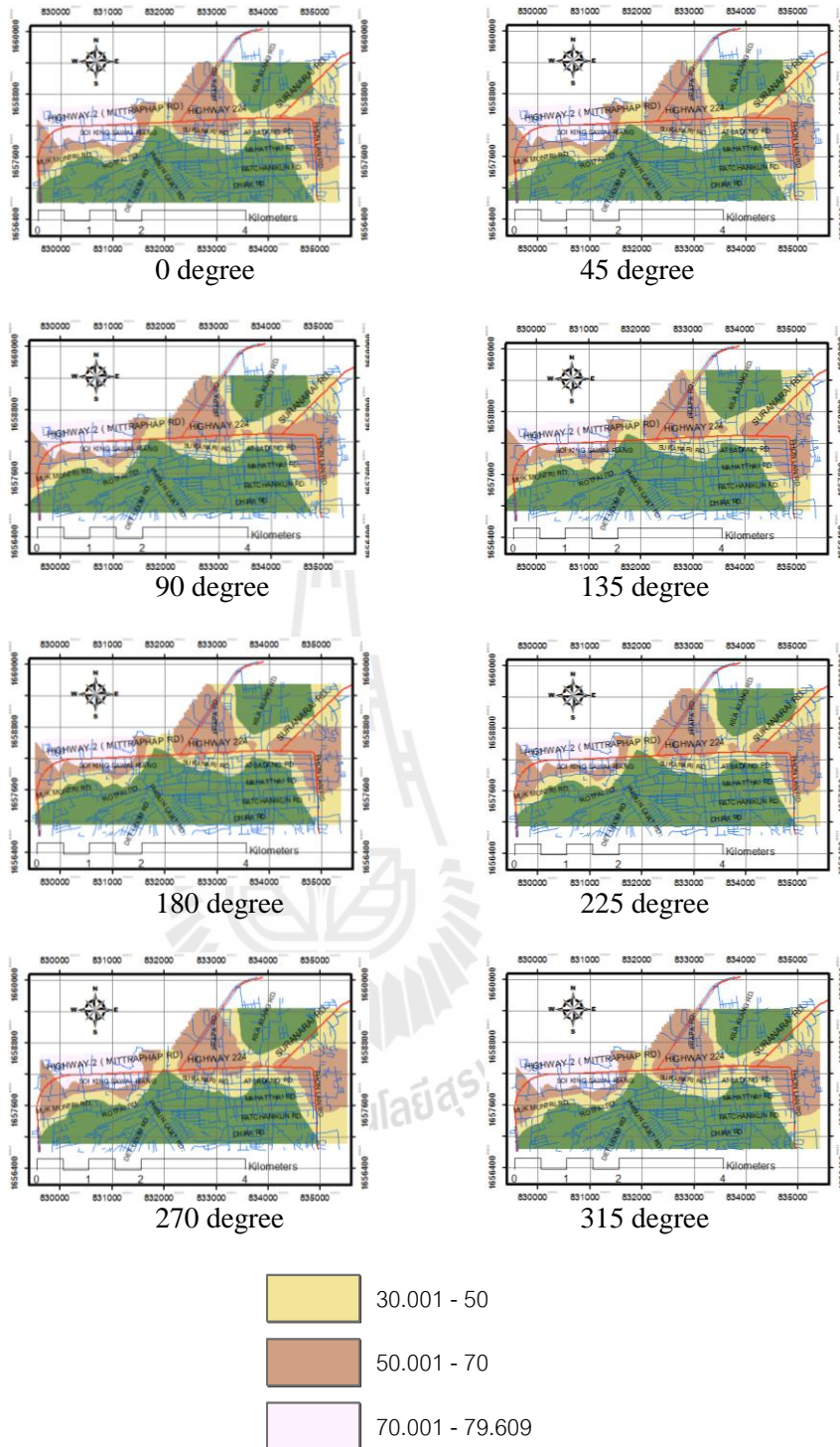


Figure H.4 NO_x concentration (ppb) dispersion maps of LDDT vehicle type during 15:00-16:00.

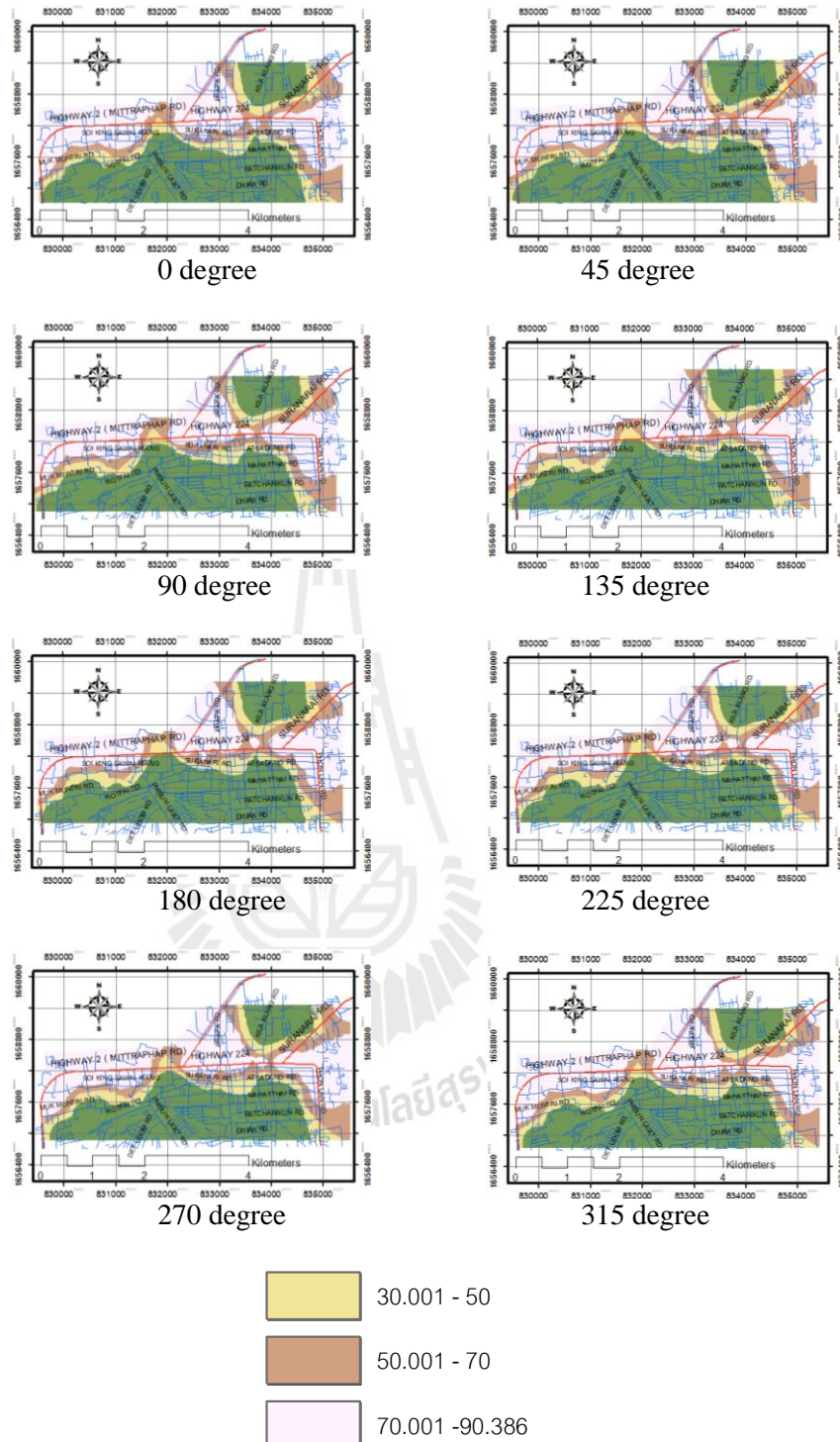


Figure H.5 NO_x concentration (ppb) dispersion maps of LDVT vehicle type during 18:00-19:00.

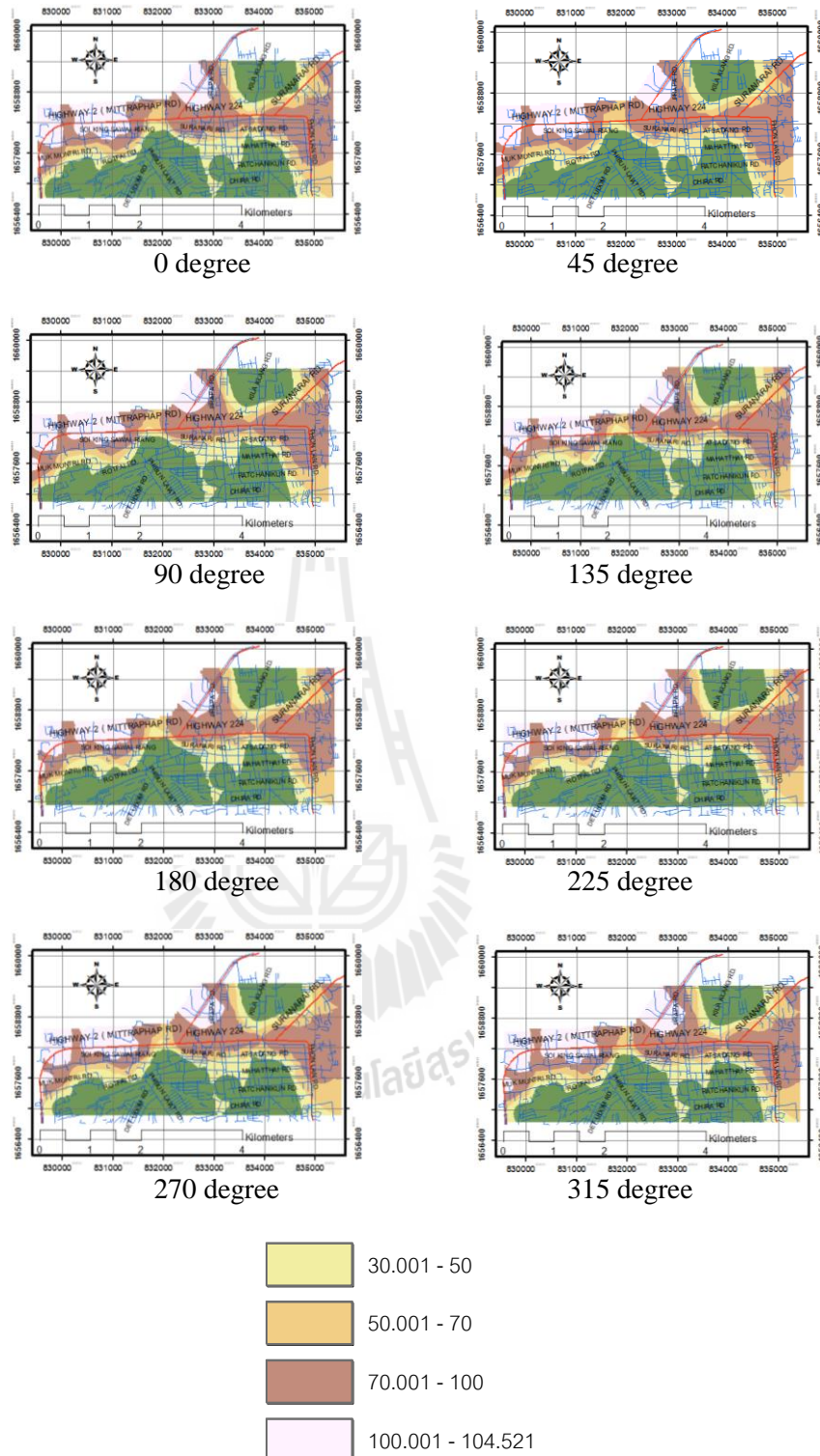


Figure H.6 NO_x concentration (ppb) dispersion maps of HDDT vehicle type during 07:00-08:00.

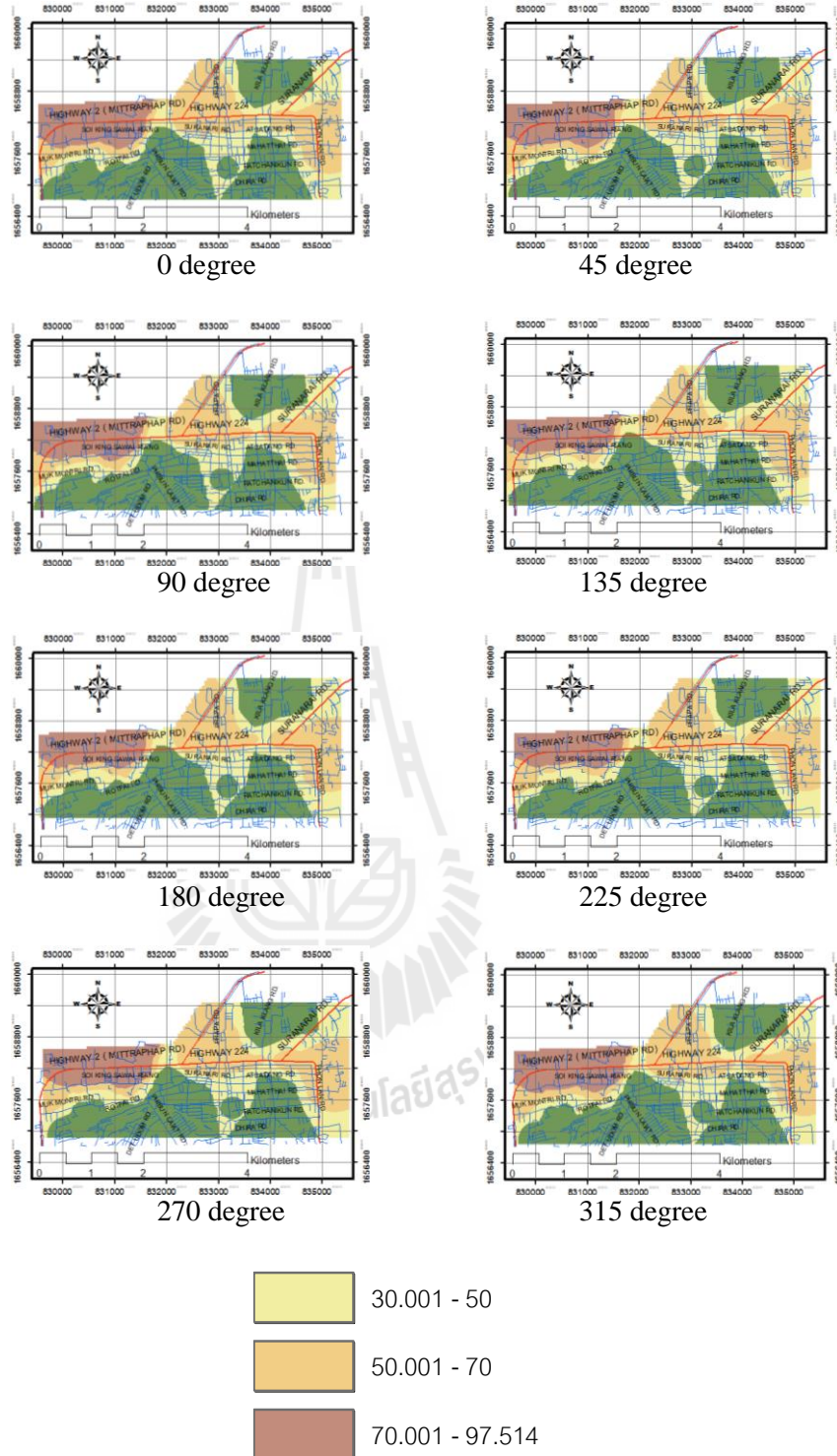


Figure H.7 NO_x concentration (ppb) dispersion maps of HDDT vehicle type during 09:00-10:00.

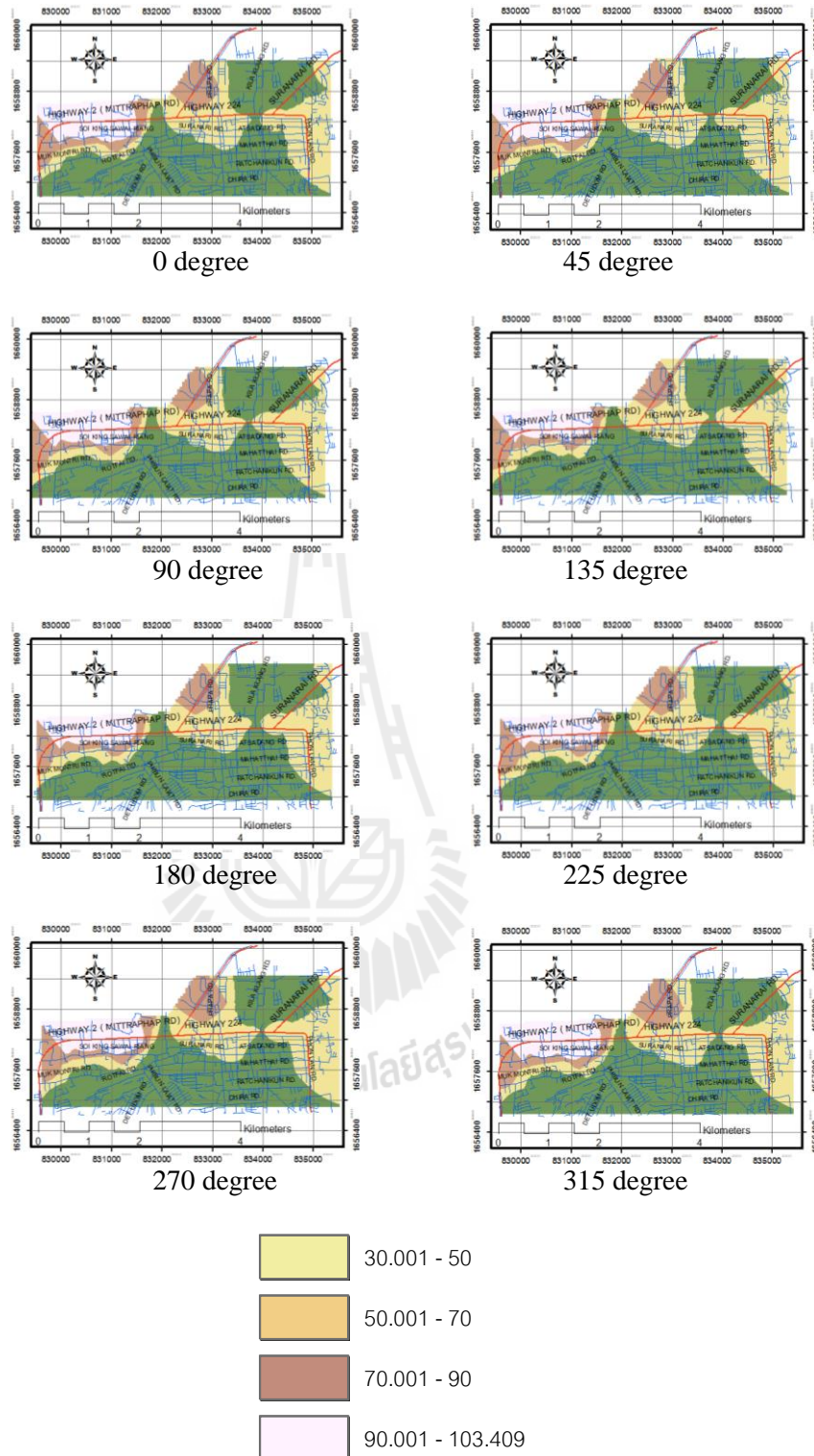


Figure H.8 NO_x concentration (ppb) dispersion maps of HDDT vehicle type during 12:00-13:00.

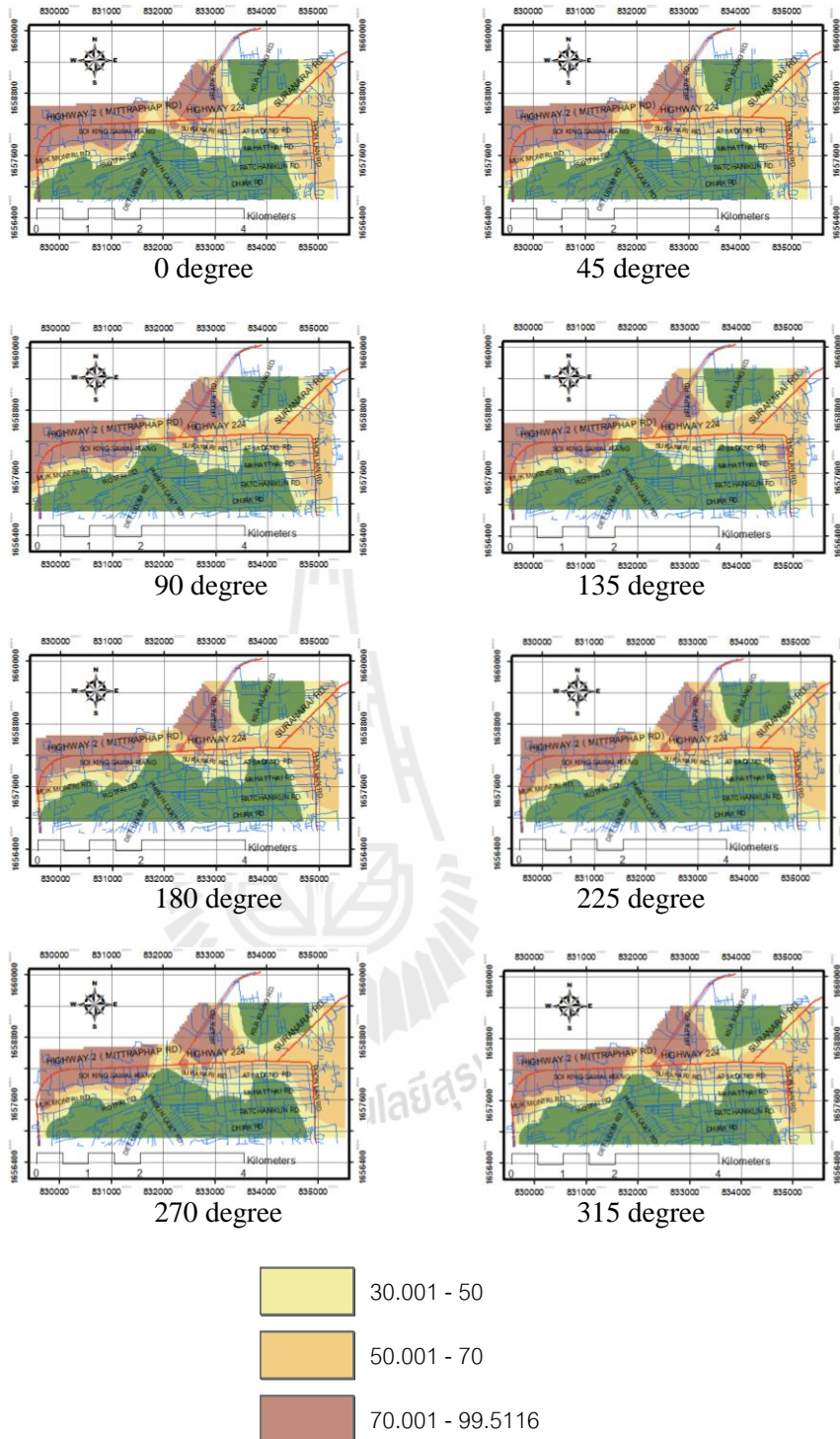


Figure H.9 NO_x concentration (ppb) dispersion maps of HDDT vehicle type during 15:00-16:00.



APPENDIX I

PM10 CONCENTRATION ($\mu\text{g}/\text{m}^3$) DISPERSION MAPS

VARIED WITH VEHICLE TYPES AND WIND

DIRECTION IN (0-315 DEGREE)

AT TIME PERIODS: (07:00-19:00)

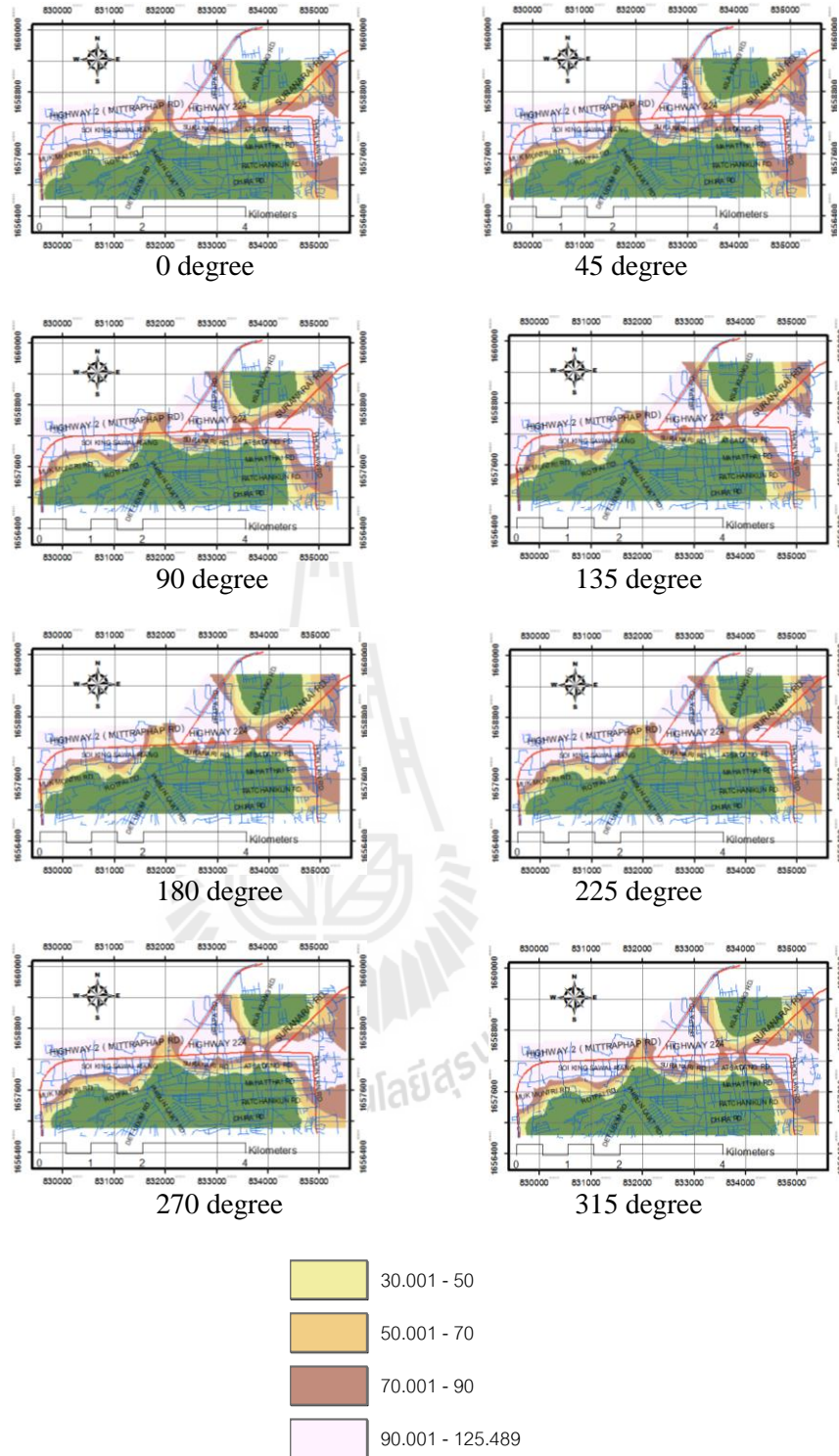


Figure I.1 PM10 concentration ($\mu\text{g}/\text{m}^3$) dispersion maps of HDDT vehicle type during 07:00-08:00.

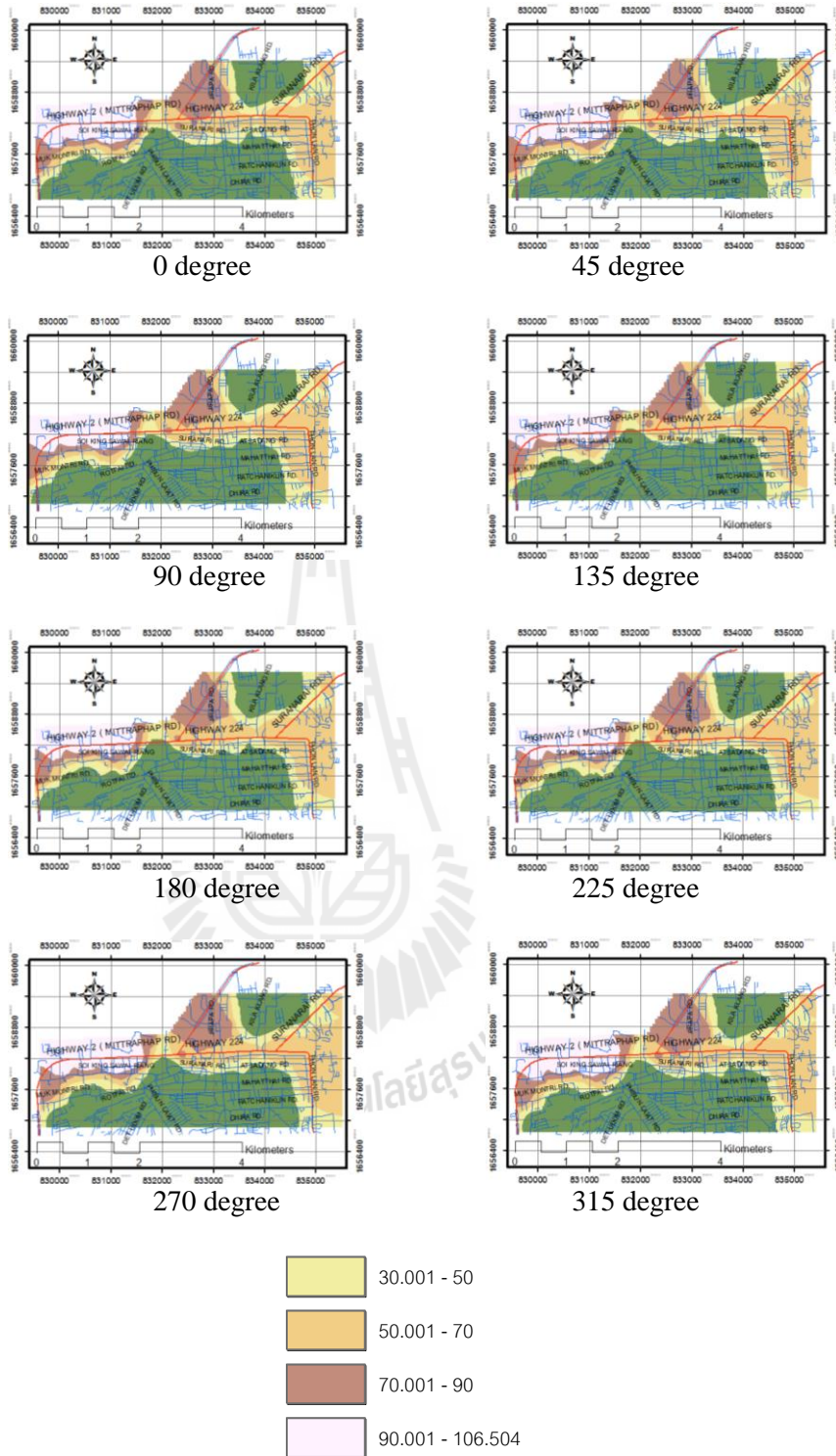


Figure I.2 PM10 concentration ($\mu\text{g}/\text{m}^3$) dispersion maps of HDDT vehicle type during 09:00-10:00.

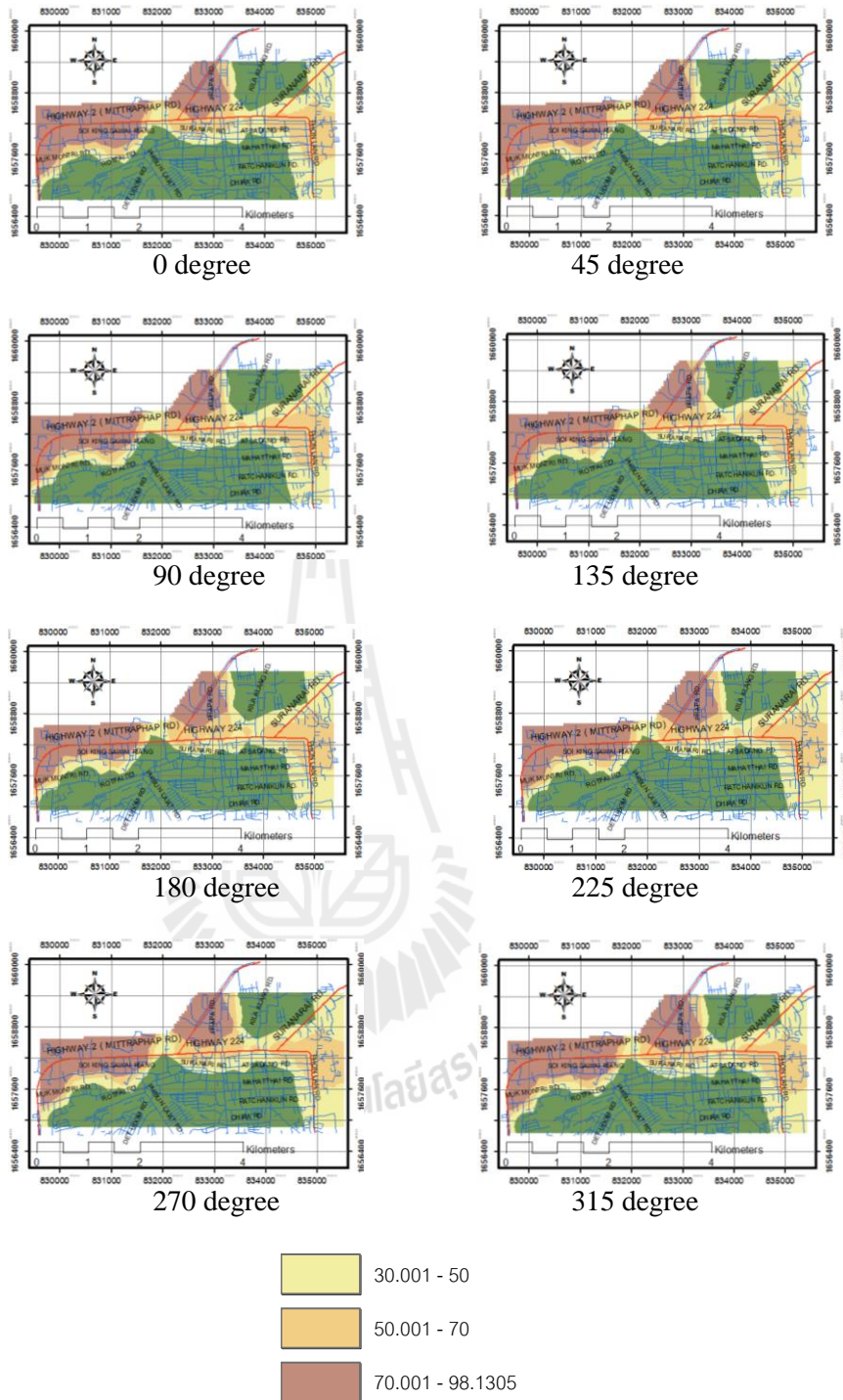


Figure I.3 PM10 concentration ($\mu\text{g}/\text{m}^3$) dispersion maps of HDDT vehicle type during 12:00-13:00.

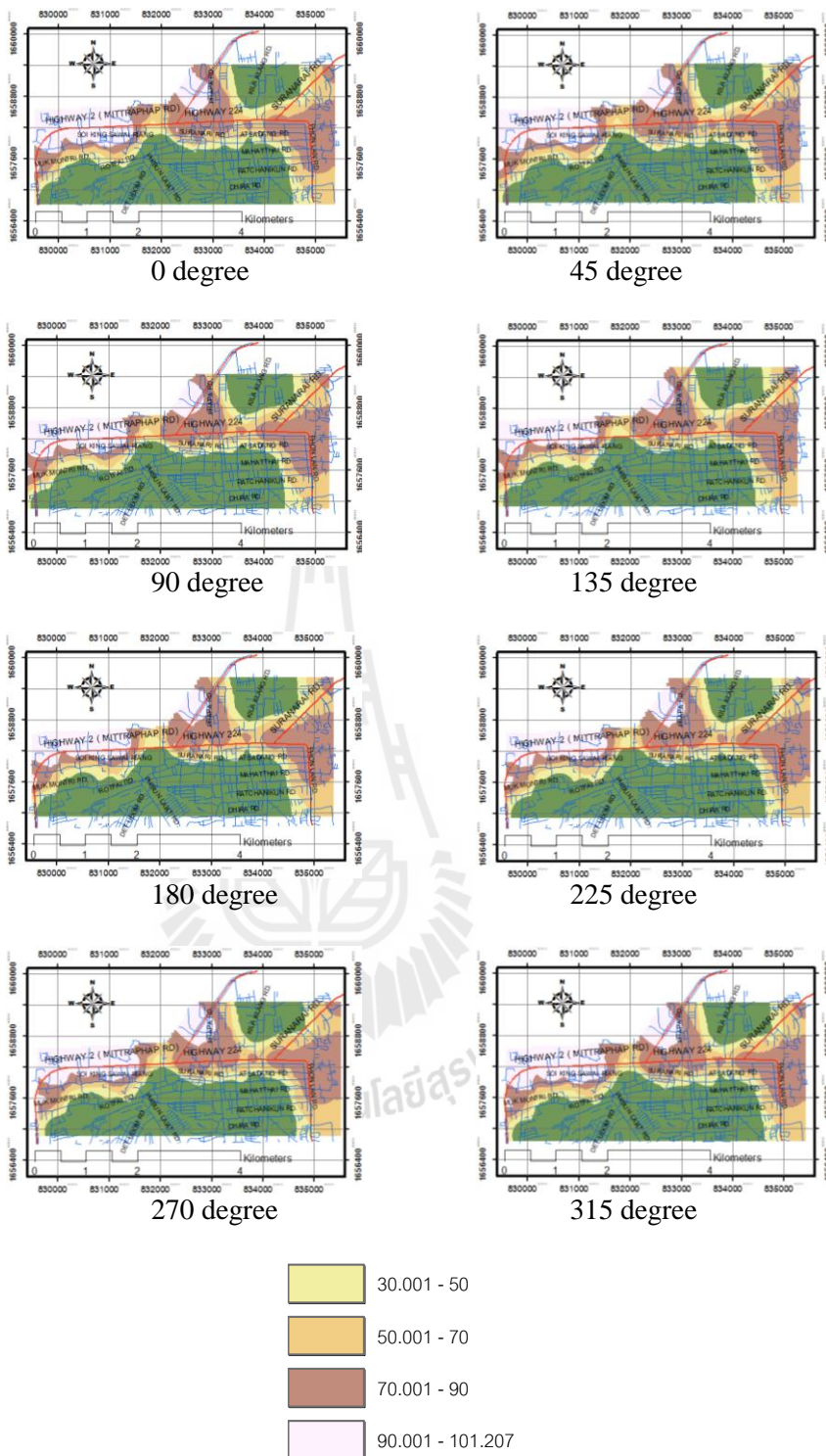


Figure I.4 PM10 concentration ($\mu\text{g}/\text{m}^3$) dispersion maps of HDDT vehicle type during 15:00-16:00.

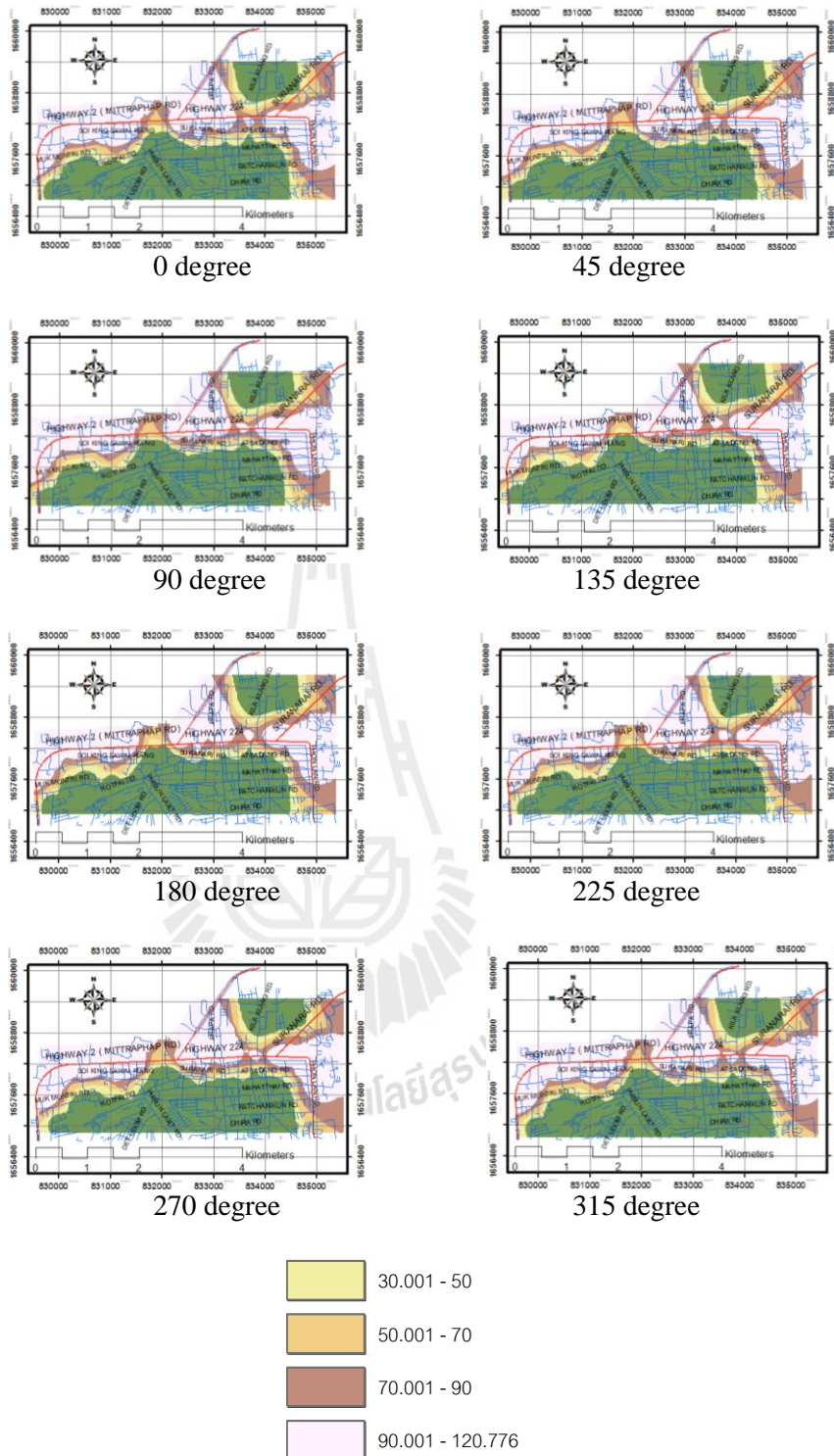


Figure I.5 PM10 concentration ($\mu\text{g}/\text{m}^3$) dispersion maps of HDDT vehicle type during 18:00-19:00.

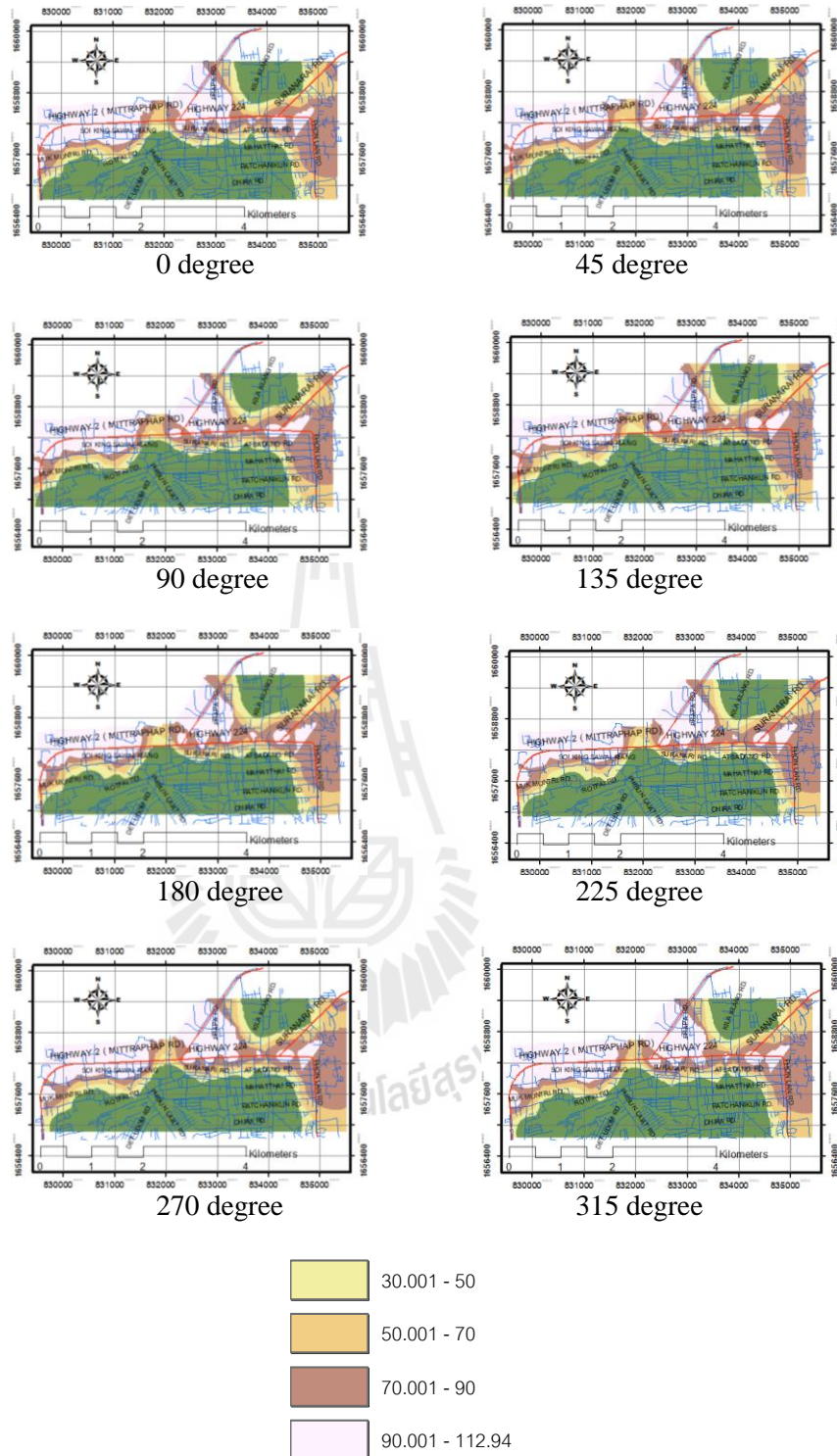


Figure I.6 PM10 concentration ($\mu\text{g}/\text{m}^3$) dispersion maps of LDDT vehicle type during 07:00-08:00.

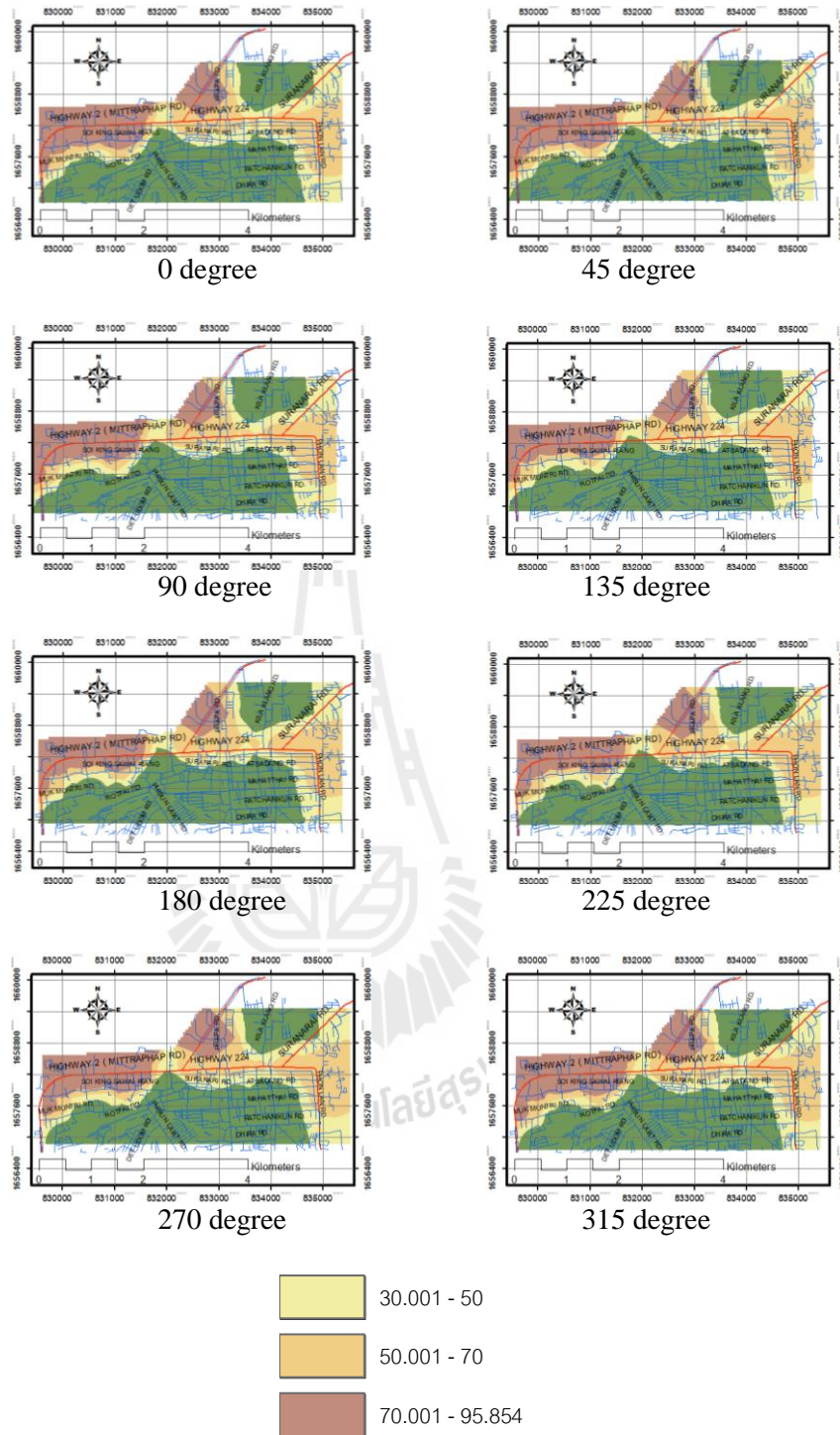


Figure I.7 PM10 concentration ($\mu\text{g}/\text{m}^3$) dispersion maps of LDDT vehicle type during 09:00-10:00.

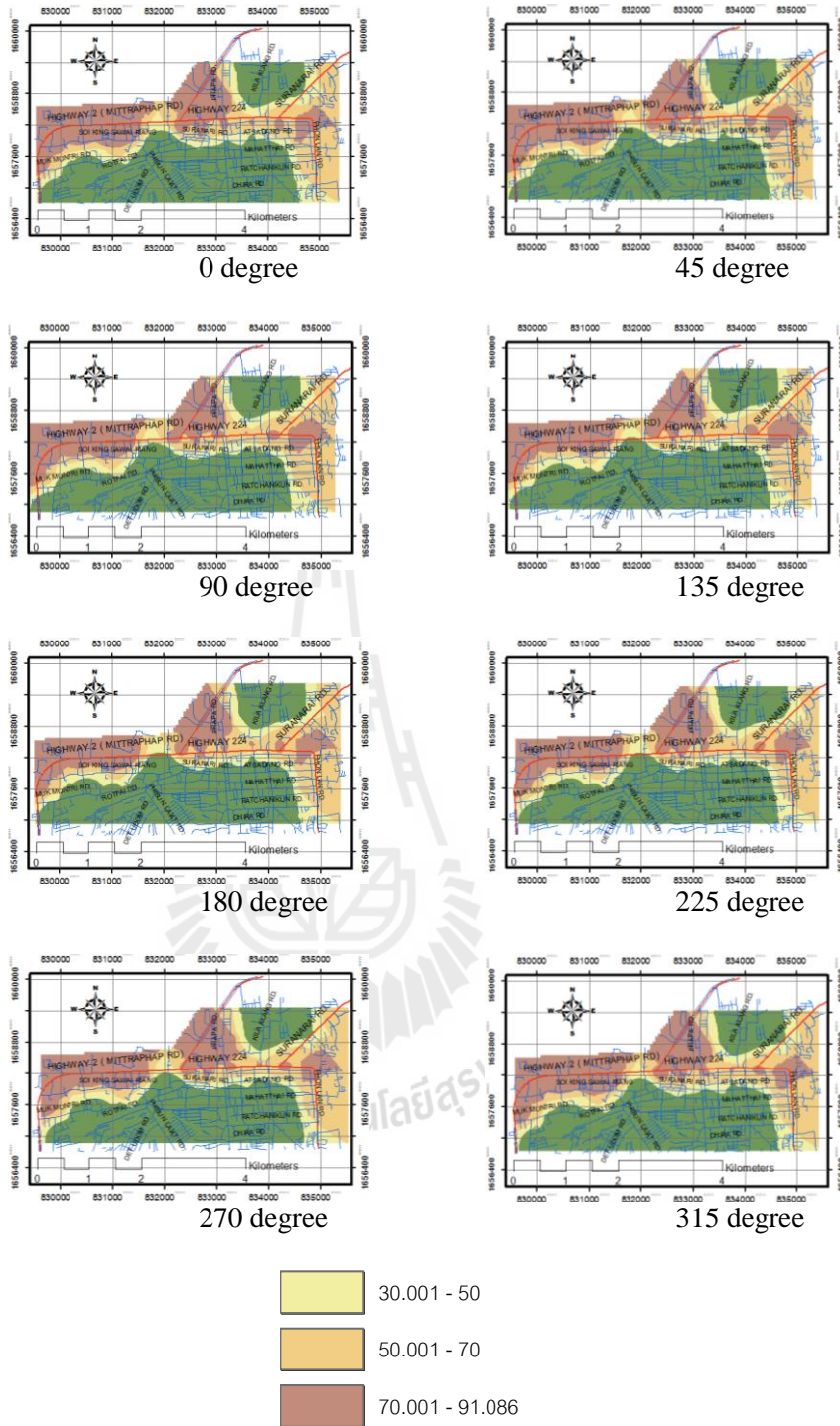


Figure I.9 PM10 concentration ($\mu\text{g}/\text{m}^3$) dispersion maps of LDDT vehicle type during 15:00-16:00.

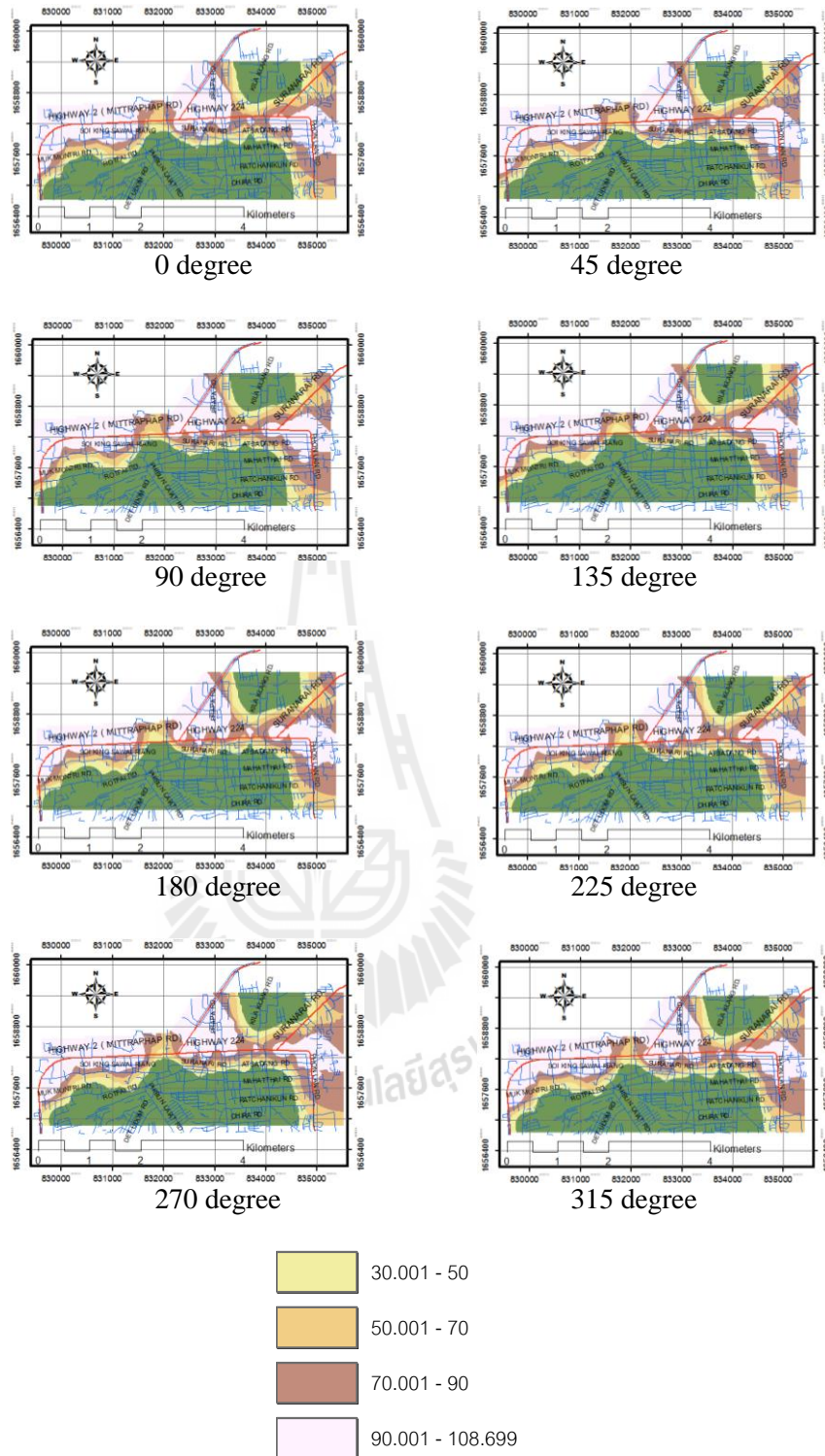


Figure I.10 PM10 concentration ($\mu\text{g}/\text{m}^3$) dispersion maps of LDDT vehicle type during 18:00-19:00.



APPENDIX J

**FREQUENCY OF VIOLENCE MAPS VARIED WITH
VEHICLE TYPES AT TIME PERIODS: (07:00-19:00)**

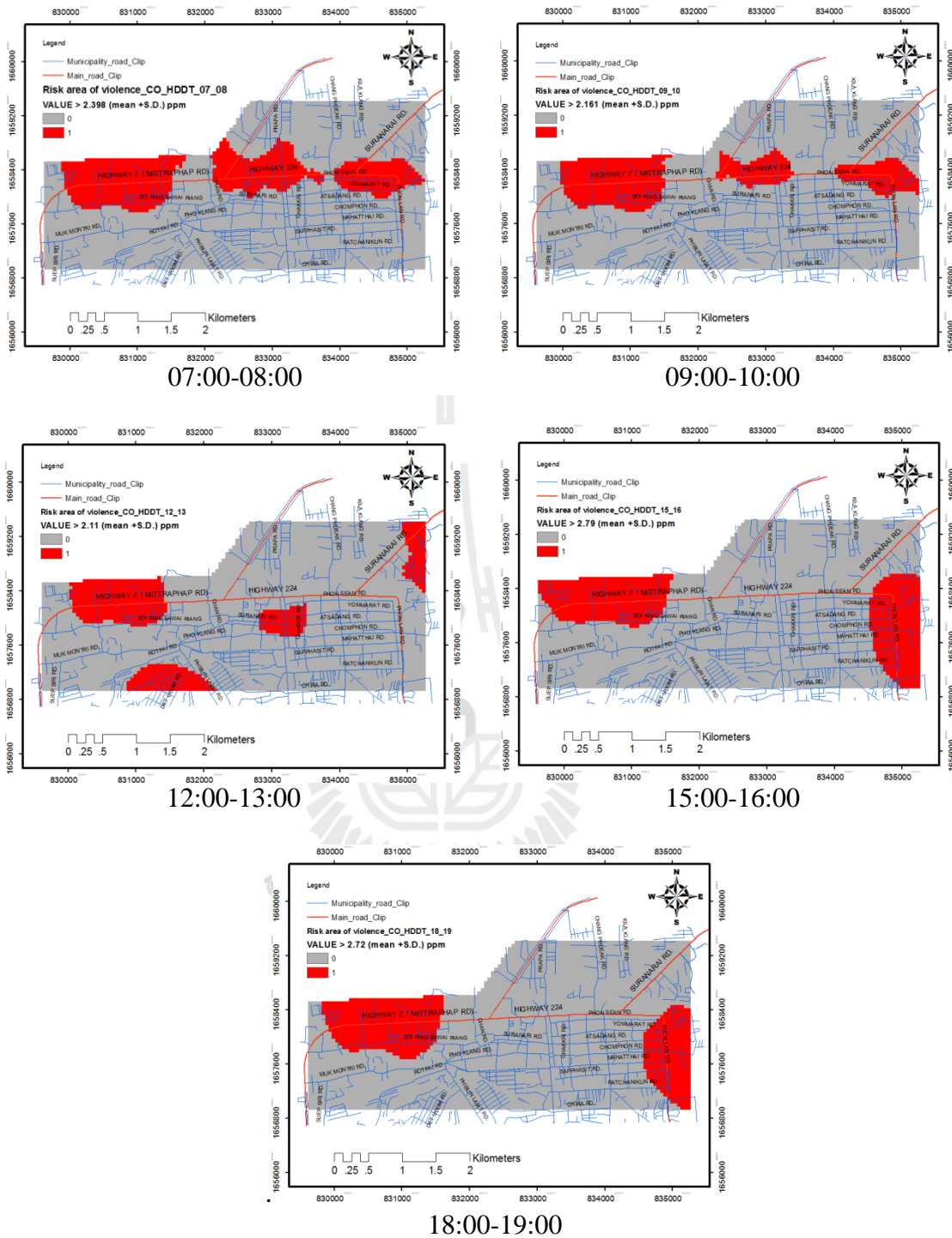


Figure J.1 CO frequency of violence map of HDDT vehicle type at 07:00-08:00, 09:00-10:00, 12:00-13:00, 15:00-16:00, and 18:00-19:00.

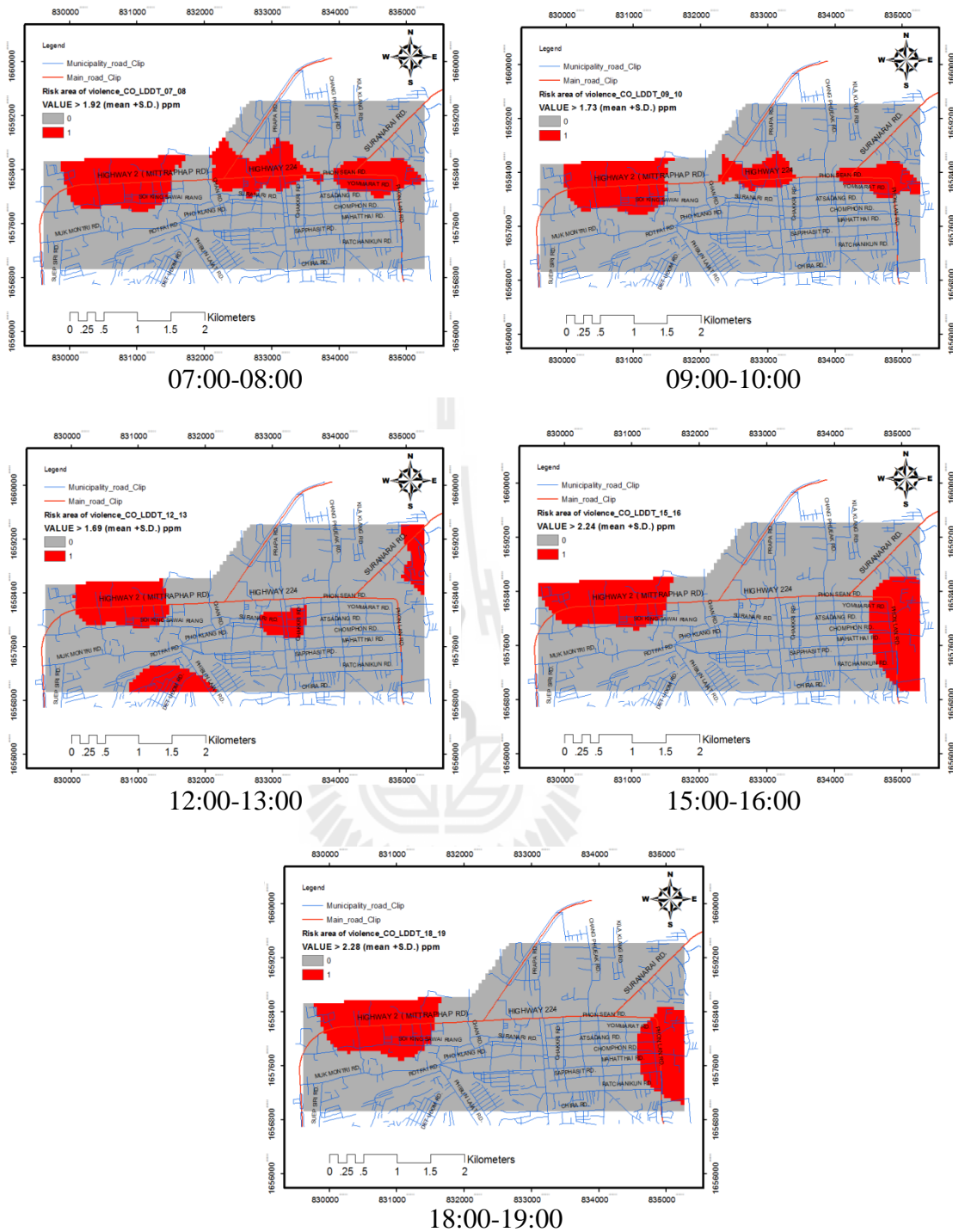


Figure J.2 CO frequency of violence map of LDDT vehicle type at 07:00-08:00, 09:00-10:00, 12:00-13:00, 15:00-16:00, and 18:00-19:00.

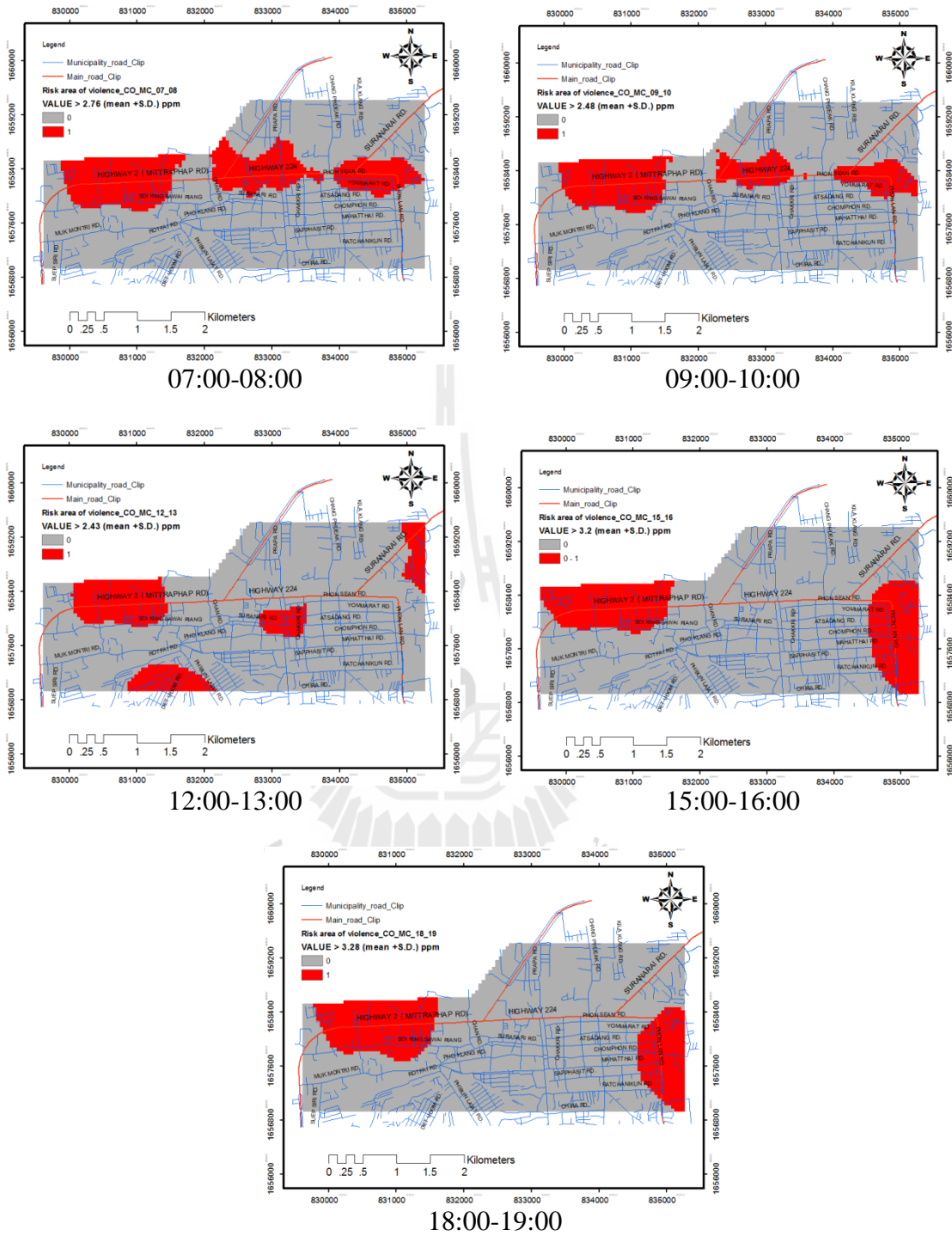


Figure J.3 CO frequency of violence map of MC vehicle type at 07:00-08:00, 09:00-10:00, 12:00-13:00, 15:00-16:00, and 18:00-19:00.

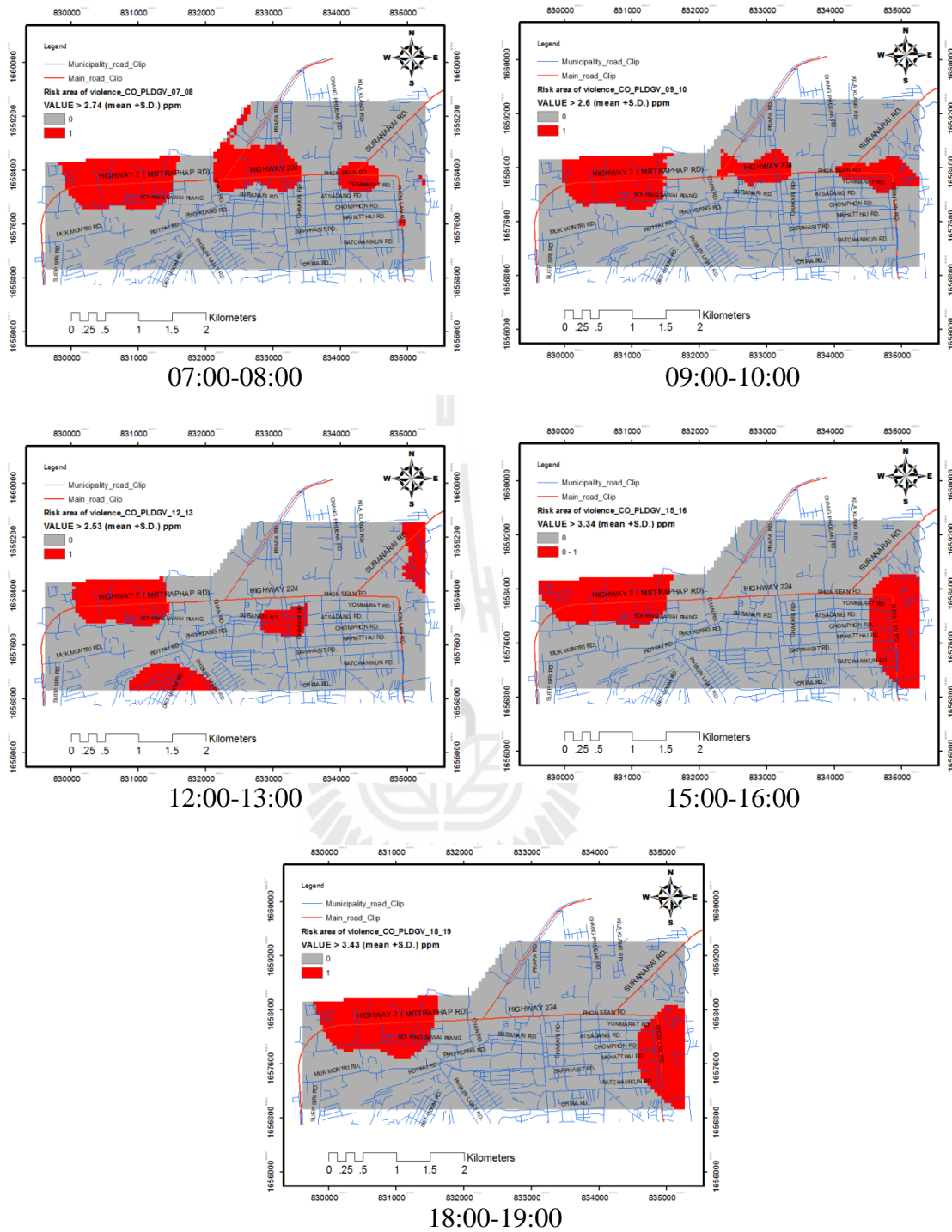


Figure J.4 CO frequency of violence map of PLDGV vehicle type at 07:00-08:00, 09:00-10:00, 12:00-13:00, 15:00-16:00, and 18:00-19:00.

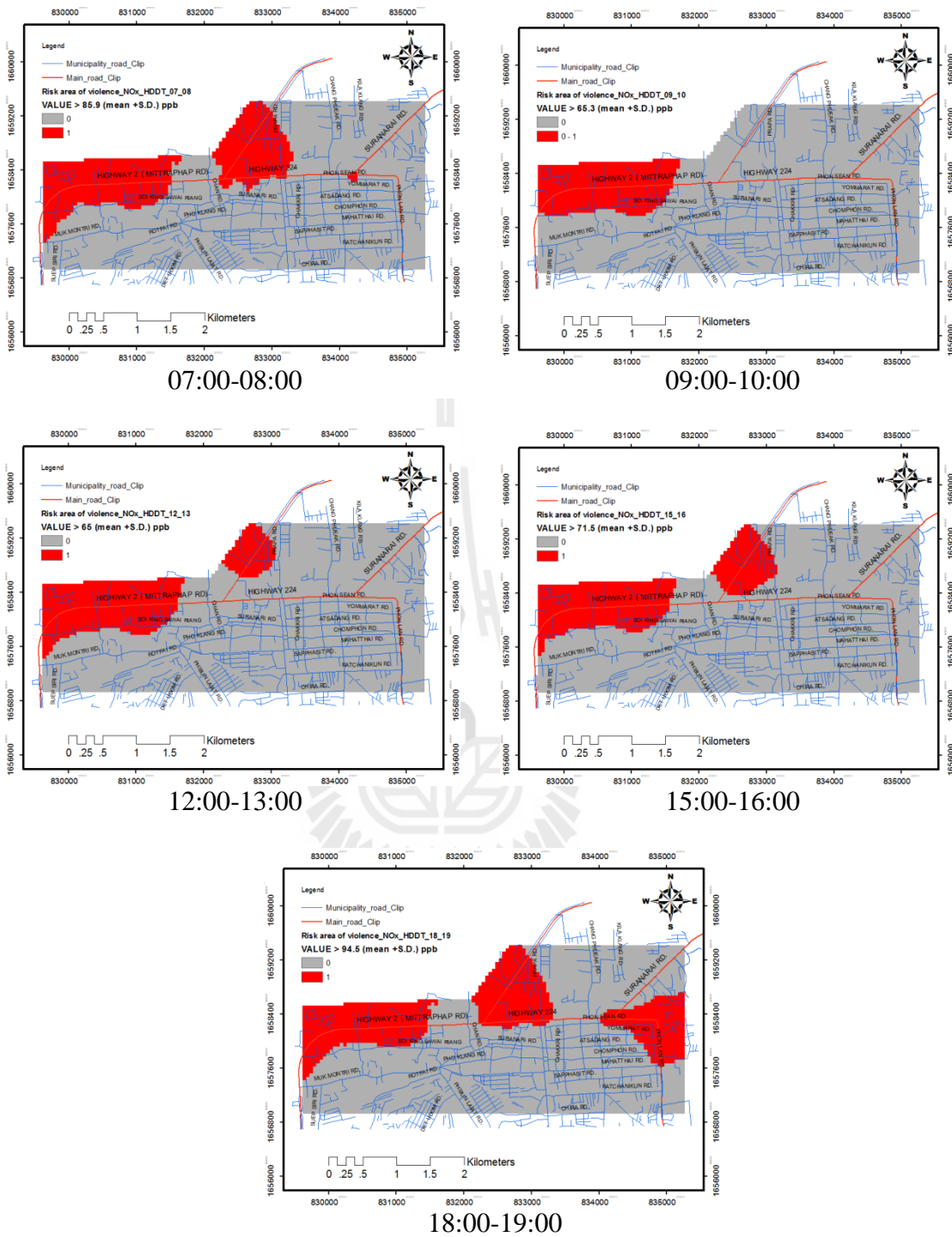


Figure J.5 NOx frequency of violence map of HDDT vehicle type at 07:00-08:00, 09:00-10:00, 12:00-13:00, 15:00-16:00, and 18:00-19:00.

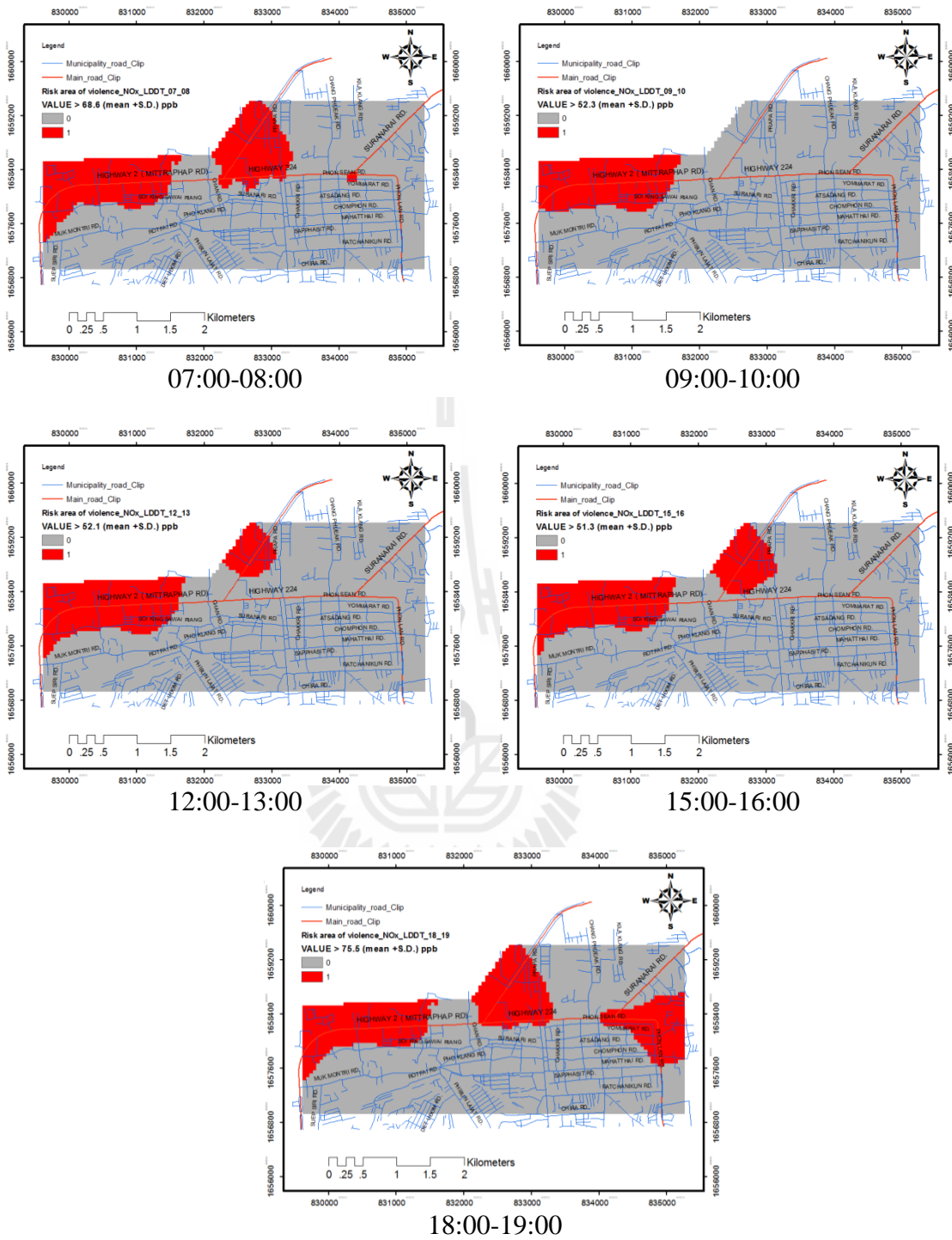


Figure J.6 NOx frequency of violence map of LDDT vehicle type at 07:00-08:00, 09:00-10:00, 12:00-13:00, 15:00-16:00, and 18:00-19:00.

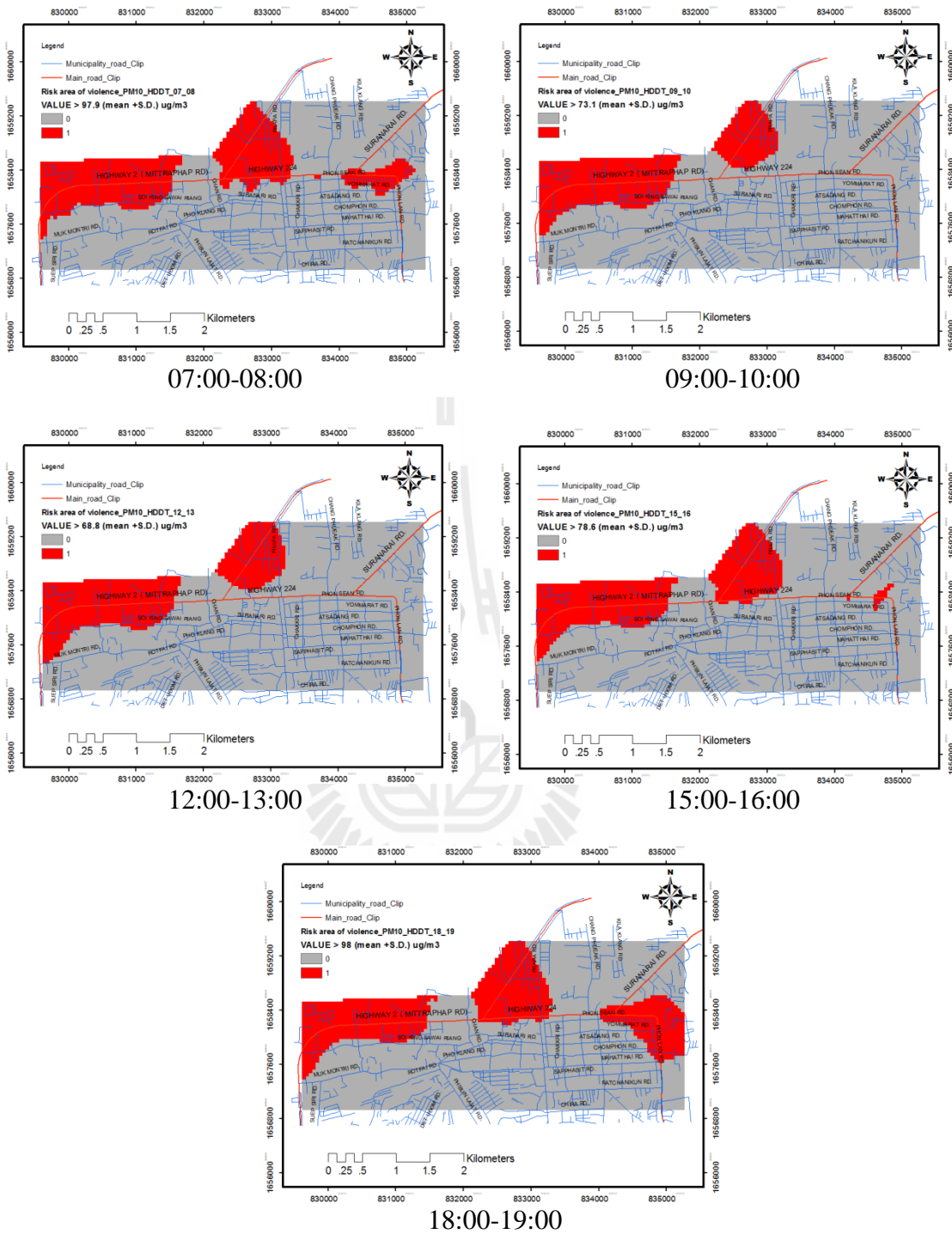


Figure J.7 PM10 frequency of violence map of HDDT vehicle type at 07:00-08:00, 09:00-10:00, 12:00-13:00, 15:00-16:00, and 18:00-19:00.

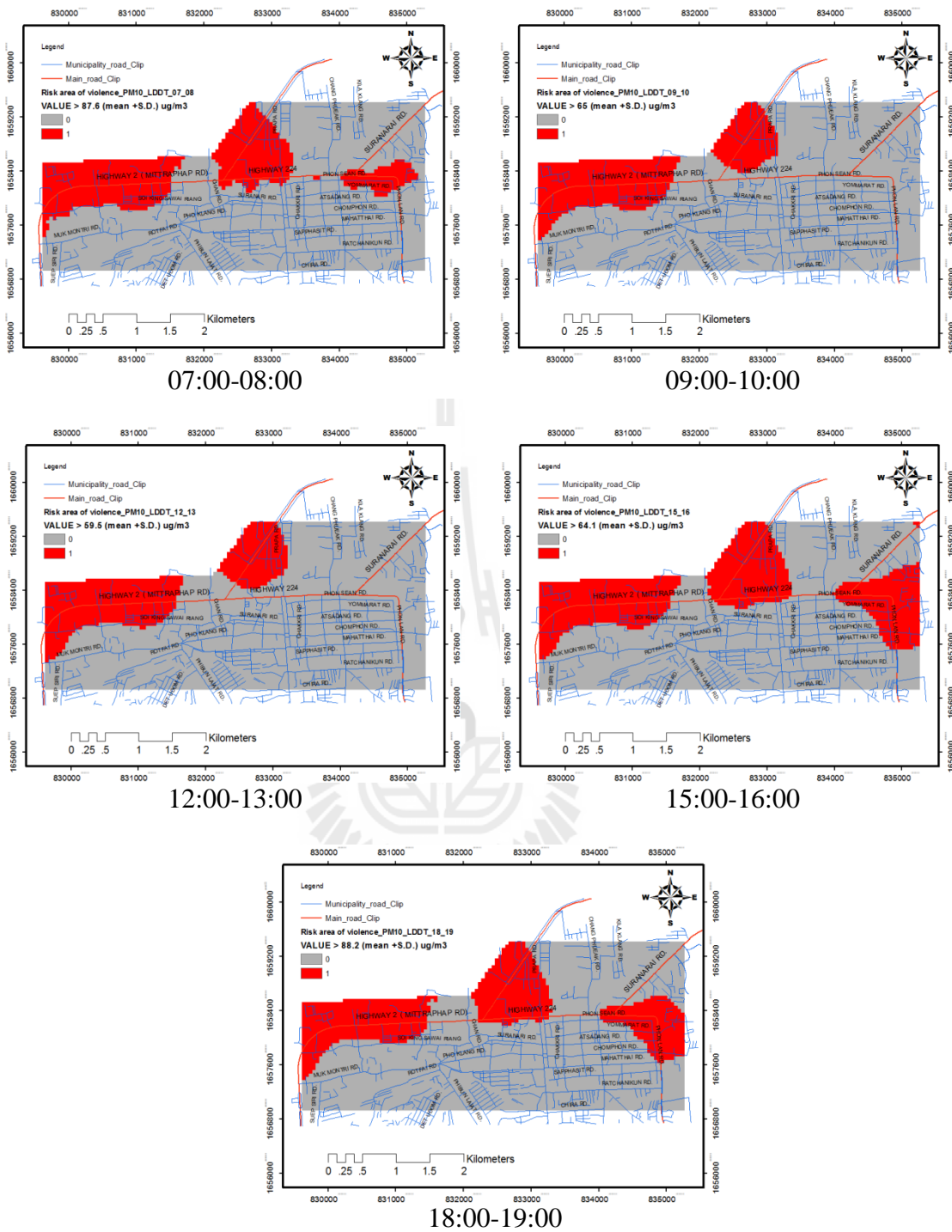
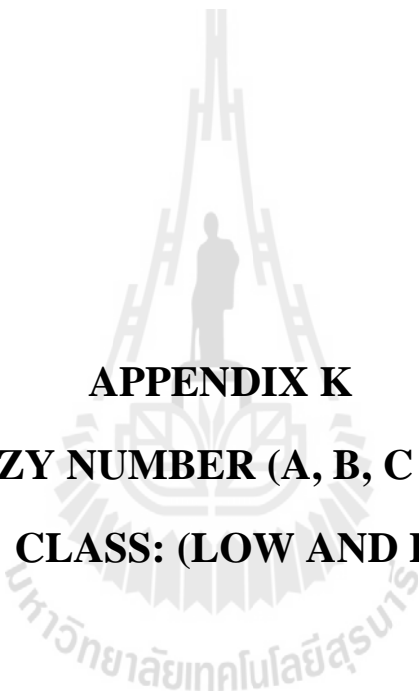


Figure J.8 PM10 frequency of violence map of LDDT vehicle type at 07:00-08:00, 09:00-10:00, 12:00-13:00, 15:00-16:00, and 18:00-19:00.



APPENDIX K
FUZZY NUMBER (A, B, C AND D) OF
CLASS: (LOW AND HIGH)

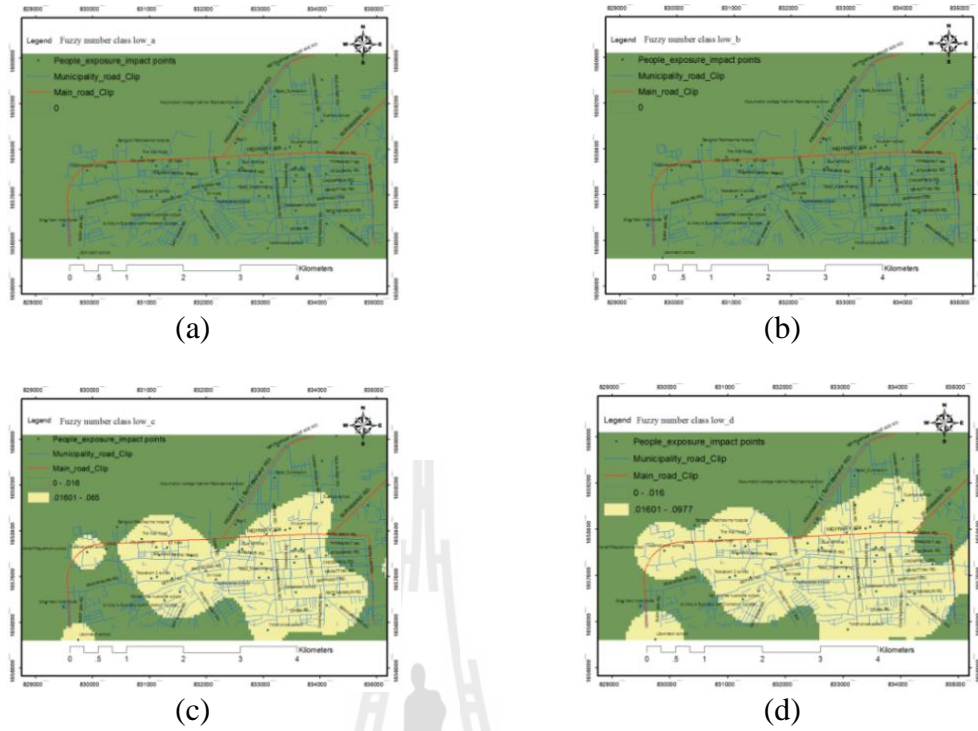


Figure K.1 The normalized fuzzy number (a, b, c, and d) of class (low).

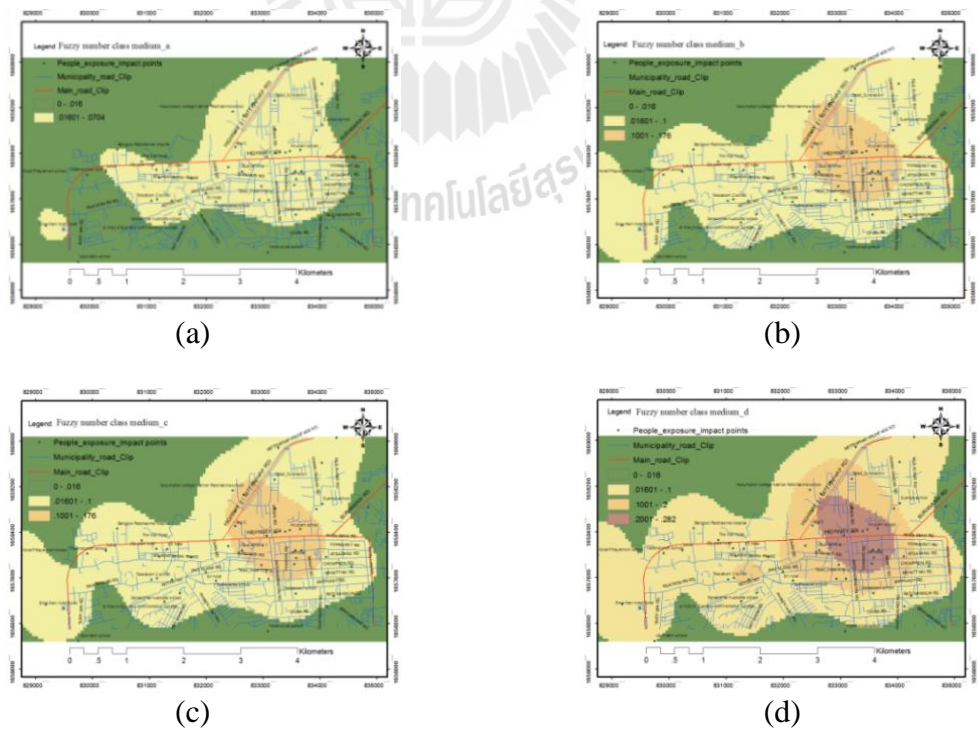


Figure K.2 The normalized fuzzy number (a, b, c and d) of class (medium).

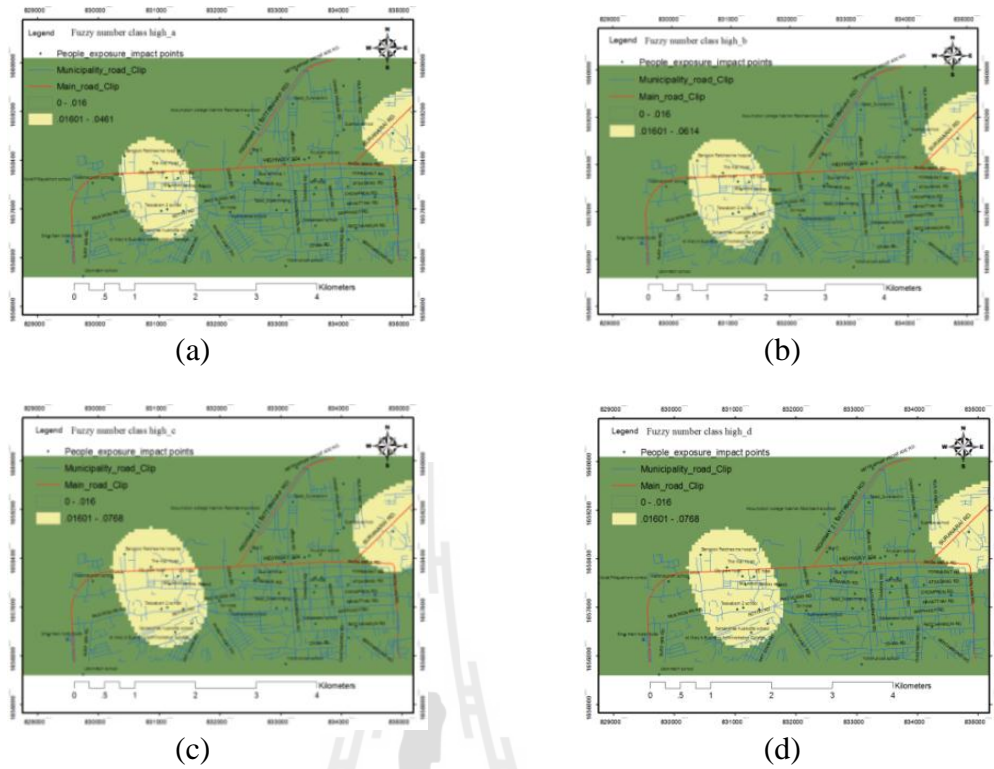


Figure K.3 The normalized fuzzy number (a, b, c, and d) of class (high).

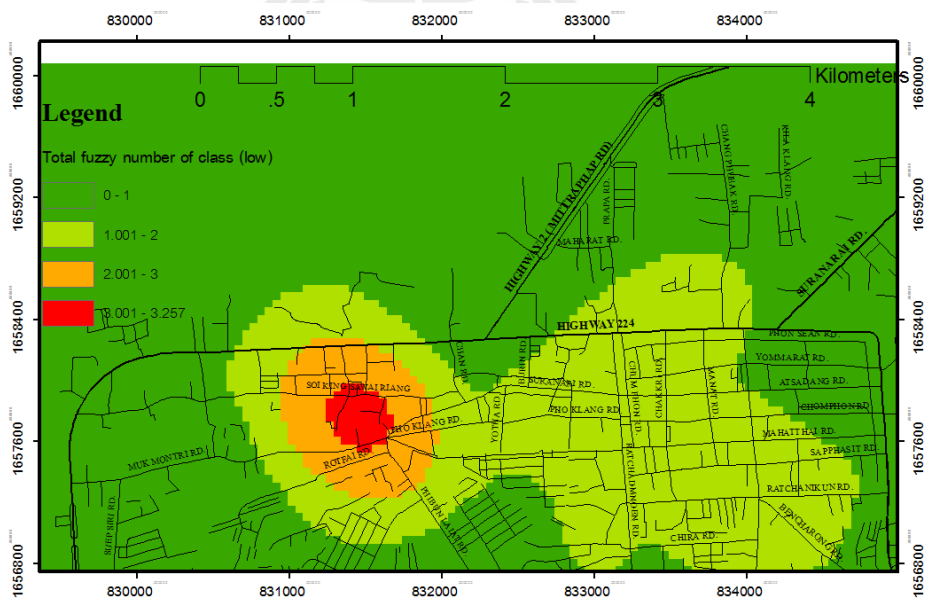


Figure K.4 Total fuzzy number (a, b, c and d) of class (low).

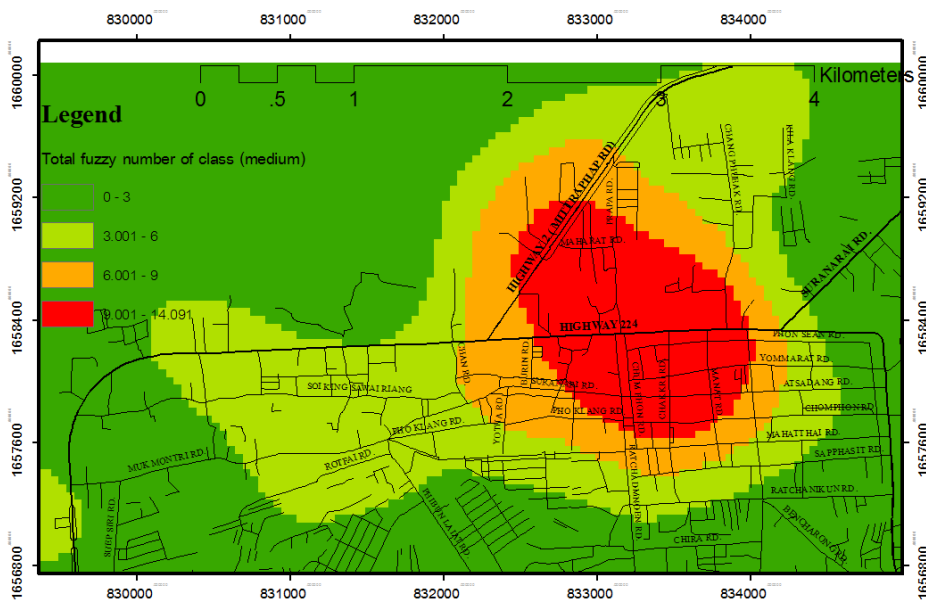


Figure K.5 Total fuzzy number (a, b, c and d) of class (medium).

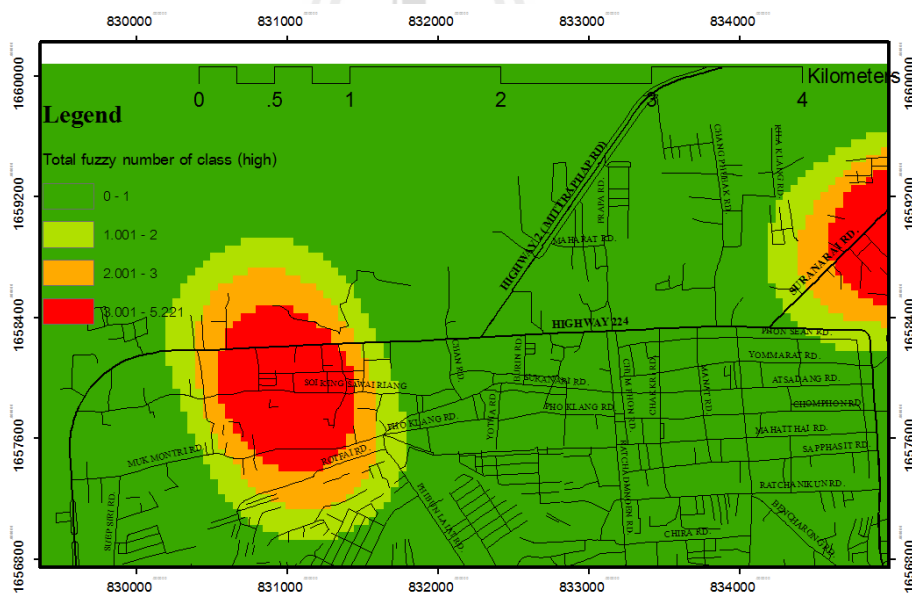


Figure K.6 Total fuzzy number (a, b, c and d) of class (high).

CURRICULUM VITAE

Name Mr PATTIWAT LITTIDEJ

Date of Birth February 3, 1980

Place of Birth Khon Kaen

Education 1999 - 2003 Bachelor of Transportation Engineering, Suranaree University of Technology, Nakhon Ratchasima, Thailand.
2005 - 2008 Master of Transportation Engineering, Suranaree University of Technology, Nakhon Ratchasima, Thailand.

Publications

Patiwat Littidej, Sunya Sarapirome, and Warunee Aunphoklang. 2012. Air Pollution Concentration Approach to Potential Area Selection of the Air Quality Monitoring Station in Nakhon Ratchasima Municipality, Thailand. **Journal of environmental science and engineering.**, (4): 484-494.

Grants and Fellowships (Ph.D) Commission on Higher Education under the CHE-PHD-THA program.